

**PHOTOCHEMISTRY OF CYCLOBUTENES AND RELATED CONSTRAINED  
*S-CIS* DIENES**

by

**JOSE ALBERTO POSTIGO, M.Sc.**

A Thesis

Submitted to the School of Graduate Studies

in Partial Fulfillment of the Requirements

for the Degree

Doctor of Philosophy

McMaster University

(c) Copyright by Jose Alberto Postigo, November 1994

**THE PHOTOCHEMISTRY OF CYCLOBUTENES AND RELATED  
CONSTRAINED *S-CIS* DIENES**

A mi mamá María Re y mi papá José Edmundo

**DOCTOR OF PHILOSOPHY (1994)**

**McMASTER UNIVERSITY**

**HAMILTON, ONTARIO**

**TITLE:** **PHOTOCHEMISTRY OF CYCLOBUTENES AND  
RELATED CONSTRAINED *S-CIS* DIENES**

**AUTHOR:** Jose Alberto Postigo, M.Sc.  
(Universidad de Buenos Aires)

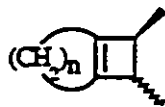
**SUPERVISOR:** Professor William J. Leigh

**NUMBER OF PAGES:** xxii, 258

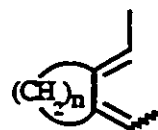
## ABSTRACT

This thesis is concerned with the development of a new qualitative model to explain the photochemistry of cyclobutene and 1,3-butadiene, in which the  $2A_g \rightarrow 1A_g$  decay channel of the van der Lugt-Oosterhoff mechanism does not actually correspond to a  $2A_g$  avoided crossing pericyclic minimum. In fact, decay from the  $2A_g$  excited state to the ground ( $1A_g$ ) state occurs at a conical intersection point (crossing between the excited state and ground state potential energy surfaces).

The study described pertains to the photochemical ring opening of a series of alkyl-substituted bicyclic cyclobutenes (structure I), and the cis,trans isomerization of related constrained s-cis dienes (structure II). The high degree of disrotatory stereospecificity observed in the ring opening of I is not related to ring strain factors induced by the ancillary ring, but rather to the decreased flexibility in the isomeric 1,3-diene products or the rotational flexibility of the substituents on the cyclobutene double bond. These results strongly suggest that orbital symmetry selection rules are important in these reactions. The effects of constraining the C-C central bond in 1,3-dienes on the cis,trans photoisomerization process and motions around C=C bond in cyclobutene photochemical ring opening are two of the direct implications of the results obtained from these experiments.



I



II

The results from the photochemical ring opening of alkyl-substituted monocyclic cyclobutenes provide evidence that orbital symmetry does play a significant role in the reaction, as indicated by the decrease in the quantum yields of ring opening upon syn-dimethyl substitution. In addition, the same results are exclusive of the presence of operative non-concerted pathways in the ring opening reaction.

The energy requirements for the photochemical ring opening of cyclobutenes have been clearly established. Thus, the inability of 1-phenylcyclobutenes to undergo ring opening reactions has been found to be related to energetic considerations rather than polarizability of their excited states.

## ACKNOWLEDGEMENTS

I would like to thank the following people who have contributed to this thesis:

My supervisor, Professor William J. Leigh who has been a source of inspiration, constant motivation and tenacity throughout the years. I thank him for the endless patience he showed since the first day I arrived at McMaster. Certainly, those first days fueled enough encouragement for the rest of my stay in Willie's group. My respect and admiration for Willie grew parallelly in both professional and personal levels. I also have to thank him for tolerating my bad spells of mood.

My committee members, Professors Dr. J. Warkentin and Dr. R.A. Bell who gave numerous suggestions throughout the years.

Mr. Brian Sayer and Dr. Don Hughes who taught me NMR spectroscopy, in both practical and theoretical ways. George Timmins for his help in most of the departmental instruments.

CIDA and McMaster for personal scholarships.

My former lab-mates K. Zheng, Nien Nguyen, Scott Mitchell, Kevin Ross, Laura DiCoco, Mark Workentin, Greg Sluggett and Zenab Musa for their perseverance in keeping our friendship; my present lab-mates Michael St. Pierre, Jo-Ann Banisch, Christine Bradaric, Dr Johnathan Lewis, Ed Lathioor, Nick Toldt, Paul Venneri, Peter Palermo, for their tolerance and friendship.

Faj Rarnelan, Dr. Richard Smith and Dr. Carol Kingsmill for their efforts in MS measurements of "non-conventional samples".

Carol Dada who generously gave of her time to help me through my first months at McMaster, and introduced me to the canadian life.

My friends in the departments of Chemistry, Physics and Psychology.

My family (Mary, Josef and Gaby) who supported me from long distance in good and bad times. I would especially like to thank my mother and father for their unconditional love and support.

## TABLE OF CONTENTS

List of Schemes	x
List of Figures	xiii
List of Tables	xix

### CHAPTER I: INTRODUCTION

1.1 The theory of Conservation of Orbital Symmetry	1
1.2 Dynamics of Photochemical Ring Opening Reactions	9
1.3 Photochemistry of Cyclobutenes	12
1.3.1 1-Aryl-substituted Cyclobutenes	12
1.3.2 The Photochemical Ring Opening of Alkyl-substituted Cyclobutenes	16
1.3.3 Excited States Responsible for Ring Opening and Cycloreversion Reactions in Alkylsubstituted Cyclobutenes	20
1.4 Mechanistic Interpretations for the Observed Nonstereospecificity Photochemical Ring Opening of Alkylsubstituted Cyclobutenes	27
1.5 The Photochemistry of Conjugated Dienes	34
1.5.1 <i>Cis,trans</i> - Photoisomerization, <i>s-cis/s-trans</i> Interconversion and Cyclobutene Formation	35
1.5.2 Bicyclo[1.1.0]butane Formation and [1,5]-H Migration	40
1.6 Theoretical Studies of the Photochemical <i>cis,trans</i> Isomerization and Electrocyclization of 1,3-Dienes	41
1.7 Statement of the Problem	55

### CHAPTER II: THE PHOTOCHEMISTRY OF 1-PHENYLCYCLOBUTENES

2.1 Introduction	58
2.2 RESULTS	
2.2.1 Preparation of 1-Phenylcyclobutenes	65



2.2.2 UV Absorption Spectra	67
2.2.3 Photochemistry of 65-70 in Aprotic Solvents	68
2.2.4 Photolyses in Hydroxylic Solvents	73
2.2.5 Fluorescence Spectra of 65-70	76
2.2.6 Singlet Lifetimes, Fluorescence and Product Quenching Experiments	78
2.2.7 Direct Detection of the Triplet	
States of 1-Phenylcyclobutene Derivatives	86
2.2.8 Cation Intermediacy in the Photolysis of	
1-Arylcyclobutenes in Hydroxylic Solvents	89
<b>2.3 DISCUSSION</b>	
2.3.1 General Aspects of the Photochemistry of 1-Phenylcyclobutenes	91
2.3.2 Substituent Effects on the Photochemistry	
and Photophysics of 1-Phenylcyclobutene	101
2.3.3 Quantitative Aspects of the Photoprotonation of 1-Arylcyclobutenes	108
<b>2.4 Summary</b>	113

### CHAPTER III: THE PHOTOCHEMISTRY OF MONOCYCLIC CYCLOBUTENE DERIVATIVES

<b>3.1 Introduction</b>	116
<b>3.2 Preparation and Characterization of Compounds</b>	117
<b>3.3 Direct Photolysis of Cyclobutenes 93-98 in Hydrocarbon Solutions</b>	119
3.3.1 Light Sources, Quantum Yield	
Determination and Product Identification	119
3.3.2 Results	120
<b>3.4 DISCUSSION</b>	125
3.4.1 C <sub>3</sub> /C <sub>4</sub> Effects on the Photochemical	
Ring Opening of Alkylcyclobutenes	125
3.4.2 Photochemical <i>versus</i> Ring Opening of 93-98	134
3.4.3 Cycloreversion of Cyclobutenes 93-98	136
<b>3.5 Conclusions</b>	136

**CHAPTER IV: THE EFFECTS OF "CENTRAL BOND"  
TORSIONAL CONSTRAINT ON THE  
PHOTOCHEMISTRY OF CYCLOBUTENE  
AND 1,3-BUTADIENE**

<b>4.1 Introduction</b>	137
<b>4.2 Preparation and Identification of Compounds</b>	141
<b>4.3 Results</b>	149
4.3.1 Direct Irradiation of Dienes	149
4.3.2 Direct Irradiation of <i>cis</i> - and <i>trans</i> -Dimethylbicyclo[n.2.0]alk-1-enes	156
<b>4.4 DISCUSSION</b>	160
4.4.1 The <i>cis,trans</i> Photoisomerization of Constrained <i>s-cis</i> Dienes	160
4.4.2 The Photochemical Ring Opening of Dimethylbicyclo[n.2.0]alk-1 <sup>n+2</sup> enes	164
<b>4.5 Summary and Conclusions</b>	171

**CHAPTER V: OVERVIEW**

<b>5.1 A New Mechanism for the Photochemical Isomerization of Cyclobutene and 1,3-Butadiene</b>	175
<b>5.2 Contributions of the Studies and Future Work</b>	176
5.2.1 Phenylcyclobutenes	176
5.2.2 Cyclobutene → Butadiene Photointerconversion	178

**CHAPTER VI: EXPERIMENTAL**

<b>6.1 1-Phenylcyclobutenes</b>	181
6.1.1 General	181
6.1.2 Commercial Solvents and Reagents Used	183
6.1.3 Preparation and Identification of Compounds	183
6.1.4 Quantum Yield Determinations and Fluorescence Lifetimes	199
6.1.5 Nanosecond Laser Flash Photolysis Experiments	200
6.1.6 Steady State Photolyses	201
<b>6.2 Monocyclic Cyclobutenes</b>	201

6.2.1 General	201
6.2.2 Commercial Solvents and Reagents Used	202
6.2.3 Preparation and Identification of Compounds	205
6.2.4 Characterization of Photoproducts	215
6.2.5 Photolyses and Quantum Yield Determinations	217
6.3 <i>Cis</i> and <i>Trans</i> -Dimethylbicyclo[n.2.0]alk-1 <sup>n+2</sup> enes	219
6.3.1 General	219
6.3.2 Commercial Solvents and Reagents Used	219
6.3.3 Preparation and Identification of Compounds	220
6.3.4 Photolyses and Quantum Yield Determinations	236
<b>REFERENCES</b>	239
<b>APPENDIX I</b>	256
<b>APPENDIX II</b>	258

## LIST OF SCHEMES

1.1.1	Symmetry elements present in the <i>conrotatory</i> and <i>disrotatory</i> motions of cyclobutene	4
1.3.3.1	Possible mechanistic pathway for the cycloreversion process in alkylsubstituted cyclobutenes	22
1.5.1.1	Relative yields for the photoisomerization processes of 2,3-dimethyl-1,3-butadiene-1,4-d <sub>2</sub>	37
1.5.1.2	<i>Cis,trans</i> isomerization and cyclobutene formation from <i>t,t</i> -39	38
1.6.1	Allylmethylene biradical mechanism for the photoisomerization of 2,4-hexadiene	43
1.6.2	<i>S-cis/s-trans</i> isomerization pathways for 1,3-butadiene	49
1.6.3	Schematic excited state pathway for ring closure of 1,3-butadiene	53
1.6.4	Possible recoupling pathways from <i>s-cis</i> excited state minima of 1,3-butadiene	53
2.1.1	Sensitized photohydration of aliphatic cycloalkenes	59
2.1.2	Mechanism for photoaddition of solvent to 1-phenylcyclohexene	61
2.1.3	Photohydration of styrene derivatives	63
2.2.1	Synthesis of 1-phenylcyclobutenes	66

2.2.3.1	Energy transfer from 4'-methoxyacetophenone triplet to 1-arylcyclobutene	71
2.2.3.2	Synthesis of 1-phenylcyclobutene- <i>d</i> <sub>3</sub>	73
2.2.4.1	Photolysis of 1-phenylcyclobutene derivatives in methanol	74
2.3.1.1	Deactivation pathways of 1-phenylcyclobutenes	91
2.3.1.2	Triplet energy transfer from arylcyclobutene to <i>trans</i> -piperylene	93
2.3.1.3	Conjectural mechanism for cycloreversion of <b>67</b> via cyclopropyl carbene	96
2.3.1.4	Mechanism for addition of methanol to 1,2-diphenylcyclobutene	97
2.3.1.5	Deactivation pathways of singlet excited 1-phenylcyclobutenes	98
2.3.1.6	Mechanism for solvent addition to 1-phenylcyclobutene showing proton transfer and nucleophilic attack by the solvent	99
2.3.3.1	Mechanism for the photoaddition of solvent in 1-arylcyclobutenes involving the formation of an exciplex	109
2.4	Photophysical and photochemical processes studied for 1-phenylcyclobutenes in the present document	114
3.4.1.1	<i>Disrotatory</i> twisting modes about C <sub>1</sub> -C <sub>4</sub> and C <sub>2</sub> -C <sub>3</sub> bonds as the C <sub>3</sub> -C <sub>4</sub> bond cleaves	128
3.4.1.2	Electrocyclization of 1,3,5-hexatriene	130
3.4.1.3	Drawing of the SCF/6-31G* transition structure for the electrocyclization of 1,3,5-hexatriene. The	

	arrows show motions in the normal mode of imaginary frequency	130
3.4.1.4	<i>E/Z</i> Diene ratios from allowed disrotatory photochemical ring opening of cyclobutenes <b>94</b> , <b>95</b> and <b>97</b>	132
4.1.1	Photochemistry of constrained <i>s-cis</i> dienes	139
4.2.1	Synthesis of 1,2- <i>bis</i> (ethylidene)cycloalkanes	141
4.2.2	Synthesis of 2,3- <i>bis</i> (ethylidene)bicyclo[2.2.1]heptane	142
4.3.2.1	Photolysis of dimethylbicyclo[ <i>n</i> .2.0]alk-1-enes	157
4.4.1	Regioselectivity observed in the photochemical ring opening of <b>128</b>	166
4.5	Conjectural surface diagram for the cyclobutene ↔ butadiene interconversion. The spheres inside the cube represent CI	173

## LIST OF FIGURES

1.1.1a	Orbital correlation diagram for the thermally-allowed interconversion of butadiene and cyclobutene	5
1.1.1b	Orbital correlation diagram for the photochemical interconversion of butadiene and cyclobutene	6
1.1.2	Relative $S_0$ (ground state) and $S_1$ (first singlet excited state) energies of 1,3-butadiene and cyclobutene	6
1.1.3	Potential energy curves for the disrotatory and conrotatory modes in the butadiene $\leftrightarrow$ cyclobutene system. The $C_s$ symmetry is preserved in the disrotatory mode and the $C_2$ symmetry is preserved in the conrotatory process. Full line: The lowest symmetric singlet $S_0$ and $S_2$ states (or $1^1A_g$ and $2^1A_g$ ). Dashed lines: the lowest antisymmetric singlet state $S_1$ or $1^1B_u$ state.	7
1.2.1	Schematic reaction coordinate for the photochemical ring opening of 1,3-butadiene	10
1.2.2	The arrows superimposed on the ground state structure of cyclobutene give the geometry changes that occur within 30 fs after excitation as a result of evolution along the indicated $CH_2-CH_2$ stretch and $CH_2$ twisting normal modes	11
1.3.3.1	UV absorption spectra of 31 - 33 in the gas phase (—) and in deoxygenated pentane solution (---)	25

1.4.1	State correlation diagram for the interconversion of dewarnaphthalene to naphthalene	28
1.4.2	Reaction pathway for the adiabatic disrotatory ring opening of 9	29
1.4.3	State correlation diagram for the butadiene $\leftrightarrow$ cyclobutene interconversion. Solid lines: Adiabatic pathway. Dashed lines: Nonadiabatic pathway	30
1.6.1a	State correlation diagram for the photoisomerization of a 1,3-butadiene system according to the avoided crossing model	42
1.6.1b	A section through the potential energy surfaces for the $^1B_u$ , $1^1A_g$ , and $2^1A_g$ states of 2-methyl-1,3-butadiene along the symmetric C=C stretches	46
1.6.2	Three-dimensional cross section of the excited state potential energy surface for butadiene	48
1.6.3	Optimized MC-SCF/4-31G structures for the central, <i>s-cisoid</i> and <i>s-transoid</i> conical intersections	50
1.6.4	Reaction coordinate diagram for twisting about the 1,3-butadiene C <sub>2</sub> -C <sub>3</sub> bond along the disrotatory (a), and conrotatory (b), <i>s-cis/</i> <i>s-trans</i> excited state isomerization pathways	52
1.6.5	Reaction funnels for the excited state and ground state surfaces and conical intersection point (vertex of the double cone)	55
2.2.3.1A,B	Moles of photoproduct vs time plots for the photolysis of 65-70 in A) pentane and B) acetonitrile deoxygenated solutions	70
2.2.6.1	Singlet lifetime decay profile and lifetime analysis for 1-phenylcyclobutene in cyclohexane deoxygenated solution	79



2.2.6.2	Quenching of the fluorescence of 70 by HFIP	81
2.2.6.3	Stern Volmer plot for the singlet lifetime quenching of 65-70 by methanol in deoxygenated acetonitrile solution	83
2.2.6.4	Stern Volmer plot for the quenching of the formation of phenylacetylene by methanol	85
2.2.6.5	Reciprocal plot of the yield of ether adduct 85 as a function of methanol concentration	85
2.2.7.1	Phosphorescence spectrum of 67 in a methylcyclohexane glass matrix recorded at 77 K	86
2.2.7.2	Triplet-triplet absorption spectra of 66-68 in acetonitrile deoxygenated solution as measured by NLFP	87
2.2.8.1	Spectral shift obtained for the transients generated upon 248 nm laser pulse excitation of 66 in acetonitrile ( $\lambda_{\text{max}} = 308 \text{ nm}$ ) and trifluoroethanol ( $\lambda_{\text{max}} = 337 \text{ nm}$ ) solutions	90
2.3.1.1	Relative energy levels for twisting about the ethylene moiety in the ground and excited state surfaces	98
2.3.2.1A,B	Hammett plot for the cycloreversion reaction of 65-70 in A) pentane and B) acetonitrile	105
2.3.2.2	Log-log plot of the rate constants for cycloreversion in methanol ( $k_2$ ) versus those for solvent addition ( $k_{\text{MeOH}}$ )	106
3.1	Cyclobutenes 93-98 to be studied	117
3.3.2.1	Moles of photoproduct versus time plots for the formation of E and Z-101 from photolysis (214 nm) of 1,2,3-trimethylcycobutene (94) in hexadecane solution	122

3.2.2.2A,B	Moles of photoproduct <i>versus</i> time plots for the formation of E,E, E,Z and Z,Z-102 from photolysis (214 nm) of A) <i>cis</i> -1,2,3,4-tetramethylcycobutene (95) and B) <i>trans</i> -1,2,3,4-tetramethylcycobutene (96) in hexadecane solution	122
3.3.2.3	Moles of photoproduct <i>versus</i> time plots for the formation of E and Z-103 from photolysis (214 nm) of 1,2,3,3,4-pentamethylcycobutene (97) in hexadecane solution	122
3.3.2.4	Total product diene yields from photolyses (214 nm) of methylated monocyclic cyclobutenes (93-98) in hexadecane deoxygenated solution	123
3.4.1.1	Plot of total quantum yield of ring opening (214 nm) as a function of methyl substitution for cyclobutenes 93-98 in hexadecane	126
3.4.2.1	Plot of activation energies <i>versus</i> number of methyl groups for the thermal ring opening of cyclobutenes 93-98	135
4.2.1	Solution phase UV absorption spectra of E,E- 124-127 and 131 measured at 23° C in pentane <i>ca.</i> $1 \times 10^{-4}$ mol dm <sup>-3</sup> solutions	146
4.2.2	Solution phase UV absorption spectra for <i>cis</i> -(—), and <i>trans</i> -(---) 128-130, and 37 measured at 23° C in pentane deoxygenated solutions	148
4.3.1.1A,B	Plots of moles of photoproduct <i>versus</i> irradiation time from photolysis of A) E,E-1,2- <i>bis</i> (ethylidene)cyclohexane (E,E-126) and B) E,Z-1,2- <i>bis</i> (ethylidene)cyclohexane (E,Z-126) in pentane deoxygenated solutions with 254 nm light	151
4.3.1.2A,B	Plots of moles of photoproduct <i>versus</i> irradiation time from photolysis of A) E,E-1,2- <i>bis</i> (ethylidene)cycloheptane (E,E-127) and B) E,Z-1,2- <i>bis</i> (ethylidene)cycloheptane (E Z-127)	

	in pentane deoxygenated solutions with 254 nm light	151
4.3.1.3A,B	Plots of moles of photoproduct <i>versus</i> irradiation time from photolysis of A) E,E-1,2-bis(ethylidene)cyclobutane (E,E-124) and B) E,Z-1,2-bis(ethylidene)cyclobutane (E,Z-124) in pentane deoxygenated solutions with 254 nm light	154
4.3.1.4A,B	Plots of moles of photoproduct <i>versus</i> irradiation time from photolysis of A) E,E-1,2-bis(ethylidene)cyclopentane (E,E-125) and B) E,Z-1,2-bis(ethylidene)cyclopentane (E,Z-125) in pentane deoxygenated solutions with 254 nm light	154
4.3.1.5A,B	Plots of moles of photoproduct <i>versus</i> irradiation time from photolysis of A) E,E-1,2-bis(ethylidene)bicyclo[2.2.1]heptane (E,E-131) and B) E,Z-1,2-bis(ethylidene)bicyclo[2.2.1]heptane (E,Z-131) in pentane deoxygenated solutions with 254 nm light	155
4.3.2.1A,B	Moles of photoproduct <i>versus</i> time plots for the photolysis (214 nm) of ca. $1 \times 10^{-2}$ mol dm <sup>-3</sup> pentane deoxygenated solutions of A) <i>cis</i> -5,6-dimethylbicyclo[2.2.0]hex-1(4)-ene ( <i>cis</i> -128) and B) <i>trans</i> -5,6-dimethylbicyclo[2.2.0]hex-1(4)-ene ( <i>trans</i> -128)	158
4.3.2.2A,B	Moles of photoproduct <i>versus</i> laser dose for the photolysis (193 nm) of ca. $1 \times 10^{-2}$ mol dm <sup>-3</sup> pentane deoxygenated solutions of A) <i>cis</i> -6,7-dimethylbicyclo[3.2.0]hept-1(5)-ene ( <i>cis</i> -129) and B) <i>trans</i> -6,7-dimethylbicyclo[3.2.0]hept-1(5)-ene ( <i>trans</i> -129)	158
4.3.2.3A,B	Moles of photoproduct <i>versus</i> laser dose for the photolysis (193 nm) of ca. $1 \times 10^{-2}$ mol dm <sup>-3</sup> pentane deoxygenated solutions of A) <i>cis</i> -7,8-dimethylbicyclo[4.2.0]oct-1(6)-ene ( <i>cis</i> -37) and B) <i>trans</i> -7,8-dimethylbicyclo[4.2.0]oct-1(6)-ene ( <i>trans</i> -37)	
4.3.2.4i,ii	Moles of photoproduct <i>versus</i> time plots for the photolysis (214 nm) of ca. $1 \times 10^{-2}$ mol dm <sup>-3</sup> pentane deoxygenated solutions of i) <i>cis</i> -8,9-dimethylbicyclo[5.2.0]non-1(7)-ene ( <i>cis</i> -130) and ii)	

	<i>trans</i> -8,9-dimethylbicyclo[5.2.0]non-1(7)-ene ( <i>trans</i> -130)	159
4.3.2.5A,B	Moles of photoproduct <i>versus</i> laser dose for the photolysis (193 nm) of <i>ca.</i> $1 \times 10^{-2}$ mol dm <sup>-3</sup> pentane deoxygenated solutions of A) <i>cis</i> -8,9-dimethylbicyclo[5.2.0]non-1(7)-ene ( <i>cis</i> -130) and B) <i>trans</i> -8,9-dimethylbicyclo[5.2.0]non-1(7)-ene ( <i>trans</i> -130)	160
4.4.1	Structure of cyclobutene at the conical intersection	170
4.5	Conjectural surface diagram for cyclobutene $\leftrightarrow$ butadiene interconversion. The spheres inside the cube represent CTs	173

## LIST OF TABLES

1.3.3.1	Gas-phase spectroscopic properties of substituted bicyclo[4.2.0]oct-7-enes 31-33	24
1.3.3.2	Product quantum yields from photolyses (193 nm) of pentane deoxygenated solutions of 31-33	26
1.4.1	Calculated and observed diene ratios from photolysis of <i>cis</i> - and <i>trans</i> - 37	32
1.4.2	Product diene yields from 214 nm photolyses of deoxygenated pentane solutions of <i>cis</i> - and <i>trans</i> -bicyclo[5.2.0]non-8-ene 23	32
1.5.1	Photoisomerization quantum yields from 2,4-hexadiene	38
2.1	Singlet fluorescence lifetimes of styrenic compounds determined in water at pH 7	64
2.2.2.1	Solution phase data for cyclobutenes 65-70 measured in acetonitrile, cyclohexane and methanol solutions	67
2.2.3.1	Quantum yields for cycloreversion of 1-arylcyclobutenes 65-70 in <i>ca.</i> $5 \times 10^{-3}$ mol dm <sup>-3</sup> acetonitrile and pentane deoxygenated solutions (254 nm)	69
2.2.4.1	Quantum yields for methanol addition and cycloreversion of 1-arylcyclobutenes 65-70 in methanol solution	75
2.2.5.1	Fluorescence emission maxima and O-O band energies for cyclobutenes 65-70	77
2.2.5.2	Quantum yields of fluorescence of cyclobutenes 65-70 determined	

	in acetonitrile and cyclohexane deoxygenated solutions using naphthalene as primary fluorescence standard	78
2.2.6.1	Fluorescence lifetimes measured by time correlated single photon counting technique for 1-arylcyclobutenes 65-70 in cyclohexane, acetonitrile, and methanol deoxygenated solutions	80
2.2.6.2	Stern Volmer values for the fluorescence quenching of compounds 65-70 by 1,1,1,3,3,3-hexafluoro-2-propanol in deoxygenated acetonitrile solutions	82
2.2.6.3	Fluorescence lifetimes of 1-phenylcyclobutene in various solvents	82
2.2.6.4	Bimolecular quenching rate constants $k_q^{\text{MeOH}}$ , Stern Volmer values $K_{SV}$ and extrapolated lifetimes in pure methanol $\tau_{\text{MeOH}}^{\text{(extr)}}$ obtained from singlet lifetime quenching experiments of cyclobutenes 65-70 by methanol in acetonitrile deoxygenated solutions	83
2.2.6.5	Quenching rate constants and Stern Volmer values	85
2.2.7.1	Triplet-triplet absorption maxima for compounds 65-70, as determined by NLFP in acetonitrile deoxygenated solutions	88
2.2.7.2	Rate constants for triplet quenching obtained by NLFP in deoxygenated solutions	89
2.3.2.1	Rate constants for fluorescence decay ( $k_f^\circ$ ), cycloreversion in cyclohexane, acetonitrile and methanol ( $k_2$ ), and solvent incorporation in methanol	103
2.4	Quantum yields for radiative and nonradiative processes for the parent 1-phenylcyclobutene	114
3.3.2.1	Relative total diene yields and isomeric diene distributions	

	from photolyses (214 nm) of cyclobutenes 93-98 in <i>ca.</i> 0.02 mol dm <sup>-3</sup> hexadecane deoxygenated solution	123
3.3.2.2	Relative yields of cycloreversion products from photolyses (214 nm) of cyclobutenes 93-98 in hexadecane deoxygenated solution	124
3.3.2.3	Absolute quantum yields for product formation from photolysis (214 nm) of cyclobutenes 93-98 in hexadecane deoxygenated solutions	125
3.4.1.1	Number of disrotatory interactions generated upon cyclobutene ring opening	129
3.4.1.2	Structures of the allowed isomers obtained from ring opening of 94, 95, and 97, and dominant steric interactions involved in the disrotatory process. Ratios of the allowed isomers are given in each case	132
3.4.2.1	Rate data for cyclobutenes 93-98 undergoing conrotatory ring opening	135
4.2.1	Diagnostic <sup>13</sup> C NMR chemical shifts of 124-127 E,E- and E,Z- diene isomers determined in deuteriochloroform as solvent	144
4.2.2	Ultraviolet absorption data for E,E- and E,Z- dienes 124-127 and 131. The spectra were recorded in <i>ca.</i> 5 x 10 <sup>-5</sup> mol dm <sup>-3</sup> deoxygenated pentane solutions	145
4.2.3	Diagnostic <sup>13</sup> C NMR chemical shifts of bicyclic cyclobutenes determined in carbon tetrachloride as solvent	147
4.3.1.1	Quantum yields for <i>cis,trans</i> photoisomerization and cyclobutene formation from 254 nm photolysis of <i>ca.</i>	

	0.02 mol dm <sup>-3</sup> pentane deoxygenated solutions of E,E- and E,Z- <b>126</b> and <b>127</b>	150
4.3.1.2	Quantum yields for <i>cis,trans</i> photoisomerization and cyclobutene formation from 254 nm photolysis of <i>ca.</i> 0.02 mol dm <sup>-3</sup> pentane deoxygenated solutions of E,E- and E,Z- <b>125</b> , <b>131</b> , and <b>124</b>	155
4.3.2.1	Quantum yields for diene formation from 193 nm and 214 nm irradiation of <i>ca.</i> 0.02 mol dm <sup>-3</sup> pentane deoxygenated solutions of <i>cis</i> - and <i>trans</i> - <b>128</b> , <b>129</b> , <b>127</b> , and <b>130</b>	157
4.4.1.1	Central bond dihedral angles at which the calculated MMX heat of formation of the corresponding <i>bis</i> (methylene)cycloalkane is 12.5 KJ mol <sup>-1</sup> higher than that of its stable ground state geometry. C <sub>1</sub> -C <sub>4</sub> distances are included (terminal methylene carbons)	161
4.4.2.1	Calculated and observed diene ratios at 193 nm and 214 nm from photolyses of cyclobutenes <b>128</b> , <b>129</b> , <b>127</b> , and <b>130</b>	166
4.4.2.2	Allowed to forbidden diene ratios from photolyses of alkylcyclobutenes in hydrocarbon solutions	168
4.4.2.3	Quantum yields for cyclobutene ring opening at 185 nm excitation wavelength	169

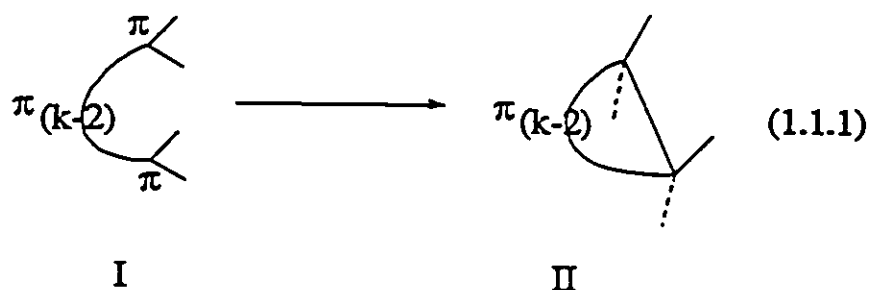


## INTRODUCTION

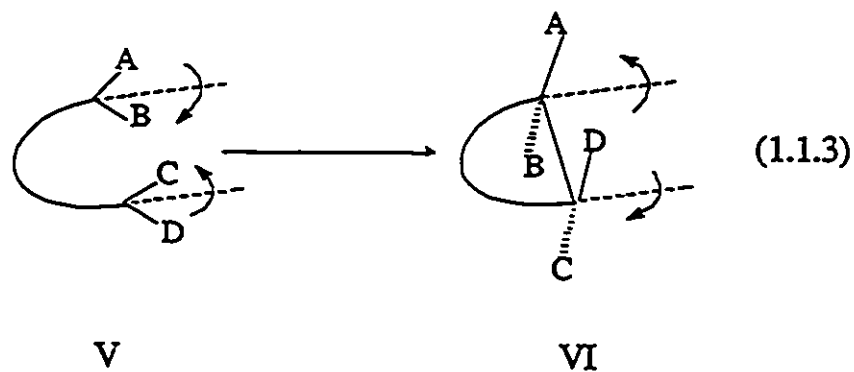
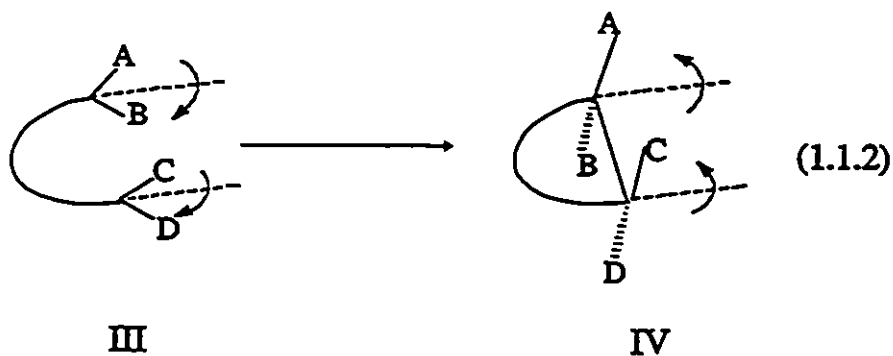
### L1 The Theory of Conservation of Orbital Symmetry

Electrocyclic reactions are among the most versatile reactions in organic chemistry. The interconversions of cyclobutene and 1,3-butadiene can be considered as a cornerstone example, put forward by the classical and famous papers by Woodward and Hoffmann on the stereochemistry of electrocyclic reactions<sup>1 - 10</sup>.

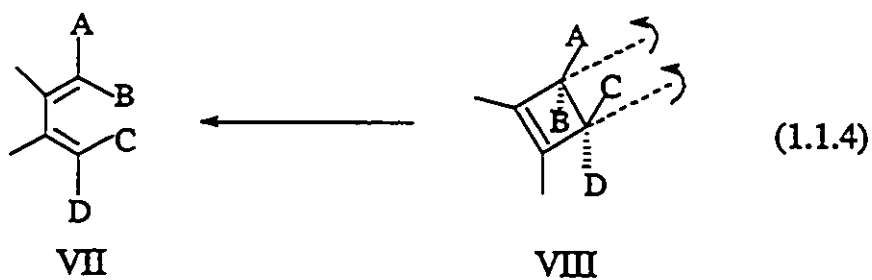
An electrocyclic transformation involves the formation of a single bond between the termini of a linear system containing  $k$   $\pi$ -electrons ( $I \rightarrow II$ , equation 1.1.1), or the converse process.



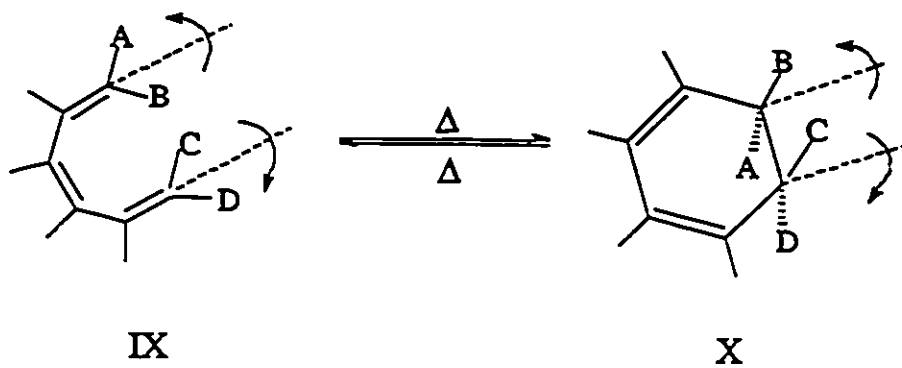
In forming or breaking the  $\sigma$  bond, the termini must rotate either in the same direction (*conrotatory*  $III \rightarrow IV$ , equation 1.1.2) or in the opposite direction (*disrotatory*  $V \rightarrow VI$ , equation 1.1.3).



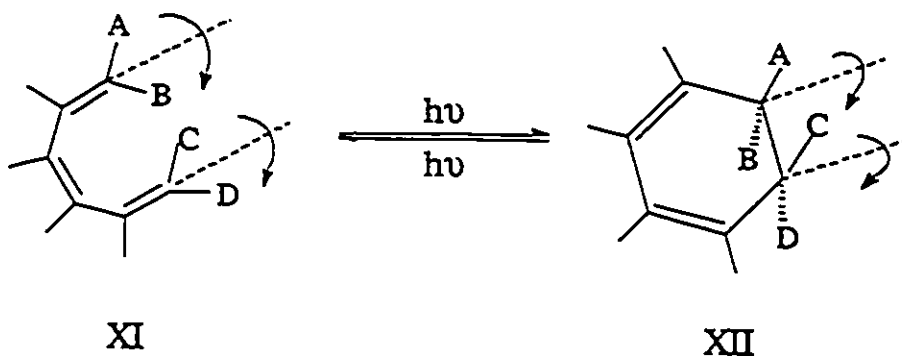
In practice, transformations of this type have been brought about thermally or photochemically. For example, the thermal isomerization of cyclobutenes is cleanly *conrotatory* (VII  $\leftarrow$  VIII, equation 1.1.4)<sup>11</sup>.



By contrast the thermal cyclization of 1,3,5-hexatrienes is uniquely *disrotatory* (IX  $\rightarrow$  X)  
12.

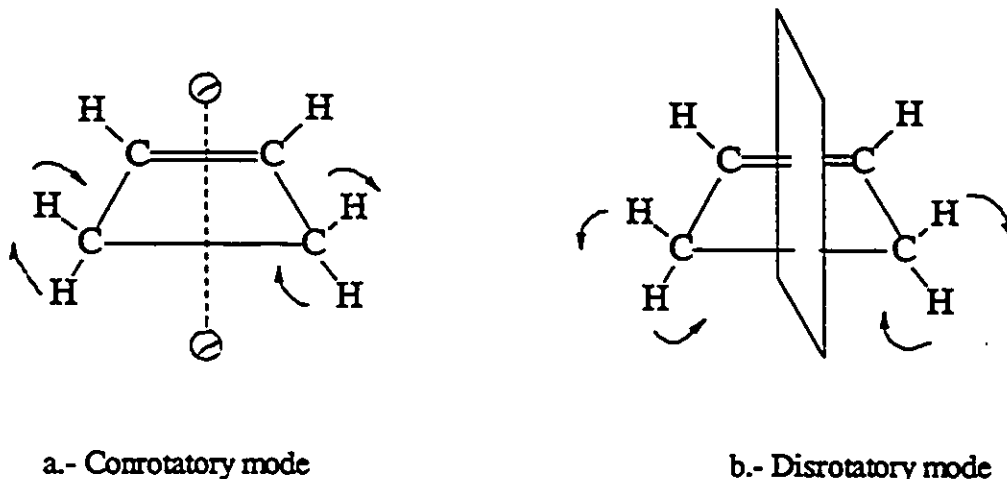


Finally, 1,3,5-hexatrienes are subjected to photochemical cyclization to 1,3-cyclohexadienes and *vice versa* by a stereospecific *conrotatory* process (XI  $\rightarrow$  XII)<sup>13</sup>.



In the electrocyclic transformation of cyclobutene to 1,3-butadiene, four molecular orbitals are involved; these are  $\sigma$ ,  $\sigma^*$ ,  $\pi$ , and  $\pi^*$ , where the first two are the bonding and antibonding orbitals of the bond which is to be broken ( $C_3-C_4$ ), and the last two refer to the carbon - carbon double bond in the cyclobutene ring. These orbitals will eventually become the molecular  $\pi$ -orbitals of butadiene, namely  $\psi_1$ ,  $\psi_2$ ,  $\psi_3$ , and  $\psi_4$ , in order of increasing energy. Each of the first set of orbitals passes adiabatically into one of the second set, and their correlation depends upon whether the isomerization proceeds in a *conrotatory* or *disrotatory* fashion (Figure 1.1.1). In the conrotatory mode, the system

preserves a twofold axis of symmetry, and each orbital is classified as A or B according to its symmetric or antisymmetric character respectively. In the *disrotatory* mode, a plane of symmetry is maintained, and each orbital remains either symmetric (A') or antisymmetric (A'') about this plane (Scheme 1.1.1)<sup>10</sup>.



Scheme 1.1.1. Symmetry elements present in the *conrotatory* and *disrotatory* motions of cyclobutene.

Figure 1.1.1a shows that in the *conrotatory* mode of cyclobutene ring opening,  $\sigma$  correlates with  $\psi_2$ ,  $\pi$  with  $\psi_1$  etc.; however, in the *disrotatory* mode,  $\sigma$  correlates with  $\psi_1$  and  $\pi^*$  with  $\psi_2$ , etc. (Figure 1.1.1b). In general, the stereochemical course of an electrocyclic reaction in the ground state is determined by the highest occupied molecular orbital (HOMO) of the reactant, as shown by extended Huckel Theory (Figure 1.1.1a). On the other hand, promotion of an electron to the lowest excited state leads to a reversal of the terminal symmetry relationships in the orbitals involved in the  $\pi$  system, with the consequence that the system which undergoes a thermally induced *disrotatory* electrocyclic transformation in the ground state should follow a conrotatory course when photochemically excited and *vice versa* (see Molecular Orbitals for Cyclobutene/Butadiene interconversion in Figure 1.1.1b).

However, when one considers that the ground state of cyclobutene is  $83.7 \text{ KJ mol}^{-1}$  less stable<sup>9</sup> than that of 1,3-butadiene, it is evident that the spectroscopic singlet of cyclobutene is about  $209\text{-}251 \text{ KJ mol}^{-1}$  higher in energy than the spectroscopic singlet of butadiene (see Figure 1.1.2). Thus the formation of the spectroscopic singlet of cyclobutene from a similar state of 1,3-butadiene was judged improbable<sup>9</sup>. By the early 1970's, although the Woodward and Hoffmann rules were gathering increasing support amongst the scientific community in predicting the stereochemical outcome of the photoinduced reaction (butadiene  $\rightarrow$  cyclobutene photointerconversion, XIII  $\rightarrow$  XIV) it was not clearly understood why the reaction took place at all.

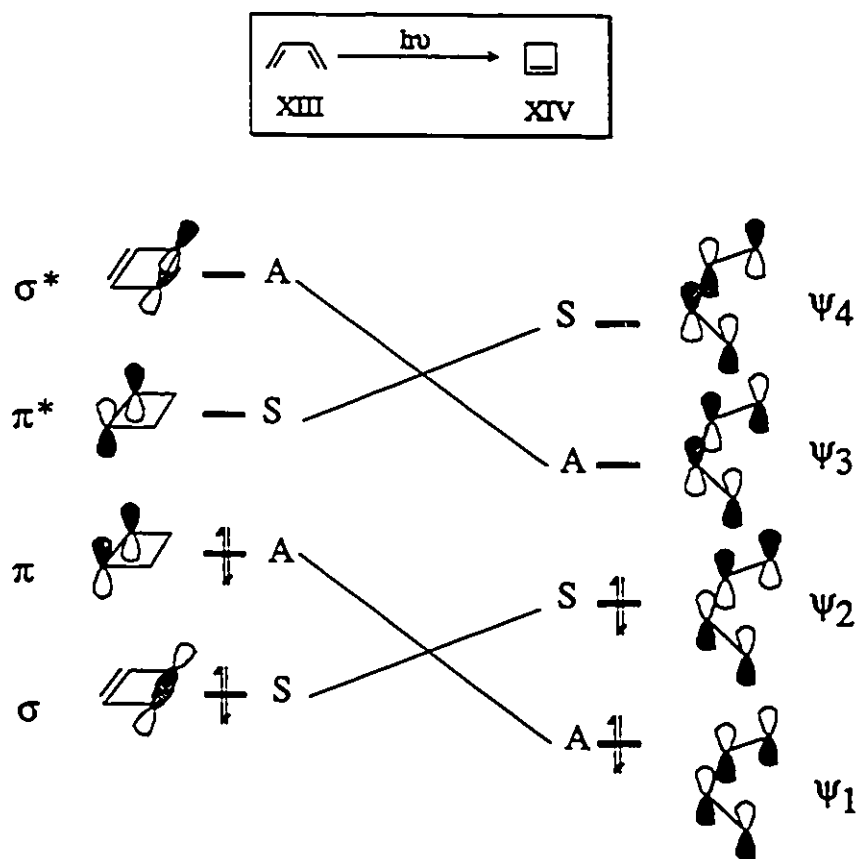


Figure 1.1.1a. Orbital correlation diagram for the thermally-allowed interconversion of butadiene and cyclobutene.

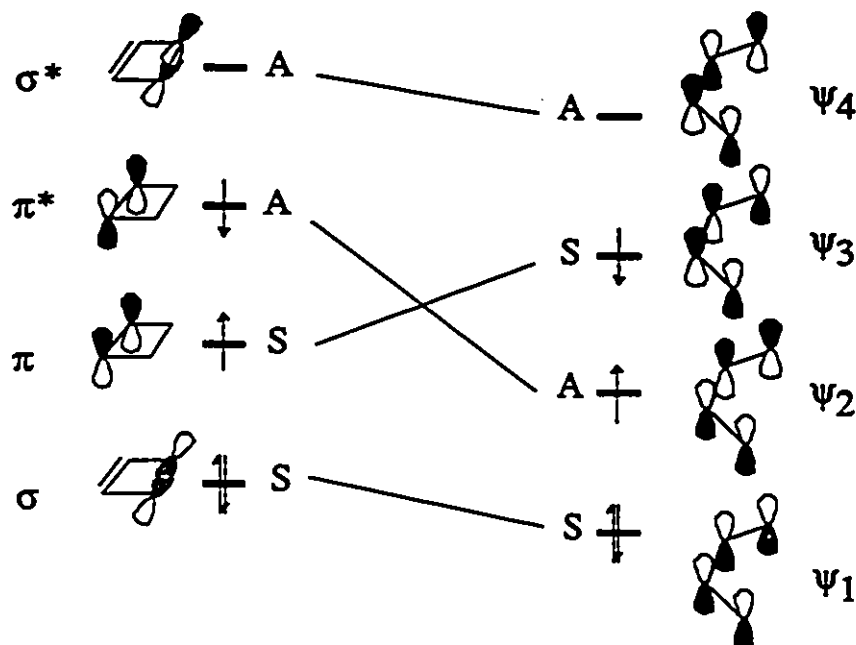


Figure 1.1.1b. Orbital correlation diagram for the allowed photochemical interconversion of butadiene and cyclobutene.

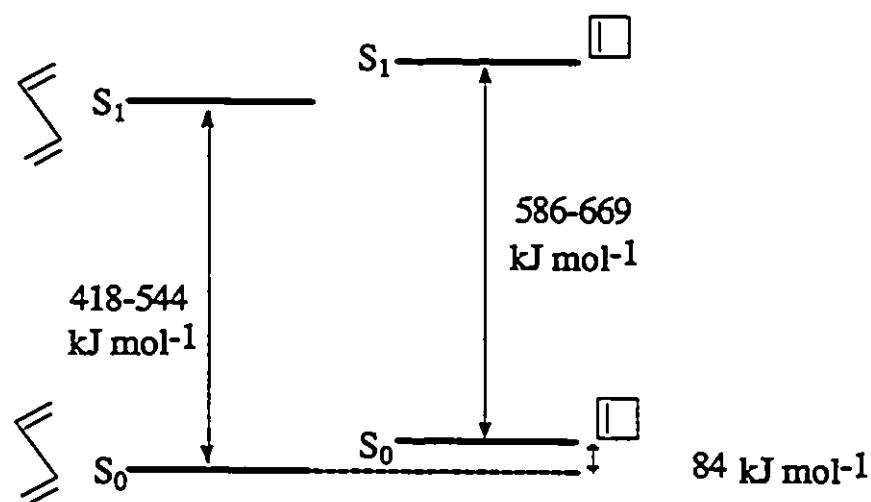


Figure 1.1.2. Relative  $S_0$  (ground state) and  $S_1$  (first singlet excited state) energies of 1,3-butadiene and cyclobutene

Van der Lugt and Oosterhoff undertook a series of quantum chemical calculations on the valence isomerization of 1,3-butadiene to cyclobutene<sup>14</sup>, with a large number of intermediate configurations, thus enabling them to establish the potential surfaces, a requisite to the discussion of the actual course of the reaction.

They found that for the thermal reaction, the *disrotatory* process of ring closure was utterly unfavorable (the energy steadily increased from -9.11 to -4.77 eV on the reaction path, which would demand an activation energy of *ca.* 418 KJ mol<sup>-1</sup>). In the *conrotatory* process, however, a much lower activation energy was found. This process is clearly depicted on the left hand side of Figure 1.1.3.

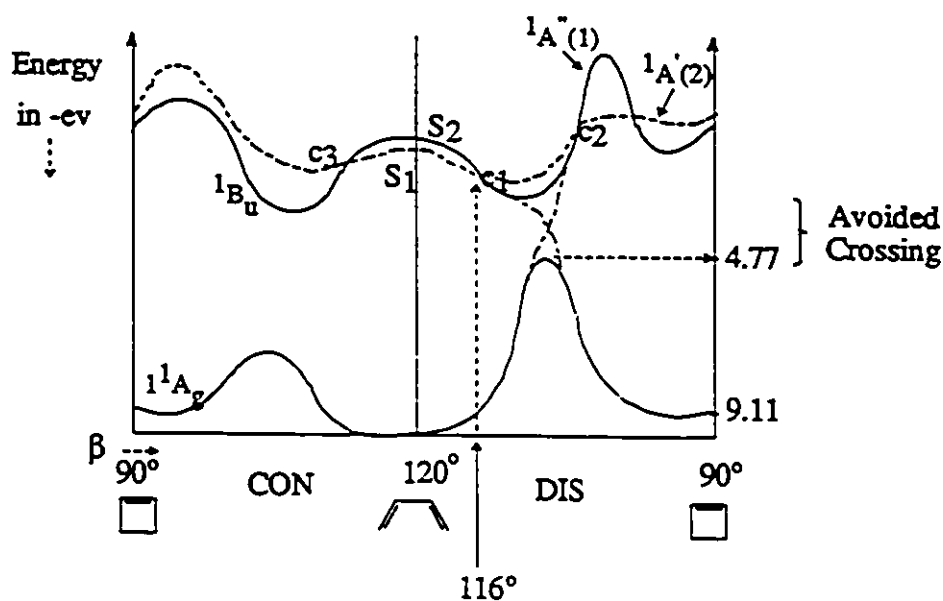


Figure 1.1.3. Potential energy curves for the disrotatory and conrotatory modes in the 1,3-butadiene / cyclobutene system. The  $C_3$  symmetry is preserved in the disrotatory mode and the  $C_2$  symmetry is preserved in the conrotatory process. Full line: The lowest singlet  $S_0$  and  $S_2$  states (or  $1^1A_g$  and  $2^1A_g$ ). Dashed lines: the lowest singlet state  $S_1$  or  $1^1B_u$  state.

When *s-cis*-1,3-butadiene is irradiated with ultraviolet light, the molecule is excited into the symmetric excited state  $S_1$  (Figure 1.1.1b). At the early stage of the cyclization process, when  $\beta \cong 116^\circ$  (angle between carbons  $C_1-C_2-C_3-C_4$  in 1,3-butadiene) in the *disrotatory* direction butadiene changes its electronic state from the symmetric  ${}^1A'(2)$  state to the antisymmetric  ${}^1A''(1)$  state through the symmetry-allowed  $c_1$  crossing (nuclear vibrations cause a molecule in *A* to pass adiabatically into *S*). In this way, the molecular electronic state  ${}^1A'(2)$  is converted into  ${}^1A''(1)$ , in which a *disrotatory* deformation can ensue. As a result, the molecule is captured in the energy well, from where it is assumed to reach the lower potential surface of the ground state. On reaching the electronic ground state, the molecule is in a nuclear configuration corresponding to the *disrotatory* transition state between butadiene and cyclobutene. The reaction can now proceed in one of two directions: either cyclobutene is formed or butadiene is regenerated. Conversely, in the *conrotatory* mode of photochemical ring closure, the energy gap between the  ${}^1B_u$  and  ${}^1A_g$  potential energy surfaces is much greater than that found in the *disrotatory* direction. The observation that the photochemical ring closure of 1,3-dienes proceeds by a stereospecific *disrotatory* mode is in agreement with the qualitative features of the potential energy diagrams depicted in Figure 1.1.3.

In the photochemical ring opening of cyclobutene to 1,3-butadiene, the energy barrier to the antisymmetric state is predicted to play a significant role for the stereospecificity. As was discussed above, there is a high energy barrier on the  ${}^1B(1)$  state for the *conrotatory* ring opening process of cyclobutene, while such a barrier is not found on the  ${}^1A''(1)$  state for the *disrotatory* mode.



The mechanism for decay to the ground state potential energy surface was suspected to be related to radiationless processes in molecules<sup>14, 15</sup> (participating collisions with other molecules were invoked as a way of return to the electronic ground state), but no information concerning the rapidity of this process was available until the mid 1980's<sup>16</sup>. The radiationless decay from the excited state to the ground state potential energy surface occurs, according to the general theoretical interpretation<sup>14</sup>, from the so-called *avoided crossing minimum* that occurs on the excited state potential energy surface (Figure 1.1.3). The rate of decay was proposed to be determined mainly by the energy gap between the ground and excited state potential energy surfaces at this point<sup>17,19-21</sup>. The decay probabilities computed by Morihashi et al<sup>18</sup> are  $10^{-4}$  and  $10^{-16}$  for *disrotatory* and *conrotatory* ring closure, respectively. They attribute the stereospecificity of the photochemical ring closure reaction to this difference.

## 1.2 Dynamics of Photochemical Ring Opening Reactions

Only recently have the dynamics and kinetics of photochemical electrocyclic ring opening reactions been explored<sup>22 - 24</sup>.

Mathies and coworkers<sup>22</sup> gave a very clear picture of photoproduct formation and vibrational relaxation dynamics in the electrocyclic photochemical ring opening of 1,3-cyclohexadiene (Figure 1.2.1). Within the first *ca.* 10 fs after excitation, 1,3-cyclohexadiene propagates along the predicted *conrotatory* reaction coordinate and undergoes rapid, nonradiative decay to the lower energy  $2A_1$ <sup>25</sup>. The *all-cis*-1,3,5-hexatriene photoproduct is then produced in upper vibrational levels of the ground state ( $^1A_1$ ) within 6 picoseconds. Although the barrier to single and double bond

isomerizations on the  $2A_1$  surface are relatively small for linear polyenes<sup>26</sup>, the initial formation of *all-cis*-ground state 1,3,5-hexatriene demonstrates that neither process is involved in internal conversion from the  $2A_1$  state. Once the ground state is populated, vibrational cooling occurs in *ca.* 9 ps, in competition with the 7-ps conformational relaxation of *all-cis*-1,3,5-hexatriene to mono-*s-cis*-1,3,5-hexatriene.

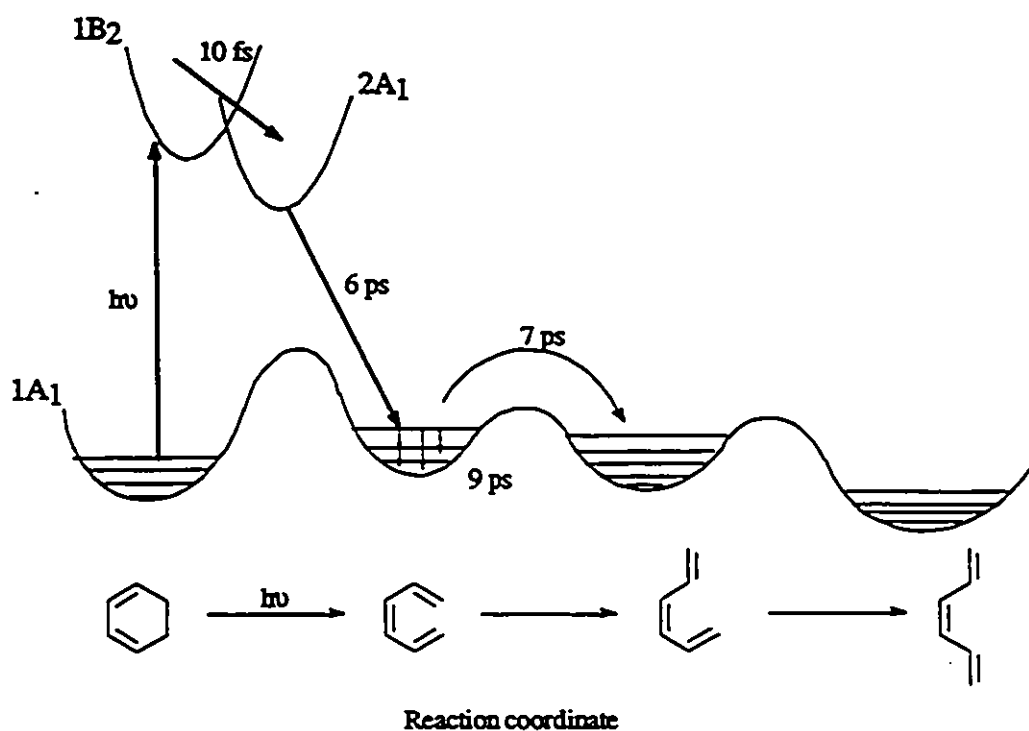


Figure 1.2.1. Schematic reaction coordinate for the photochemical ring opening of 1,3-cyclohexadiene.

Recent results on the photochemical ring opening dynamics of *cyclobutene* itself<sup>27</sup> obtained by Laser Resonance Raman Intensities, indicate that the initial photochemical

motions are directed along the Woodward-Hoffmann-predicted *disrotatory* ring opening reaction coordinates (see Figure 1.2.2). Upon excitation, an increase in the equilibrium bond distance of the methylene groups is observed (the CH<sub>2</sub>-CH<sub>2</sub> bond breaks, as the ring opening proceeds). A resonance mode directly related to the disrotatory twist of the CH<sub>2</sub> groups is also observed. It was noticeable from close inspection of the Resonance Raman spectrum, that the initial dynamics of the ring opening reaction of cyclobutene involve a torsion about the C=C bond (the CH<sub>2</sub> groups in the *s-cis* diene product are expected to assume a gauche conformation and a torsion would be necessary to bring the planar cyclobutene ring to this geometry). In conclusion, after excitation, planar cyclobutene evolves immediately along the *orbital symmetry-predicted* reaction coordinate.

The preceding examples afford strong indications that there exists a high degree of concertedness along the reaction coordinates for these electrocyclic reactions as suggested by the early works of Woodward and Hoffmann (*vide supra*).

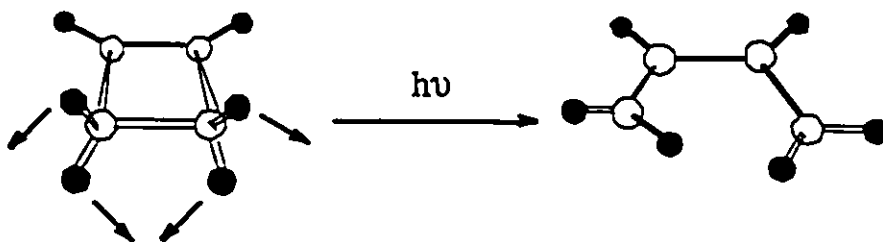
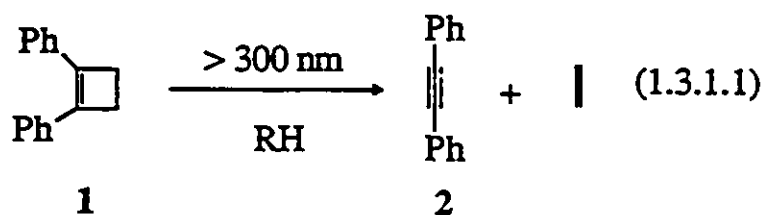


Figure 1.2.2. The arrows superimposed on the ground state structure of cyclobutene give the geometry changes that occur within 30 fs after excitation as a result of evolution along the indicated CH<sub>2</sub>-CH<sub>2</sub> stretch and CH<sub>2</sub> twist normal modes

### 1.3 Photochemistry of Cyclobutenes

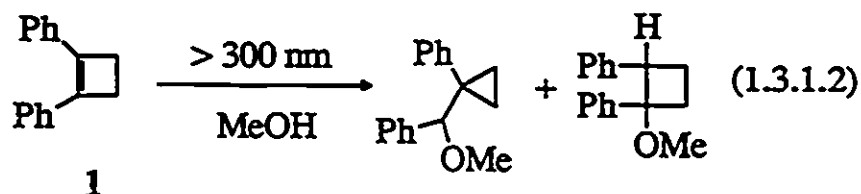
#### 1.3.1 1-Aryl-substituted Cyclobutenes:

Classically, cyclobutenes have been studied in the readily accessible regions (wavelengths  $\geq 254$  nm) by substitution with chromophores at the double bond. These chromophores interact conjugatively with the double bond, thereby lowering the energy of the excited state and drastically altering its electronic character, resulting in a complete modification in the spectroscopic and photochemical behavior of the chromophore. A notable case is the photochemistry of 1,2-diphenylcyclobutene <sup>128 - 30</sup>. De Boer and Schlessinger<sup>28</sup> reported that the singlet excited state of **1** is very efficiently deactivated by fluorescence ( $\phi_f = 1$ ). In this work, the authors only observed dimers as products. This system was reexamined by Kaupp and coworkers<sup>29</sup> who reported the fluorescence quantum yield to be *ca.* 0.9 (equation 1.3.1.1) and observed the formation of 1,2-diphenylacetylene **2** and ethylene in low quantum yield ( $\phi = 0.001$ ).

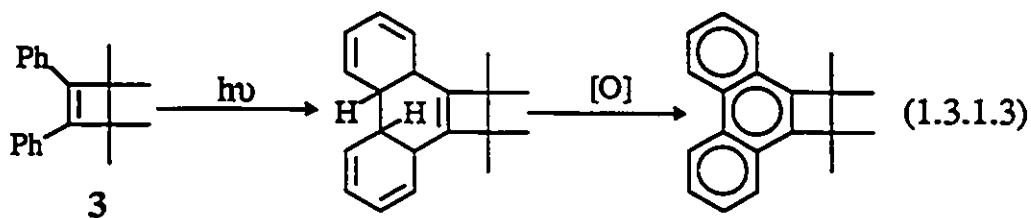


Irradiation of **1** with 300 nm light in nucleophilic solvents such as methanol or acetic acid leads to the formation of solvent addition products as shown in equation 1.3.1.2. The photochemical ionic addition to **1** is thought to proceed via protonation of the first singlet

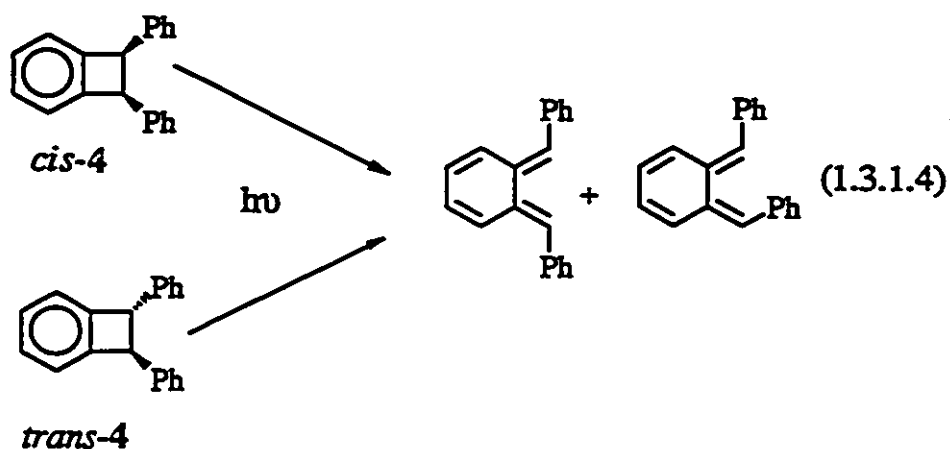
excited state of the cyclobutene, yielding a cyclobutyl cation intermediate that can rearrange to a cyclopropyl cation.



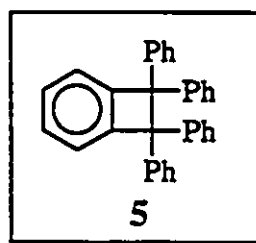
In contrast to the behaviour of 1, 1,2-diphenyl-3,3,4,4-tetramethylcyclobutene 3 cyclizes inefficiently to yield a cyclobutaphenanthrene derivative in solution (equation 1.3.1.3)<sup>31</sup>.



Photochemical ring opening can be promoted by the introduction of ring strain, as in the case of benzocyclobutene derivatives<sup>32 - 35</sup>. Low temperature studies have provided evidence that suggests that the photochemical ring opening of *cis*- and *trans*-diphenylbenzocyclobutene 4 occurs *nonstereospecifically* (equation 1.3.1.4)<sup>35</sup>. The thermal ring opening of these compounds has been shown to obey orbital symmetry selection rules<sup>32</sup>.

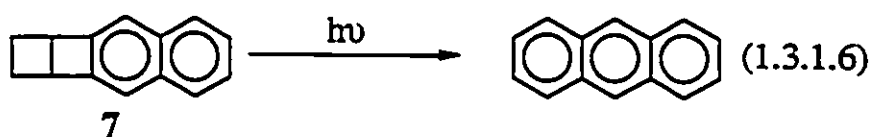
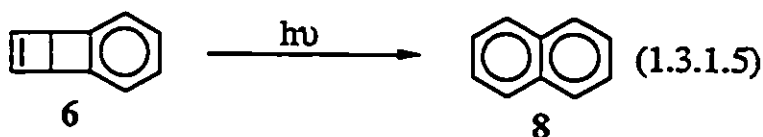


The ring opening of 4 has been shown to proceed from both the singlet and triplet excited states. The nonstereoselective nature of the ring opening reaction has been explained as being due to the involvement of upper triplet excited states. Triplet reactivity has also been shown to play a role in the ring opening of the tetrasubstituted cyclobutene 5.

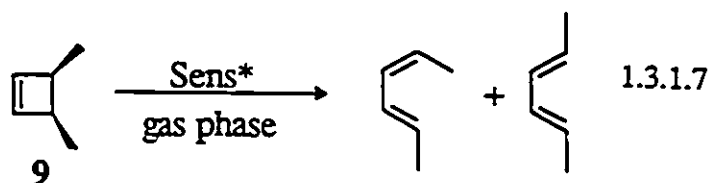


Photoexcited 1,4-dewarnaphthalene<sup>36</sup> and anthracene<sup>37</sup> (6 and 7, respectively) undergo ring opening with high efficiency (see equations 1.3.1.5 and 1.3.1.6). The ring opening process occurs adiabatically in both the singlet and triplet manifolds, as evidenced

by the characteristic naphthalene and anthracene excited state emissions that result from excitation of their dewar isomers. The phenyl substituents in these cases change the electronic character of the singlet excited states. Singlet excited states, which do not normally intersystem cross to the triplet manifolds in alkylsubstituted cyclobutenes, are perturbed by the phenyl substituents to such an extent in the examples depicted, that reaction entirely within the singlet manifold appears impossible.



Triplet reactivity in alkylcyclobutenes has been explored and found not only to be possible, but quite complex as well<sup>38, 39</sup>. Srinivasan<sup>39</sup> investigated the mercury sensitized photolysis of *cis*-3,4-dimethylcyclobutene (*cis*-9), in the gas phase and observed *nonstereospecific* ring opening. The formation of the symmetry forbidden *cis*, *trans*-2,4-hexadiene was postulated to arise from a vibrationally hot ground state of *cis*-9 (equation 1.3.1.7).

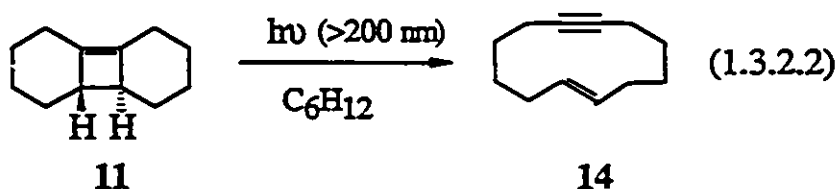
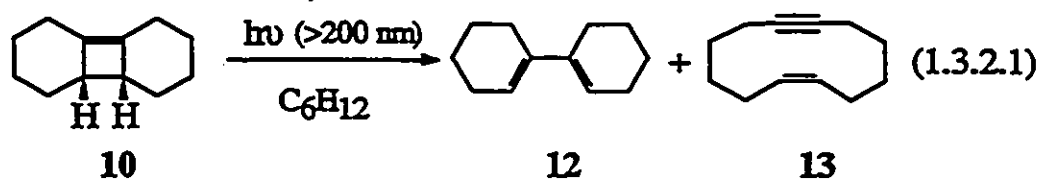


### 1.3.2 The Photochemical Ring Opening of Alkylsubstituted Cyclobutenes:

According to the State Correlation diagram shown in Figure 1.1.3, the electrocyclic ring opening of simple cyclobutenes initiated by light should proceed in a *disrotatory* fashion.

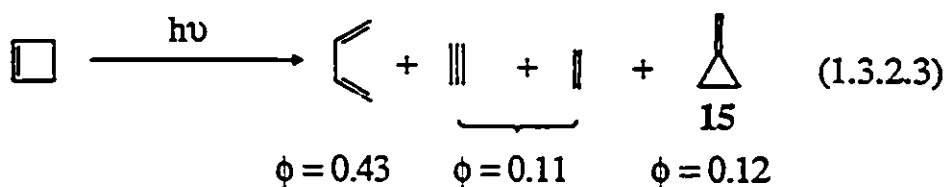
There are few reported examples in the early literature that illustrate the photochemical ring opening of alkylsubstituted cyclobutenes. The reason for this is mainly a practical one, related to the fact that these compounds absorb only in the far-UV region of the spectrum ( $\leq 230$  nm). Until 1987, there was only one report that offered stereochemical information on the photochemical electrocyclic ring opening of cyclobutene<sup>40</sup>. Saltiel and Lim reported the photochemistry of the tricyclic cyclobutene derivatives **10** and **11** (equations 1.3.2.1 and 1.3.2.2), providing results which strongly suggest that the photochemical ring opening does indeed proceed by the symmetry-allowed *disrotatory* pathway. The authors argued that disrotatory opening of **11** would yield the highly strained *cis,trans*-1,1'-bicyclohexenyl **12**, and that the failure of **11** to yield the stable *cis,cis* isomer indicated that *conrotatory* photochemical ring opening did not occur to any significant extent. Other photoproducts of the reaction consisted of **13** and **14**, which are known as "cycloreversion or fragmentation products".





For many years, the results of this study have provided the prototypical examples that illustrate the stereochemistry associated with two seminal photochemical pericyclic reactions: the electrocyclic ring opening of cyclobutene and the  $[\sigma_{2s} + \sigma_{2s}]$  cycloreversion reaction of four-membered cyclic hydrocarbons.

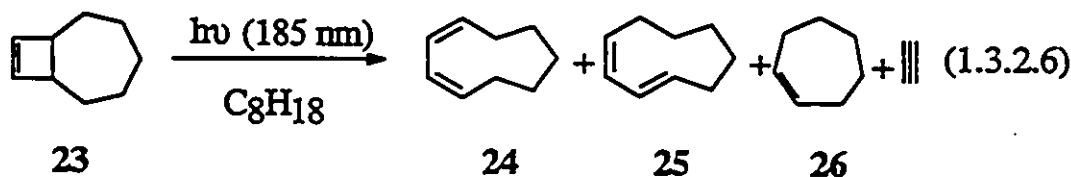
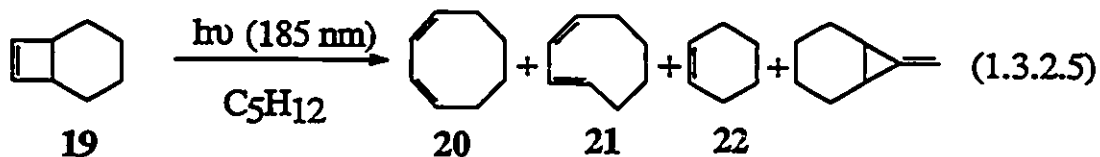
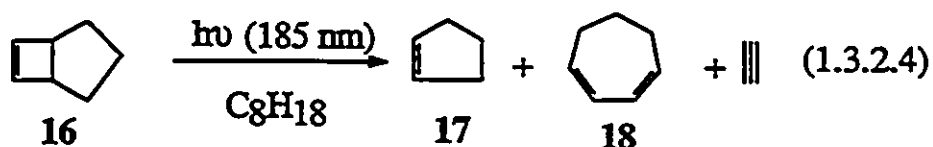
The solution phase photochemistry of cyclobutene itself was reported by Adam and coworkers<sup>41</sup> (equation 1.3.2.3).



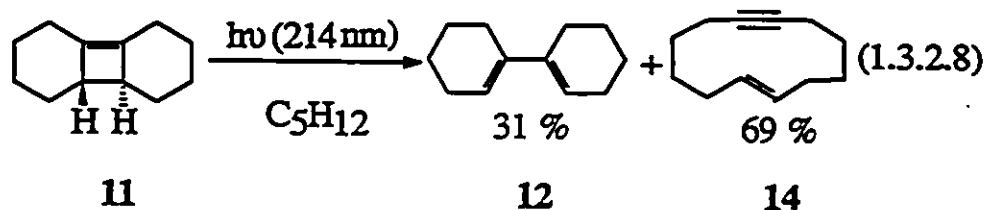
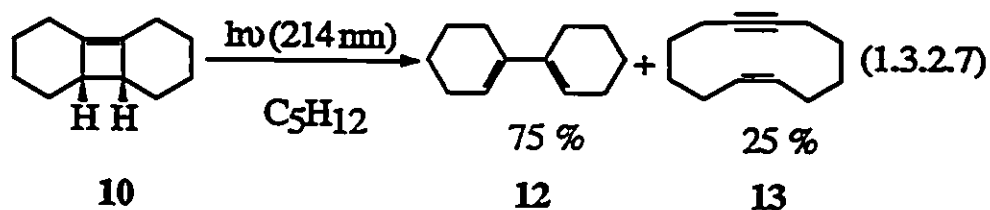
In addition to ring opening and molecular fragmentation products, measurable yields of methylenecyclopropane (15) were observed. 1,3-Butadiene was thought to arise from electrocyclic ring opening from the  $\pi, \pi^*$  excited state. The remaining photoproducts were rationalized in terms of the intermediacy of carbenes formed by [1,2]alkyl and hydrogen shifts after  $\pi, R(3s)$  excitation. These carbenes were suggested to be cyclopropylmethyl

carbene and cyclobutylidene, precursors to the minor primary photoproducts acetylene, ethylene and methylenecyclopropane 15.

Further investigations on the photochemistry of three simple cyclobutene derivatives in solution was conducted by Leigh and coworkers<sup>42 - 44</sup>. They found that apart from the competitive fragmentation and ring opening reactions, the electrocyclic ring opening formally proceeds *nonstereospecifically*, yielding mixtures of 1,3 - diene geometric isomers in each case (see equations 1.3.2.4 - 6).



The photochemistry of the tricyclic hydrocarbons 10 and 11 was reinvestigated<sup>43</sup>. The direct photolysis produced mixtures of two major products in each case: diene 12 and the enynes 13 or 14.



Both isomers (**10** and **11**), undergo photochemical ring opening upon direct photolysis in solution. The tentative detection of **10** from the photolysis of the *trans* isomer and an estimate of its relative yield indicated that the highly strained *cis,trans* isomer of **12** may be formed directly, along with the *cis,cis* isomer, in the case of **11**, see equations 1.3.2.7 and 1.3.2.8. These results verified that photochemical ring opening of simple alkylcyclobutene derivatives is *nonstereospecific*, in general.

In contrast to the nonstereospecificity associated with the ring opening reaction of alkylsubstituted cyclobutenes observed to this point, it is well established that the photofragmentation process is highly *stereospecific*<sup>42</sup>. The stereochemistry about the adjacent saturated carbons in the cyclobutene moiety is retained in the alkene fragment from the reaction. This is the expected result if fragmentation proceeds by concerted [ $\sigma 2s+\sigma 2s$ ] cycloreversion<sup>40</sup>, but there are alternative pathways that could lead to the same result<sup>41, 44, 45</sup>.

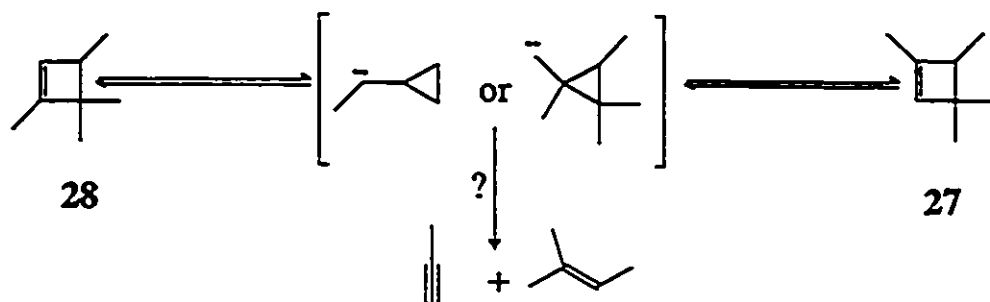
### 1.3.3 Excited States Responsible for the Ring Opening and Cycloreversion Reactions in Alkylsubstituted Cyclobutenes.

Spectroscopic results for alkylcyclobutenes, as well as simpler alkenes, indicate that at least three excited singlet states are accessible in the far UV region in the gas phase and in solution<sup>46 - 49</sup>. These are the  $\pi,\pi^*$  and the  $\sigma,\pi^*$  valence states and the  $\pi,R(3s)$  Rydberg state. The Rydberg transitions may be substantially mixed with valence transitions (such as the  $\sigma,\pi^*$ ), particularly in solution. In principle, either the valence or the Rydberg-like transitions could be involved in the photochemistry of simple cyclobutenes, though via very different mechanisms.

It is known that alkyl substitution lowers the gas-phase energy of the  $\pi,R(3s)$  state in simple alkenes while having only marginal effects on the energy of the valence state (gas phase absorption spectra reveal that the 0,0 band of the  $\pi,R(3s)$  absorption moves more rapidly to the red than that of the  $\pi,\pi^*$  band with increasing numbers of alkyl substituents on ethylene<sup>47</sup>). This can be explained by considering that excitation to the Rydberg state involves promotion of a valence  $\pi$ -electron to a spatially diffuse  $3s$  orbital. Thus the electronic character of alkene Rydberg states bears some resemblance to a radical cation. Consequently, the substituent effect on alkene Rydberg state energies parallels that on the  $\pi$ -ionization potential ( $\pi$ -IP). Cyclobutene radical cations are known to undergo thermal ring opening in the gas phase<sup>50 - 52</sup>. Furthermore, a recent report<sup>53</sup> indicates that photolysis of cyclobutene radical cation in cryogenic media leads to *s-trans*-1,3-butadiene radical cation and that *s-cis*-1,3-butadiene radical cation does not occur as an intermediate; consequently, the photochemical ring opening of cyclobutene radical cation does not proceed in a concerted electrocyclic fashion. It is then possible that involvement of the  $\pi,R(3s)$  state in the photochemical ring opening of alkylcyclobutenes could account



least one common intermediate in the direct photolysis of these compounds. Whether or not cyclopropyl carbenes are involved in the cycloreversion reaction is not clear. The cycloreversion products are formed in substantially higher yield than rearrangement products. This is opposite to the known behavior of these species, which usually yield cyclobutenes as the major products upon thermal or photochemical generation from diazo precursors<sup>55</sup>.

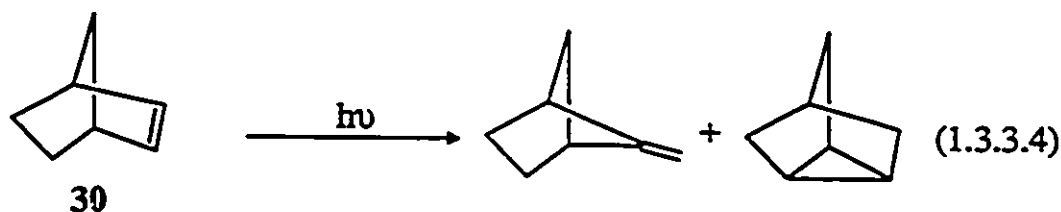
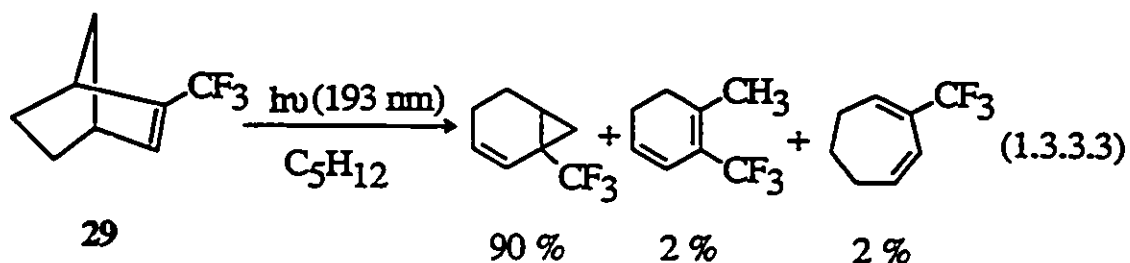


Scheme 1.3.3.1. Possible mechanistic pathway for the cycloreversion process in alkylsubstituted cyclobutenes

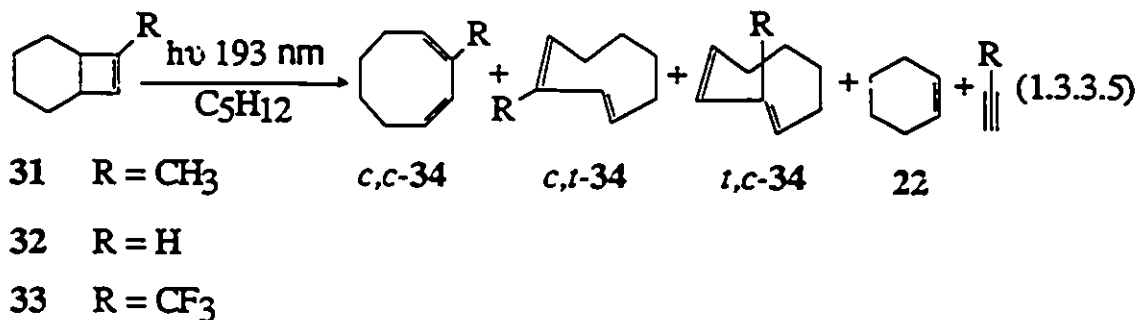
While spectroscopic studies show that increasing alkyl substitution has the same effect on the relative ordering of the valence and Rydberg excited states of cyclobutenes in the gas phase as is found with simpler alkenes, the product distributions from the photolysis of a series of methyl-substituted monocyclic cyclobutenes derivatives in solution showed<sup>42, 63, 83</sup> no consistent variations that would help to define how the various excited states that can be populated in solution contribute to the different products observed.

It has been shown that trifluoromethyl substitution (at the C=C bond) has the effect of raising the gas-phase Rydberg state energies in alkenes such as norbornene, without altering the energy or localized character of the alkene  $\pi, \pi^*$  state<sup>58, 59</sup>. This substituent effect on the gas-phase excited state manifold is manifested in the solution phase

photochemistry of the alkene. The photochemistry of 2-(trifluoromethyl)norbornene (29 in equation 1.3.3.3) is much different than that observed for norbornene (30 in equation 1.3.3.4)<sup>58</sup> and has been assigned to exclusive reaction from the  $\pi,\pi^*$  singlet state exclusively.



Leigh and coworkers<sup>60</sup> undertook a study of the spectroscopy and photochemistry of three simple *cis*-fused bicyclic cyclobutene derivatives (31-33), which bear substituents chosen so as to alter systematically the ordering and separation of the  $\pi,\pi^*$  and Rydberg states in the parent compound. The photolyses of these compounds is depicted in equation 1.3.3.5.



As it is illustrated in Figure 1.3.3.1 the gas phase UV absorption spectra of 31-33 each show a prominent, relatively intense band with an apparent maximum at 185 nm. The remaining features of the gas phase spectra vary dramatically with substituent. The spectrum of 32 shows a weak shoulder absorption at 195 nm, which is shifted to 210 nm in that of 31. This absorption is not present in the spectrum of 33, but believed to be located at wavelengths shorter than 187 nm. The variation of the position of this band throughout the series of compounds parallels the variation in the lowest vertical  $\pi$ -IP from the photoelectron spectra of 31-33 (see Table 1.3.3.1). This behavior led to the assignment of those bands as deriving from  $\pi, R(3s)$  transitions. The results summarized in Table 1.3.3.2 indicate that the photochemistry of 31-33 also shows consistent trends with substitution at the double bond.

**Table 1.3.3.1.** Gas-phase spectroscopic properties of substituted bicyclo[4.2.0]oct-7-enes 31-33

compound	$\pi$ IP <sup>a</sup> , eV	$E_{\pi, R(3s)}$ <sup>b</sup> , eV	$E_{\pi, \pi}$ , eV
		( $\tau$ , eV) <sup>c</sup>	( $\tau$ , eV) <sup>c</sup>
31	$8.5 \pm 0.1$	5.91 (2.6)	6.40 (2.1)
32	$9.0 \pm 0.1$	6.37 (2.6)	$\geq 6.70$
33	$9.7 \pm 0.2$	$> 6.7$ (3.0)	$\geq 6.62$ ( $\leq 3.1$ )

a Lowest vertical ionization potential (IP) from photoelectron spectrum.

b Absorption maximum in gas phase UV.

c Term value.



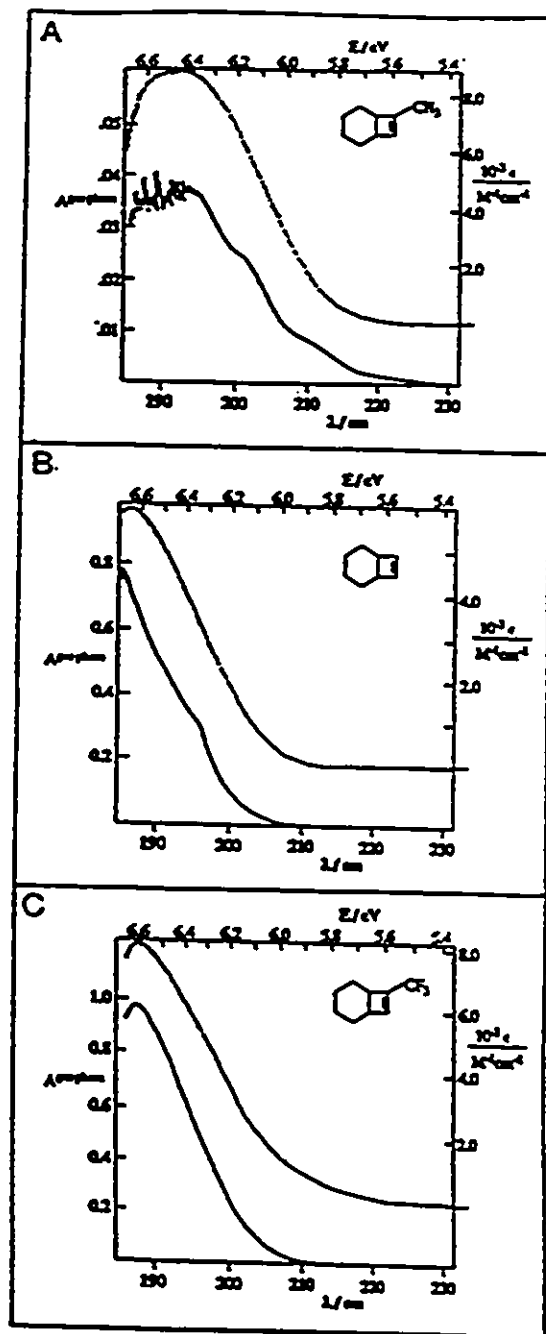


Figure 1.3.3.1. UV Absorption spectra of 31 - 33 in the gas phase (—) and in deoxygenated pentane solution (---)

First it is observed that the quantum yields of isomeric dienes from photochemical ring opening of 31-33 increase systematically throughout the series, while the characteristics of the process with respect to the distribution of isomeric dienes obtained is almost constant.

Table 1.3.3.2. Product quantum yields from photolyses (193 nm) of deoxygenated pentane solutions of 31-33 at 22° C

cyclobutene	$\phi_{c.c-12}$	$\phi_{(c.t + t.c)-12}$	$\phi_{\text{cyclohexene}}$
31	0.049	0.038	0.13
32	0.100	0.075	0.14
33	0.186	0.106	0.030

This is consistent with this aspect of photoreactivity being derived exclusively from the excitation to the  $\pi,\pi^*$  singlet state. From this study it was inferred that the nonstereospecificity associated with the photochemical ring opening of alkylsubstituted cyclobutenes cannot be attributed to some component of the reaction that arises from Rydberg state excitation.

The fragmentation process depicted in equation 1.3.3.5 and summarized in Table 1.3.3.2 also shows a pronounced trend in quantum yields as a function of substitution. The quantum yield for cycloreversion is decreased substantially in 33 compared to those in 31 and 32, suggesting that the formal cycloreversion reaction is derived mainly from the Rydberg-like excited state.

#### 1.4 Mechanistic Interpretations for the Observed Nonstereospecific Photochemical Ring Opening of Alkylsubstituted Cyclobutenes.

Several mechanistic possibilities have been suggested to explain the apparent nonstereospecificity of the photochemical ring opening<sup>61 - 63</sup>; (a) the electronically excited reactant molecule may pass directly to the electronically excited state of the product, followed by *cis,trans* isomerization, *adiabatic mechanism*; (b) the process occurs via non-concerted pathways involving intermediates which decay to a distribution of isomeric dienes; (c) the electronically excited reactant molecule crosses directly to a vibrationally excited or "hot" ground state of the reactant which then undergoes a thermal reaction to give ground state products; or (d) reactive excited state decay occurs at a *conical intersection* of the ground and excited state surfaces, which effectively mixes diene excited state decay modes (*i.e. cis,trans* isomerization) with those of cyclobutene.

##### (a) Adiabatic Mechanism.

The overall nonstereospecificity observed in the ring opening reaction of alkylcyclobutenes could be explained on the grounds of an adiabatic ring opening process. Precedent for an adiabatic photochemical ring opening of a cyclobutene exists in the literature. Yang and Michl<sup>35, 36</sup> demonstrated that in condensed media, excited 1,4-dewamaphthalene **6**, converts efficiently to excited naphthalene **8** in both the singlet and triplet manifolds (equation 1.3.1.5). The state correlation diagram for the conversion of **6** to **8** is depicted in Figure 1.4.1. In this figure, the solid lines represent the *adiabatic* reaction pathway, while the dotted lines represent the avoided crossing of the ground and

excited state potential energy surfaces that would be followed by a *nonadiabatic* mechanism.

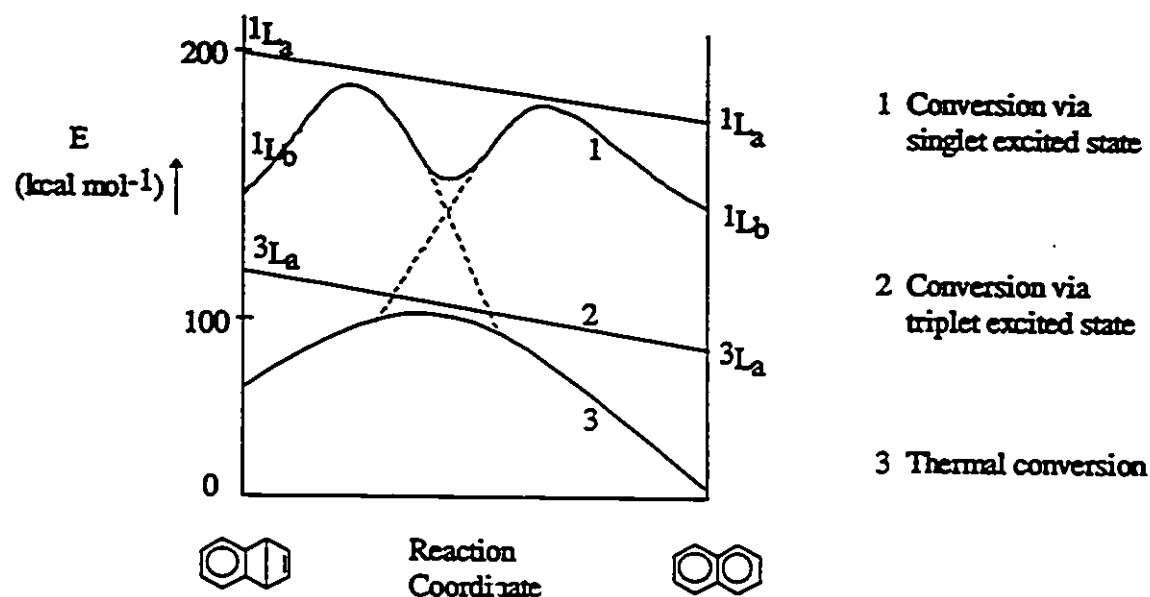
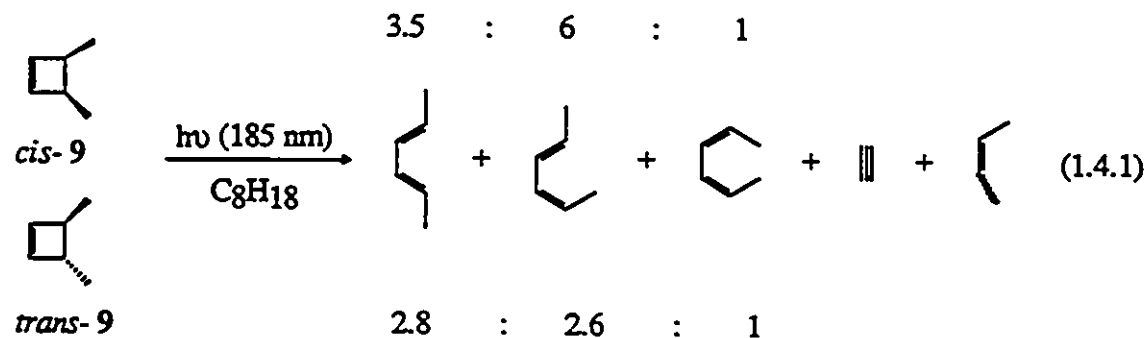
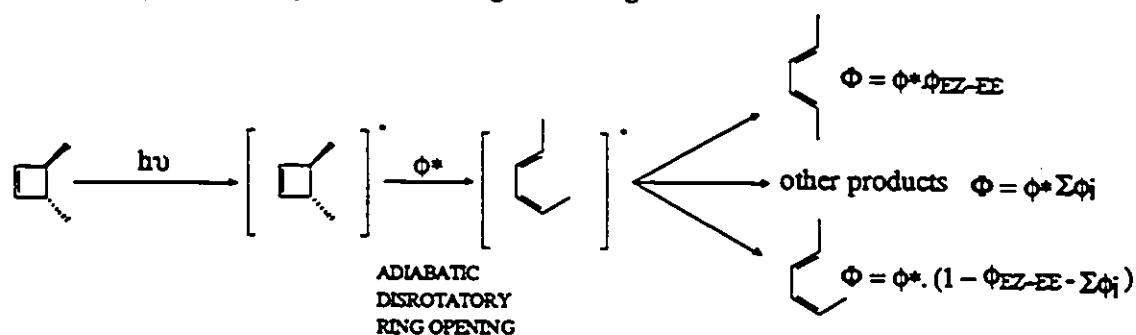


Figure 1.4.1. State correlation diagram for the interconversion of dewarnaphthalene to naphthalene

The direct photolysis of *cis*- and *trans*-3,4-dimethylcyclobutene, 9, affords all three of the possible isomers of 2,4-hexadiene in each case, but in different relative amounts (equation 1.4.1)<sup>64</sup>.



In both cases, the diene mixture obtained was weighted toward the formally forbidden *conrotatory* ring opening pathway. A simple calculation of the "expected" relative yields of the isomeric 2,4-hexadienes, using the quantum yields for their *cis,trans* photoisomerization<sup>64</sup> and the assumption that ring opening occurred exclusively by the adiabatic, *disrotatory* pathway, yields ratios which are not in agreement with the ratios obtained from photolysis of *cis* and *trans*-3,4-dimethylcyclobutene. It was noted that this discrepancy could be attributed to the fact that cyclobutene ring opening could be expected to yield the diene initially in an *s-cis* conformation, while the direct diene photoisomerization quantum yields report on the behavior of the *s-trans* diene conformers<sup>65, 66</sup>. The excited state decay characteristics of *s-cis* and *s-trans* dienes are known to differ considerably<sup>42</sup>. A conjectural adiabatic mechanism for photochemical ring opening of *trans*-cyclobutene 9 is given in Figure 1.4.2.



$$\text{Predicted (E,E/E,Z)} = \frac{\phi_{EZ-EE}}{(1 - \phi_{EZ-EE} - \sum\phi_i)}$$

Figure 1.4.2. Reaction pathway for the adiabatic disrotatory ring opening of 9.  $\phi^*$  Denotes the quantum yield for production of excited *s-cis*-E,Z-2,4-hexadiene.  $\phi_{EZ-EE}$  Denotes the quantum yield for isomerization of E,Z-2,4-hexadiene to the E,E isomer.  $\sum\phi_i$  Denotes the quantum yields for other processes observed

Figure 1.4.3 shows the state correlation diagram for the ring opening of cyclobutene (solid lines). In this mechanism, the cyclobutene is excited into its lowest singlet excited manifold  $S_1$ , from which crossing to the  $S_2$  surface occurs and the excited state pericyclic minimum is reached. Complete traversal to the excited diene could occur (in competition with decay at the pericyclic minimum) if further motion on the excited state surface is not subject to a substantial energy barrier. Recent *ab-initio* calculations by Morihashi and Kukuchi<sup>18</sup> suggest that this may be the case. Thus, the orbital symmetry allowed excited diene that is formed by disrotatory ring opening relaxes to ground state diene by *cis,trans* isomerization or returns to ground state diene precursor.

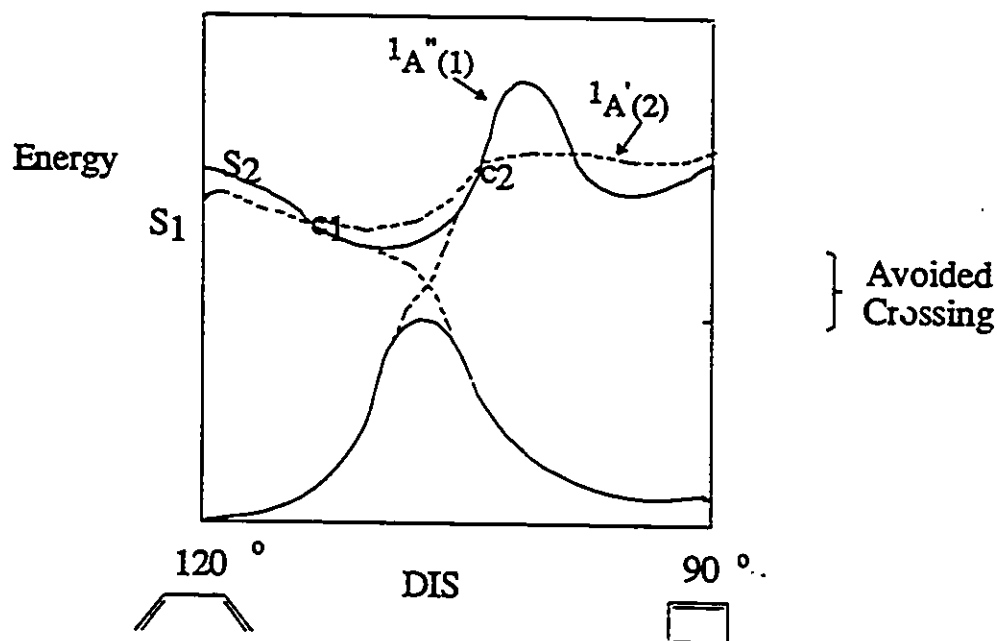
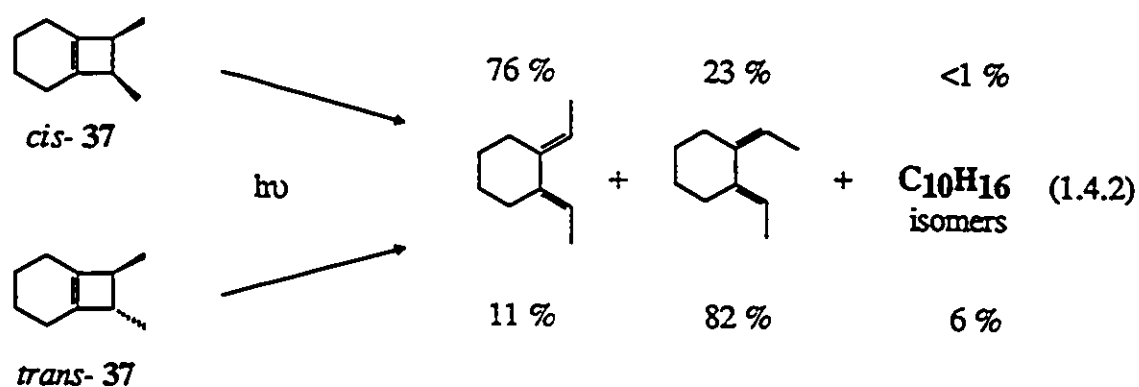


Figure 1.4.3. State correlation diagram for the Butadiene/Cyclobutene interconversion. Solid lines: Adiabatic pathway. Dashed line: Non-adiabatic pathway

In 1992, Leigh and coworkers<sup>67</sup> investigated the photochemistry of two cyclobutenes, *cis*- and *trans*-**37** and the isomeric constrained *s-cis* 1,3-dienes, in an attempt to test the hypothesis of *adiabaticity* in cyclobutene ring opening. Irradiation of *cis*- and *trans*-**37** produced a mixture of dienes according to equation 1.4.2. Table 1.4.1 illustrates the expected (that would be formed if ring opening of **37** proceeded by a disrotatory adiabatic pathway) and observed diene ratios for cyclobutene ring opening. The results revealed that for *cis*-**37**, there is reasonable agreement between the calculated and observed diene ratios, while for *trans*-**37**, the discrepancy between those values is significant. At this point, to discern the presence of an operative *adiabatic* mechanism, or to support the hypothesis of *nonadiabaticity* was judged premature. An operating *adiabatic* mechanism could not be confirmed or ruled out without further recourse to experiments. However, the surprising aspect of this photochemical reaction was the high degree of *disrotatory* stereoselectivity observed. The *cis*- isomer of **37** afforded more than 75 % of the formally allowed *E,E*- diene isomer, whereas *trans*- **37** yielded more than 80 % of the symmetry allowed *E,Z*- diene isomer.



**Table 1.4.1.** Calculated and observed diene ratios from photolysis of *cis*- and *trans*-37

	<i>cis</i> -37 (E,E/E,Z)	<i>trans</i> -37 (E,Z/E,E)
<i>calculated</i>	2.4	2.4
<i>observed</i>	3.3	7.5

**(b) Excited State Ring Opening Proceeds by a Biradicaloid Mechanism**

Photolysis of *cis* and *trans* 23<sup>83</sup> afforded mixtures of the products shown in equation 1.3.2.6. The diene distribution derived from their photochemical ring opening reactions is summarized in Table 1.4.2.

**Table 1.4.2.** Product diene yields from 214 nm photolyses of deoxygenated pentane solutions of *cis*- and *trans*- bicyclo[5.2.0]non-8-ene 23.

<i>Cyclobutene</i>	24	25
<i>cis</i> -23	15	33
<i>trans</i> -23	14	50

On the basis of the similarity in the distributions of isomeric dienes obtained upon photolyses of *cis* and *trans*- 23<sup>83</sup>, it was proposed that cyclobutene ring opening might proceed largely by a nonconcerted pathway involving biradical intermediates. Due to the



geometric constraints imposed by the cyclic structures of 23, ring opening of the two isomers would yield common biradical intermediates, or at least a set of biradicals that decay to a common distribution of products.

In a similar fashion, the corresponding biradicals that would be formed from ring opening of 10 and 11 (equations 1.3.2.7-8) are subject to even greater geometric constraints than those from *cis* and *trans*- 23, and it is expected that both compounds should yield the *cis* isomer 12 predominantly. The low estimated yield of *cis,trans*- 12 from photolysis of 11 is consistent with this expectation<sup>43</sup>.

However, results from Mathies and coworkers (Section 1.2), suggest that photochemical ring opening reactions proceed with a high degree of concertedness, and that the first motions are indeed directed along the predicted *disrotatory* reaction coordinates.

(c) Ring Opening from Vibrationally Excited Ground States.

Another mechanism that has been suggested to be able to account for the nonstereospecificity of cyclobutene ring opening attributes the formation of formally forbidden diene isomers to conrotatory reaction from upper vibrational levels of the ground state, which are populated by internal conversion in competition with disrotatory ring opening.

A distinction between a reaction involving an electronic excited state *versus* vibrational excited ground states is difficult to make. However, most photochemical reactions are carried out in solution where the excess energy of the photoexcitation is dissipated rapidly to the surroundings. Thus, it is reasonable to assume that the excited state system follows only low energy reaction paths on the surface.

#### (d) Internal Conversion by Conical Intersections

The presence of different reaction paths at the conical intersection point of a given reaction coordinate for cyclobutene ring opening provides a rationalization for the observation that cyclobutene ring opening is *nonstereospecific* in general. A detailed description of this process will be discussed in Section 1.6 of the present chapter, following a review of conjugated diene photochemistry.

### 1.5 The Photochemistry of Conjugated Dienes

The photochemistry of 1,3-dienes has been exhaustively studied<sup>36 - 37, 68 - 70, 125, 132</sup>. The excited singlet state deactivation pathways which are important in conjugated dienes are:

- (i) *cis,trans* isomerization
- (ii) *s-cis/s-trans* conformer interconversion
- (iii) cyclobutene formation (from *s-cis* dienes)
- (iv) bicyclo[1.1.0]butane formation (from *s-trans* dienes)
- (v) [1,5]-H migration (in appropriately substituted *s-cis* dienes)

In general, fluorescence and intersystem crossing are slow compared to reactive excited state deactivation processes (i.e. (i)-(v)). For instance, 1,3-butadiene and 1,3,5-hexatriene show no fluorescence. 1,3,5-Octatriene boasts a quite substantial quantum

yield of fluorescence, and this decreases as the chain length increases and, finally, there is again no fluorescence in the very long polyene limit, i.e., trans-polyacetylene<sup>19</sup>.

Theoretical studies<sup>21</sup> suggest that for conjugated polyenes as well as for 1-aryl-1,3-butadienes<sup>71</sup> there exist two low lying singlet excited states,  $1^1B_u$  and the  $2^1A_g$ , of very similar energies.

The large  $S_1 \rightarrow T_1$  energy gap and the rapid  $S_0 \leftarrow S_1$  radiationless decay of 1,3-dienes<sup>71</sup> (Section 1.2) both contribute in making the population of 1,3-diene triplets via intersystem crossing from  $S_1$  of negligible significance. The most direct information on the spectroscopy of short polyene triplet states comes from the electron impact spectra measured for 1,3-butadiene and 1,3,5-hexatriene<sup>72, 73</sup>. It is reasonably well established that the lowest triplet state of *trans*-1,3-butadiene is the  $^3B_u$  state. A second triplet has been assigned to  $^3A_g$ . High oxygen pressures have been used to enhance the  $S_0 \rightarrow T_1$  transitions of 1,3-dienes<sup>74</sup>. Since triplet states of conjugated dienes are readily obtained through energy transfer from triplet photosensitizers, it is the general belief that these are the reactive species which give rise to processes such as dimerization by reaction with ground state diene molecule. *cis,trans* Isomerization can also be effected by triplet sensitization<sup>75</sup>.

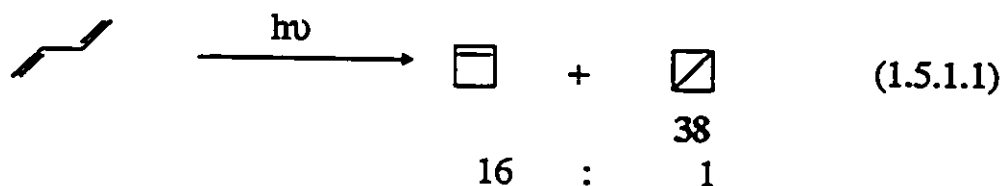
### 1.5.1 *cis,trans* Photoisomerization, *s-cis/s-trans* Interconversion, and Cyclobutene Formation.

The direct *cis,trans* isomerization of conjugated dienes is a process that has been studied in great detail<sup>75</sup>. Polyene isomers in general, differing by their conformation about an essential double bond, exist as distinguishable chemical species. The thermal and

photochemical interconversion of these isomers is of fundamental importance. It is the basic step in a large number of chemical and biological transformations. Because of its special role as the visual chromophore, retinal has received considerable attention<sup>76, 77, 78</sup>.

Aryl-substituted 1,3-dienes generally undergo *cis,trans* photoisomerization efficiently and show very weak fluorescence, but do not undergo cyclization to cyclobutene or bicyclobutanes. Under triplet state excitation conditions bicyclobutanes are not formed (see section 1.5.2) and there is only one known instance of sensitized cyclobutene formation<sup>9</sup>.

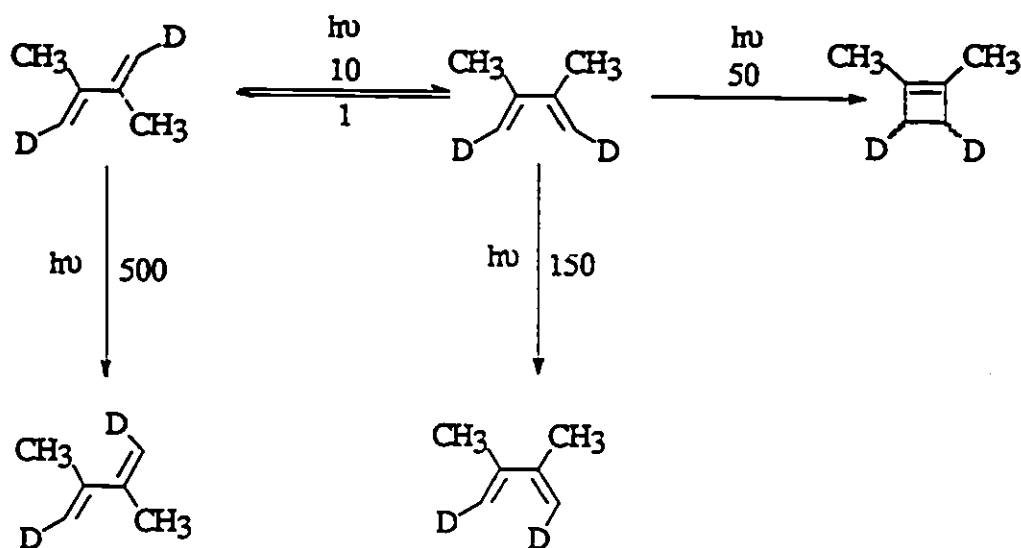
Direct irradiation of 1,3-butadiene in hydrocarbon solution yields cyclobutene and bicyclo[1.1.0]butane 38 (equation 1.5.1.1). Irradiation of the isolated *s-cis* and *s-trans* conformers in an argon matrix at 20 K results in the facile interconversion of the two species<sup>9</sup>.



Squillacote et al. showed for the first time in 1990 that the *s-cis* conformer of an acyclic 1,3-diene undergoes both electrocyclic closure and double bond isomerization<sup>79</sup>. It had been reported earlier that when *trans*-1,3-pentadiene (see Scheme 1.5.1.1) is photolyzed with 254 nm light a 1:2.8 ratio of closure to isomerization is observed, but upon irradiation at 229 nm no closure is apparent<sup>80</sup>. While these results were initially

interpreted to wavelength-dependent photochemistry, the above authors showed that the *s-cis* conformer of *trans*-1,3-pentadiene is the primary absorbing species at 254 nm. They also found that double bond isomerization and cyclobutene production are competitive processes even at 20 K.

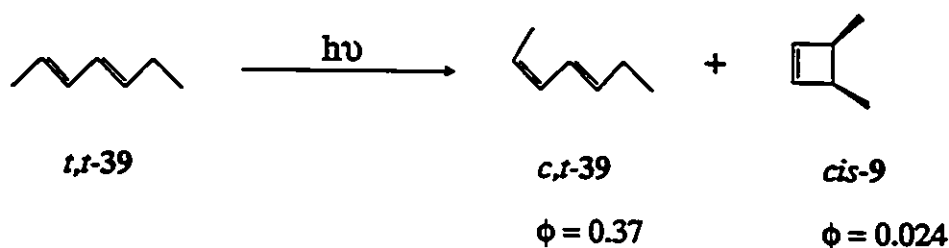
*cis,trans* Isomerization, which presumably partitions equally between starting material and product, occurs only about six times more efficiently than electrocyclic ring closure.



Scheme 1.5.1.1. Relative yields for the photoisomerization processes of 2,3-dimethyl-1,3-butadiene-1,4-d<sub>2</sub>

It then follows that ring closure is the second most efficient reaction from *s-cis*-1,3-diene singlet states (a 1:3 ratio of closure to isomerization is experimentally obtained for 2,3-dimethyl-1,3-butadiene-1,4 d<sub>2</sub> according to Scheme 1.5.1.1). In general, in acyclic dienes, cyclobutene formation occurs only when there is a significant population of *s-cis*

conformers present in solution<sup>74</sup>. Thus, in the case of  $\pi$ -2,4-hexadiene the geometric  $\pi \rightarrow ct$  photoisomerization (see Scheme 1.5.1.2) is accompanied by the formation of *cis*-3,4-dimethylcyclobutene **9** as a minor product, whereas irradiation of the  $tc$  and  $cc$ -2,4-hexadiene isomers under the same experimental conditions leads only to *cis,trans* isomerization. The quantum yields for these various processes are summarized in Table 1.5.1.

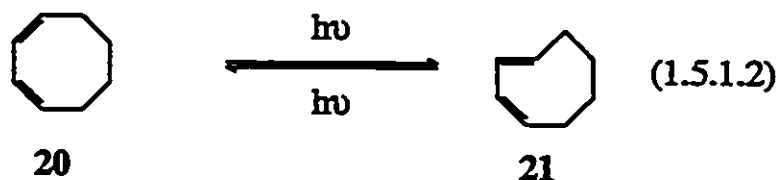


Scheme 1.5.1.2. *Cis,trans* isomerization and cyclobutene formation from *t,t*-39.

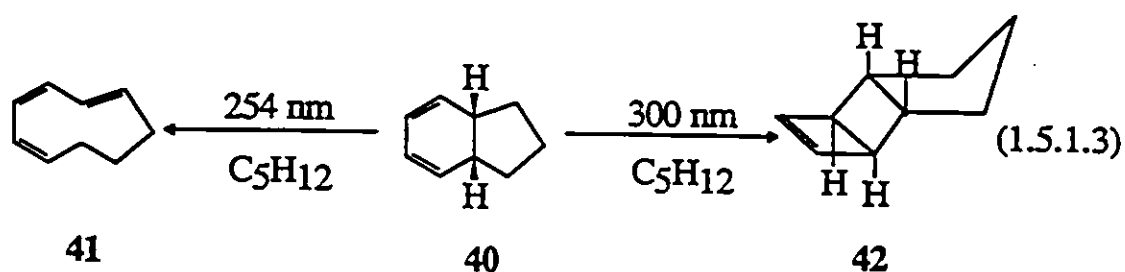
Table 1.5.1. Photoisomerization quantum yields from 2,4-hexadiene

$\phi_{\pi \rightarrow ct}$	$\phi_{cc \rightarrow ct}$	$\phi_{ct \rightarrow \pi}$	$\phi_{cc \rightarrow \pi}$	$\phi_{ct \rightarrow cc}$	$\phi_{\pi \rightarrow cc}$
0.37	0.41	0.18	0	0.29	0

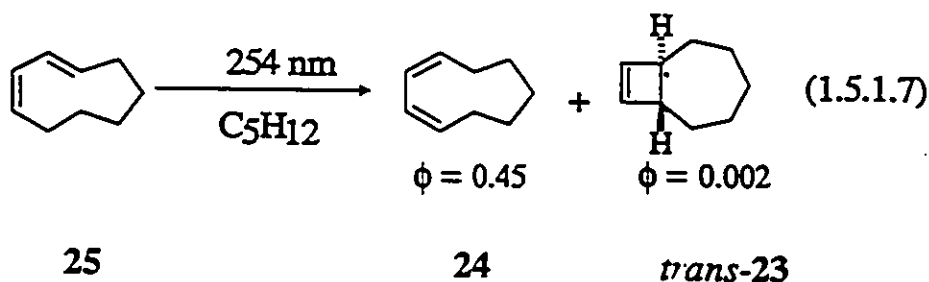
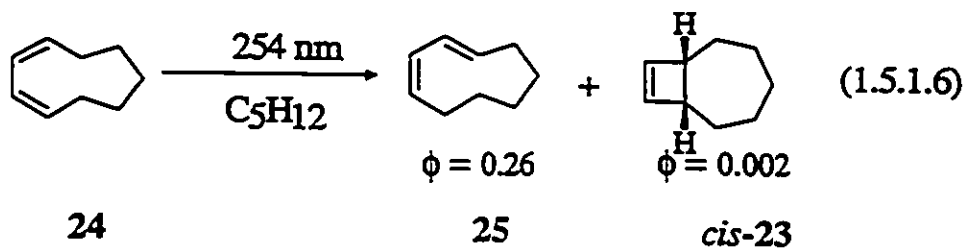
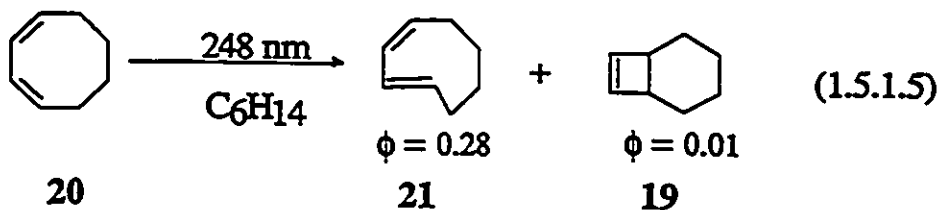
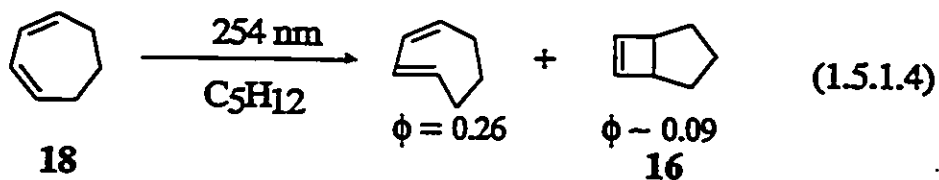
Direct excitation of *cis,cis*- or *cis,trans*-1,3-cyclooctadiene with 248 nm light gives *cis,trans* isomerization as the main chemical reaction (equation 1.5.1.2). The sum of the photoisomerization quantum yields,  $\phi_{cc \rightarrow ct} = 0.28$  and  $\phi_{ct \rightarrow cc} = 0.80^{81}$ , is close to unity and it was suggested that vibrational relaxation of the initially produced *cis,cis* and *cis,trans* excited singlet states leads to a common distorted intermediate which partitions between the two isomers.



The photochemistry of **40** is wavelength dependent (equation 1.5.1.3). Upon photolysis at 254 nm, **40** gives rise to *cis,cis,trans*-1,3,5-cyclononatriene **41** as the only detectable product, but on irradiation at 300 nm slowly yields the tricyclic cyclobutene **42**<sup>82</sup>. The photostationary state ratio between **40**/**41** at 300 nm is 99 % **40** and 1 % **41**. The ring opening of **40** to yield **41** was suggested to result from excitation of the more stable, twisted *s-cis* conformer of diene **40**. Formation of compound **42** was attributed to excitation of a planar diene conformer of **40**.



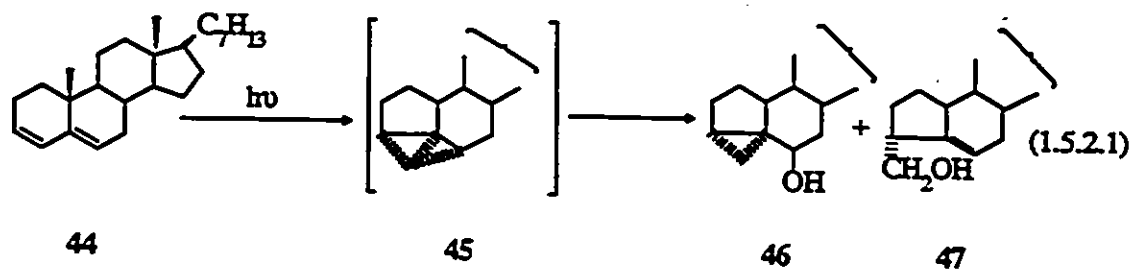
It is well documented that the photochemical ring closure of 1,3-dienes is a highly *stereospecific* process. The efficiency of photochemical ring closure of large cyclic dienes decreases as ring size increases, as is shown in equations 1.5.1.4-781, 83 - 86.



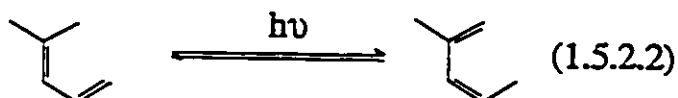
### 1.5.2 Bicyclo[1.1.0]butane Formation and [1,5]-H Migration.

Bicyclobutane<sup>87</sup> formation<sup>41, 88 - 90</sup> can be forced to be the major reactive process in flexible *s-trans* dienes which are incapable of undergoing *cis,trans* isomerization; an example of this is 3,5-cholestadiene (44 in equation 1.5.2.1)<sup>91, 92</sup>.





Finally, direct irradiation of *s-cis* 1,3-pentadienyl systems can also lead to [1,5]-hydrogen migration in appropriately substituted cases (equation 1.5.2.2)<sup>93</sup>.



## 1.6 Theoretical Studies of the Photochemical *cis,trans* Isomerization and Electrocyclization of 1,3-Dienes.

### (A) Avoided Surface Crossing Models

The accepted mechanism for the cyclization of *s-cis*-1,3-butadiene is that initially suggested by Oosterhoff et al<sup>14</sup> (Figure 1.4.3). This mechanism involves planarization of the carbon framework on the excited state potential energy surface plus synchronous<sup>15</sup> (or asynchronous, *vide infra*<sup>79</sup>) rotation of the terminal methylenes leading to an avoided crossing minimum (Figure 1.1.3), followed by internal conversion to the ground state potential energy surface and ring closure or regeneration of reactant. The carbon framework of the system remains planar along the reaction pathway and thus the reaction path bears no resemblance to the reaction path leading to *s-cis/s-trans* interconversion.

The proposed reaction coordinate for double bond *cis,trans* isomerization (Figure 1.6.1a) involves an initial rotation of a single terminal methylene by 90° on the excited state potential energy surface (while the rest of the structure remains almost unchanged) leading to an excited state minimum. The remainder of the rotation occurs on the ground state surface after internal conversion from the excited state minimum. For both reactions in Figures 1.4.3 and 1.6.1a, as well as for the *s-cis/s-trans* interconversion, the reaction funnels (which separates the part of the reaction path that lies on the excited state and the part that lies on the ground state, Figure 1.1.3) are assumed to be different excited state minima located along different excited state paths connecting reactants and products.

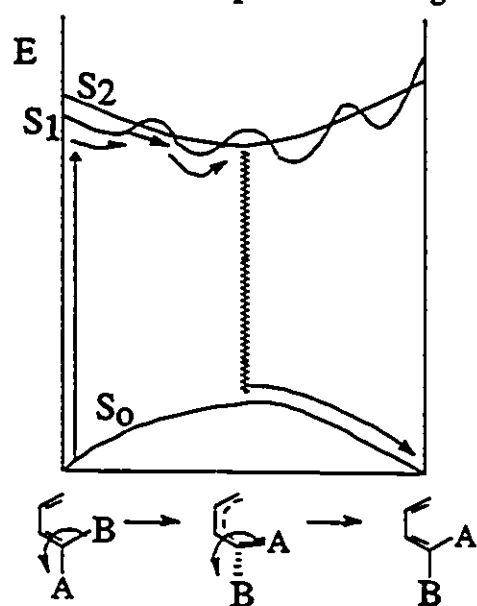
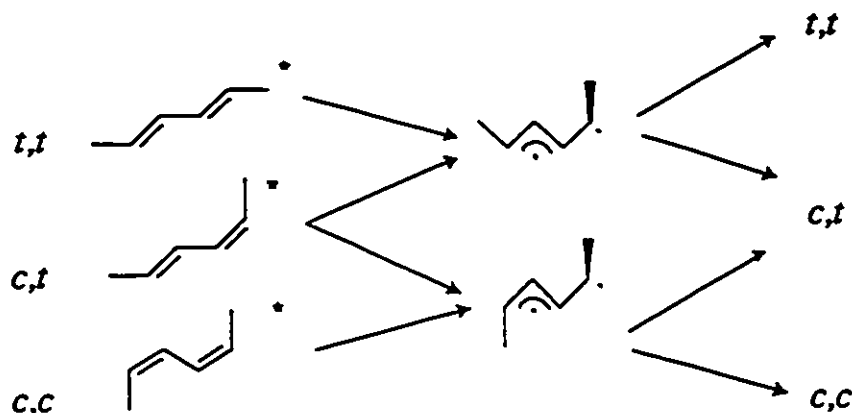


Figure 1.6.1a. State correlation diagram for the photoisomerization of a 1,3-butadiene system according to the avoided crossing model

The ramifications of the allylmethylene mechanism are best described using the photoisomerization of 2,4-hexadienes, as depicted in Scheme 1.6.1. The isomerization process commences with torsional relaxation of the initially planar singlet excited diene

about one double bond and continues through relaxed, noninterconverting, diradicaloid excited states which either isomerize or revert to the starting material.



Scheme 1.6.1. Allylmethylene biradical mechanism for the photoisomerization of 2,4-hexadiene

Most calculations<sup>94</sup> seem to suggest that there is little or no energy barrier to photochemical double bond isomerization. At the same time, calculations for disrotatory electrocyclic closure show a substantial barrier<sup>95</sup>. Experimentally, a 1:2.8 ratio of closure to isomerization is obtained starting from an *s-cis*-1,3-diene (Scheme 1.5.1.1). Squillacote et al explained this apparent conflict between calculations and experimental evidence by postulating an excited state potential energy surface for a nonsynchronous ring closure, which avoids the barrier of the synchronous disrotatory reaction (the reaction path presented avoids the barrier of  $17\text{-}33\text{ KJ mol}^{-1}$  by initially rotating around only one of the double bonds). Continuation of this rotation leads to a well that represents an allylmethylene zwitterionic species and thus eventual double bond isomerization.

Since the proposal of the above mechanism, many studies have emphasized the stability of  $C_5$  symmetry allylmethylene structures, in which a single  $C=C$  bond has been

twisted  $90^\circ$  from the molecular plane. For example, a semiempirical study of 1,3-pentadiene (piperylene) yielded a saddle point in the C=C-CH<sub>3</sub> twist potential energy surface, implicating a direct barrierless isomerization on the  $IB_u$  surface as the dominant photochemical pathway<sup>96</sup>. However, a recent study on 2-methyl-1,3-butadiene utilizing Absolute Resonance Raman Intensities has demonstrated the effect of methyl group substitution on the  $\pi$ -system. If the methyl group were to stabilize a particular allylmethylene structure, the C-C-C-C bend and the ethylenic stretch would be expected to show fundamental intensity; however, those features do not appear in the resonance Raman spectrum of 2-methyl-1,3-butadiene<sup>21</sup>. The authors concluded that in the  $IB_u$  state of 2-methyl-1,3-butadiene, the distortions of the C=C bond lengths and the C-C-C bond angles are nearly equal at each end, and that the terminal C-C bonds retain significant  $\pi$  character in the  $IB_u$  state; thus, the experimental evidence obtained is not entirely compatible with the development of an allylmethylene structure along this potential energy surface.

The model proposed by Van der Lugt and Oosterhoff has been widely used to explain the photochemical and photophysical aspects of the cyclobutene $\leftrightarrow$ butadiene interconversion. In addition to the photochemistry just discussed, a related photophysical effect is assumed to result from rapid traversal to and through excited state minima: the absence of fluorescence from *s-trans* butadiene. Zerbetto et al<sup>19</sup> explained the origin of this phenomenon by computing radiationless decay rates, which were found to be much shorter than the time frames required by fluorescence decay, but nevertheless finite<sup>20</sup>. They concluded that the non-planarity of butadiene in its lowest excited vibronic state leads to a dramatic increase in the rate of  $S_1 \rightarrow S_0$  radiationless decay. In this fast radiationless decay, out-of-plane torsional modes are responsible for the internal

conversion of the lowest excited singlet state to the ground state. Internal conversion in 1,3-butadiene is therefore *fast enough* to quench fluorescence completely.

Similarly, the weakness of fluorescence from isoprene ( $\phi_f \sim 10^{-6}$ ) was interpreted as being due primarily to strong nonadiabatic coupling and internal conversion from the Franck-Condon excited  $1B_u$  state (single excitation from HOMO to LUMO of the  $\pi$  system or  $S_1$  state) to another electronic manifold by an allowed crossing with an electronic state of different symmetry; this state was identified as the  $2A_g$  (double excitation from HOMO to LUMO or  $S_2$  state), as depicted in Figure 1.6.1b<sup>21</sup>. The time scale of the internal conversion process was calculated to be 10 fs.

Cyclobutene formation ensues from a synchronous (or asynchronous) rotation<sup>97</sup> about the C<sub>1</sub>-C<sub>2</sub> and C<sub>3</sub>-C<sub>4</sub> bonds of the 1,3-butadiene moiety according to this model. Upon relaxation to the energy minimum, decay to the ground state surface (by coupling of the discrete vibrational levels of  $S_2$  with the quasi-continuum of the  $S_0$  vibrational levels) produces cyclobutene or regenerates diene (Figure 1.4.3). As mentioned in Section 1.1, the disrotatory pathway for 1,3-butadiene closure is preferred overall because the ground state surface for this pathway is higher in energy than that for the conrotatory pathway (see Figure 1.1.3), and consequently, internal conversion to the ground state is faster for the *disrotatory* mode of cyclization. This interpretation supports the fact that photochemical ring closure of a 1,3-diene is a highly stereospecific process; however, it is incompatible with the nonstereospecificity observed *in general* for the reverse reaction (cyclobutene ring opening, Section 1.3.1).

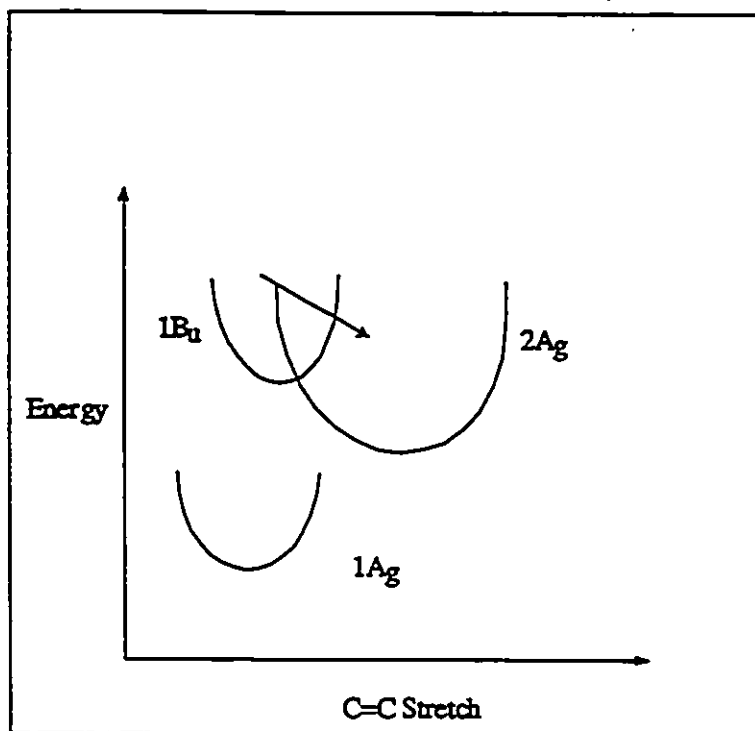


Figure 1.6.1b. A section through the potential energy surfaces for the  $1^1B_u$ ,  $1^1A_g$  and  $2^1A_g$  states of 2-methyl-1,3-butadiene along the symmetric C=C stretches.

### (B) Conical Intersection Model

Diene photoisomerization and photochemical ring opening reactions are processes that appear to be very fast (well below 1 picosecond, see Section 1.2<sup>77, 98</sup>) and are often associated with a complete lack of fluorescence<sup>19</sup>. These facts are incompatible with a mechanism where a relatively stable excited state intermediate is generated (*i.e.* allyl methylene biradical) and with the presence of a substantial energy gap between two potential energy surfaces.

Recent *ab-initio* (MC SCF) calculations, postulate the existence of *conical intersection* regions (where the ground and excited state potential energy surfaces intersect) in the isomerization pathways of 1,3-butadiene and in several other photochemical reactions<sup>100 - 102</sup>. The degeneracy of the two surfaces at a conical intersection allows a very rapid decay process that has been theoretically demonstrated to take place within a single vibrational period<sup>103</sup>. The photoexcited reactant can then pass directly to the ground state. The funnel (conical intersection) between the excited state and the ground state surfaces (Figure 1.6.5) of the reaction coordinate plays a role in a photochemical reaction similar to the transition state for a thermal reaction (the photoexcited reactant must necessarily assume the structure of a conical intersection point, or the rate of decay to the ground state surface would be much slower).

The geometries of the conical intersections (CI's) found for the excited singlet state surface of 1,3-butadiene are tetraradicaloid structures (four quasi-unpaired electrons where almost all the bonding is lost) with all three C-C bonds twisted, as a result of substantial pyramidalization at one of the two central carbons and twisting of the two terminal C-C bonds<sup>104</sup>. Figure 1.6.2 illustrates a pictorial representation of the reaction paths and minima for 1,3-butadiene isomerization within a three dimensional cross section (obtained by MM-VB, molecular mechanics valence bond calculations) of the excited state potential energy surface. The variable  $\beta$  depicts the *s-cis/s-trans* interconversion process, and the coordinates  $\alpha_1$  and  $\alpha_2$  describe the *cis,trans* isomerization of the two terminal double bonds, which can change in both a synchronous and asynchronous fashion (*cf.* with avoided crossing model) at the time  $\beta$  is approaching a value of  $90^\circ$ . The center of the box (90,90,90) in Figure 1.6.2, which has been shaded, corresponds to a point where all the  $\pi$  bonds are twisted by  $90^\circ$ . This is one of the conical intersection regions.

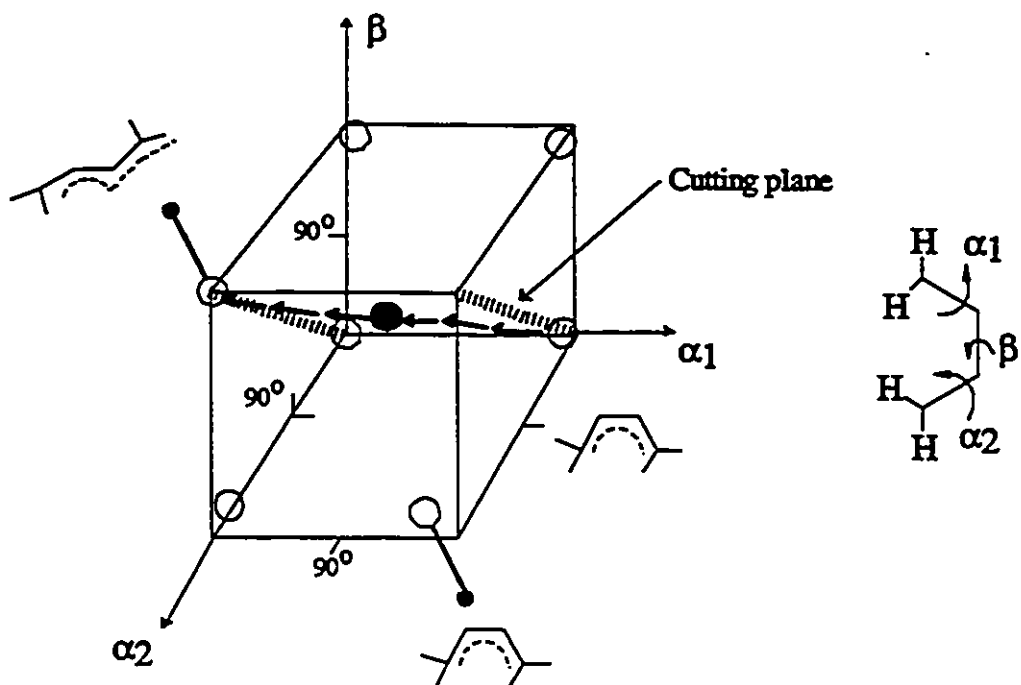
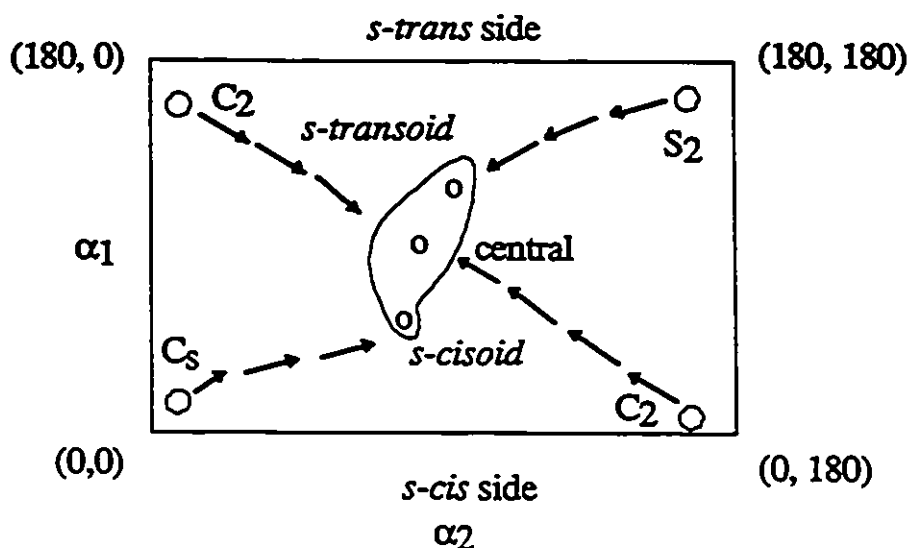


Figure 1.6.2. Three-dimensional cross section of the excited state potential energy surface for butadiene. The coordinates  $\alpha_1$ ,  $\alpha_2$ , and  $\beta$  correspond to rotations about the three C-C  $\sigma$  bonds of the butadiene framework and span a range from 0 to 180°. The circles represent the excited state stable structures. The central volume represents the conical intersection region centered on the (90,90,90) point. The diagonals correspond to *conrotatory* and *disrotatory* pathways going from *s-cis* to *s-trans* minima

The location of the *s-cis* and *s-trans* minima that correspond to the excited state of 1,3-butadiene are indicated by spheres near the bottom face and the top face of the box, respectively. The *s-cis/s-trans* interconversion pathways can be envisaged by plotting potential energy surfaces in the special cutting plane defined by the dashed lines in Figure 1.6.2. This cutting plane is depicted in Scheme 1.6.2.





Scheme 1.6.2. *s-cis/s-trans* Isomerization pathways for 1,3-butadiene

Two stable *s-cis* conformations were found (at the MC-SCF/4-31 G level of theory) which correspond to  $C_2$  and  $C_s$  symmetry. The two *s-trans* conformations found have symmetry  $C_2$  and  $S_2$ . In the *s-cis/s-trans* transition region, no real transition structure for the *s-cis/s-trans* interconversion process was found, rather only points of degeneracy between the first excited state and ground state seem to occur in these calculations. Thus, there exists a large continuous region of "touching" between the ground and excited state potential energy surfaces along the *s-cis/s-trans* isomerization path. However, three quite different critical points were found on the conical intersection region, denoted as *s-transoid*, *s-cisoid*, and *central*. The structures of these points are depicted in Figure 1.6.3. If the photoprocess starts from the *s-trans* conformer ( $S_2$  symmetry) a stationary point on the conical intersection which lies  $13.4 \text{ kJ mol}^{-1}$  below the  $S_2$  *s-trans* minimum is reached. This point is the lowest energy point on the excited state surface.

Similarly, starting from the  $C_s$  *s-cis* conformer, an *s-cisoid* stationary point is encountered on the conical intersection at  $15.5 \text{ kJ mol}^{-1}$  above the excited state

minimum. The pathways to the conical intersections involve the nonsynchronous rotation of the two terminal  $\text{CH}_2$ 's of 1,3-butadiene along with central C-C bond rotation. A third stationary point on the conical intersection found in these calculations lies 25.1  $\text{kJ mol}^{-1}$  above the  $\text{C}_s$  and  $\text{S}_2$  minima (central conical intersection in Figure 1.6.3). These three conical intersection structures are stationary points on the touching region and hence they give an indication of the accessibility of the conical intersection region by following the possible excited state *s-cis/s-trans* interconversion pathway. The location and energy of the conical intersection stationary points is schematically illustrated in Figure 1.6.4, where the geometric parameter  $\beta$  (from Figure 1.6.2) is used as the reaction coordinate.

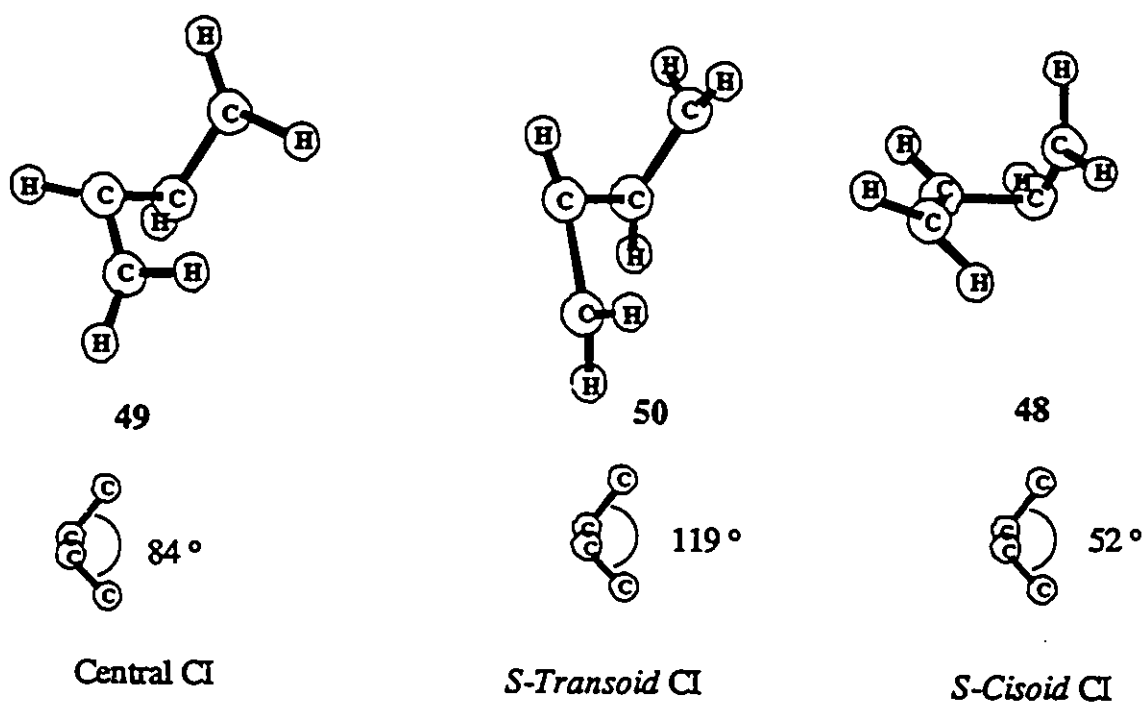


Figure 1.6.3. Optimized MC-SCF/4-31G structures for the central, *s-cisoid* and *s-transoid* conical intersections

The *s-cisoid* conical intersection (48, Figure 1.6.3) occurs at a C-C-C-C dihedral angle of  $52^\circ$  while the central conical intersection (49, Figure 1.6.3) is located at  $84^\circ$ . Similarly, the *s-transoid* conical intersection (50), occurs at a C-C-C-C dihedral angle of  $119^\circ$ . The conical intersection is approached very soon starting from the  $C_5$  *s-cis* minimum or from the  $S_2$  *s-trans* minimum near the *s-cisoid* or *s-transoid* conical intersection stationary points respectively. These calculations provide the foundation for understanding the disrotatory stereochemical preference which is observed for the photochemical ring closure of 1,3-dienes to cyclobutenes .

Scheme 1.6.2 depicts the reaction pathways from the energy minima of the *s-cis* and *s-trans* conformers of 1,3-butadiene for *s-cis/s-trans* conformer interconversion, *cis,trans* isomerization and cyclobutene formation. If the decay commences from the *s-cis* region, the system after photoexcitation undergoes relaxation to the low energy region of the potential energy surface where the excited state minima and the *conical intersection region* are located and a very fast return to the ground state potential energy surface is assured. There are two stereochemically different pathways connecting the two *s-cis* minima ( $C_5$  and  $C_2$ ) to the conical intersection region. Along the disrotatory pathway (the one starting from the  $C_5$  minimum) the system approaches the conical intersection region, located  $16.7 \text{ kJ mol}^{-1}$  above the minimum, (*vide supra*) with a value of  $\beta$  below  $50^\circ$  (see Figure 1.6.4). The situation is different along the conrotatory pathway, where the system must enter the *central conical intersection region*, about  $25.1 \text{ kJ mol}^{-1}$  above the minimum, with a value of the  $\beta$  torsional angle larger than  $80^\circ$ . As is shown in Scheme 1.6.2, the location of the edge of the conical intersection is consistent with an immediate passage into the conical intersection region and thus to the ground state when the system moves along the disrotatory pathway, while the conrotatory pathway corresponds to a less

favorable route. The *stereochemical* decision is thus made mainly on the excited state surface of the reaction pathway.

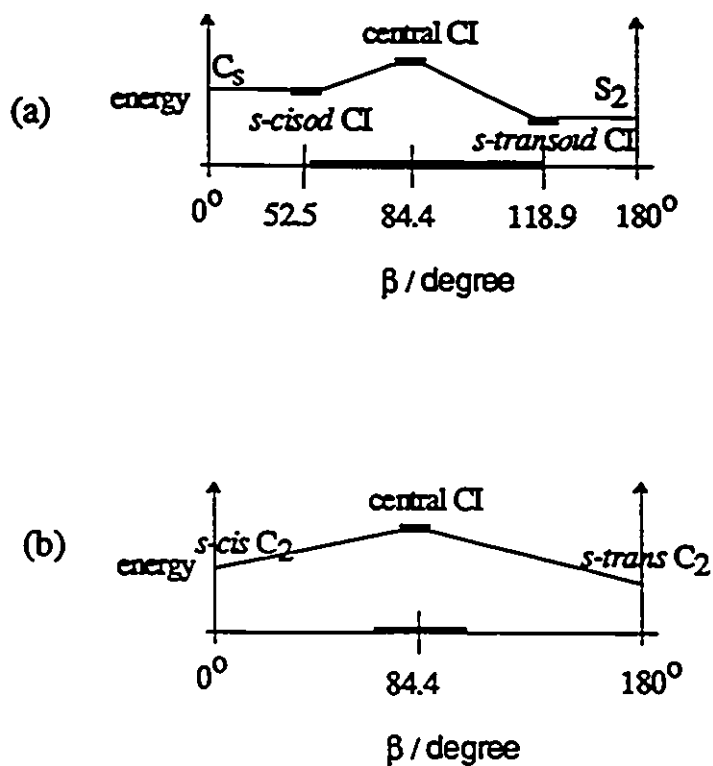
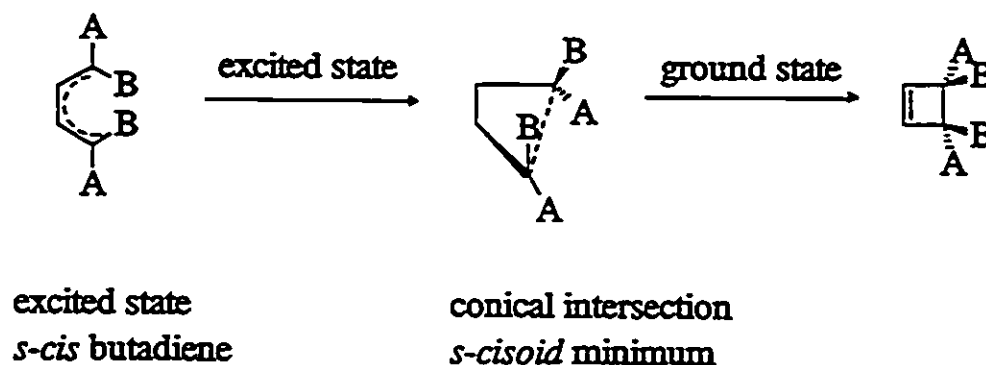
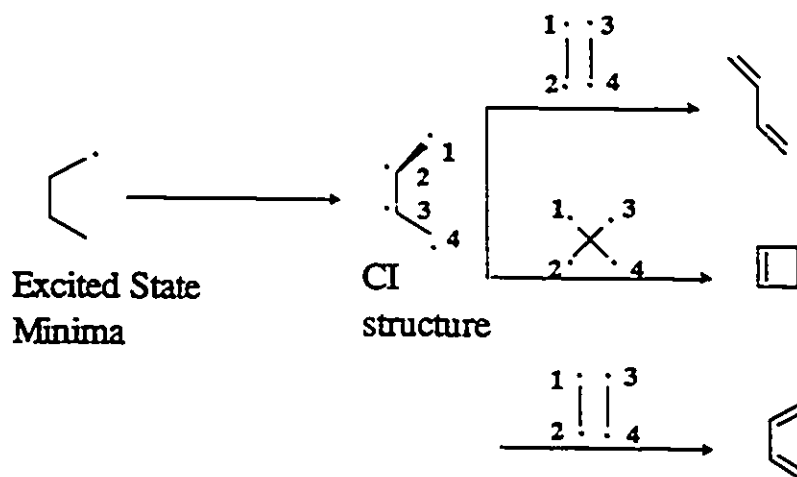


Figure 1.6.4. Reaction coordinate diagram for twisting about the 1,3-butadiene  $C_2$ - $C_3$  bond along the disrotatory (a), and conrotatory (b), *s-cis/s-trans* excited state isomerization pathways



Scheme 1.6.3. Schematic excited state pathway for ring closure of 1,3-butadiene.

A recoupling process, described in Scheme 1.6.4, will dominate the ground state stage of the reaction, which commences at the *conical intersection* region and branches to the various ground state minima corresponding to different photoproducts. Branching to the different recoupling pathways will be dictated by the structure of the molecule at the conical intersection point and the momentum vectors associated with individual atomic trajectories that are established during the approach of the molecule to the conical intersection.



Scheme 1.6.4. Possible recoupling pathways from *s-cis* excited state minima of 1,3-butadiene

This mechanism can explain the different degrees of stereospecificity in the ring opening and ring closure reactions. A simple picture of the ring opening process involves an initial excitation to a noncovalent electronic state, which then relaxes very rapidly to the doubly excited ( $2^1A_g$ ) state at a geometry close to that of the original ground state reactant (after few oscillations the molecule will decay to the  $2^1A_g$  state and evolve on the  $2A_g$  potential energy surface). The nonstereospecificity obtained is proposed to result from what occurs on the ground state part of the reaction coordinate, after passage through the conical intersection. Relaxation on the ground state surface is dominated by twisting motions of two  $CH_2$  groups, but this can occur in conrotatory or disrotatory fashion.

Olivucci and coworkers<sup>61</sup> undertook a theoretical study on the photochemistry of 7-methylbicyclo[4.2.0]oct-1(6)-ene 31 using *ab initio* CAS-SCF (Complete Active Space-Self Consistent Field) computations at the 4-31G level of theory. They demonstrated that the formation of the three diene products in the photochemistry of 31 (see equation 1.3.3.5) can be rationalized via a reaction path that passes from the excited state to the ground state via three different *transition points*<sup>62</sup>. The photochemical reaction is divided into two stages. The first stage, which occurs on the excited state potential energy surface before the transition point, corresponds to *ring opening*, involving primarily  $C_2-C_3$  rotation (numbering from 1,3-butadiene moiety). The *conrotatory or disrotatory motion* occurs in the second stage of the reaction, on the ground state surface after the transition point, and there are three possible ground-state paths from each conical intersection. Thus the stereochemical outcome is decided in the second stage of the reaction by the nature of the path which is actually followed from the conical intersections to the products. The possibility of these different relaxation routes from each conical intersection provides a

mechanistic rationalization for the observation that ring opening of 31 is *nonstereospecific*. Figure 1.6.5 shows, pictorially, a representation of the reaction funnel, where the vertex symbolizes the conical intersection point.

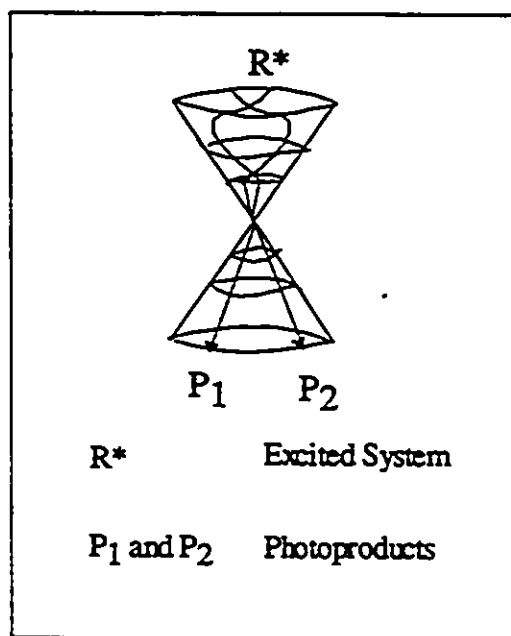


Figure 1.6.5. Reaction funnels for the excited state and ground state surfaces and conical intersection point (vertex of the double cone)

### L7 Statement of the problem:

Three cyclobutene systems will be investigated in this study: 1-Phenyl substituted cyclobutenes; Alkylsubstituted monocyclic cyclobutenes, and Bicyclo[n.2.0]alkenes.

Phenyl-substituted cyclobutenes (section 1.3) are known to fluoresce with high quantum yields to the exclusion of ring opening. The reason for this distinct behavior will

be investigated employing a series of appropriately substituted 1-phenyl cyclobutenes. In particular, the presence of a polarized excited state will be researched as a possible cause for the lack of ring opening reaction.

Results from Leigh and coworkers<sup>43</sup> (see section 1.3.1 and equations 1.3.1.7 and 1.3.1.8) on the photochemical ring opening of *cis*- and *trans*-tricyclo[6.4.0.0.]dodec-1-ene (10 and 11 respectively) suggested that orbital symmetry does play a role in the initial stages of the ring opening reaction. Also, the dynamics of the photochemical ring opening reaction point towards symmetry-allowed *disrotatory* pathways, as explained in section 1.2. Our study is to be concerned with a series of alkylsubstituted cyclobutenes with increasing alkyl substitution at C<sub>3</sub>/C<sub>4</sub> (and therefore diminishing modes for *disrotation*) to provide further evidence, that despite the general nonstereospecificity observed in the ring opening reaction of monocyclic cyclobutenes, the initial motions are directed towards orbital symmetry-allowed *disrotatory* control.

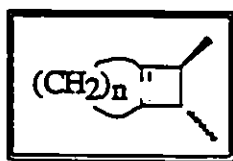


A study of the *cis,trans* photoisomerization of a series of *EE* and *EZ* constrained *s-cis* dienes will be undertaken in Chapter IV. This study will focus on the role of central C-C bond torsion on the *cis,trans* photoisomerization process of *s-cis* dienes.

According to section 1.4, equation 1.4.2, cyclobutenes such as *cis* and *trans*- 37 undergo photochemical ring opening with an unusually high degree of stereoselectivity. In order to elucidate the reasons why such structural effects prejudice the stereochemical outcome of the photochemical ring opening reaction, the study of a series of bicyclic



cyclobutenes with varying ancillary ring sizes will be analyzed. The question posed is whether the stereoselectivity observed (e.g. equation 1.4.2) is a function of constraint in the cyclobutene ring. Particularly, the role of C=C torsional motions in cyclobutene ring opening will be discussed and paralleled with the motions around C<sub>2</sub>-C<sub>3</sub> (1,3-butadiene numbering) in the *cis,trans* photoisomerization of 1,3-dienes.



$n = 2, 3, 4, \text{ and } 5$

Comparisons of the product distributions obtained from photolysis of these compounds with the quantum yields for *cis,trans* photoisomerization of the corresponding isomeric dienes will also be carried out, in a more comprehensive consideration of the adiabatic mechanism for cyclobutene ring opening.

The majority of the results and observations will be discussed in the context of recent theoretical calculations for cyclobutene  $\leftrightarrow$  butadiene interconversion.

## CHAPTER II

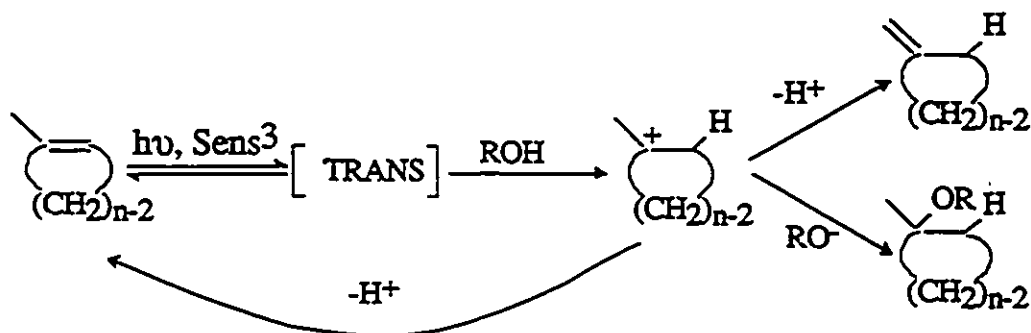
### THE PHOTOCHEMISTRY OF 1-PHENYLCYCLOBUTENES

#### 2.1 Introduction

The photochemistry of 1,2-diphenylcyclobutene (**1**) in aprotic solvents was illustrated in equation 1.3.3.1 (Chapter 1.3.1). Compound **1** does not undergo ring opening upon photolysis, but cycloreverts to 1,2-diphenylacetylene with very low quantum efficiency. The major photochemical deactivation pathway of the singlet excited state of **1** is fluorescence ( $\phi_f = 0.9$ ). This contrasts with the behavior of benzocyclobutenes and dewar aromatics, which both undergo efficient ring opening upon photolysis in condensed media (equations 1.3.1.4-6). It has been suggested that the failure of arylcyclobutenes to undergo excited state ring opening may be due to simple energetic considerations; the  $\pi, \pi^*$  singlet state energy is too low to enable cleavage of the cyclobutene C<sub>3</sub>-C<sub>4</sub> bond. A second possibility is that the lack of reactivity towards ring opening is for some reason due to polarization of the styrenic C=C bond in the  $\pi, \pi^*$  excited singlet state. That such polarization is present is indicated by the fact that photolysis of arylcyclobutenes (and simple styrene derivatives) in alcohol solution results in the formation of ethers consistent with initial protonation of the lowest excited singlet state by the solvent (equation 1.3.3.2).

The addition of hydroxylic solvents to optically excited olefins is a well-studied reaction in organic photochemistry. Evidence that these reactions involve protonation of the olefin and the intermediacy of the resulting carbocation is compelling<sup>105a</sup>.

The triplet-sensitized photohydration of aliphatic cycloalkenes in protic media is summarized in Scheme 2.1.1. The proposed mechanism is supported by evidence<sup>105a</sup> which includes direct detection of the *trans*-alkene and incorporation of deuterium when the reaction is run in methanol-*d*.

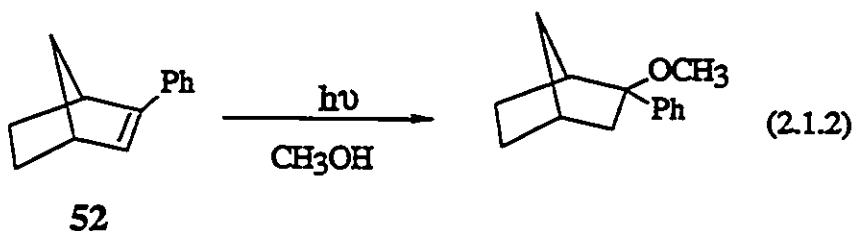
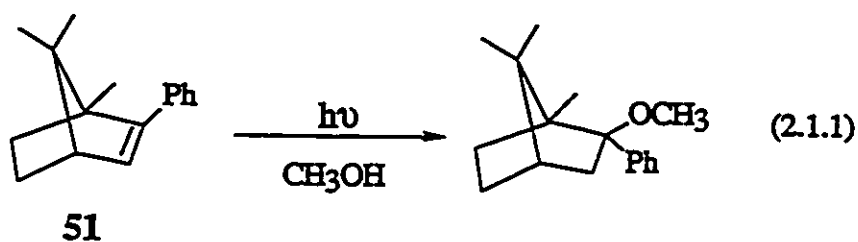


Scheme 2.1.1. Sensitized photohydration of aliphatic cycloalkenes.

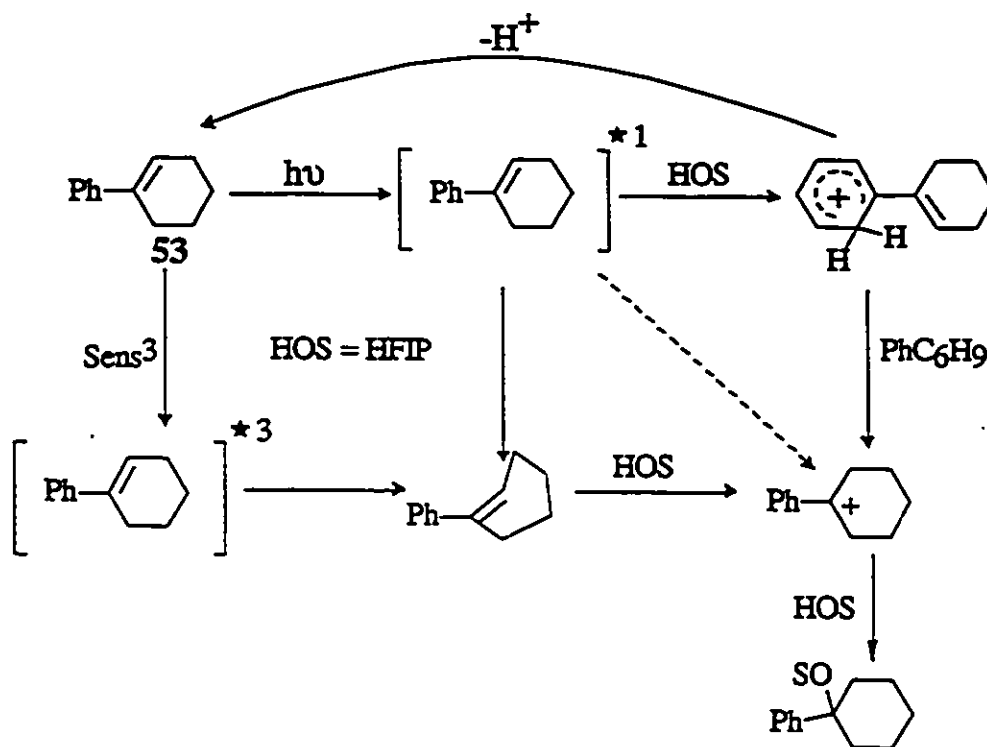
Photoprotonation of aliphatic cycloalkenes also takes place on direct irradiation. The pathway is believed to involve formation of the *trans*-cycloalkene<sup>106</sup>, the same intermediate obtained on sensitized irradiation.

Aliphatic acyclic alkenes do not undergo photoaddition on sensitized irradiation but do add hydroxylic solvents on direct photolysis. Kropp<sup>105a, 106</sup> has interpreted these photoadditions in terms of nucleophilic trapping of the Rydberg  $\pi, R(3s)$  state. The photochemistry of simple aromatic alkenes and alkynes has been rationalized as deriving from  $\pi, \pi^*$  excited states, since they are much lower in energy than other available states.

Singlet states have been postulated to be involved in the photoaddition of methanol to 2-phenyl-2-bornene **51** and 2-phenyl-2-norbornene **52**<sup>105a</sup> (equations 2.1.1 and 2.1.2). In addition, methanol was found to quench the fluorescence of 2-phenyl-2-bornene.



McClelland and coworkers<sup>107</sup> investigated the photochemistry of 1-phenylcyclohexene 53 in 1,1,1,3,3,3-hexafluoro-2-propanol (HFIP). They observed the cation directly as a transient species by laser flash photolysis, using both direct irradiation at 248 nm and benzophenone sensitized irradiation at 308 nm. In this case, the cation is formed by direct protonation of the singlet state, as well as ground state protonation of *trans*-53 which is formed by excited state *cis,trans*- isomerization. Triplet sensitized formation of the cation involves the *trans*- cycloalkene exclusively. In the direct irradiation, their results suggest that protonation occurs predominantly on the aromatic ring to give the 2-benzenonium ion, which ultimately yields the benzylic cation by proton transfer to ground state alkene. The entire mechanism is depicted in Scheme 2.1.2. Direct protonation of the singlet state at the styrenic double bond to give the cyclohexyl cation directly cannot be ruled out, but the authors concluded that that pathway is likely to be of minor importance in this case.

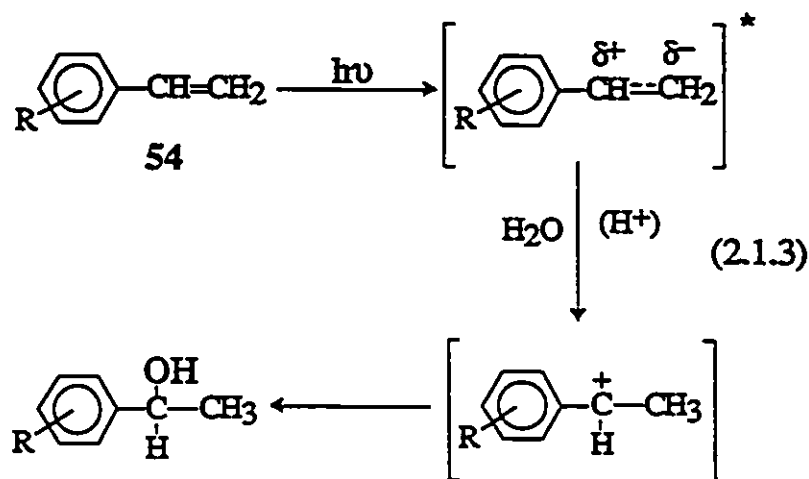


Scheme 2.1.2. Mechanism for photoaddition of solvent to 1-phenylcyclohexene

The acid-base properties of aromatic compounds in the excited state have been a topic of great interest<sup>105b,c</sup>. Phenols and hydroxyaromatic compounds become much stronger acids ( $\Delta pK_a$  can be  $> 6$ ) in  $S_1$ <sup>105d,e</sup>. For aromatic alkenes, the  $pK$  shifts on excitation ( $\Delta pK = pK^* - pK$ ) to  $S_1$  are of the order of 8 logarithmic units or more. A typical example is given by styrene systems.

Yates and coworkers<sup>108</sup> have shown that the photohydration of styrenes **54** are generally subject to acid catalysis, the reaction proceeding via a polarized  $S_1$  state (equation 2.1.3). These authors also examined the reactivity-selectivity relationships for the photoaddition reactions of different nucleophiles to alkenes and alkynes. They found that the photochemically generated carbenium ion exhibits greater selectivity than its

thermal counterpart generated in identical media, suggesting that the cation is produced in the excited state.

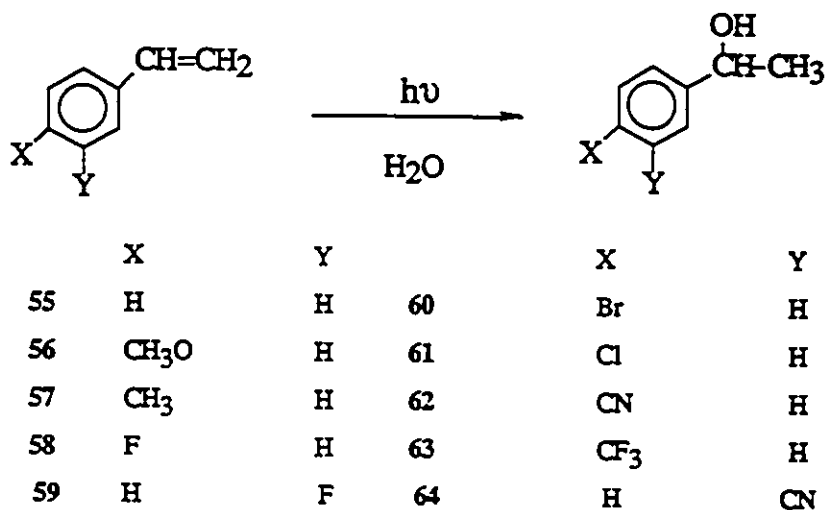


In another mechanistic study<sup>109</sup> it was demonstrated that while the triplet states of styrenes (nitrosubstituted derivatives excluded) are not inert in aqueous acid, they do not undergo photoprotonation.

The singlet states of nonnitro-substituted aromatic alkenes and alkynes most likely possess charge transfer character, thus facilitating protonation at the  $\beta$ -carbon and hence hydration. The triplet states of these molecules are thought to be of a diradicaloid nature. Yates and coworkers compared the ground state protonation rate constants with those from the excited state and found that the latter is approximately  $10^{11}$ - $10^{14}$  times more reactive to protonation than the ground state. This was explained as being principally due to the ground state electronic configurations and geometries involved and the need for rehybridization upon protonation<sup>109 - 111</sup>. Since the excited state electronic distribution is quite different, the activation barrier to proton transfer may be reduced significantly. If

however, the excited states are assumed to have twisted or bent geometries, with charge transfer character, then the need for rehybridization on protonation is avoided.

A study on the structure-reactivity relationship of the photohydration reaction of aromatic alkenes was undertaken by Yates and coworkers<sup>112</sup> with a series of substituted styrenes. Irradiation of alkenes 55–64, (see Scheme 2.1.3.) in neutral water or dilute acid at 254 nm resulted in efficient conversion to the corresponding 1-arylethanol. Sensitization and quenching experiments indicated a singlet reaction; solvent isotope effects and the observation of general acid catalysis was consistent with protonation being the rate determining step in the hydration of  $S_1$ . Table 2.1 summarizes the singlet fluorescence lifetimes of several styrenic compounds in aqueous solution. It is observed that the stronger the electron donating ability of the substituent, the shorter the lifetime of the styrene derivative. From the results of fluorescence quenching experiments, it was concluded that this is the result of a substantial effect on the rate of protonation of  $S_1$  by the solvent.



Scheme 2.1.3. Photohydration of styrene derivatives.

**Table 2.1.** Singlet fluorescence lifetimes of styrenic compounds determined in water at pH

7

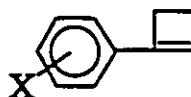
<i>Styrene</i>	$\tau_s$ [ns]
55	7.5
56	1.2
57	4.5
58	4.9
59	4.3

Yates and coworkers could not detect photohydration products for styrenes with substituents of greater electron-withdrawing character than that of fluorine, and thus concluded that for photohydration to take place, *the electron-donating ability of the substituent had to be higher or equal to that of fluorine in  $S_1$ .*

As pointed out earlier, arylcyclobutenes do not undergo ring opening upon photolysis in solution. In principle, this could be due to the lower energy and/or more extended delocalization in the lowest excited singlet state of aryl- compared to alkyl- derivatives. It may also be the result of the  $\pi, \pi^*$  singlet state being more extensively polarized than in alkyl derivatives. If the latter is true, then reducing the intrinsic polarization of the C=C bond in the cyclobutene ring through substitution in the phenyl ring should result in an increase in the rate constant for ring opening, to the point where the ring opening reaction may be detectable.



With that goal in mind, the photochemistry and photophysics of six 1-arylcyclobutene derivatives **65-70** shown below will be studied in aprotic solvents.



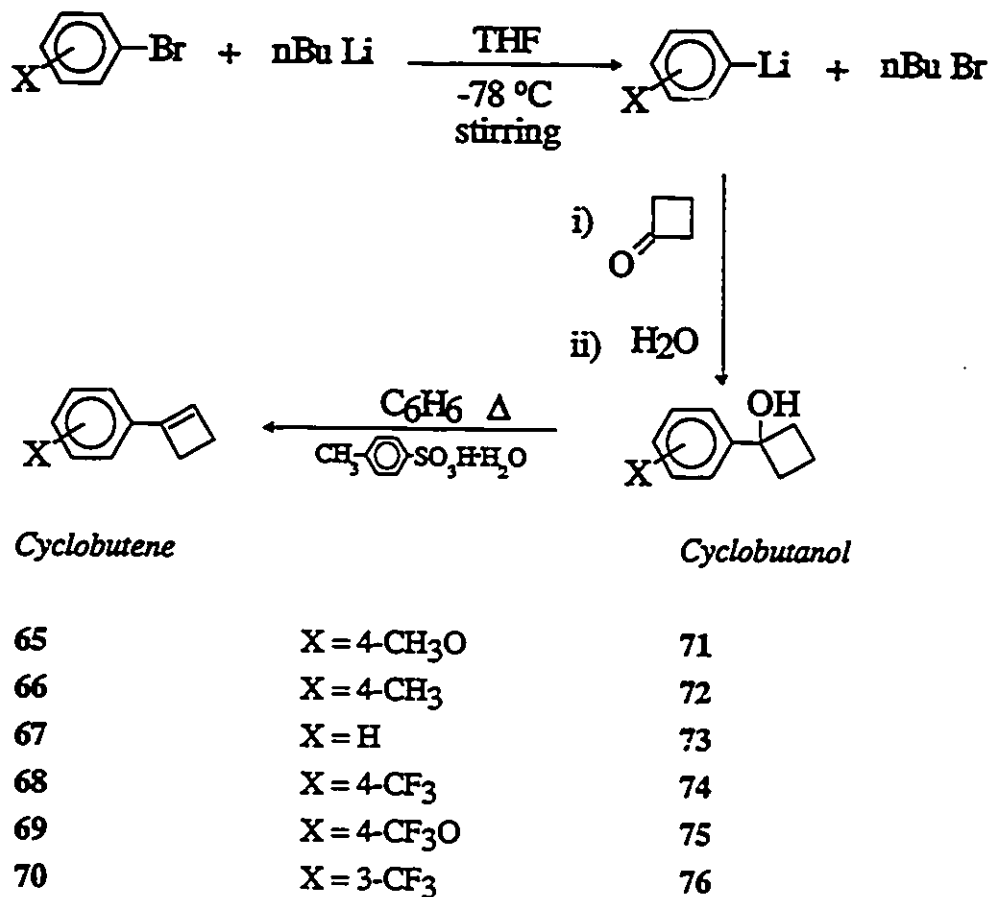
X =	4-CH <sub>3</sub> O	4-CH <sub>3</sub>	H	4-CF <sub>3</sub>	4-CF <sub>3</sub> O	3-CF <sub>3</sub>
	<b>65</b>	<b>66</b>	<b>67</b>	<b>68</b>	<b>69</b>	<b>70</b>

These compounds also afford the opportunity to examine the effect of geometrical constraints on the photoprotonation of substituted styrene derivatives. Thus the photochemistry of **65-70** in the presence of alcohols will also be investigated in order to establish a qualitative comparison with the analogously substituted styrenes.

## 2.2 RESULTS

### 2.2.1 Preparation of 1-Phenylcyclobutenes

The six 1-arylcyclobutenes were prepared by arylation of cyclobutanone with the corresponding aryl-lithium reagent, followed by acid-catalyzed dehydration of the intermediate 1-arylcyclobutanols according to Scheme 2.2.1.



Scheme 2.2.1. Synthesis of 1-phenylcyclobutenes

Initial purification of cyclobutenes 65-70 was carried out by bulb-to-bulb distillation. Further purification was achieved by semipreparative gas chromatography. Identification of 65-70, as well as the intermediate 1-aryl-1-cyclobutanols, was performed on the basis of their <sup>1</sup>H and <sup>13</sup>C NMR, UV, IR and mass spectra and High Resolution Mass Spectrometry measurements.

## 2.2.2 UV Absorption Spectra

The UV absorption spectra of compounds 65-70 were obtained in dilute deoxygenated cyclohexane (or pentane), acetonitrile and methanol solutions. Each compound displays a rather broad absorption, devoid of any fine structure. The absorption maxima and the molar extinction coefficients are summarized in Table 2.2.2.1.

**Table 2.2.2.1.** Solution phase UV absorption data for cyclobutenes 65-70 measured in acetonitrile (CH<sub>3</sub>CN), cyclohexane (C<sub>6</sub>H<sub>12</sub>) and methanol (CH<sub>3</sub>OH) solutions at 23°C.

<i>Cyclobutene</i>	$\lambda_{\max}$ [nm] <sup>a</sup>		
	CH <sub>3</sub> CN	C <sub>6</sub> H <sub>12</sub>	CH <sub>3</sub> OH
65	260 (~16000)	260 (17900)	265 (16050)
66	256 (15500)	258 (14500)	247 (16000)
67	252 (13000)	256 (12882)	252 (12950)
68	260 (14800)	260 (16000)	260 (15730)
69	254 (17000)	254 (17400)	260
70	254 (15100)	254 (16500)	260

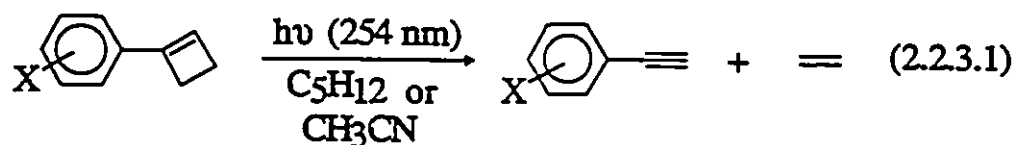
a Wavelength of maximum absorption.

b Molar extinction coefficient at  $\lambda_{\max}$

### 2.2.3 Photochemistry of 65-70 in Aprotic Solvents

Photolysis of cyclobutenes 65-70 in deoxygenated pentane and acetonitrile (*ca*  $5 \times 10^{-3}$  mol dm<sup>-3</sup>) solutions with 254 nm light produces the product mixtures shown in equation 2.2.3.1. No attempt was made to identify ethylene in the photoreaction mixtures, but the phenylacetylenes 77-82 (cycloreversion products), were identified by GC/MS analyses, GC/FTIR analyses and by coinjection with authentic samples where available. The chemical yields of the 1-phenylacetylenes obtained in this manner range from 80 - 95 % (at conversions lower than 10 %).

No ring opening product (2-aryl-1,3-butadiene) was observed within the limits of detection of the technique employed (either by gas chromatography or high field NMR), allowing an upper limit of 1 % relative to that of phenylacetylene formation.



*Cyclobutene*

*Phenylacetylene*

65	X = 4-CH <sub>3</sub> O	77
66	X = 4-CH <sub>3</sub>	78
67	X = H	79
68	X = 4-CF <sub>3</sub>	80
69	X = 4-CF <sub>3</sub> O	81
70	X = 3-CF <sub>3</sub>	82

Yields for phenylacetylene formation from photolyses of cyclobutenes 65-70 in deoxygenated acetonitrile and pentane solutions were determined from the slopes of moles

of photoproduct *versus* irradiation time plots (Figure 2.2.3.1A and B). These experiments were carried out in a merry-go-round apparatus, with the photolysis of 68 as a standard, with monitoring of photoproduct formation by gas chromatographic techniques. Absolute quantum yields for product formation from photolysis of 68 as deoxygenated  $ca. 5 \times 10^{-3} \text{ mol dm}^{-3}$  solutions in pentane, acetonitrile, and methanol were determined by electronic actinometry<sup>113 - 115</sup> (Appendix 1). Absolute quantum yields for product formation from 65-67, 69-70 were then calculated using the slopes of product concentration versus time plots, and the absolute quantum yields for reaction of the reference compound 68 as measured above. These quantum yields are exhibited in Table 2.2.3.1.

Table 2.2.3.1. Quantum yields for cycloreversion of 1-arylcyclobutenes 65-70 in  $ca. 5 \times 10^{-3} \text{ mol dm}^{-3}$  deoxygenated acetonitrile and pentane solutions at 23°C with 254 nm Light

<i>Cyclobutene</i>	$\phi_1$ (acetonitrile)	$\phi_2$ (pentane)
65	$0.18 \pm 0.02$	$0.20 \pm 0.02$
66	$0.12 \pm 0.05$	$0.15 \pm 0.02$
67	$0.09 \pm 0.02$	$0.09 \pm 0.01$
68	$0.08 \pm 0.01$	$0.07 \pm 0.01$
69	$0.035 \pm 0.009$	$0.022 \pm 0.003$
70	$0.0090 \pm 0.0006$	$0.0045 \pm 0.0006$

A)

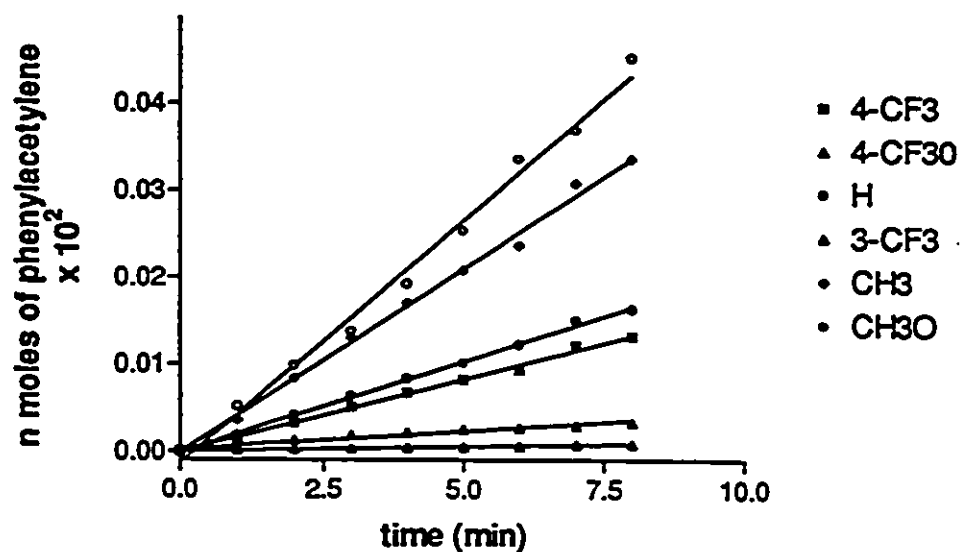


Figure 2.2.3.1A. Moles of photoproduct vs. time plots for the photolysis of 65-70 in deoxygenated pentane solution at  $23 \pm 1^\circ\text{C}$ .

B)

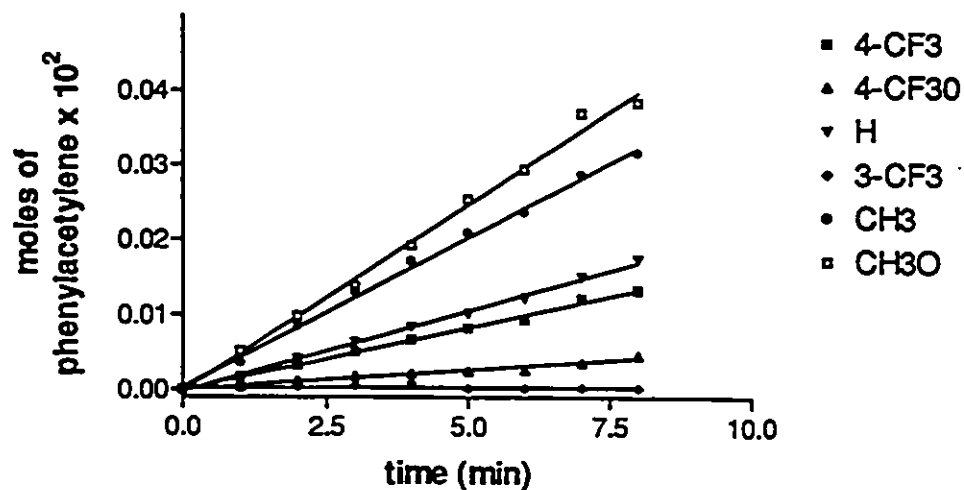
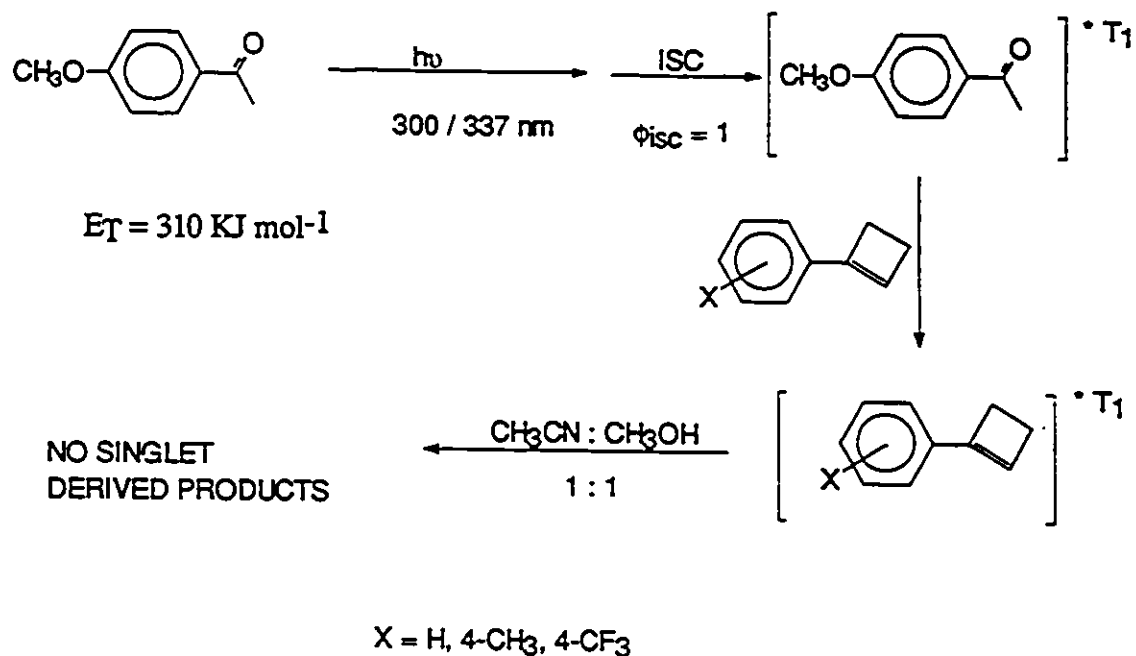


Figure 2.2.3.1B. Moles of photoproduct vs. time plots for the photolysis of 65-70 in deoxygenated acetonitrile solution at  $23 \pm 1^\circ\text{C}$ .

Irradiation of acetonitrile solutions of compounds 66-68 in the presence of 4'-methoxyacetophenone with 300 nm light (conditions where the ketone absorbs > 99 % of the light), resulted in the formation of high molecular weight products which were shown to be dimers of 66-68 by GC/MS analysis. No significant accumulation of the corresponding phenylacetylene was observed in any of the cases studied. Scheme 2.2.3.1 depicts the sensitization process. 4'-Methoxyacetophenone was chosen as sensitizer due to its triplet energy ( $310 \text{ KJ mol}^{-1}$ ) being somewhat higher than that of 1-phenylcyclobutene itself ( $\sim 245 \text{ KJ mol}^{-1}$  116). Triplet energy transfer was verified to occur at near the diffusion controlled rate by nanosecond laser flash photolysis experiments (*vide infra*).



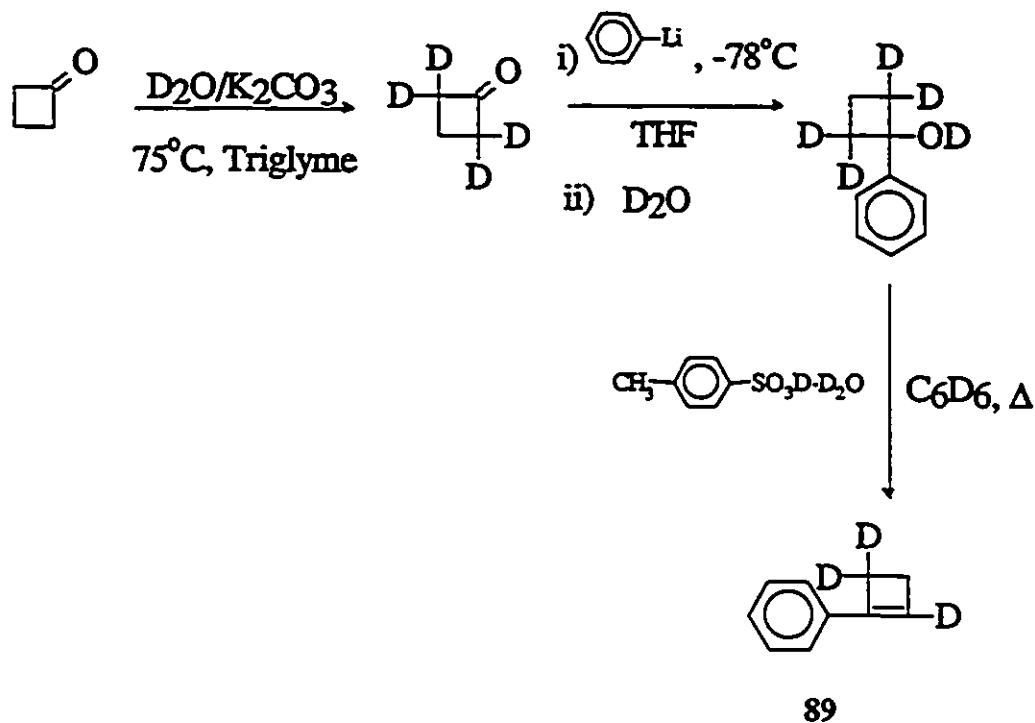
Scheme 2.2.3.1. Energy transfer from 4'-methoxyacetophenone triplet to 1-aryl cyclobutene

Irradiation of cyclohexane solutions of compounds 66-68 in the presence of *trans*-piperylene (*ca.*  $2 \times 10^{-3}$  mol dm<sup>-3</sup>) led to the formation of the corresponding phenylacetylene (78, 79, and 80 respectively) in similar yields to those obtained in the absence of the diene. The last two experiments supported the conclusion that the cycloreversion reaction derives from excitation into the singlet manifold of the 1-phenylcyclobutenes.

In one case (70) direct irradiation led to the formation of substantial amounts of high molecular weight material. These high molecular weight products were tentatively identified as dimers on the basis of GC/MS analyses. These products are not observed, within our limits of detection, upon direct photolyses of compounds 65-69 in dilute deoxygenated pentane or acetonitrile solutions. Photolysis of 70 in pentane in the presence of 1,3-cyclohexadiene in concentration of 0.02 mol dm<sup>-3</sup>, (which has a triplet energy of 219 KJ mol<sup>-1</sup> 117) with 254 nm light resulted in complete suppression of the formation of dimeric products. This experiment seems to indicate that the dimeric products obtained from direct photolysis of 70 are triplet-derived.

The possibility that photocycloreversion proceeds via a similar mechanism to that of alkylcyclobutenes (Introduction 1.3.3) has been investigated with 1-phenylcyclobutene-2,4,4-*d*<sub>3</sub> (89). This compound was synthesized by the route shown in Scheme 2.2.3.2. Photolysis (254 nm) of 89 in deoxygenated acetonitrile solution was carried out to *ca.* 50 % conversion and the starting material was reisolated by semipreparative GC. The <sup>1</sup>H NMR spectrum of the recovered material was indistinguishable from that of freshly-synthesized sample.

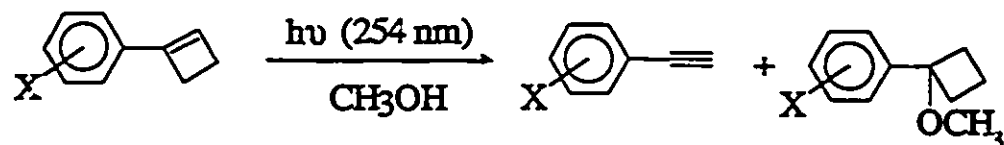




Scheme 2.2.3.2. Synthesis of 1-phenylcyclobutene-d<sub>3</sub>.

#### 2.2.4 Photolyses in Hydroxylic Solvents.

Photolysis of 65-70 in deoxygenated *ca.*  $5 \times 10^{-3}$  mol dm<sup>-3</sup> methanol solutions with 254 nm light affords the respective 1-arylcyclobutyl methyl ethers, 83-88, in high chemical yields (65-90 %) and the respective cycloreversion products, as depicted in Scheme 2.2.4.1. No other products were detected in higher than 5 % yield.

*Cyclobutene**Solvent adduct*

65	X = 4-CH <sub>3</sub> O	83
66	X = 4-CH <sub>3</sub>	84
67	X = H	85
68	X = 4-CF <sub>3</sub>	86
69	X = 4-CF <sub>3</sub> O	87
70	X = 3-CF <sub>3</sub>	88

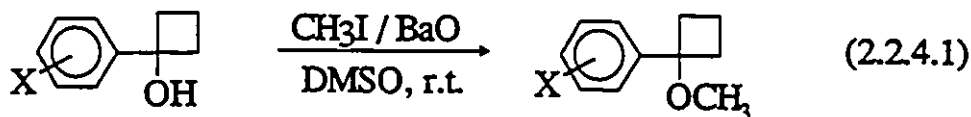
Scheme 2.2.4.1. Photolysis of 1-phenylcyclobutene derivatives in methanol.

Relative quantum yields for the formation of 83-88 from photolyses of cyclobutenes 65-70 in deoxygenated methanolic solutions were calculated from the slopes of photoproduct concentration *versus* irradiation time plots (see Section 2.2.3). Product formation was monitored by gas chromatographic analysis. The relative yields obtained in this fashion were transformed into absolute quantum yield figures by the use of the actinic conversion (Section 2.2.3). These quantum yields are shown in Table 2.2.4.1 (see Appendix 1 for quantum yield calculations).

**Table 2.2.4.1.** Quantum yields for methanol addition and cycloreversion of 1-arylcyclobutenes 65-70 in methanol solution at 23° C.

<i>Cyclobutene</i>	$\phi$ methanol adduct	$\phi$ phenylacetylene
65	0.13 ± 0.02	0.05 ± 0.02
66	0.10 ± 0.02	0.03 ± 0.02
67	0.08 ± 0.01	0.010 ± 0.005
68	0.05 ± 0.01	0.016 ± 0.003
69	0.024 ± 0.007	0.005 ± 0.002
70	0.0006 ± 0.0001	0.0001 ± 0.0001

The 1-arylcyclobutyl methyl ethers (83-88) were identified by coinjection with authentic samples, and by comparison of the mass and infrared spectra of isolated samples with those obtained from the authentic samples. The authentic samples were prepared by methylation of the 1-arylcyclobutanols (71-76) with iodomethane in dimethylsulphoxide in the presence of barium oxide (equation 2.2.4.1), and were identified on the basis of their



<i>Cyclobutanol</i>		<i>Solvent adduct</i>
71	X = 4-CH <sub>3</sub> O	83
72	X = 4-CH <sub>3</sub>	84
73	X = H	85
74	X = 4-CF <sub>3</sub>	86
75	X = 4-CF <sub>3</sub> O	87
76	X = 3-CF <sub>3</sub>	88

$^1\text{H}$  and  $^{13}\text{C}$  NMR, IR and mass spectra and by High Resolution Mass Spectrometry.

Irradiation of acetonitrile : methanol (50:50) solutions of compounds 66-68 in the presence of 4'-methoxyacetophenone with 300 nm light (where compounds 66-68 show only minimal residual absorption), produced no 1-arylcyclobutyl methyl ether or phenylacetylene, but again, high molecular weight material was detected in the reaction mixture. Scheme 2.2.3.1 depicts the sensitization process.

In order to elucidate the extent of reversibility of the protonation step in the photoaddition of solvent to 1-phenylcyclobutenes, an experiment involving the photolysis of 1-phenylcyclobutene 67 in deoxygenated methanol- $\text{d}_4$  was conducted. If the protonation step is reversible, deuterium incorporation in reisolated starting material is expected. The results of the experiment indicate that the recovered starting material contained < 0.5 % of a single deuterium after 50 % conversion of the starting material, as analyzed by mass spectrometric techniques.

### 2.2.5 Fluorescence Spectra of Cyclobutenes 65-70

The fluorescence emission spectra of compounds 65-70 were recorded as very dilute solutions (*ca.*  $5 \times 10^{-6}$  mol  $\text{dm}^{-3}$ ) in acetonitrile, cyclohexane and methanol. The fluorescence excitation spectra of 65-70 match the absorption spectra very closely in all the compounds of the series. Table 2.2.5.1 summarizes the  $\lambda_{\text{max}}$  of fluorescence (emission) along with the singlet excited state energies obtained from the O-O band

(excitation-emission) overlap. The wavelengths for optical excitation are the  $\lambda_{\max}$  values in the respective solvents (Table 2.2.2.1).

**Table 2.2.5.1.** Fluorescence emission maxima and O-O band energies for cyclobutenes 65-70

Solvent	Acetonitrile		Methanol		Pentane	
	$\lambda_{\max}$ em [nm]	$E_{S1}$ [KJ mol <sup>-1</sup> ]	$\lambda_{\max}$ em [nm]	$E_{S1}$ [KJ mol <sup>-1</sup> ]	$\lambda_{\max}$ em [nm]	$E_{S1}$ [KJ mol <sup>-1</sup> ]
<i>Cyclobutene</i>						
65	331	362	-	-	330	363
66	318	376	320	374	335	357
67	320	373	318	377	309	387
68	322	371	320	374	309	387
69	337	355	328	365	335	357
70	331	362	331	361	337	355

Quantum yields of fluorescence were determined in both cyclohexane and acetonitrile as dilute, scrupulously deoxygenated solutions utilizing a primary fluorescence standard (naphthalene,  $\phi_f = 0.23$ ) and are summarized in Table 2.2.5.2 (see Appendix 1 for fluorescence quantum yield determinations).

**Table 2.2.5.2.** Quantum yields of fluorescence of cyclobutenes 65 - 70 determined in deoxygenated acetonitrile (CH<sub>3</sub>CN) and cyclohexane (C<sub>6</sub>H<sub>12</sub>) solutions at 23°C using naphthalene as primary fluorescence standard (estimated error – ± 20 %)

<i>Cyclobutene</i>	$\phi_f$ (CH <sub>3</sub> CN)	$\phi_f$ (C <sub>6</sub> H <sub>12</sub> )
65	0.20	0.20
66	0.22	0.21
67	0.24	0.25
68	0.27	0.25
69	0.31	0.30
70	0.18	0.31

### 2.2.6 Singlet Lifetimes, Fluorescence and Product Quenching Experiments.

Singlet lifetimes were determined by the Time Correlated Single Photon Counting technique in deoxygenated cyclohexane, acetonitrile, and methanol solutions at 23°C. The solvents were checked for background fluorescence before use. A typical fluorescence decay profile and lifetime analysis is shown in Figure 2.2.6.1 for 1-phenylcyclobutene, 67, in dilute, deoxygenated cyclohexane solution. The decays were deconvoluted as single exponentials using a maximum of 10000 total counts in 512 channels. The quality of the fit was judged by the value of the reduced chi square ( $\chi_r^2 \sim 0.9 - 1.1$ ) and the distribution of the residuals. Each lifetime is the average of at least six determinations. These lifetimes are presented in Table 2.2.6.1.

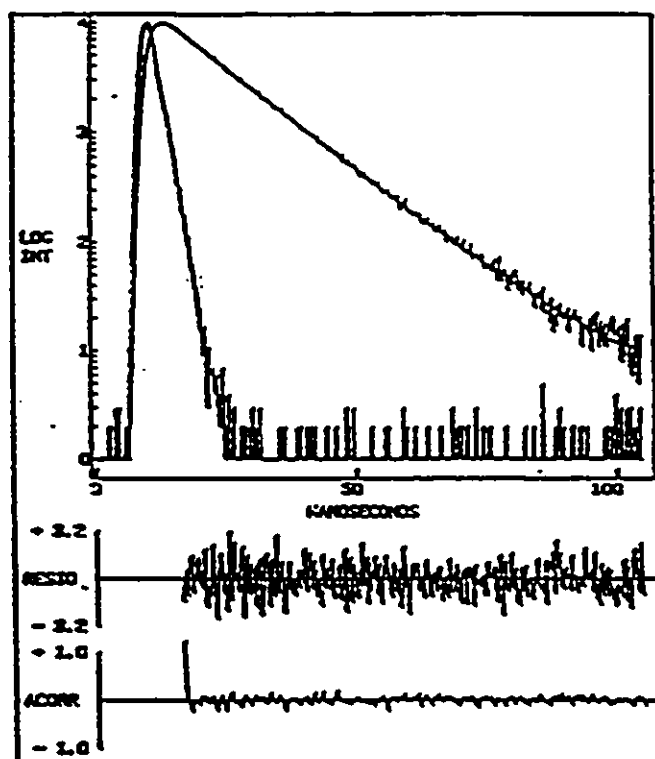


Figure 2.2.6.1. Singlet lifetime decay profile and lifetime analysis for 1-phenylcyclobutene in deoxygenated cyclohexane solution.

**Table 2.2.6.1.** Fluorescence lifetimes measured by the time correlated single photon counting technique for 1-arylcylobutenes 65-70 in deoxygenated cyclohexane, acetonitrile and methanol solutions at 23° C.

<i>Cyclobutene</i>	$\tau$ [ns] <sup>a</sup>		
	C <sub>6</sub> H <sub>12</sub>	CH <sub>3</sub> CN	CH <sub>3</sub> OH
65	12.9	10.2	5.6
66	12.1	9.7	6.6
67	12.2	9.0	7.4
68	12.1	11.8	11.5
69	12.5	11.6	10.8
70	6.7	7.5	7.0

a estimated error ~ 10 %

The steady state fluorescence spectra of compounds 65-70 in dilute deoxygenated acetonitrile solutions were quenched efficiently with 1,1,1,3,3,3-hexafluoro-2-propanol, (HFIP), a hydroxylic solvent of higher acidity and lower nucleophilicity than methanol. Plots of the ratio  $I_0/I$  for compounds 65-70 against HFIP concentration were fitted to the Stern Volmer equation 2.2.6.1, where  $I_0$  and  $I$  signify the fluorescence intensity of compounds 65-70 in the absence and in the presence of HFIP of concentration  $[Q]$ ;  $k_q$  is the rate constant for quenching by HFIP;  $\tau_0$  is the fluorescence lifetime of 65-70 in the absence of HFIP. The  $k_q\tau_0$  values obtained from the slopes of these plots (exemplified in Figure 2.2.6.2 for the quenching of 70 by HFIP) are summarized in Table 2.2.6.2.

$$I_0/I = 1 + k_q\tau_0 [Q] \quad (2.2.6.1)$$



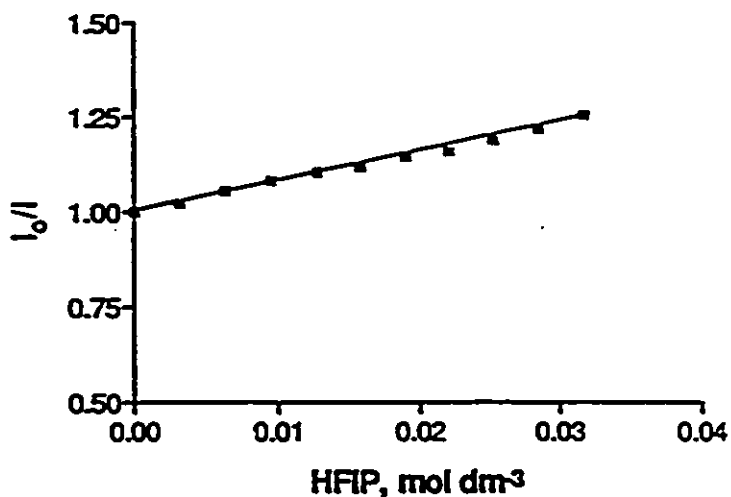


Figure 2.2.6.2. Quenching of the fluorescence of 70 by 1,1,1,3,3,3-hexafluoro-2-propanol

Singlet lifetimes were also determined in neat 2,2,2-trifluoroethanol and HFIP for the unsubstituted 1-phenylcyclobutene derivative 67, and are summarized in Table 2.2.6.3.

Singlet lifetime quenching experiments for 65-67 in dilute deoxygenated acetonitrile solutions were also attempted, using methanol as quencher. These plots are shown in Figure 2.2.6.3. Bimolecular quenching rate constants ( $k_q^{\text{MeOH}}$ ) were estimated from the slopes of the low concentration portions of these plots ( $\leq 0.7 \text{ mol dm}^{-3}$ ) according to equation 2.2.6.2 (where  $\tau_{(\text{MeOH})_x}$  is the lifetime of the phenylcyclobutene in the presence of methanol and  $\tau^\circ$  is the lifetime in acetonitrile), and are listed in Table 2.2.6.4 along with the Stern-Volmer constants  $K_{SV}$  resulting from the product  $k_q^{\text{MeOH}} \times \tau^\circ$ . The extrapolated singlet lifetimes (at pure methanol concentration) resulting from these plots are also shown in Table 2.2.6.4 as  $\tau_{\text{MeOH}}(\text{ext.})$ .

$$1/\tau_{(\text{MeOH})_x} = 1/\tau^\circ + [\text{MeOH}]_x k_q^{\text{MeOH}} \quad (2.2.6.2)$$

**Table 2.2.6.2.** Stern Volmer values for the fluorescence quenching of compounds 65-70 by hexafluoroisopropanol in deoxygenated acetonitrile solutions

<i>Cyclobutene</i>	$k_q \tau$ [mol <sup>-1</sup> dm <sup>3</sup> ]	$\lambda_{em}$ [nm]
65	25 ± 2	331
66	22 ± 1	318
67	15 ± 2	320
68	10 ± 1	322
69	7.6 ± 0.6	337
70	6.5 ± 0.4	331

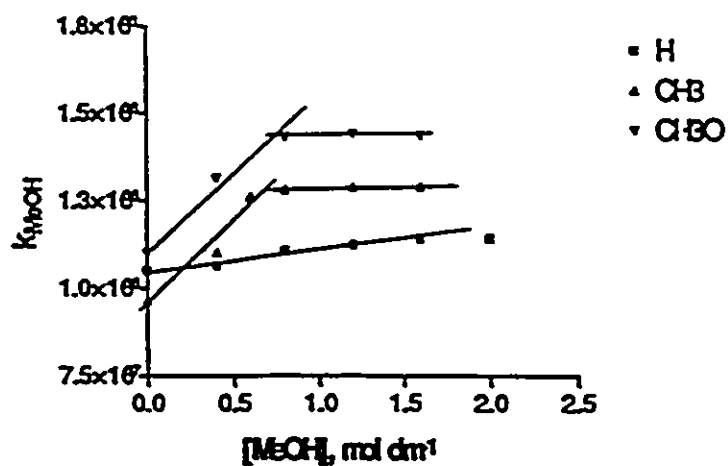
**Table 2.2.6.3.** Fluorescence lifetimes of 1-phenylcyclobutene in various solvents, measured at 23° C.

SOLVENT	$\tau$ [ns] ± 10 %
C <sub>6</sub> H <sub>12</sub>	12.2
CH <sub>3</sub> CN	9.0
CH <sub>3</sub> OH	7.4
CF <sub>3</sub> CH <sub>2</sub> OH	2.8
CF <sub>3</sub> CHOHCF <sub>3</sub>	0.5

**Table 2.2.6.4.** Bimolecular quenching rate constants  $k_q^{\text{MeOH}}$ , Stern Volmer values  $K_{\text{SV}}^1$  and extrapolated lifetimes in pure methanol  $\tau_{\text{MeOH}}(\text{ext.})^1$ , obtained from singlet lifetime quenching experiments of cyclobutenes 65-67 by methanol in deoxygenated acetonitrile solutions.

<i>Cyclobutene</i>	$k_q^{\text{MeOH}}$ [mol <sup>-1</sup> dm <sup>3</sup> s <sup>-1</sup> ]	$K_{\text{SV}}$ [mol <sup>-1</sup> dm <sup>3</sup> ] ( $\epsilon \sim \pm 20\%$ )	$\tau_{\text{MeOH}}(\text{ext.})$ [ns]
65	$1.5 \times 10^8 \pm 0.6 \times 10^8$	1.5	7
66	$5.0 \times 10^7 \pm 1.0 \times 10^7$	0.49	8
67	$5.8 \times 10^6 \pm 0.5 \times 10^6$	0.043	9

1 Defined in the preceding text



**Figure 2.2.6.3.** Stern Volmer plot for the singlet lifetime quenching of 65-67 by methanol in deoxygenated acetonitrile solution.

The fluorescence of 1-phenylcyclobutene 67 is readily quenched by oxygen. It was found that the rate constant for quenching of the singlet excited state of 67 with oxygen

approaches diffusion control in acetonitrile solution, and it was assigned a value of  $2.0 \times 10^{10} \text{ mol}^{-1} \text{ dm}^3 \text{ s}^{-1}$ , obtained from the lifetimes of 67 in nitrogen and air saturated solutions (9.0 and 6.0 ns, respectively).

The photolysis of compound 67 in deoxygenated acetonitrile solution containing varying amounts of methanol with 254 nm light was undertaken. This experiment was aimed at constructing a Stern Volmer plot for the quenching of the singlet excited state of 67 by methanol utilizing product analyses instead of fluorescence quenching measurements. The plot for the quenching of 1-phenylacetylene formation by methanol is illustrated in Figure 2.2.6.4. From the slope of this plot ( $k_q\tau$  value, see equation 2.2.6.1) a value of the Stern-Volmer constant for the quenching of 1-phenylacetylene formation by methanol was found to be  $0.046 \pm 0.003 \text{ mol}^{-1} \text{ dm}^3$ .

Figure 2.2.6.5 shows a reciprocal plot of the yield of the ether adduct 85 obtained in these experiments as a function of methanol concentration. The intercept/slope ratio calculated by least squares analyses of the data (using equation 2.2.6.3) affords  $k_q\tau = 0.02 \pm 0.01 \text{ mol}^{-1} \text{ dm}^3$ . In this equation,  $\phi_{\text{methanol}}$  signifies the yield of the ether adduct,  $k_q$  is the overall rate constant for formation of the methanol adduct,  $k_q^{\text{MeOH}}$  is the rate constant for excited state quenching by methanol, and  $\Sigma k'$  is the inverse of the lifetime of 67 in the given solvent. This value of  $k_q\tau$  is considered to be a lower limit owing to the poor precision of the data at lower methanol concentrations.

$$1/\phi_{\text{methanol}} = (\Sigma k')/k_q^{\text{MeOH}} 1/[\text{MeOH}] + k_q/k_q^{\text{MeOH}} \quad (2.2.6.3)$$

Table 2.2.6.5 summarizes the Stern-Volmer constants for the quenching of singlet excited 67 by methanol obtained according to the experiments described above.

Table 2.2.6.5. Quenching rate constants and Stern Volmer values.

<i>Method</i>	<i>Figure</i>	$k_Q\tau$ [mol <sup>-1</sup> dm <sup>3</sup> ]	$k_Q$ [mol <sup>-1</sup> dm <sup>3</sup> s <sup>-1</sup> ]
Singlet Lifetime Quenching	2.2.6.3	0.043±0.005	5.8 x 10 <sup>6</sup> ±0.5 x 10 <sup>6</sup>
Phenylacetylene Quenching	2.2.6.4	0.046±0.003	6.2 x 10 <sup>6</sup> ±0.4 x 10 <sup>6</sup>
Inverse [Ether] vs. [MeOH]	2.2.6.5	0.02±0.01	3 x 10 <sup>6</sup> ±2 x 10 <sup>6</sup>

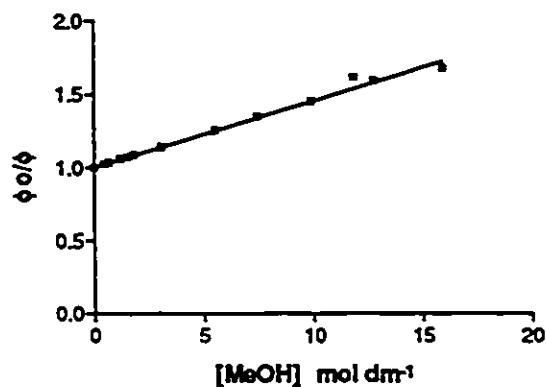


Figure 2.2.6.4. Stern Volmer plot for the quenching of the formation of phenylacetylene by methanol.

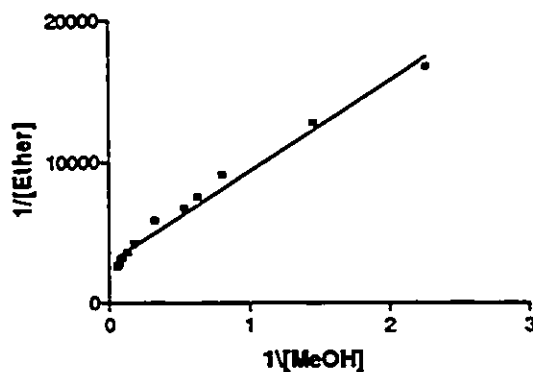


Figure 2.2.6.5. Reciprocal plot of the yield of ether adduct 85 as a function of methanol concentration

### 2.2.7 Direct Detection of the Triplet States of 1-Phenylcyclobutene Derivatives.

The phosphorescence emission spectrum of compound **67**<sup>116</sup> was recorded in a methylocyclohexane glass matrix at 77 K and is shown in Figure 2.2.7.1. The triplet lifetime of compound **67** was measured under these conditions and found to be 4.1118a ms .

Triplet-triplet absorption spectra were measured for compounds 66-68 in rigorously deoxygenated acetonitrile solutions by Nanosecond Laser Flash Photolysis techniques (NLFP) and are shown in Figure 2.2.7.2. Table 2.2.7.1 summarizes the triplet-triplet absorption maxima of compounds 66-68.

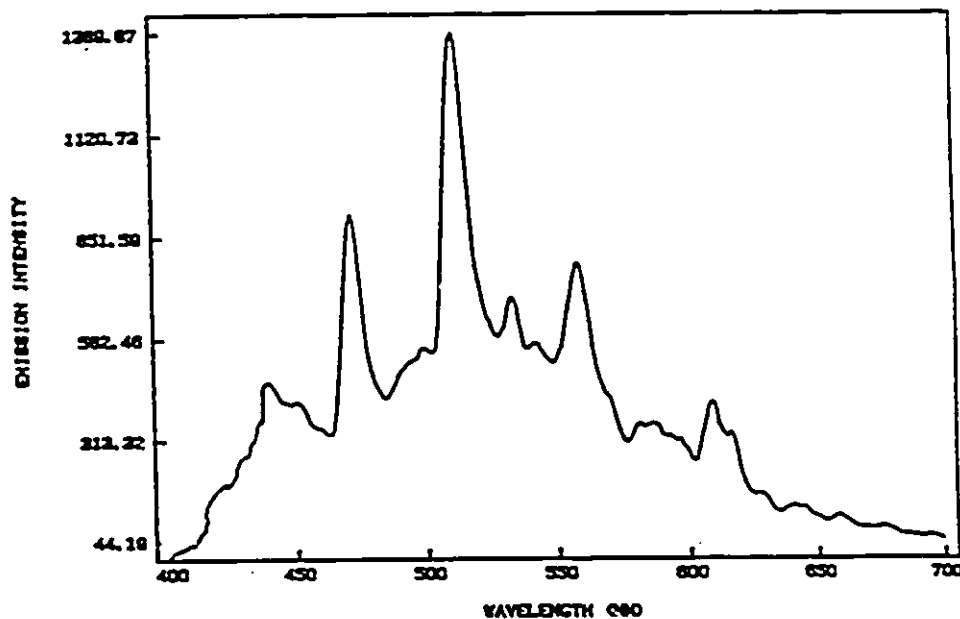


Figure 2.2.7.1. Phosphorescence spectrum of **67** in a methylocyclohexane glass matrix recorded at 77 K

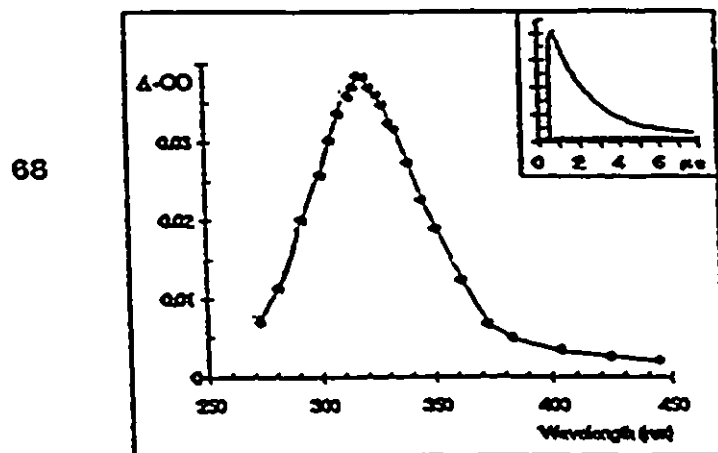
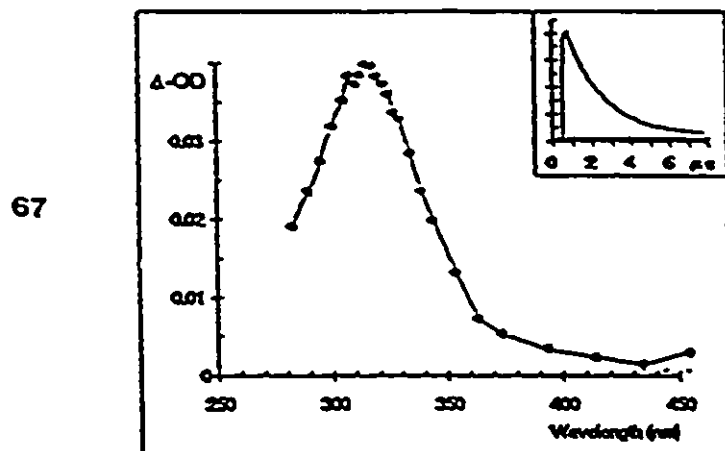
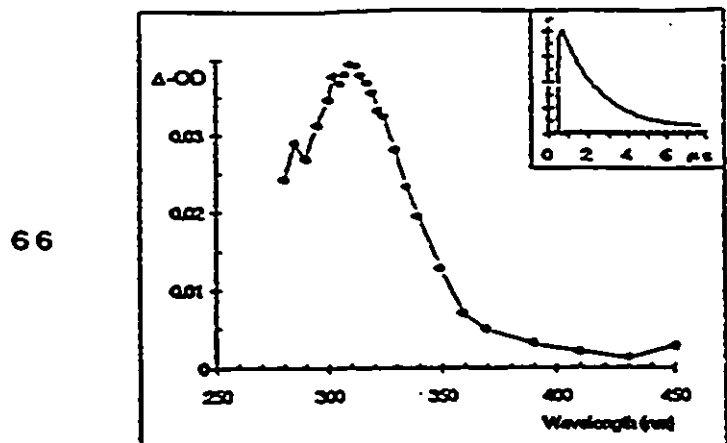


Figure 2.2.7.2. Triplet-Triplet absorption spectra of 66-68 in deoxygenated acetonitrile solution as measured by NLFP

**Table 2.2.7.1.** Triplet-Triplet absorption maxima for compounds 66-68, as determined by NLFP in deoxygenated acetonitrile solutions





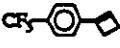





<i>Cyclobutene</i>	$\lambda_{\max}$ [nm]
66	312
67	308
68	320

The triplet state assignment for these spectra was confirmed by standard quenching experiments, in that the lifetimes of the transients giving rise to the spectra in Figure 2.2.7.2 are shortened in the presence of *trans*-piperylene. Table 2.2.7.2 summarizes the rate constants for triplet quenching of compounds 66-68 by *trans*-piperylene and other quenchers, obtained according to equation 2.2.7.1 (where  $k_d$  represents the pseudo first order rate constant for decay, and  $k_0$  is the rate constant for decay in the absence of added quencher Q). It was also verified by NLFP techniques that 1-phenylcyclobutene quenches 4'-methoxyacetophenone triplets with a rate constant of  $(2.71 \pm 0.09) \times 10^9 \text{ dm}^3 \text{ mol}^{-1} \text{ s}^{-1}$  in acetonitrile solution.

$$k_d = k_0 + k_q [Q] \quad (2.2.7.1)$$



**Table 2.2.7.2.** Rate constants for triplet quenching obtained by NLFP in deoxygenated solutions

<i>compound</i>	$\lambda_{exc.}$ [nm]	$\lambda_{analysis}$ [nm]	<i>Solvent</i>	<i>Quencher</i>	$k_q \times 10^{-9}$ [s mol <sup>-1</sup> dm <sup>3</sup> ]
 67	248	320	C <sub>6</sub> H <sub>12</sub>		1.58±0.06
 67	248	320	C <sub>8</sub> H <sub>18</sub>		4.6±0.8
 68	248	320	C <sub>8</sub> H <sub>18</sub>		1.70±0.06
 66	248	310	C <sub>6</sub> H <sub>12</sub>		1.44±0.06
 66	337	385	CH <sub>3</sub> CN		2.71±0.09

### 2.2.8 Cation Intermediacy in the Photolysis of 1-Arylcyclobutenes in hydroxylic solvents.

Nanosecond Laser Flash Photolysis experiments were conducted utilizing a deoxygenated solution of 66 in 2,2,2-trifluoroethanol. The transient spectrum thus obtained is shifted to longer wavelengths with respect to that of the triplet obtained in acetonitrile solution (see Figure 2.2.7.1). This spectral shift is illustrated in Figure 2.2.8.1.

The lifetime of the intermediate was shortened by addition of methanol to the solution, yielding a bimolecular rate constant of  $3.2 \pm 0.8 \times 10^5 \text{ mol}^{-1} \text{ s}^{-1} \text{ dm}^3$ .

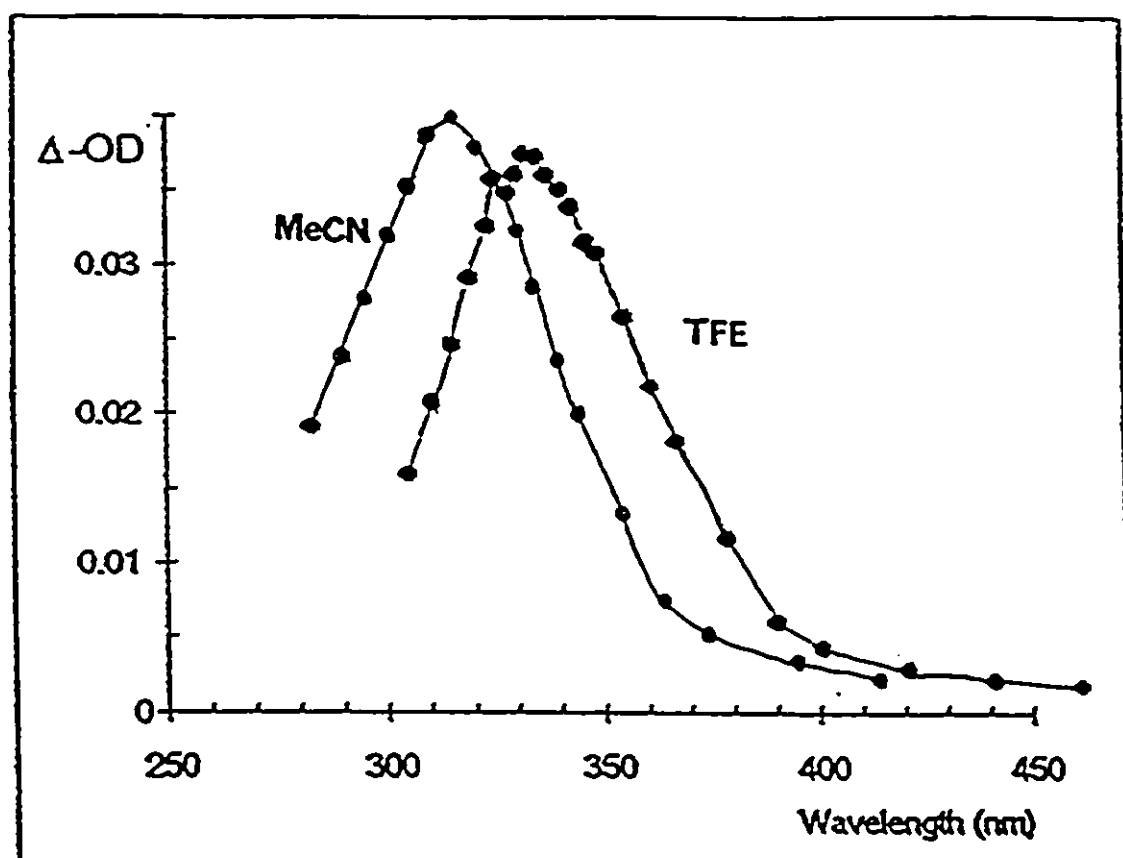
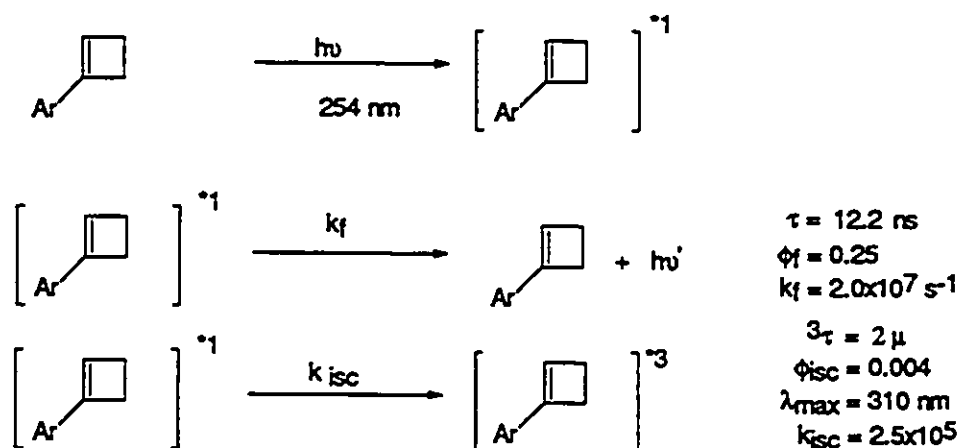


Figure 2.2.8.1. Spectral shift obtained for the transients generated upon 248 nm laser pulse excitation of 66 in acetonitrile ( $\lambda_{\text{max}} = 308 \text{ nm}$ ) and trifluoroethanol ( $\lambda_{\text{max}} = 337 \text{ nm}$ ) solutions.

## 2.3 DISCUSSION

### 2.3.1 General Aspects of the Photochemistry and Photophysics of 1-Phenylcyclobutenes

The values of  $\phi_f$  (= 0.24) and  $\tau_s$  (= 12.2 ns) reported for **67** in pentane solution at room temperature are both in reasonable agreement with those reported by H.E. Zimmerman and coworkers for the same compound in methylcyclohexane / isopentane solution at 27°C ( $\phi_f$  = 0.27;  $\tau_s$  = 15.9 ns  $\pm$  0.9 ns<sup>118a</sup>). These authors also reported a value of  $\phi_{ISC}$  = 0.004 for the quantum yield of intersystem crossing in **67**, determined by the biacetyl phosphorescence sensitization method<sup>118b</sup>. Thus, intersystem crossing is over an order of magnitude less efficient than either fluorescence or reaction via [2 + 2]-cycloreversion ( $\phi_{79}$  = 0.09), and the combination of these three processes accounts for only about 40 % of excited state decay events. Presumably, nonproductive radiationless decay processes account for the rest (see Scheme 2.3.1.1).

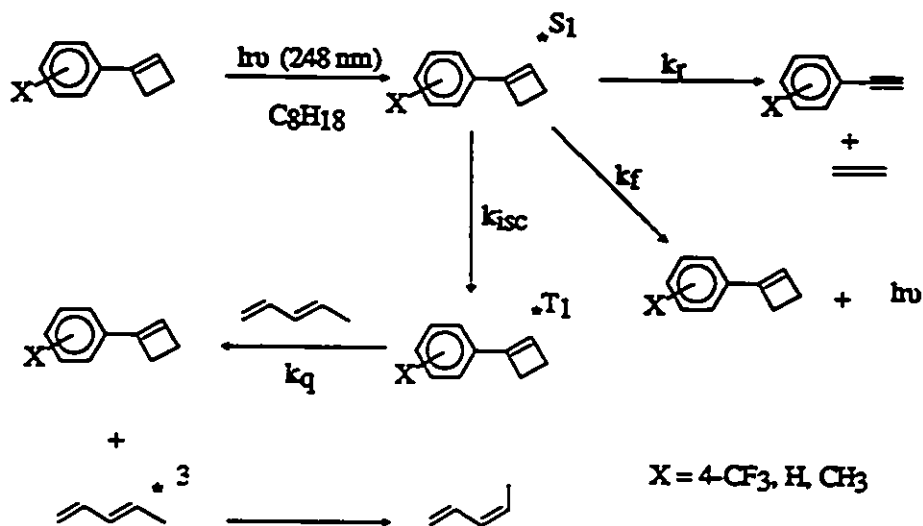


Scheme 2.3.1.1. Deactivation pathways of 1-phenylcyclobutene

Ramamurthy and coworkers<sup>116</sup> observed phosphorescence from 1-phenylcyclobutene (**67**) included in a thallium - exchanged zeolite at 77 K. Our results demonstrate that it is possible to detect phosphorescence from **67** in a rigid glass such as methylcyclohexane at 77 K (Figure 2.2.7.1). The triplet lifetime for compound **67** has been estimated by Zimmerman and coworkers<sup>118a</sup> to be ca.  $3.6 \pm 2.0$  ms; the value reported in this thesis is  $4.3 \pm 0.1$  ms.

Triplet states of 1-arylcyclobutenes can also be readily detected by Nanosecond Laser Flash Photolysis (NLFP) techniques. The triplet-triplet absorption spectra of **66-68** are shown in Figure 2.2.7.2. The triplet-triplet absorption maximum for **67** is similar to that reported by Caldwell and coworkers for 1-phenylcyclopentene<sup>137</sup>. The triplet lifetimes and the triplet-triplet absorption spectra of **66-68** appear to be rather insensitive to substituent on the aryl ring or solvent polarity. The rate constants for triplet quenching by dienes (*e.g.*, *trans*-piperylene, Table 2.2.7.2) are significantly slower than the diffusion-controlled rates in both acetonitrile and isooctane. This is not surprising, since the triplet energy of **67** is ca.  $240 \text{ KJ mol}^{-1}$ <sup>118</sup>, approximately isothermal with the diene triplet energy. The triplet energy transfer process from arylcyclobutene to *trans*-piperylene is depicted in Scheme 2.3.1.2.

As was mentioned in Section 2.2.3, direct triplet reactivity was observed upon photolysis of **70** in aprotic solvents. Direct irradiation of **70** led to the formation of substantial amounts of high molecular weight products, which were suppressed when the irradiation was carried out in the presence of 1,3-cyclohexadiene, indicating that the high molecular weight products are triplet-derived. GCMS evidence suggests that these products are dimers of **70**. The propensity of phenylalkene triplets towards dimerization is well documented<sup>106</sup>.



Scheme 2.3.1.2. Triple energy transfer from arylcyclobutene to *trans*-piperylene

The results from these series of experiments confirm that in spite of the low quantum yield of intersystem crossing observed for 67, its triplet state is readily detectable upon direct irradiation by NLFP or phosphorescence techniques (Figures 2.2.7.1 and 2.2.7.2 respectively). Furthermore, the triplet state can alternatively be produced by triplet sensitization, or quenched by dienes (Scheme 2.2.3.1 and 2.3.1.2 respectively).

The fluorescence emission maxima of 65-70 vary slightly between 320-330 nm, but show no regular variation with substituent or solvent throughout the series (Table 2.2.5.1). The emission bands show minor fine structure in pentane, but are approximately gaussian in acetonitrile solution. On the other hand, the fluorescence quantum yields increase throughout the series in both solvents (Table 2.2.5.2) while the singlet lifetimes remain approximately invariant, with the exception of that of 70 (Table 2.2.6.1).

Irradiation of 65-70 in aprotic solvents results in the formation of the corresponding phenylacetylenes 77-82 (equation 2.2.3.1) in high chemical yield. The

reaction is singlet-derived, as evidenced by the lack of observable quenching of the formation of 78-80 from photolysis of 66-68 in the presence of diene (Scheme 2.3.1.2), and the fact that 77-82 are not formed under triplet sensitization conditions (Scheme 2.2.3.1). Irradiation of 65-70 in methanol solution affords the corresponding solvent adducts 83-88 and the phenylacetylenes 77-82 (equation 2.2.4.1). The former reaction also occurs from the lowest excited singlet state, as evidenced by the shorter fluorescence lifetimes observed for 65-67 in methanol compared to those in acetonitrile (Table 2.2.6.1), the substantial quenching of the formation of cycloreversion products in methanol and methanol-acetonitrile, and the fact that the reaction is not quenched by dienes (Scheme 2.3.1.2). In the case of 67, the Stern Volmer constant obtained from the quenching of phenylacetylene formation by methanol in acetonitrile (Figure 2.2.6.4) agrees with that obtained from the reciprocal plot for the formation of cyclobutyl ether 85 (Figure 2.2.6.5). The Stern Volmer constant ( $k_q\tau = 0.046 \pm 0.003 \text{ mol}^{-1} \text{ dm}^3$ ) affords a quenching rate constant  $k_q = 5.1 \times 10^6 \text{ mol}^{-1} \text{ dm}^3 \text{ s}^{-1}$ , in satisfactory agreement with the rather imprecise value measured by single photon counting techniques ( $k_q = (5.1 \pm 1.4) \times 10^6 \text{ mol}^{-1} \text{ dm}^3 \text{ s}^{-1}$ ). These experiments support the idea that both cycloreversion and solvent addition photoreactions arise from the lowest excited singlet states of 1-arylcyclobutenes.

By simple inspection of Table 2.2.3.1, those phenylcyclobutenes with electron withdrawing substituents (68-70) show reduced quantum yields for cycloreversion. An analogous situation was observed for the bicyclic alkylcyclobutenes 31-33, equation 1.3.3.5, for which quantum yields of cycloreversion are summarized in Table 1.3.3.2. The fragmentation yield for compound 33 (with trifluoromethyl substitution) is five times lower than that for the unsubstituted bicyclic cyclobutene 32. However, in these systems, as was previously pointed out, the reactive manifold towards fragmentation ( $\pi, R(3s)$ ) is

destabilized by an electron withdrawing group such as trifluoromethyl. This analogy with 1-phenylcyclobutenes could be only coincidental, as the reactive singlet manifold in 1-aryl-substituted cyclobutenes is the  $\pi,\pi^*$  state which is expected to be practically invariant to that kind of substitution<sup>1</sup>. The mechanism of [2 + 2] photocycloreversion in alkylcyclobutenes may involve the intermediacy of cyclopropyl carbenes (Introduction 1.3.3).

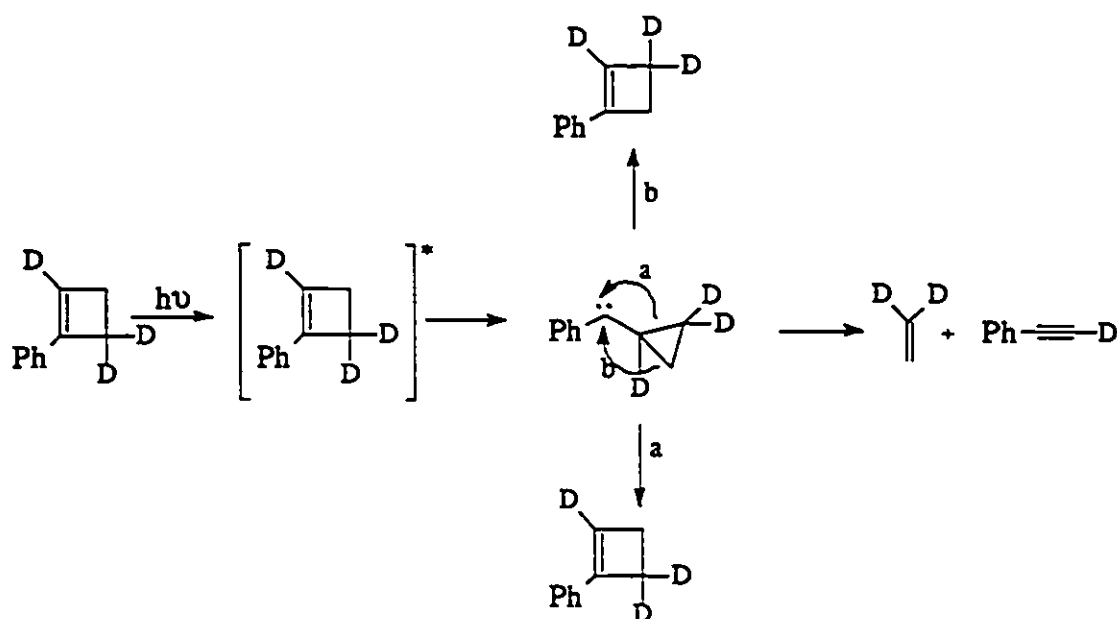
While there is substantial precedent for Rydberg-derived [1,2]-shifts in the photochemistry of aliphatic alkenes and cycloalkenes<sup>119b</sup>, there appear to be few examples<sup>119c</sup> of such processes yielding carbenes in phenylalkene photochemistry. Although the excited singlet state behavior of most of the phenylalkenes that have been studied is dominated by torsional relaxation (with the consequence that carbene-derived products might be difficult to detect in significant yield, particularly when the carbene intermediate can revert to starting olefin), rearrangements of this type have not been observed even in the torsionally constrained phenylcycloalkenes that have been investigated in detail<sup>119d</sup>.

The photochemistry of 2,2,4-trideuterio-1-phenylcyclobutene (89) in acetonitrile solution was investigated in order to probe for skeletal rearrangements which might be indicative of the intermediacy of a cyclopropyl carbene in the [2 + 2] cycloreversion process. If cycloreversion proceeds via such an intermediate (Scheme 2.3.1.3), then one would expect to observe scrambling of deuteria between positions 3 and 4 of the cyclobutyl ring, since carbenes of this type are known to undergo ring expansion to the corresponding cyclobutene in addition to fragmentation to alkene and alkyne<sup>45, 55</sup>.

---

<sup>1</sup>If this analogy is not purely coincidental, then the involvement of the  $\pi,\pi^*$  state in the cycloreversion process of alkyl-substituted cyclobutenes could be playing a role. The tacit implication is therefore that the retrocycloaddition reaction in alkyl-substituted cyclobutenes could arise from both valence ( $\pi,\pi^*$ ) and Rydberg ( $\pi,R(3s)$ ) excited states.

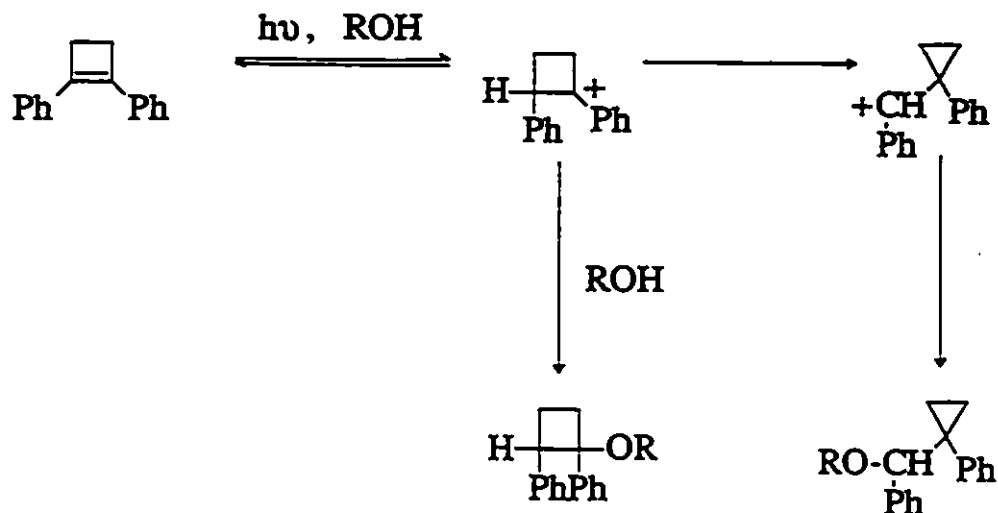
Examination of the  $^1\text{H}$  NMR spectrum of an irradiated  $0.02 \text{ mol dm}^{-3}$  solution of **89** after *ca.* 50 % conversion affords no evidence for significant scrambling of the label between the two positions. We thus conclude that 1,2-rearrangements leading to cyclopropylcarbenes are unimportant in this case. This is consistent with cycloreversion occurring by a concerted  $[\sigma_{2s} + \sigma_{2s}]$  mechanism.



Scheme 2.3.1.3. Conjectural mechanism for cycloreversion of **67** via cyclopropyl carbene intermediates

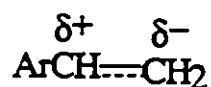
In 1974, Hasegawa and coworkers reported the photoaddition of methanol to 1,2-diphenylcyclobutene (equation 1.3.1.2). They interpreted the addition as taking place via a cyclobutyl and cyclopropylmethyl cations, according to Scheme 2.3.1.4.





Scheme 2.3.1.4. Mechanism for addition of methanol to 1,2-diphenylcyclobutene

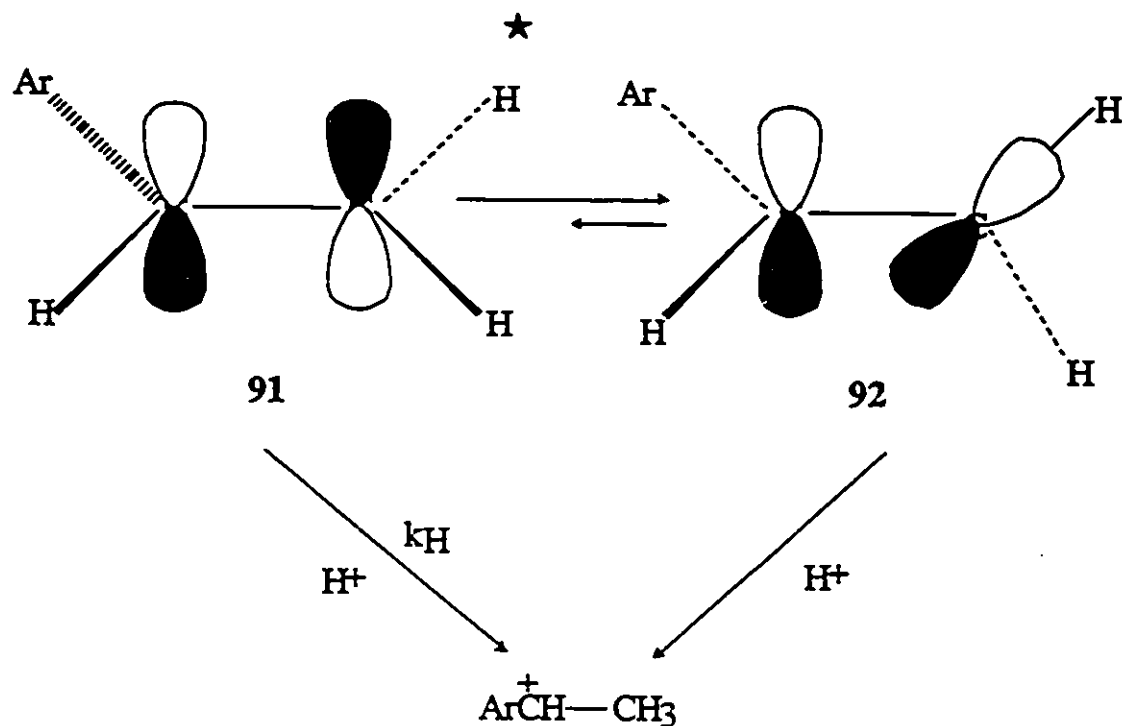
The polarized nature of the excited state of styrenic compounds has been well established by Yates and coworkers<sup>109, 110, 120 - 132</sup>, who rationalized the facile photoprotonation of these systems by postulating that the  $S_1$  state possesses charge-transfer character, as shown by 90.



90

Since fluorescence quenching was observed concurrently with acid-catalyzed photohydration, the protonation step,  $k_H$ , must be to the planar vertical  $S_1$  state (91) of these alkenes, rather than the twisted zwitterionic state (92) (Scheme 2.3.1.5). Twisted zwitterionic (or diradicaloid) states of alkenes are nonfluorescent since they can readily deactivate to  $S_0$  via rapid internal conversion<sup>110</sup> (Figure 2.3.1.1). Theoretical calculations by Nebot - Gil and Malrieu suggested that the lowest ionic singlet state of

styrene has the benzyl moiety with the positive charge, and the  $\beta$  carbon (where protonation takes place) bears the negative charge<sup>133</sup>.



Scheme 2.3.1.5. Deactivation pathways of singlet excited 1-phenylcyclobutenes

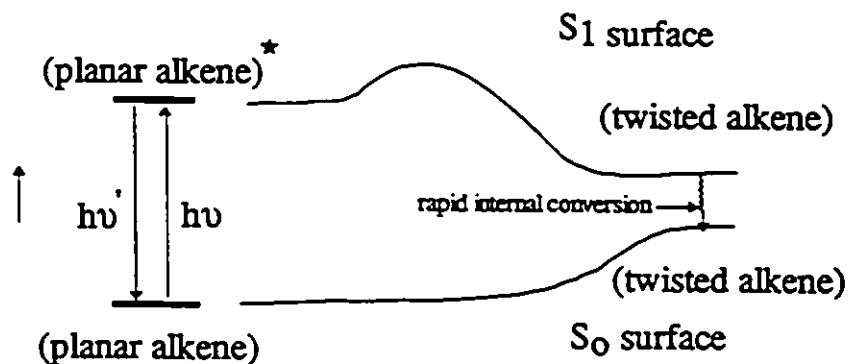
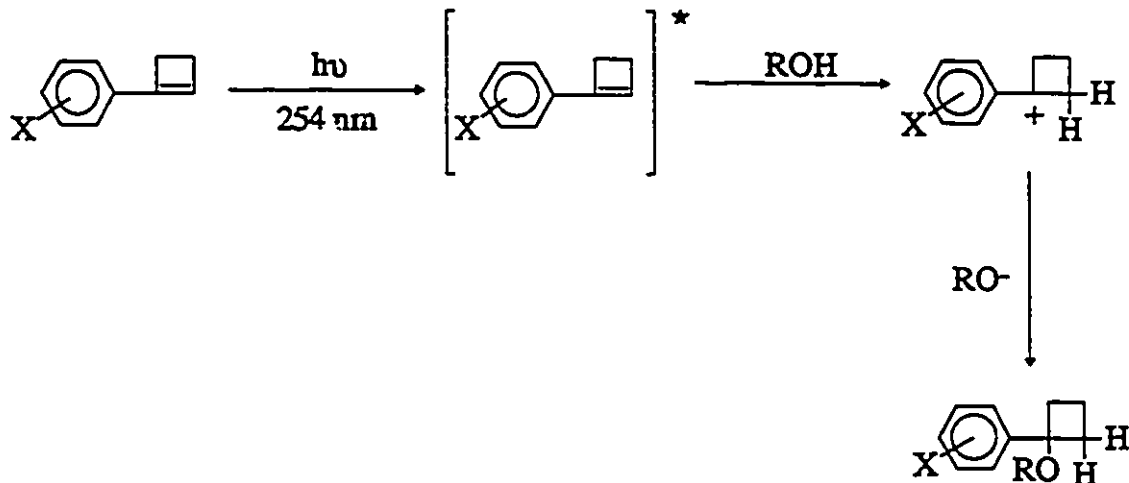


Figure 2.3.1.1. Relative energy levels for twisting about the ethylene moiety in the ground and excited state surfaces

It is reasonable to assume that a similar mechanism is in operation for the photoaddition of solvent to 1-arylcyclobutenes, and that mechanism is proposed in Scheme 2.3.1.6, with proton addition as the rate determining step for excited state decay followed by nucleophilic attack of the arylcyclobutyl cation by the solvent (methanol). This mechanism is supported by the fact that the fluorescence of compounds 65-70 is readily quenched by acidic solvents such as 2,2,2-trifluoroethanol (TFE) and 1,1,1,3,3,3-hexafluoro-2-propanol (HFIP). If the rate determining step in the photoreaction of 1-arylcyclobutenes with methanol were nucleophilic attack by the solvent, an opposite trend to that observed would be expected (the singlet lifetimes would correlate with the solvent nucleophilicity rather than with the solvent acidity). Table 2.2.6.3 shows the dependence of the singlet fluorescence lifetime on the solvent acidity.



Scheme 2.3.1.6. Mechanism for solvent addition to 1-phenylcyclobutene showing proton transfer and nucleophilic attack by the solvent

McClelland and coworkers<sup>142a</sup> reported the observation of a number of substituted benzyl cations by nanosecond laser flash photolysis experiments conducted in solvents

such as TFE and HFIP. They found that the UV absorption maxima of the transients generated upon 248 nm laser excitation lie between 310 and 320 nm. The same authors also investigated the cumyl and phenylethyl cations, which exhibit red shifted absorptions with respect to the benzyl cations. Particularly, for the 4-methylcumyl cation, a maximum of absorption at 340 nm with a shoulder at 380 nm was reported in TFE as solvent. The lifetime of the 4-methylcumyl cation in TFE was measured to be 100 ns.

In the present study, a maximum of absorption at 337 nm was obtained for the transient generated upon photolysis of 4-tolylcyclobutene (66) in TFE with 248 nm laser flash photolysis. The transient  $\lambda_{\text{max}}$  is red-shifted 25 nm with respect to the triplet-triplet transient absorption spectrum measured for the same compound in acetonitrile solution, and is at a similar position to that of the 4-methylcumyl cation reported by McClelland. The transient at 337 nm is thus tentatively assigned to the 1-(p-tolyl)-cyclobutyl cation (Figure 2.2.8.1). Its lifetime is shortened by addition of methanol to the solution, yielding a bimolecular rate constant of  $3.2 \pm 0.8 \times 10^5 \text{ mol}^{-1} \text{ s}^{-1} \text{ dm}^3$ . This is in good agreement with the value of  $3.4 \times 10^5 \text{ mol}^{-1} \text{ s}^{-1} \text{ dm}^3$  reported by McClelland and coworkers<sup>142a</sup> for the quenching of the cumyl cation by methanol in HFIP. It is tentatively concluded that 1-arylcyclobutyl ions are true intermediates in the photoaddition of hydroxylic solvents to 1-phenylcyclobutene derivatives.

Scheme 2.2.4.2 depicts the absence of deuterium incorporation in the starting material upon photolysis of 1-phenylcyclobutene (67) in methanol- $\text{d}_4$ . This experiment rules out the possibility that photoprotonation of 1-phenylcyclobutene derivatives is reversible, either in the excited state or in the ground state of the cation.

Yates and coworkers used emission decay profiles as an indication of reversibility of the photoprotonation reaction<sup>130</sup>. Their emission decays were single-exponential and

hence they concluded that the feed-back step  $k_{\text{F}}$  (from Scheme 2.3.1.6) was negligible. As mentioned in Section 2.2.6, the singlet lifetimes for compounds of 65-70 are also single exponentials, which supports the idea that excited state photoprotonation proceeds irreversibly.

### 2.3.2 Substituent Effects on the Photochemistry and Photophysics of 1-Phenylcyclobutene

Reported experimental reactivity data on excited states have generally been analyzed in terms of ground state substituent constants<sup>119</sup> ( $\sigma$ ,  $\sigma^+$ ,  $\sigma^-$ ), implying that substituent effects are not affected by changing the electronic state. Data on excited state reactivity are most readily available for singlet acidities<sup>120</sup>, and a particularly large number of results are available for the  $\text{pK}_a^*$  values of substituted phenols. These data correlate only qualitatively with ground state substituent constants, the correlation being particularly poor for *meta* substituents. Wehry and Rogers<sup>124</sup> showed that conjugative effects are much more important than inductive effects in electronically excited states and that direct resonance interactions involving *meta* substituents are considerably more significant in the excited state than they are in the ground state.

Yates and coworkers<sup>125</sup> attempted to derive a substituent parameter scale for excited-state reactions based on the acid catalyzed photoaddition of water across the multiple bond of the side chain of styrenes and phenylacetylenes. However, their choice of substituents was limited to hydrogen, fluoro, alkyl and alkoxy groups. The trifluoromethyl group could not be included in their scale due to its extremely slow photoprotonation

reaction compared to other modes of excited state decay. Similarly, bromo and chloro substituents could not be evaluated (these substituents lead to homolytic cleavage and biphenyl type products).

Baldry<sup>126</sup> derived a set of substituent constants for the excited state,  $\sigma_{ex}$ , using the  $pK_a^*$  of phenols obtained from Forster cycle analysis of the 0-0 fluorescence bands of the protonated and unprotonated species, or from the pH dependence of fluorescence. He defined  $\sigma_{ex}$  according to equation 2.3.2.1:

$$\sigma_{ex} = (pK_a^* - 3.804)/-3.10 \quad (2.3.2.1)$$

Zimmerman and coworkers<sup>127</sup> investigated the so called *meta* effect of substituents in the excited state. The observation that a methoxy substituent in the *meta* position exerts an effect that is contrary to ground state expectations was rationalized by the changes in charge density (as calculated by Hückel MO theory) that occur on excitation. In the excited state, a methoxy group is predicted to be a better electron donor from the 3-position (i.e. *meta*) than from the 4-position<sup>128</sup>. In an analogous fashion, a trifluoromethyl group is predicted to be a better electron withdrawing group from the 3-position than from the 4-position in the excited state.

In order to establish a correlation with substituent constants, it is necessary to extract rate constants for the photoprocesses of interest. This is possible using quantum yield data in conjunction with lifetime data. The rate constants for fluorescence decay  $k_f$  are calculated from equation 2.3.2.2 (where  $\phi_f$  signifies the quantum yield of fluorescence in the appropriate solvent, and  $\tau_s$  the singlet lifetime determined by time correlated singlet photon counting techniques in the specific solvent). In a similar fashion, the rate constants

for cycloreversion ( $k_2$ ) in acetonitrile and cyclohexane and solvent incorporation in neat methanol  $k_{\text{meth}}$  can be calculated according to equations 2.3.2.3 and 2.3.2.4, respectively (where  $\phi_2$  and  $\phi_{\text{ether}}$  are the quantum yields for cycloreversion and solvent incorporation, respectively). All the rate constants are summarized in Table 2.3.2.1.

$$\phi_f = k_f \tau_s \quad (2.3.2.2)$$

$$\phi_2 = k_2 \tau_s \quad (2.3.2.3)$$

$$\phi_{\text{ether}} = k_{\text{meth}} \tau_s \quad (2.3.2.4)$$

**Table 2.3.2.1.** Rate constants for fluorescence decay ( $k_f^0$ ), cycloreversion in cyclohexane, acetonitrile and methanol ( $k_2$ ) and solvent incorporation in methanol ( $k_{\text{meth}}$ )

	C <sub>6</sub> H <sub>12</sub>		CH <sub>3</sub> CN		CH <sub>3</sub> OH	
<i>Cyclobutene</i>	$k_f^0$ [s <sup>-1</sup> ] x 10 <sup>-7</sup>	$k_2$ [s <sup>-1</sup> ] x 10 <sup>-7</sup>	$k_f^0$ [s <sup>-1</sup> ] x 10 <sup>-7</sup>	$k_2$ [s <sup>-1</sup> ] x 10 <sup>-7</sup>	$k_2$ [s <sup>-1</sup> ] x 10 <sup>-7</sup>	$k_{\text{meth}}$ [s <sup>-1</sup> ] x 10 <sup>-7</sup>
65	1.6 ± 0.2	1.6 ± 0.2	2.2 ± 0.3	2.0 ± 0.2	0.88	2.32 ± 0.3
66	1.7 ± 0.2	1.2 ± 0.2	2.4 ± 0.3	1.3 ± 0.5	0.46	1.5 ± 0.2
67	2.0 ± 0.2	0.74 ± 0.07	2.6 ± 0.3	1.0 ± 0.2	0.135	1.1 ± 0.2
68	2.4 ± ?	0.58 ± 0.08	3.0 ± 0.4	0.7 ± 0.1	0.139	0.4 ± 0.1
69	3.4 ± 0.3	0.18 ± 0.02	3.6 ± 0.4	0.3 ± 0.1	0.046	0.2 ± 0.1
70	4.6 ± 0.5	0.07 ± 0.01	2.9 ± 0.3	0.14 ± 0.02	0.0014	0.0086 ± 0.001

The rate constants for cycloreversion of 65-70 in cyclohexane and acetonitrile and for solvent incorporation in methanol (Table 2.3.2.1) correlate only qualitatively with the ground state substituent constants  $\sigma$  or  $\sigma^+$  (e.g.:  $\rho = -1.2 \pm 0.5$  ( $r^2 = 0.60$ ) for the cycloreversion reaction in acetonitrile). Correlations with the  $\sigma_{ex}$ -values of Baldry are somewhat better (Figure 2.3.2.1), but still fail to deal adequately with the *meta* trifluoromethyl substituent.

Qualitatively, it is evident by simple inspection of these plots that the rate of cycloreversion decreases as the electron withdrawing ability of the substituent increases. To our knowledge, this is the first reported example of a substituent effect on a photochemical cycloreversion process that can clearly be attributed to the  $\pi,\pi^*$  singlet state. The observed substituent effect on  $k_2$  (Table 2.3.2.1) seems to indicate that there is substantial dipolar character developed in the  $\sigma$ -bond framework during the cycloreversion process, with positive charge developing at C<sub>1</sub> of the cyclobutene ring

The common assumption in organic photochemistry is that the central feature in the mechanism of [2 + 2] cycloaddition (and fragmentation) reactions is the existence of an avoided surface crossing that allows for the occurrence of a radiationless jump from S<sub>1</sub> to S<sub>0</sub>, whose rate is controlled by the energy gap between the two surfaces. Recent theoretical calculations<sup>142c</sup> predict that it is possible to reduce the S<sub>1</sub>-S<sub>0</sub> energy gap to zero in photocycloaddition (and cycloreversion) reactions by introducing a difference in the energies of the localized nonbonding orbitals involved. This can be accomplished by making the diagonals of the forming or fragmenting cycloadduct unequal. In this way, asymmetrically substituted rings are predicted to generate perturbation parameters ( $\delta_{AB}$ ) which are significantly different from zero, increasing the contribution from zwitterionic resonance structures on the excited state potential energy surface for cycloaddition and



cycloreversion reactions. These concepts have been verified by *ab-initio* large scale CI calculations on perturbed square cyclobutadienes<sup>142d</sup>. The substituent effect on the rate of excited state cycloreversion of 65-70 provides the first experimental verification of these theoretical predictions.

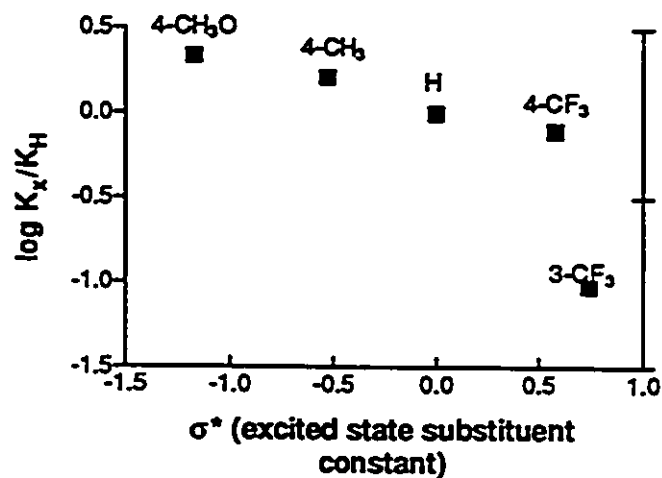


Figure 2.3.2.1A. Hammett plot for the cycloreversion reaction of 65-70 in pentane

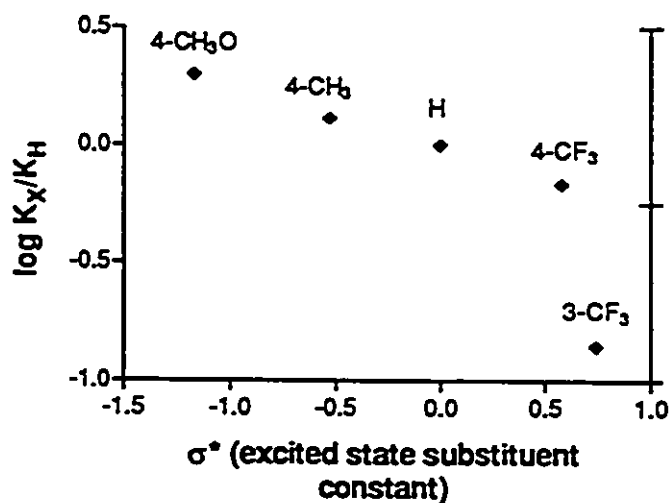


Figure 2.3.2.1B. Hammett plot for the cycloreversion reaction of 65-70 in acetonitrile

As is the case for the cycloreversion reaction of these compounds in non-hydroxylic solvents, the solvent photoaddition reaction is also sensitive to substituent effects, as indicated by the trend in rate constants  $k_{\text{meth}}$  given in Table 2.3.2.1. This trend can be rationalized in terms of the basicity of the excited state, which is enhanced in phenylcyclobutenes that bear electron donating substituents.

While the rate constants for cycloreversion and methanol addition correlate poorly with ground or excited state substituent constants, they do correlate well with each other. Figure 2.3.2.2 shows a log-log plot of the rate constants for photocycloreversion in methanol  $k_2$  versus those for solvent photoaddition  $k_{\text{meth}}$ . The slope ( $1.1 \pm 0.2$ ;  $r^2 = 0.97$ ) indicates that there is an almost exact correspondence between the substituent effects on the two processes.

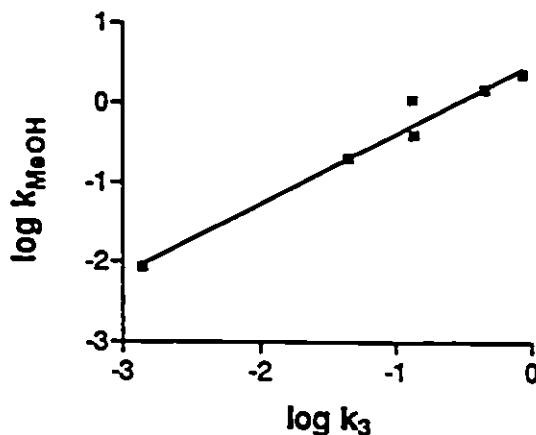


Figure 2.3.2.2. Log-log plot of the rate constants for cycloreversion in methanol ( $k_2$ ) versus those for solvent addition ( $k_{\text{MeOH}}$ ).

There is no consistent variation in the singlet lifetimes of 65-70 with substituent in any of the solvents studied. However, a trend is manifested in the rate constants for fluorescence decay ( $k_f^\circ$ ) as shown in Table 2.3.2.1. The rate constants for fluorescence

decay increase (in cyclohexane solution) as the electron withdrawing ability of the substituent increases.

The singlet lifetimes of 65-67 are very sensitive to the presence of oxygen in solution, and it has been determined that the rate constant for quenching of the singlet excited state of 67 with oxygen approaches the diffusion limit in acetonitrile solution ( $2.0 \times 10^{10} \text{ mol}^{-1} \text{ dm}^{-3} \text{ s}^{-1}$ ). In contrast, the singlet lifetimes of those phenylcyclobutenes with electron withdrawing groups (68-70) are more or less insensitive to the presence of oxygen in solution (depending on the electron withdrawing ability of the substituent). Thus, the singlet lifetime of 70 (with the strongest electron withdrawing group in the excited state) measured in air saturated acetonitrile solution coincides with that measured in deoxygenated acetonitrile solution ( $\sim 7 \text{ ns}$ ). The effect of oxygen on the singlet lifetimes of 65-67 is thus tentatively attributed to electron transfer quenching<sup>134b,c</sup>, which should lead to the formation of cyclobutene radical cation and superoxide ion.

Electrocyclic ring opening to the corresponding 2-aryl-1,3-butadiene does not occur in detectable yield with any of the compounds studied in this work. The inability of 1-arylcyclobutenes to undergo photochemical ring opening as opposed to alkylsubstituted cyclobutenes is thus most likely related to energetic considerations and not to the polarizability of the  $S_1$  state. We conclude that *for photochemical ring opening to occur, the  $S_1$  state energy has to be higher than the Bond Dissociation Energy of the cyclobutenyl C3-C4 bond.* This condition is easily satisfied by alkylsubstituted cyclobutenes whose  $S_1$  energies are in the order of 544-607 KJ mol<sup>-1</sup>. Singlet state energies for 1-arylcyclobutenes are summarized in Table 2.2.5.1.

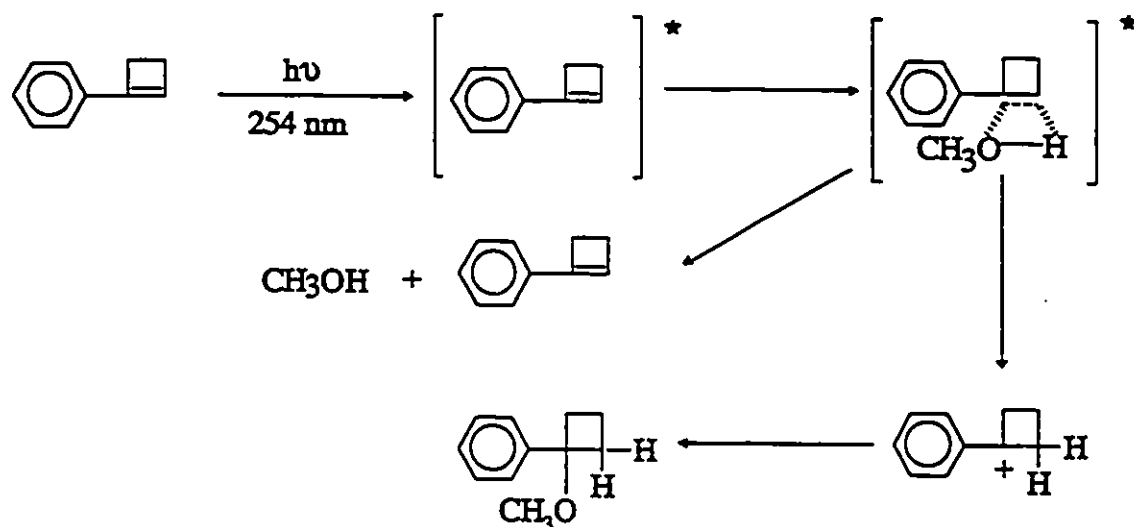
### 2.3.3 Quantitative Aspects of the Photoprotonation of 1-Arylcyclobutenes

It is observed that the rate constant for addition of methanol in neat methanol for the unsubstituted 1-phenylcyclobutene **67**, ( $k_{\text{meth}} = 4.4 \times 10^5 \text{ s}^{-1} \text{ mol}^{-1} \text{ dm}^3$ ; Table 2.3.2.1) does not match with the rate constant for quenching of the excited state of **67** by methanol ( $k_{\text{q}} \sim 6 \times 10^6 \text{ s}^{-1} \text{ mol}^{-1} \text{ dm}^3$ ; Table 2.2.6.5). This discrepancy can be due to [a] the protonation step in Scheme 2.3.1.6 being reversible, [b] the presence of an exciplex in the mechanism for solvent adduct formation; or [c] a special solvent effect on the singlet lifetimes of **65-70** in methanol solution.

Dauben and coworkers<sup>136</sup> found that the fluorescence of 1-phenylcyclohexene in methanol is quenched upon addition of moderately low concentrations of sulfuric acid. This quenching was fairly effective, but it does not correlate quantitatively with the formation of the solvent adduct (the addition of methanol across the double bond in a Markovnikov fashion). This implies that excited state quenching does not lead to formation of the solvent adduct with unit efficiency<sup>137</sup>. McClelland and coworkers<sup>107</sup> (see Scheme 2.1.2) suggested that the source of the inefficiency may be competitive protonation on the aromatic ring. In the present study, the mass spectrum of recovered 1-phenylcyclobutene from the photoreaction mixture in methanol- $\text{d}_4$  shows less than 0.5 % deuterium incorporation (after 80 % conversion) in the molecular ion region. The lower detection limit for deuterium incorporation in the aromatic fragment-ion region of the mass spectrum is calculated to be less than 0.01 %.

Exciplex intermediates have been invoked for numerous photochemical reactions, among which it is worth mentioning those proposed in arene-alkene photocycloadditions<sup>138</sup>. The standard mechanism for exciplex formation has been shown

to be valid in several systems<sup>139</sup>. In the present case, a mechanism involving an exciplex intermediate could explain the discrepancy between the rate constants for methanol addition in neat methanol (Table 2.3.2.1) and for quenching of the excited state in acetonitrile by methanol (Table 2.2.6.5). This mechanism is depicted in Scheme 2.3.3.1. In this mechanism, an excited complex is formed between the excited 1-phenylcyclobutene and a molecule of methanol, which can either collapse to return to ground state 1-phenylcyclobutene or be quenched by proton transfer to yield the ground state phenylcyclobutyl cation, which in turn is trapped by the solvent to form the Markovnikov solvent adduct.



Scheme 2.3.3.1. Mechanism for the photoaddition of solvent in 1-arylcyclobutenes involving the formation of an exciplex

Solvents effects [c] could also be responsible for the difference found in the rate constants for solvent addition and quenching of excited phenylcyclobutene by methanol (*vide supra*). Figure 2.2.6.3 shows the peculiar behavior obtained from the quenching of the singlet lifetimes of compounds 65, 66 and 67 by methanol in acetonitrile solutions.

The slopes of those plots reach a plateau at a distinct methanol concentration. The lifetimes obtained from the plateau regions of the plots ( $[\text{MeOH}] > 0.7 \text{ mol dm}^{-3}$ ) do correspond to the measured lifetimes of 65, 66 and 67 in methanol within experimental error. However, the extrapolated lifetimes at neat methanol concentration (obtained from the low methanol concentration portions of this plot where  $[\text{MeOH}] < 0.7 \text{ mol dm}^{-3}$ ) are much shorter than the measured lifetimes of 65-67 in neat methanol. It is then possible that at certain methanol concentration, the quenching interactions between excited phenylcyclobutene and methanol (or methanol aggregates) become such that normal linear behavior is no longer operative (only particular orientations of the aggregates and excited 1-arylcyclobutene are required for effective quenching to take place, as some orientations may not be quenched at all, giving rise to longer lifetimes). A model of this type implies that specific solvent-excited state arylcyclobutene interactions have to be considered. It has also been suggested<sup>138</sup> that the transient diffusion term (see Appendix 2) makes an important contribution to the quenching process. This is possible since the concentration of the quencher (methanol) is high (and probably removed from its activity value) and the unquenched lifetime is long.

It has also been proposed that *dielectric friction*<sup>140</sup> can also contribute to the relaxation dynamics of molecules which undergo a sudden change in charge distribution upon excitation (e.g. 1-arylcyclobutenes). Thus, dielectric friction<sup>141</sup> may be an important source of coupling to the solvent if changes occur along the relaxation coordinate. Any polarity dependent changes in the shapes of the potential energy surfaces traversed during the relaxation process may therefore affect the decay dynamics, and consequently the intrinsic lifetimes, in the given solvents. Since only small changes in the absorption and emission bands occur under the experimental conditions employed (see

Tables 2.2.3.1 and 2.2.4.1), there do not appear to be large changes in the ground and excited state potential energy surfaces with solvent polarity. However, the relaxation coordinates of 1-arylcyclobutenes in a solvent such as methanol, may probe regions of the potential energy surfaces which are not represented in the static absorption or emission processes<sup>141</sup>. Therefore, solvent dependent changes in the form of the relaxation coordinate cannot be unequivocally excluded.

We tentatively conclude that the methanol quenching experiments reflect the combination of two opposite and counterbalancing effects on the excited singlet state lifetimes of 1-phenylcyclobutenes. The singlet lifetimes observed in acetonitrile also reflect solvent polarity effects, as compared to the singlet lifetimes obtained in cyclohexane solvent (Table 2.2.6.1).

As has been reported for styrene systems<sup>112</sup>, photoaddition of alcohol to 4-methoxyphenylcyclobutene is the most efficient, followed by the 4-methyl and unsubstituted compounds (65, 66 and 67 respectively). Yates and coworkers<sup>125, 130</sup> reported that 4-trifluoromethylstyrene (63) is unreactive towards photoprotonation, and argued that this is due to insufficient charge transfer character in the excited singlet state. This is clearly not the case in the corresponding arylcyclobutene (68) which undergoes methanol photoaddition with measurable efficiency. The difference in behaviour between 63 and 68 presumably results from the fact that excited state torsional relaxation is blocked in the cyclic compound 68, allowing relatively slow protonation to proceed with measurable efficiency.

The above results show that the basicity of the excited state in 1-phenylcyclobutenes in hydroxylic solvents can be readily altered by proper substitution, as is the case for

styrene systems. However, the compounds presented in this study can be used as a probe of electron - withdrawing substituent effects in  $S_1$ , a measure which is not attainable with the acyclic derivatives utilized by Yates and coworkers. Thus, our results allow the conclusion that the electron withdrawing power of 4-trifluoromethoxy substituent in the excited state falls in between that of 3-trifluoromethyl and 4-trifluoromethyl groups in the excited state.

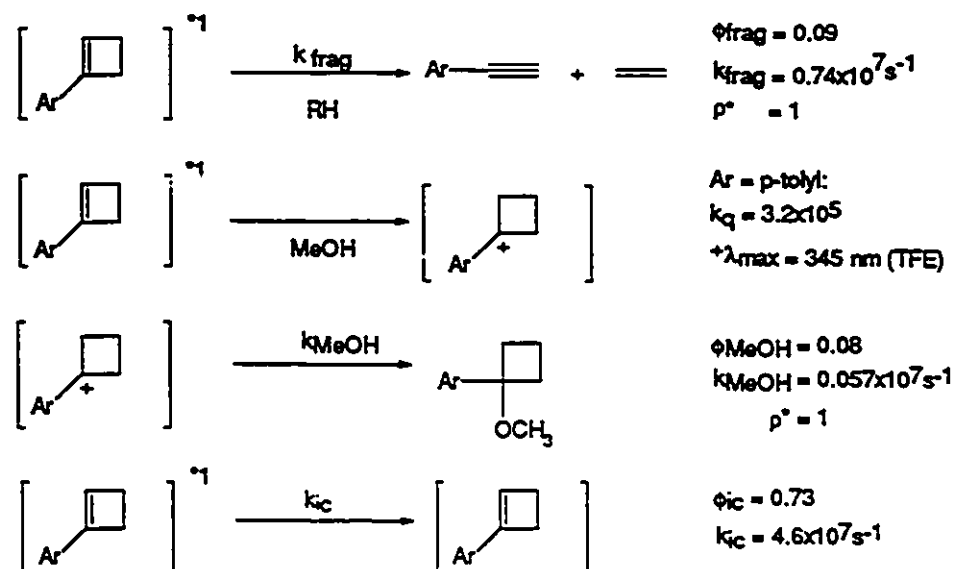
It is also of interest to compare the absolute rates of methanol addition to 65-67 to those reported by Yates and coworkers for water addition to the corresponding styrene derivatives<sup>125</sup>. The rates of water catalyzed photohydration of substituted styrenes in neutral aqueous solution were reported to be  $1.86 \times 10^4 \text{ mol}^{-1} \text{ s}^{-1} \text{ dm}^3$  for styrene itself,  $3.8 \times 10^4 \text{ mol}^{-1} \text{ s}^{-1} \text{ dm}^3$  for 4-methylstyrene, and  $2.45 \times 10^5 \text{ mol}^{-1} \text{ s}^{-1} \text{ dm}^3$  for 4-methoxystyrene. In contrast, the  $k_{\text{MeOH}}$  values for addition of methanol to 65-67 in methanol (Table 2.3.2.1) vary by a factor of about two throughout the series of the three compounds. Converting the  $k_{\text{MeOH}}$  values to second order rate constants (by correcting for solvent concentration) indicates that for the parent compound, the rate of addition of methanol to excited 67 is ~ 25 times faster than the rate of water addition to styrene in water. The enhanced reactivity towards protonation in the phenylcyclobutene series (Table 2.3.2.1), as compared to styrenes<sup>125</sup>, may be attributed to relief of ring strain in the former series of compounds upon protonation. The much less-prominent substituent effect on the rates of methanol photoaddition to phenylcyclobutenes compared to that on the rates of water photoaddition to styrenes may be the consequence of this substantial variance in absolute reactivity, although it will clearly be necessary to study the photochemistry of the two sets of compounds under more similar reaction conditions before reliable conclusions can be made in this regard.



## 2.4 Summary.

Electrocyclic ring opening to the corresponding 2-aryl-1,3-butadiene does not occur in detectable yields upon photolysis of any of the 1-phenylcyclobutenes 65-70 studied.

The photophysics of 1-phenylcyclobutene was partially outlined in Scheme 2.3.1.1. Scheme 2.4 depicts the remainder of the photophysical and photochemical processes studied for this series of compounds. As is the case for other 1-phenylated cyclobutenes, compounds 65 through 70 fluoresce with appreciable quantum yields. Table 2.4 summarizes the radiative, reaction and non-radiative<sup>118</sup> quantum yields for the parent compound 1-phenylcyclobutene 67. Non-productive internal conversion is then rendered the major deactivation pathway of the singlet excited state of these molecules. The quantum yields of reaction are fairly low, and can be attributed to the short singlet lifetimes of these compounds, which are presumably due to high internal conversion rates. The intersystem crossing rate constant was calculated to be ca.  $2.5 \times 10^5 \text{ s}^{-1}$  for 67 by Zimmermann and coworkers<sup>118</sup>; when compared to the rate constant for internal conversion ( $3 \times 10^7 \text{ s}^{-1}$ ) the inefficiency of the former process ( $\phi_{\text{ISC}} = 0.004$ ) is understandable. It is likely that the significant triplet reactivity exhibited by 70 upon direct photolysis in n-pentane or acetonitrile solution, is the simple result of markedly diminished singlet reactivity, and not the result of an increase in the rate of intersystem crossing.



Scheme 2.4. Photophysical and photochemical processes studied for 1-phenylcyclobutenes in the present document.

Table 2.4. Quantum yields for radiative and non-radiative processes for the parent 1-phenylcyclobutene

$\Phi_{\text{fluorescence}}^{\dagger}$	$\Phi_{\text{ISC}}^{\ddagger}$	$\Phi_{\text{phenylacetylene}}^{\dagger}$	$\Phi_{\text{IC}}^{\ddagger}$
0.25	0.0031	0.09	0.73

$\ddagger$  From Zimmermann and coworkers.

$\dagger$  Measured in cyclohexane as solvent.

The transient absorption spectrum obtained from flash photolysis of 66 in 2,2,2-trifluoroethanol was assigned to the p-tolyl-cyclobutyl carbenium ion, though further characterization is necessary to establish firmly the validity of this assignment. All the compounds in the series undergo photoprotonation in alcohol solution; it may therefore be possible to generate the corresponding cations in non-nucleophilic solvents and study their

chemistry directly by flash photolysis techniques. However, the fact that the triplet state is readily observable in aprotic solvents, and has  $\lambda_{\text{max}}$  similar to that of the cation, may pose difficulties in the direct observation of those ionic intermediates. Further work in this area is expected to provide valuable information on these reactive intermediates.

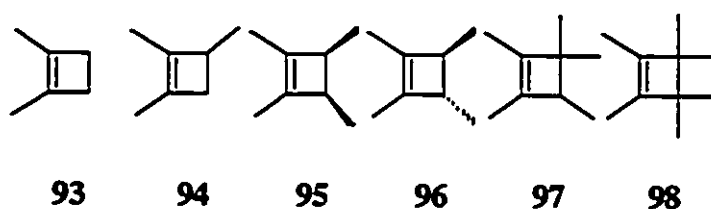
CHAPTER III  
THE PHOTOCHEMISTRY OF MONOCYCLIC CYCLOBUTENE  
DERIVATIVES

3.1 Introduction

One of the fundamental questions pertaining to the photochemical ring opening of cyclobutene, given its overall nonstereospecificity, is whether orbital symmetry selection rules play any role in the process at all. Several mechanisms were presented in Chapter I to explain the nonstereospecificity; most of them involve the presumption that the loss of stereospecificity occurs *after* ring opening has initiated (in disrotatory fashion) on the excited state surface. Theoretical calculations, at various levels of theory<sup>15, 18, 30, 61, 62</sup>, universally predict that orbital symmetry *should* play a role in the reaction. Only two experimental studies suggest that this may indeed be the case. One is the study of the photochemistry of the isomeric tricyclic cyclobutenes 10 and 11 (see Chapter 1.3.2). Another is the study of cyclobutene ring opening on the femtosecond time scale<sup>27</sup> by Resonance Raman Spectroscopy (Chapter 1.2). Clearly, the development of a comprehensive mechanistic picture to explain the apparent failure of cyclobutene to follow orbital symmetry selection rules would be facilitated by the acquisition of additional experimental examples that illustrate the possible role of orbital symmetry selection rules in the early stages of the reaction on the excited state surface.

The study to be described in this chapter examines the effects of alkyl substitution at C<sub>3</sub>-C<sub>4</sub> on the efficiency of the process, using the series of monocyclic cyclobutenes depicted in Figure 3.1.

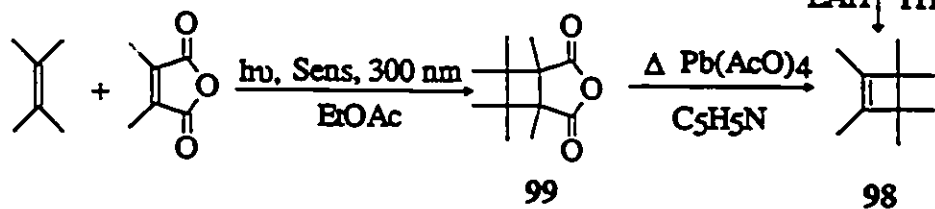
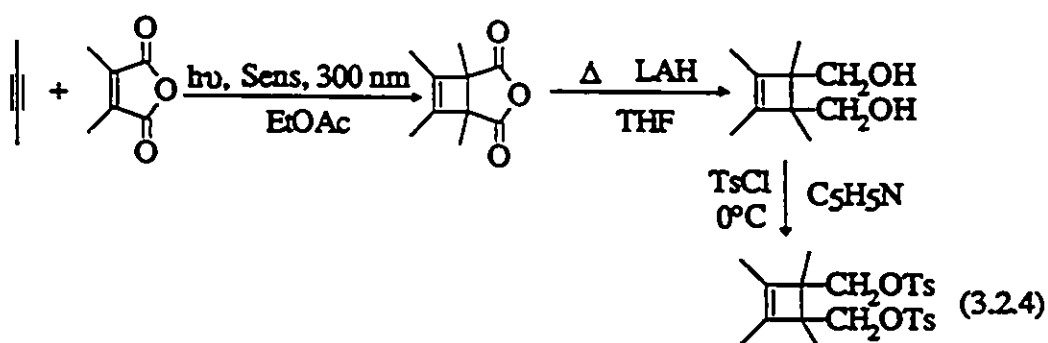
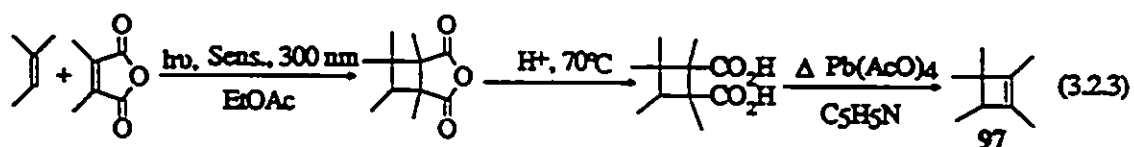
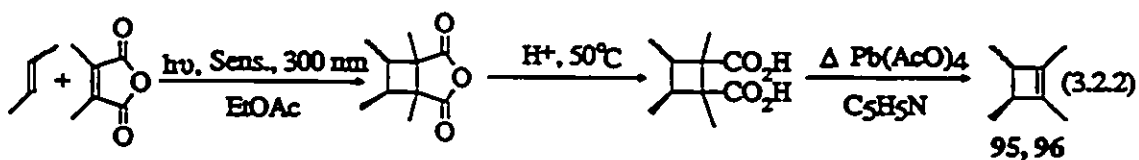
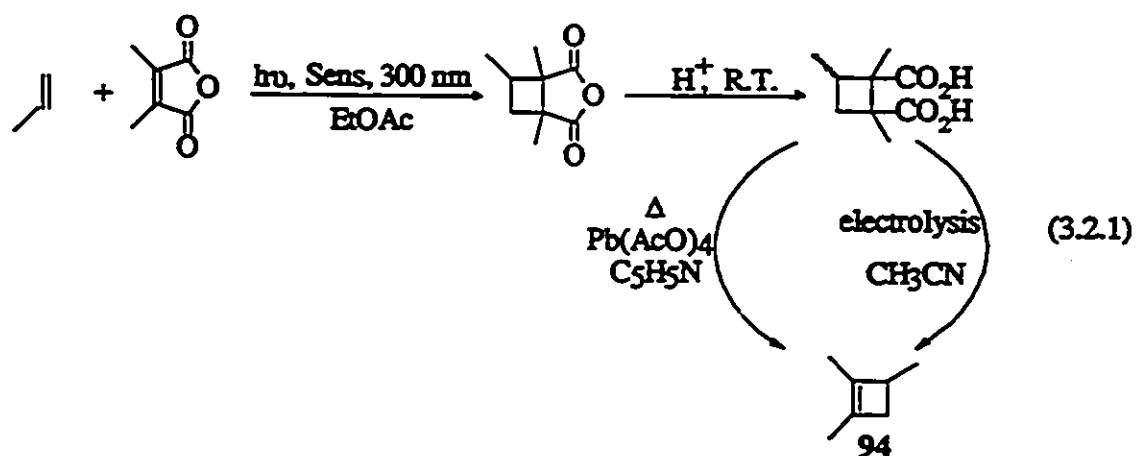
FIGURE 3.1



### 3.2 Preparation and Characterization of Compounds

*1,2-Dimethylcyclobutene*<sup>93</sup> (93) was synthesized by preparative photolysis of 2,3-dimethyl-1,3-butadiene<sup>143, 144</sup>. Compound 93 was purified by semipreparative gas-chromatography (vpc) and its structure was assigned on the basis of its <sup>1</sup>H NMR and <sup>13</sup>C NMR spectra.

*1,2,3-Trimethylcyclobutene*<sup>145 - 149</sup> (94), *cis-* and *trans-1,2,3,4-tetramethylcyclobutene*<sup>46</sup> (95, 96), *1,2,3,3,4-pentamethylcyclobutene*<sup>150, 151</sup> (97), and *hexamethylcyclobutene*<sup>150, 151</sup> (98) were prepared according to the procedures shown in equations 3.2.1-4. The cyclobutenes were isolated and purified by semipreparative gas chromatography. All compounds and synthetic intermediates were characterized by <sup>1</sup>H NMR, mass and IR spectroscopy<sup>145</sup>.



Ultraviolet absorption spectra of the six compounds were recorded in deoxygenated hexadecane solution at 23° C. Those of 95 and 96 are similar to the previously reported spectra in isooctane solution<sup>46</sup>. The spectra of the other four compounds are similar to one another, showing only edge absorption extending to *ca.* 225 nm in the spectral region above 185 nm. The molar extinction coefficients at 214 nm are in the range 1000-2000 mol<sup>-1</sup> cm<sup>-1</sup> dm<sup>3</sup> for all the compounds in the series.

### 3.3 Direct Photolysis of Cyclobutenes 93-98 in Hydrocarbon Solutions

#### 3.3.1 Light Sources, Quantum Yield Determinations and Product Identification

Irradiations were performed using 214 nm light provided by a 16W zinc resonance lamp situated in the center of a merry-go-round apparatus. The solvent used was n-hexadecane, which was chosen because it allows quantitation and identification of the very volatile photoproducts from the photolysis of 93-98 (equations 3.3.2.1-3) by gas chromatography analyses. In the present study, it was possible to obtain n-hexadecane of very low optical density in the far-UV region (less than 0.05 at 200 nm) by a series of repetitive purification processes (see Chapter VI). This approach improved the sensitivity of the results and shortened the photolysis times considerably compared to those required with less extensively purified hydrocarbon solvents. Photolyses were carried out to conversions of starting material of 5 % or less, in order to avoid secondary photolysis of the primary photoproducts.

The quantum yield for formation of 2,3-dimethyl-1,3-butadiene from photolysis (214 nm) of 1,2-dimethylcyclobutene (93) in deoxygenated hexadecane solution was

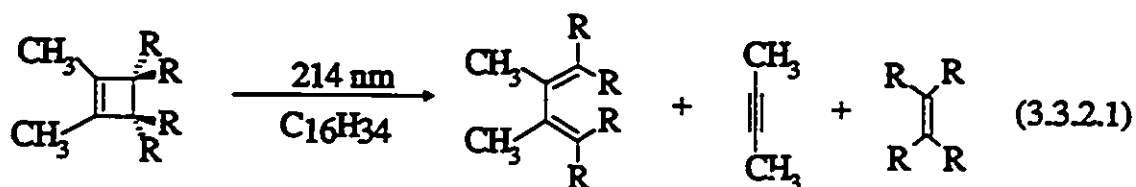
determined by uranyl oxalate actinometry<sup>113, 152 - 154</sup>, and is the average of triplicate determinations. Quantum yields for 2-butyne formation from **93** and for diene and 2-butyne formation from **94-98** in hexadecane solutions were determined by merry-go-round photolyses relative to the quantum yield for formation of 2,3-dimethyl-1,3-butadiene from **93** in the same solvent. Product quantum yields were determined for each compound from the slopes of moles of photoproduct *versus* time plots. The dienes obtained from the photolysis of cyclobutenes **93-98** were identified on the basis of their <sup>1</sup>H NMR, mass, UV and IR spectra.

### 3.3.2 Results

Irradiation (214 nm) of **93-98** as deoxygenated, 0.018 M solutions in n-hexadecane containing *ca.*  $2 \times 10^{-3}$  mol dm<sup>-3</sup> n-heptane as internal standard with 214 nm light generates the product mixtures depicted in equations 3.3.2.1-3. Two types of photoproducts are observed, the ring opening products which are substituted 1,3-butadiene derivatives, and cycloreversion-derived products which consist of mixtures of an alkene and 2-butyne. Relative yields of the isomeric dienes (Section 3.3.1) were determined by merry-go-round photolyses (relative to the formation of 2,3-dimethyl-1,3-butadiene (**100**) from photolysis of 1,2-dimethylcyclobutene (**93**) in the same solvent) from the slopes of concentration *versus* photolysis time plots as depicted in Figures 3.3.2.1-3. Figure 3.3.2.4 shows a plot of total diene yield *versus* irradiation time for all six compounds. Relative total diene yields (after normalizing that of **100** from photolysis of **93** to a value of 1.0) are listed in Table 3.3.2.1. The table also lists the distributions of isomeric dienes obtained from photolysis of **94-97**. The relative yields of 2-butyne and the



alkene derived from the cycloreversion reaction of cyclobutenes 93-98 were determined in similar fashion and are summarized in Table 3.3.2.2.



Ring Opening Products

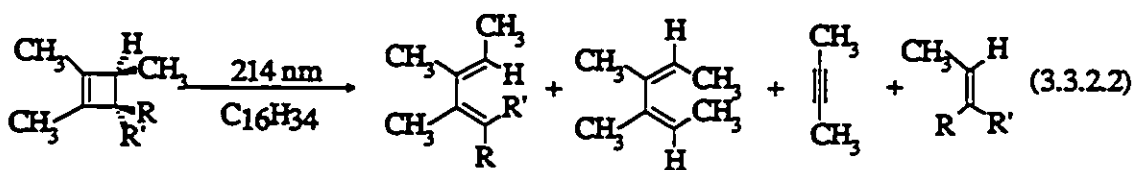
Fragmentation Products

93 R = H

100

98 R = CH<sub>3</sub>

104



Ring Opening Products

Fragmentation Products

95 R = CH<sub>3</sub>, R' = H

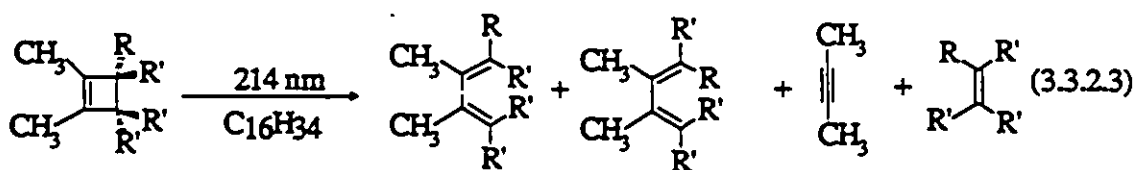
E,E-102 (R = CH<sub>3</sub>, R' = H)    Z,Z-102

105

96 R = H, R' = CH<sub>3</sub>

E,Z-102 (R = H, R' = CH<sub>3</sub>)

106



Ring Opening Products

Fragmentation Products

94 R = CH<sub>3</sub>, R' = H

E-101    Z-101

97 R = H, R' = CH<sub>3</sub>

Z-103    E-103

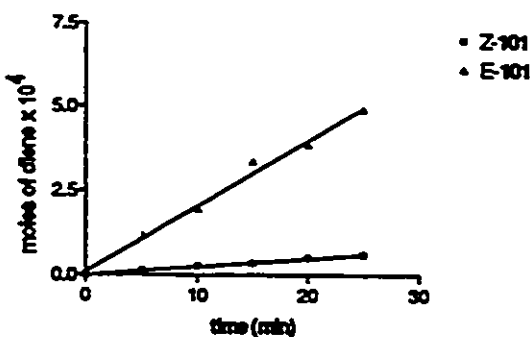


Figure 3.3.2.1. Moles of photoproduct *versus* time plots for the formation of E and Z-101 from photolysis (214 nm) of 1,2,3-trimethylcyclobutene (94) in hexadecane solution.

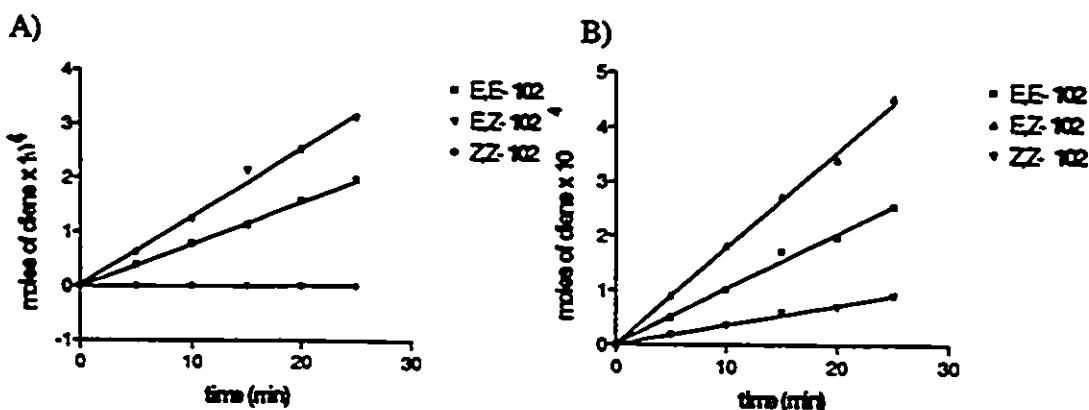


Figure 3.3.2.2. Moles of photoproduct *versus* time plots for the formation of E,E; E,Z; and Z,Z-102 from photolysis (214 nm) of A) *cis*-1,2,3,4-tetramethylcyclobutene (95) and B) *trans*-1,2,3,4-tetramethylcyclobutene (96) in deoxygenated hexadecane solution.

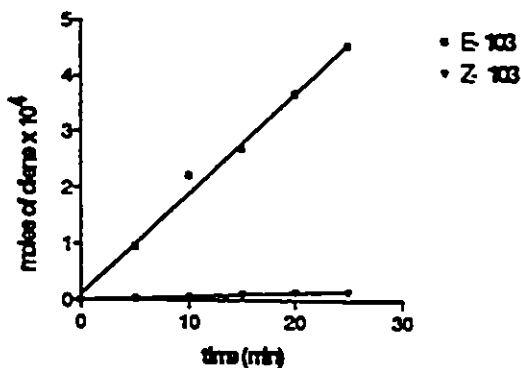


Figure 3.3.2.3. Moles of photoproduct *versus* time plots for the formation of E, and Z-103 from photolysis (214 nm) of 1,2,3,3,4-pentamethylcyclobutene (97) in deoxygenated hexadecane solution

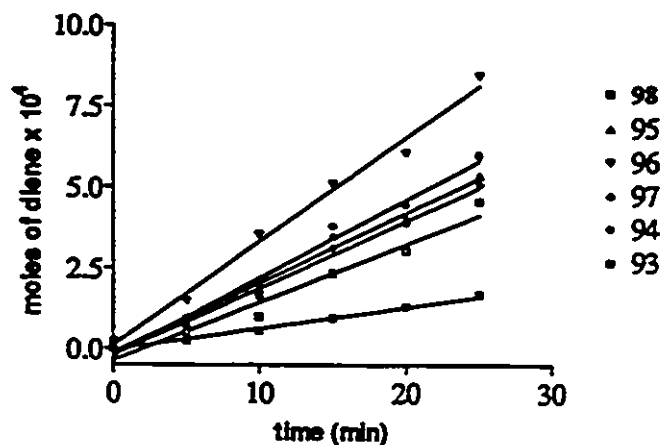


Figure 3.3.2.4. Total product diene yields from photolyses (214 nm) of methylated monocyclic cyclobutenes (93-98) in deoxygenated hexadecane solutions

Table 3.3.2.1. Relative total diene yields<sup>a</sup> and isomeric diene distributions<sup>b</sup> from photolyses (214 nm) of cyclobutenes 93-98 in *ca.* 0.02 mol dm<sup>-1</sup> deoxygenated *n*-hexadecane solutions at 20°C.

<i>Cyclobutene</i>	Total Diene Yield	<i>E,E</i> or <i>E</i> diene	<i>E,Z</i> or <i>Z</i> diene	<i>Z,Z</i> diene
93	1			
94	4.09	90.3	9.7	
95	3.33	40.7	59	0.3
96	4.49	34.7	54.2	11.1
97	3.09	96.8	3.2	
98	0.89			

a. Calculated from the slopes of the plots shown in Figure 3.3.2.4 and normalized relative to that of 100 from 93.

b. Calculated from the slopes of the plots shown in Figures 3.3.2.1-3 and normalized to a total of 100 % for each diene.

**Table 3.3.2.2.** Relative yields of cycloreversion products from photolyses (214 nm) of cyclobutenes 93-98 in *ca.* 0.02 mol dm<sup>-1</sup> deoxygenated n-hexadecane solutions at 20°C

<i>Cyclobutene</i>	Relative Yield of 2-Butyne
93	1
94	1.43
95	1.59
96	1.94
97	2.76
98	0.98

Table 3.3.2.3 lists absolute quantum yields for the formation of dienes 100-104 and 2-butyne from photolysis of 93-98 under these conditions. These data were calculated from the data in Tables 3.3.2.1-2 using the actinic conversion. Total quantum yields for diene formation are also listed in the table.

**Table 3.3.2.3.** Absolute quantum yields for product formation from photolysis (214 nm) of cyclobutenes 93-98 in *ca.* 0.02 mol dm<sup>-1</sup> deoxygenated n-hexadecane solutions at 20° C.

<i>Cyclobutene</i>	$\phi_{\text{diene}}^{\text{a, b}}$	$\phi_{EE.\text{or } E}^{\text{b}}$	$\phi_{EZ.\text{or } Z}^{\text{b}}$	$\phi_{ZZ}^{\text{b}}$	$\phi_{\text{butyne}}^{\text{b}}$
93	0.063				0.11
94	0.258	0.23	0.025		0.028
95	0.210	0.085	0.124	0.0006	0.019
96	0.283	0.098	0.153	0.031	0.016
97	0.195	0.0189	0.0062		0.024
98	0.051				0.011

a.  $\phi_{\text{diene}}$  is the sum of the quantum yields for formation of isomeric dienes in each case.

b. Estimated error ~ 20 %.

GC spiking experiments with authentic samples verified that the formation of alkenes 105 and 106 occur with > 99 % stereospecificity from photolysis of 95 and 96 respectively.

### 3.4 Discussion

#### 3.4.1 C<sub>3</sub>/C<sub>4</sub> Effects on the Photochemical Ring Opening of Alkylcyclobutenes

The varying structural feature in 93-98 is the number of methyl groups attached to carbons 3 and 4 of the 1,2-dimethylcyclobutene ring. The data listed in Table 3.3.2.3

indicate that this structural variation results in a marked effect on the quantum yield for diene formation. These data are summarized in a more revealing way in Figure 3.4.1.1, which depicts the total quantum yield for diene formation *versus* the number of C<sub>3</sub>/C<sub>4</sub> methyl groups (*n*). As *n* increases throughout the series,  $\phi_{\text{diene}}$  increases to a maximum value at *n* = 2 (*trans*) and then decreases as *n* increases further.

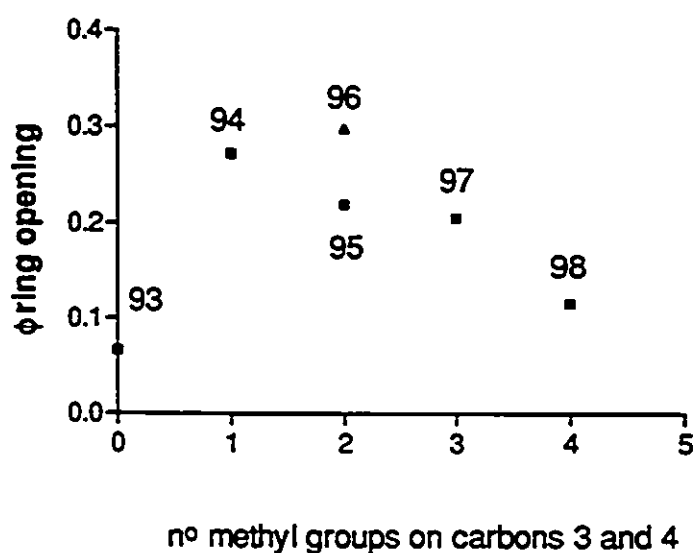
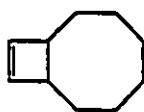


Figure 3.4.1.1. Plot of total quantum yield of ring opening (214 nm) as a function of methyl substitution for cyclobutenes 93-98 in hexadecane

One of the factors that controls the efficiency of the photochemical ring opening of alkylcyclobutenes is the C<sub>3</sub>-C<sub>4</sub> bond strength<sup>83</sup>, just as is the case in ground state electrocyclic ring opening reactions<sup>169</sup>. This is demonstrated by a comparison of the diene/alkene ratios derived from photolysis of compounds *cis*-107 (*ca.* 1.0) and *cis*-108 (*ca.* 3.6)<sup>170</sup>. Molecular modeling studies show that the  $\pi$ -system of the cyclooctenyl C=C double bond in *cis*-108 is almost coplanar with the fragmenting cyclobutenyl C-C bond, a geometry which would be expected to weaken the C<sub>3</sub>-C<sub>4</sub> bond substantially

compared to that in 107. This effect is also manifested in the relative rates of thermal ring opening of the two compounds<sup>43, 170</sup>. Another example which illustrates the role of C<sub>3</sub>-C<sub>4</sub> bond dissociation energy on the ring opening reaction

*cis-107**cis-108*

shall be presented in Chapter IV. The increase in  $\phi$  diene between  $n = 0$  and  $n = 2$  *trans* (compounds 93, 94, and 96) is consistent with the expected progressive weakening of the C<sub>3</sub>-C<sub>4</sub> bond in 93 with increasing methyl substitution.

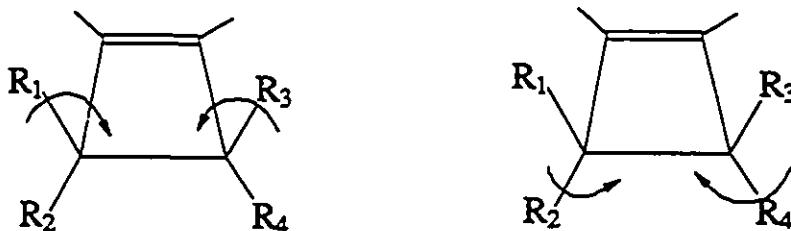
The quantum yield ratios fall off again in compounds 95, 97, and 98. From the point of view of bond-strength arguments alone, these values would be expected to *increase* continuously with increasing methyl substitution at C<sub>3</sub>/C<sub>4</sub>; in the case of 95, the C<sub>3</sub>-C<sub>4</sub> bond strength might in fact be expected to be even smaller than that in the *trans*- isomer 96 owing to eclipsing of the methyl groups. *Syn*- dimethyl substitution clearly causes a diminution in both the absolute and relative quantum yields for ring opening compared to what might be expected on the basis of bond strength arguments alone. Thus the present data are not compatible with a simple biradical mechanism for the process, in which ring opening occurs by homolytic C<sub>3</sub>-C<sub>4</sub> bond scission to yield a 1,4-biradical, which then relaxes to yield a mixture of diene isomers<sup>43, 83</sup>.

A reasonable explanation for the reduced quantum yields of diene formation from photochemical ring opening of those cyclobutenes containing *syn*-dimethyl substitution (95, 97, and 98) is that the rate of excited state ring opening is altered by steric effects

between *syn*- substituents at C<sub>3</sub>/C<sub>4</sub>. Such effects would be expected if ring opening proceeds by *disrotation* in the early stages on the excited state reaction coordinate. Ring opening involving *disrotatory* twisting about C<sub>1</sub>-C<sub>4</sub> and C<sub>2</sub>-C<sub>3</sub> bonds as the C<sub>3</sub>-C<sub>4</sub> bond cleaves can occur by two pathways as illustrated in Scheme 3.4.1.1. The types of steric interactions (H-H, H-CH<sub>3</sub>, and CH<sub>3</sub>-CH<sub>3</sub>) that are involved in the two possible *disrotatory* ring opening modes of 93-98 are summarized in Table 3.4.1.1.

The increase in  $\phi_{\text{diene}}$  throughout the initial three members of the series (93, 94, and 96) suggests that no appreciable loss in efficiency results from replacing one pathway involving a hydrogen-hydrogen interaction with one involving a methyl-hydrogen interaction.

Replacement of one H-H or H-CH<sub>3</sub> interaction with a CH<sub>3</sub>-CH<sub>3</sub> interaction (95 and 97) results in a significant reduction in  $\phi_{\text{diene}}$ . Two CH<sub>3</sub>-CH<sub>3</sub> interactions (*i.e.* 98) result in a further reduction in  $\phi_{\text{diene}}$ ; it is noteworthy that  $\phi_{\text{diene}}$  for 98 is similar to that of unsubstituted compound 93, which possesses a much stronger (in a linear sense) C<sub>3</sub>-C<sub>4</sub> bond.



Scheme 3.4.1.1. *Disrotatory* twisting modes about C<sub>1</sub>-C<sub>4</sub> and C<sub>2</sub>-C<sub>3</sub> bonds as the C<sub>3</sub>-C<sub>4</sub> bond cleaves.

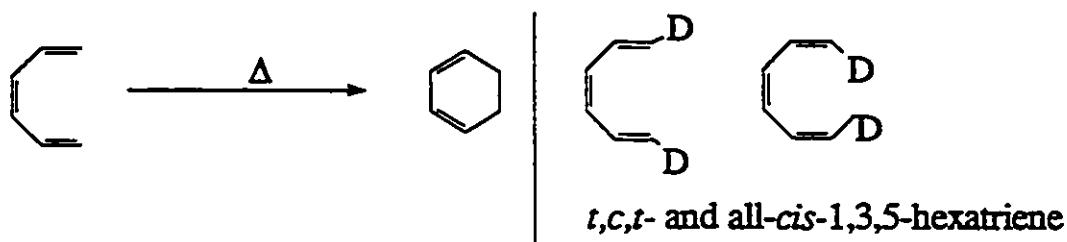


**Table 3.4.1.1.** Number of *disrotatory* interactions generated upon cyclobutene ring opening

cyclobutene	<i>Disrotatory</i> Interactions		
	H-H	H-CH <sub>3</sub>	CH <sub>3</sub> -CH <sub>3</sub>
93	2	0	0
94	1	1	0
95	1	0	1
96	0	2	0
97	0	1	1
98	0	0	2

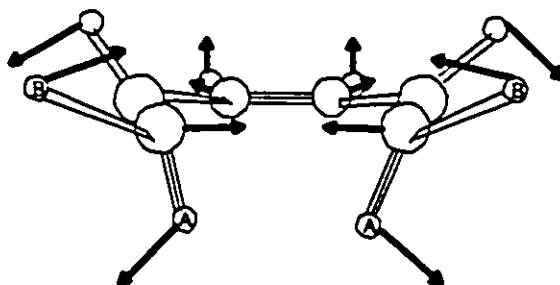
The importance of steric factors in *ground state* disrotatory electrocycloreversions has not been extensively documented<sup>5a,b</sup>, due to the fact that six-electron electrocycloreversions are relatively uncommon because of the greater thermodynamic stability of 1,3-cyclohexadienes relative to their open chain 1,3,5-hexatriene isomers. However, there is evidence to suggest that increasing the steric bulk at C<sub>5</sub>/C<sub>6</sub> of a cyclohexadienyl system does result in an increase in the activation energy for ring opening<sup>5b</sup> when the process does occur. It is expected that the effects of such interactions should be more pronounced on the rates of excited state disrotatory electrocyclic processes, since excited state pericyclic reactions are normally subject to quite small activation barriers.

Baldwin and coworkers have measured the secondary deuterium isotope effect ( $k_H/k_D$ ) for the *disrotatory* thermal electrocyclicization of hexa-1,3,5-triene<sup>167, 168</sup>. The secondary isotope effects for the *disrotatory* electrocyclic reactions of *t,c,t*- and all-*cis*-1,3,5-hexatriene (Scheme 3.4.1.2)



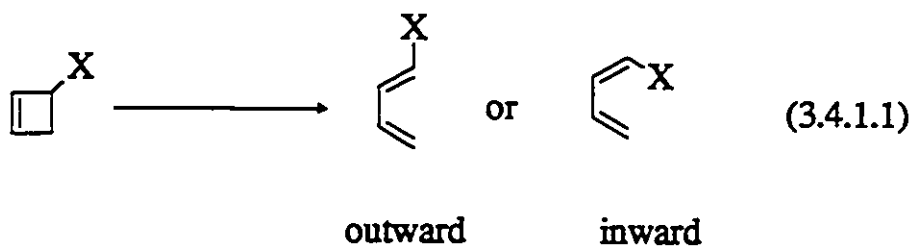
Scheme 3.4.1.2. Electrocyclization of 1,3,5-hexatriene.

are  $1.05 \pm 0.03$  and  $0.88 \pm 0.02$ , respectively. The authors demonstrated (through *ab-initio* calculations) that the former is the expected secondary isotope effect caused by very slight changes in hybridization at C<sub>1</sub> and C<sub>6</sub> in the transition state for electrocyclization. The strong inverse effect observed for the all-*cis*-deuterated compound can then be ascribed to steric effects between the "A" hydrogens in Scheme 3.4.1.3. Steric isotope effects are always less than unity because C-D bonds are shorter than the corresponding C-H bonds<sup>119a</sup>.



Scheme 3.4.1.3. Drawing of the SCF/6-31G\* transition structure for the electrocyclicization of 1,3,5-hexatriene. The arrows show motions in the normal mode of imaginary frequency



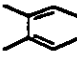

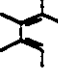
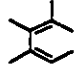


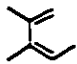
Stereoelectronic effects on thermal cyclobutene ring opening have been extensively studied by Houk and coworkers<sup>156, 157</sup>. They introduced the term torquoselectivity to describe the selectivity exhibited in the thermal conrotatory ring opening of 3-substituted cyclobutenes, which may proceed by outward or inward rotation of the C<sub>3</sub>/C<sub>4</sub> substituents to afford *E*- or *Z*- dienes (equation 3.4.1.1). Using quantum mechanical calculations, it was predicted that electron donor and weak electron acceptor substituents should prefer to rotate outwards, while very strong electron acceptor substituents should prefer to rotate inwards<sup>158, 159</sup>. The same authors reported several experimental verifications of those predictions<sup>160 - 162</sup>. They also agreed with the conclusions of Frey and coworkers who demonstrated that torquoselectivity is approximately additive in polysubstituted cyclobutenes<sup>165</sup>. Electronic effects related to differences in hybridization of the C-substituent bonds during outward and inward rotation, are thought to outweigh steric effects in conrotatory electrocyclic reactions. This is born out by recent studies of secondary deuterium kinetic isotope effects on the thermal ring opening of cyclobutenes<sup>168</sup>.

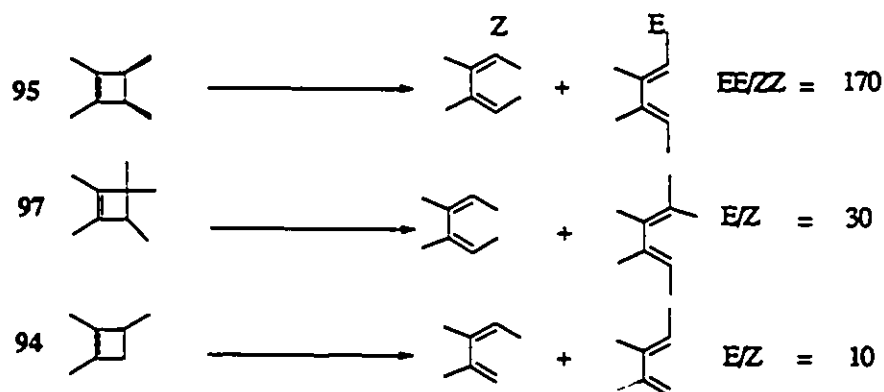


Another indication that steric factors play a role in the photochemical ring opening of cyclobutenes is afforded by a comparison of the relative yields of isomeric dienes obtained from **94**, **95**, and **97** (Scheme 3.4.1.4). Table 3.4.1.2 shows the three cyclobutene derivatives, the structure of the formally allowed diene isomers obtained from ring opening, and the dominant steric interaction that will be involved in the disrotatory ring opening mode leading to the formation of each isomer. In these three derivatives, the

two disrotatory ring opening modes lead to different diene isomers. The decreasing relative yields of E/Z (or E,E/ZZ) dienes in the series 95>97>94 is consistent with a decrease in steric discrimination between the two possible modes throughout the series.

Table 3.4.1.2. Structures of the allowed diene isomers obtained from ring opening of 94, 95, and 97, and dominant steric interactions involved in the disrotatory process. Ratios of the allowed isomers are given in each case.

Cyclobutene	Isomer 1	Steric Interaction	Isomer 2	Steric Interaction	Isomer 1/ Isomer 2
		H vs H		CH <sub>3</sub> vs CH <sub>3</sub>	170
		H vs CH <sub>3</sub>		CH <sub>3</sub> vs CH <sub>3</sub>	30
		H vs CH <sub>3</sub>		H vs CH <sub>3</sub>	10



Scheme 3.4.1.4. E/Z Diene ratios from allowed disrotatory photochemical ring opening of cyclobutenes 94, 95, and 97.

The degree of steric discrimination follows the difference in the acuteness of the *disrotatory* interactions involved in the two ring opening pathways (Scheme 3.4.1.4).

It is also instructive to compare the diene distributions from photolyses of **95** and **96** which are summarized in Table 3.3.2.1. The relative yields of *E,E*-, *E,Z*-, and *Z,Z*-**102** obtained from photolysis of **95** and **96** are similar to those reported previously<sup>46</sup>. The absolute quantum yield for formation of *Z,Z*-2,3-dimethyl-2,4-hexadiene (*Z,Z*-**102**) from photolysis of **96** is 50 times higher than that obtained from **95**. *Z,Z*-**102** is a formally forbidden product from **96**; its substantially higher yield from **96** than from **95** is consistent with its formation by two different pathways (with different steric requirements) from **95** and **96**. Clearly, those steric requirements involved in the formation of *Z,Z*-**102** from **96** are less demanding than those involved in its formation from **95**.

While the trends noted above are consistent with other indications that, in spite of the overall nonstereospecificity of the photochemical ring opening of alkyl substituted cyclobutenes, *disrotatory* motions are involved in the initial stages of the process on the excited state potential energy surface, there are clearly other possible explanations that must be examined. One is that the observed substituent effect on the quantum yield of ring opening might be due to an effect on some other excited state decay process in addition to ring opening (*e.g.* cycloreversion). A complete analysis would therefore require calculation of rate constants for the photochemical ring opening reaction. Unfortunately, the excited singlet state lifetimes necessary for the calculation cannot be determined by the technique available to us.

### 3.4.2 Photochemical *versus* Thermal Ring Opening of 93-98

Rate constants and activation parameters for the thermal ring opening of alkylcyclobutenes have been determined for a wide variety of compounds (including 93-98) by Frey and coworkers<sup>143 - 149, 155</sup> and Criegee and Seebach<sup>150, 151</sup> and have been reviewed by Marvell<sup>5</sup>. Table 3.4.2.1 lists rate constants and free energies of activation for the thermal electrocycloreversion of 93-98, and Figure 3.4.2.1 shows a plot of Arrhenius activation energy *versus*  $n$ . The similarity of the trend in activation energy for thermal ring opening of these compounds to that in the quantum yields for the photochemical process is striking, but it is difficult to ascertain its cause. The thermal process occurs with high degree of conrotatory stereospecificity, and is certainly a fundamentally different process mechanistically from the photochemical one. The trend in thermal activation energy for these compounds has been ascribed to a combination of steric and electronic effects<sup>145 - 149, 151</sup>. More recent theoretical studies have led to the conclusion that the latter dominates, however<sup>157, 161, 163-166</sup>.

One possible explanation for the similarity is that the photochemical process involves a dominant contribution from vibrationally excited ground state molecules, which might be formed by internal conversion in competition with disrotatory ring opening on the excited state surface. This could explain the general nonstereoselectivity of the reaction, since the hot ground state component would be expected to proceed with conrotatory stereochemistry. However, it would be difficult to explain the substantial yield of *Z,Z*-102 obtained from photolysis of 96 (*Z,Z/E,E* ~ 0.3), since the *Z,Z* diene is not formed in detectable yields (*i.e.* < 1 % of that of *E,E*-102) in the thermal ring opening of this compound.

**Table 3.4.2.1.** Rate data for cyclobutenes 93-98 undergoing *conrotatory* ring opening<sup>S</sup>

<i>Cyclobutene</i>	$k \times 10^9$ [s <sup>-1</sup> ] <sup>‡</sup>	$\Delta G$ [KJ mol <sup>-1</sup> ]
93	0.68	143.3
94	1.32	138.6
95	2.26	146.7
96	5.61	133.1
97	2.60	142.7 <sup>†</sup>
98	0.45	167.4 <sup>†</sup>

<sup>‡</sup> Calculated at 448 K

<sup>†</sup> Reference 151.

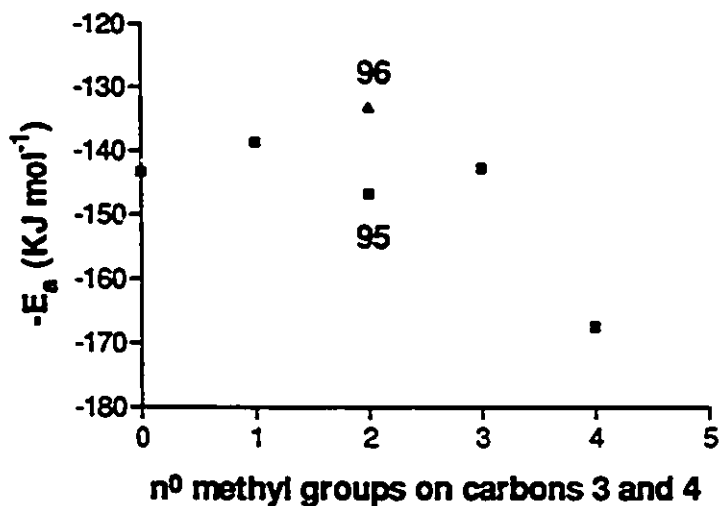


Figure 3.4.2.1. Plot of activation energies *versus* number of methyl groups for the thermal ring opening of cyclobutenes 93-98

### 3.4.3 Cycloreversion of Cyclobutenes 93-98

The photocycloreversion of 95 and 96 yields *cis*- and *trans*- 2-butene, respectively, with a high (> 99 %) degree of stereospecificity, verifying previous conclusions regarding the process<sup>46</sup>.

The quantum yields for cycloreversion (Table 3.3.2.3) do not vary markedly throughout the series of cyclobutenes 93-98. This is consistent with the Rydberg state assignment for this reaction; 93-98 all possess similar Rydberg state energies. This is understandable since the chromophore (C=C) remains unchanged along the series of alkyl-substituted cyclobutenes.

## 3.5 Conclusions

The present results provide evidence that orbital symmetry *does* play a significant role in the photochemical ring opening of cyclobutene, in spite of the general nonstereospecificity of the reaction. These results are also in agreement with those obtained by Mathies and coworkers<sup>27</sup>, which show that the photochemical ring opening dynamics of cyclobutene (in the first 10 - 20 femtoseconds following Franck Condon excitation) are those predicted by orbital symmetry selection rules.



## CHAPTER IV

### THE EFFECTS OF "CENTRAL BOND" TORSIONAL CONSTRAINT ON THE PHOTOCHEMISTRY OF CYCLOBUTENE AND 1,3-BUTADIENE

#### 4.1 Introduction

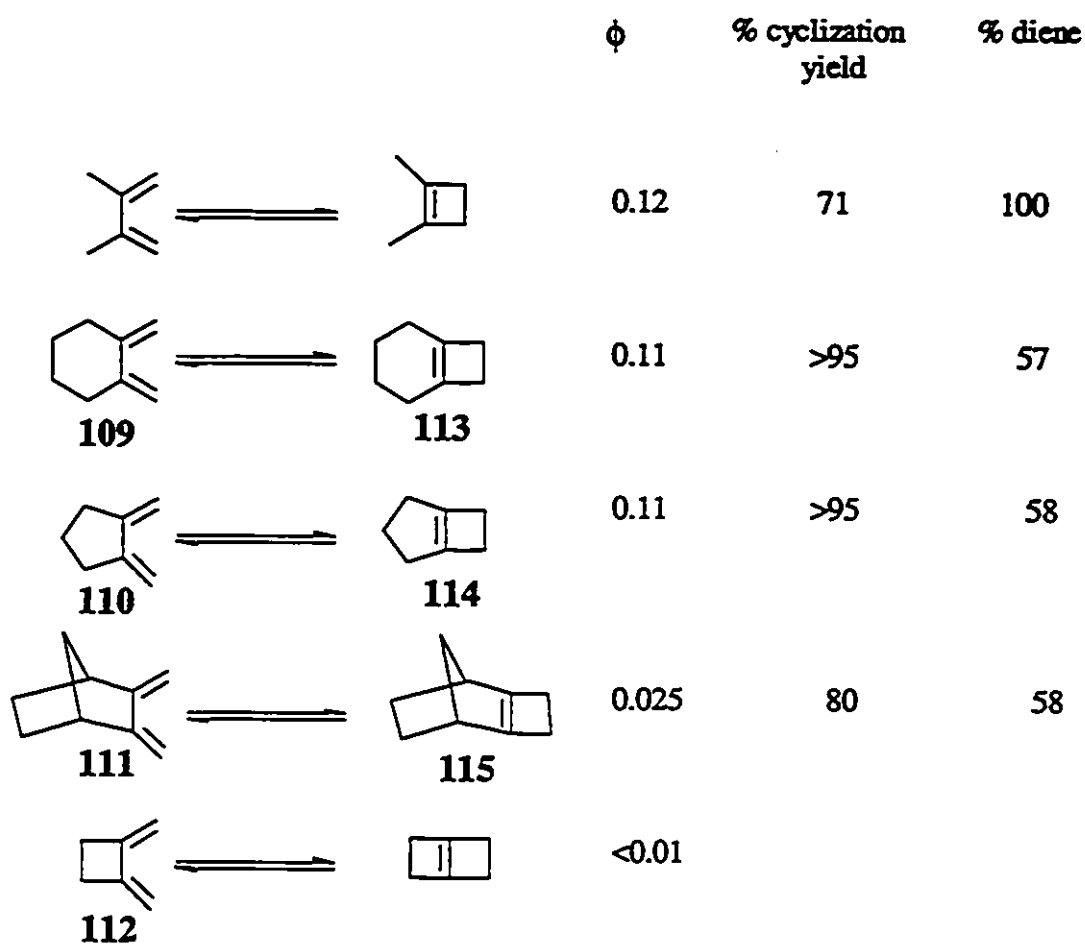
Recent theoretical calculations have led to the proposal of a fully efficient internal conversion mechanism for the photoisomerization processes of conjugated dienes, which is described in detail in Chapter I. These studies are based on the tenet that excited-to-ground state internal conversion processes occur at *conical intersections*- geometries where the two surfaces actually touch<sup>61, 100 - 104</sup> -rather than at avoided surface crossings. According to MC-SCF *ab-initio* calculations, the structures at the conical intersection geometries for the  $2^1A_g$  surface of 1,3-butadiene are tetraradicaloid with all three C-C bonds twisted<sup>102</sup>. In the *s-cis*- like conical intersection (48 in Figure 1.6.3), which is proposed to be involved in the photochemistry of *s-cis*-dienes, the two terminal bonds are twisted by *ca.* 20° and 80°, while the central bond is twisted by *ca.* 50°. This should be compared to the *planar* allylmethylene biradical, which is commonly thought to be the lowest energy structure on the excited singlet state surface of 1,3-butadiene, and postulated to be involved in the *cis,trans*- photoisomerization process. This model, in which the allylmethylene biradical geometry is simply that at the avoided surface crossing for *cis,trans* isomerization, would predict that the efficiency of the process should be independent of structural constraints which would prevent torsion of the central C-C

bond. The opposite would be expected for the conical intersection model, since it predicts that *cis,trans* photoisomerization about one or the other double bond involves simultaneous torsional motions about the central C-C bond. It is interesting that similar skeletal motions have been suggested to be important in the photoisomerization of opsin-bound retinal<sup>77 - 78</sup>.

This same model postulates that the pathway for cyclobutene ring opening is dominated by the twisting motion of one or two almost independent methylene groups, and that the nonstereospecificity of cyclobutene ring opening is due to the way in which the photoexcited reactant traverses the excited state potential energy surface as it approaches the conical intersection region. The theory predicts that torsional motions about the cyclobutene C=C bond (central single bond in 1,3-butadiene) accompany disrotatory torsion of the C<sub>1</sub>-C<sub>4</sub>/C<sub>2</sub>-C<sub>3</sub> bonds.<sup>87</sup>

There already appears to be some experimental evidence that contradicts the predictions of the avoided crossing model for *cis,trans*- photoisomerization. On the basis of resonance Raman spectroscopic results for isoprene, Mathies and coworkers<sup>21, 96</sup> proposed that the initial relaxation modes (after Franck Condon excitation to the <sup>1</sup>B<sub>u</sub> state) include torsion about the central bond. This is also suggested by gas-phase spectroscopic studies of acyclic dienes<sup>21, 24</sup>.

Aue and coworkers<sup>91</sup> reported the photochemical ring closure of constrained *s-cis* exocyclic dienes **109-112** (see Scheme 4.1.1). They found that the photoconversions of 1,2-dimethylenecyclohexane (**109**) to bicyclo[4.2.0]oct-1(2)ene (**113**) and 1,2-dimethylenecyclopentane (**110**) to **114** proceed in high (> 95 %) chemical yield, and with quantum yield of about 0.1.

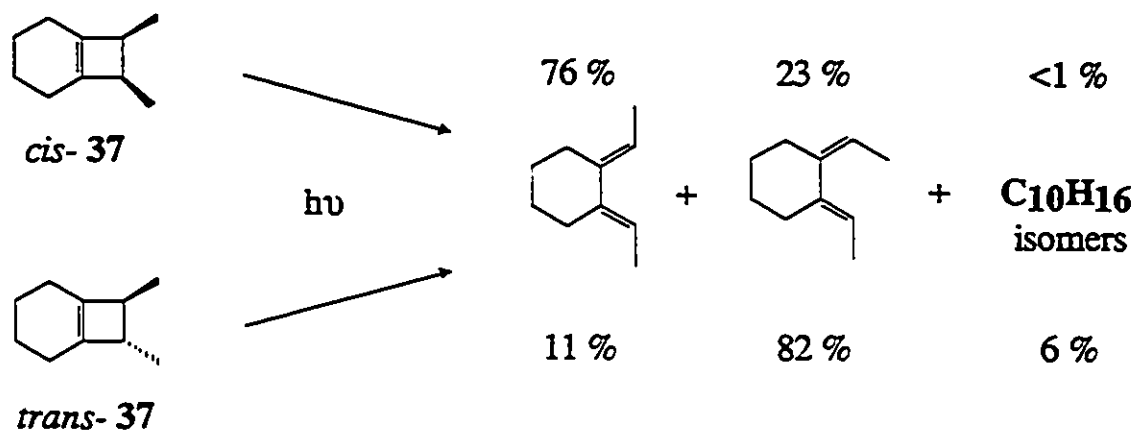


Scheme 4.1.1. Photochemistry of constrained *s-cis* dienes.

The substantially lower quantum yields for photocyclization of **111** and **112** were ascribed to strain effects on the rates and quantum yields of photochemical ring closure, since the diene chromophores are essentially identical and were assumed to possess similar excited state lifetimes.

The conical intersection model<sup>61, 102, 104, 177</sup> rationalizes the trend observed for these compounds as due to variations in the torsional flexibility of the central bond throughout the series.

The report from Leigh and coworkers<sup>67</sup> on the photochemistry of *cis*- and *trans*-**37** (*vide infra*) provided a strong indication that orbital symmetry factors do play a role in the photochemical ring opening of cyclobutenes<sup>33</sup>. The high degree of disrotatory stereoselectivity observed in this photochemical ring opening reaction (> 75 % of the formally allowed *E,E* isomer from ring opening of *cis*- cyclobutene **37**, and > 80 % of the allowed *E,Z* isomer from ring opening of *trans*-**37**) was the first clear example that suggests that orbital symmetry factors may be important.



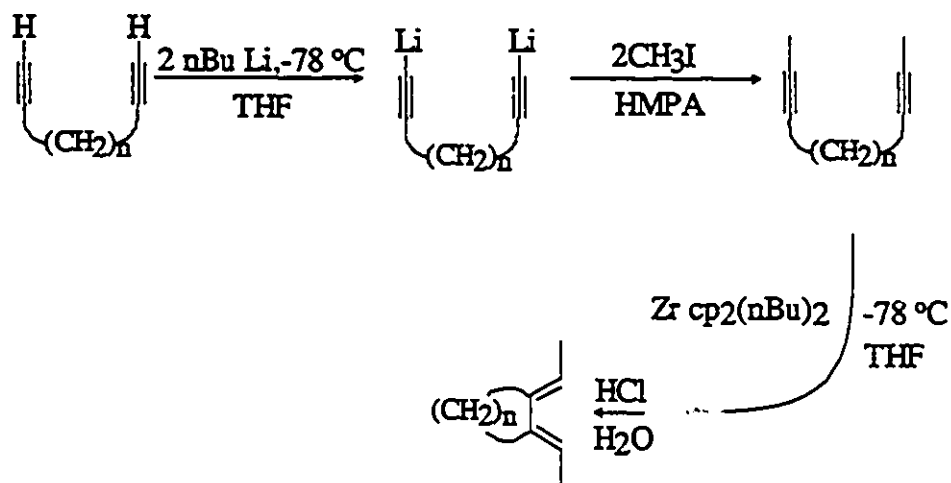
It is possible that the special structure of **37** is the dominant factor responsible for the high degree of disrotatory selectivity in the photochemical ring opening of these compounds. *cis*- And *trans*-**37** would be expected to experience reduced central bond torsional flexibility as ring opening commences, and may be indicative of the validity of the conical intersection mechanism for cyclobutene ring opening.

This chapter describes a study directed at assessing the importance of central bond torsional motions in both diene and cyclobutene photochemistry. The study involves an investigation of the photochemistry of an expanded series of cyclobutenes and their isomeric dienes. Determination of the quantum yields for *cis,trans*- photoisomerization of the dienes will allow us to test the effects of central bond torsional constraint on the

efficiency of the photoisomerization processes of conjugated dienes. They will also allow a more comprehensive test of the adiabatic ring opening mechanism that was described in Chapter 1.4.

## 4.2 Preparation and Identification of Compounds

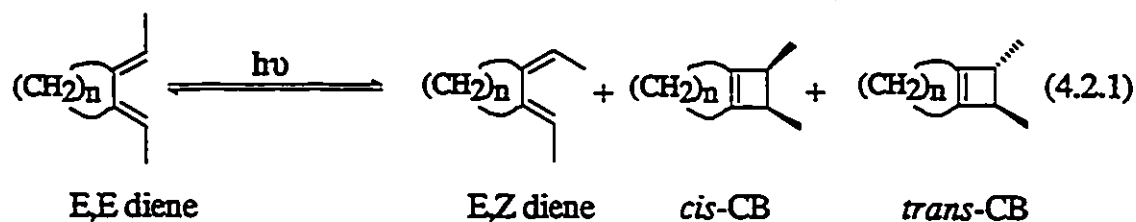
Synthesis of the *E,E* isomers of the 1,2-bis(ethylidene)cycloalkanes 124-127 was effected by zirconocene-mediated intramolecular coupling<sup>180</sup> of the corresponding dialkynes 116-119, which in turn were synthesized by methylation of the terminal dialkynes 120-123, (see Scheme 4.2.1).



<i>Terminal dialkyne</i>	<i>Diene</i>	<i>Methylated alkyne</i>
n		
2    120	124	116
3    121	125	117
4    122	126	118
5    123	127	119

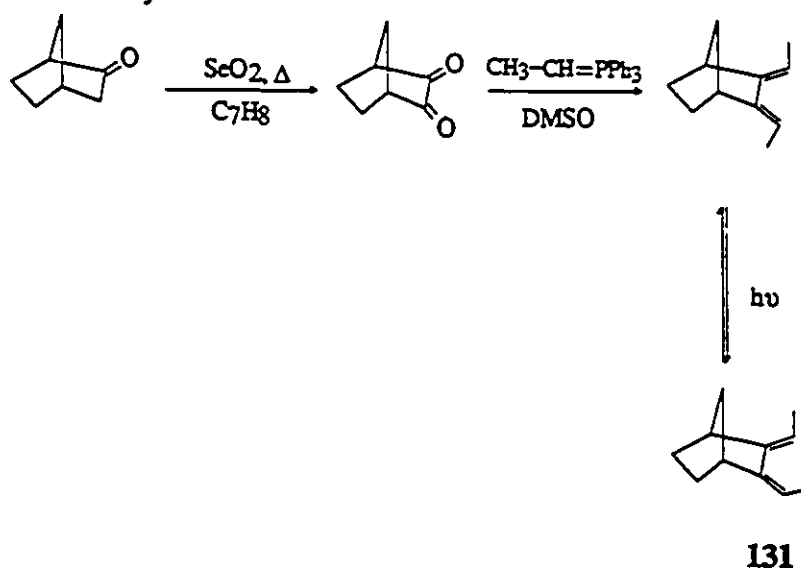
Scheme 4.2.1. Synthesis of 1,2-bis(ethylidene)-cycloalkanes

Exhaustive irradiation (254 nm) of the *E,E*-diene isomers was then carried out to afford a mixture of the *E,E*- and *E,Z*-dienes and the *cis*- and *trans*-cyclobutenes, which were separated and purified by semipreparative gas chromatography (equation 4.2.1).



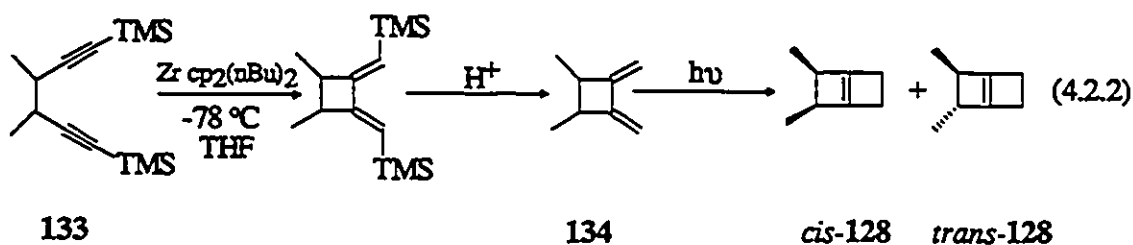
<i>n</i>	<i>diene</i>	<i>cyclobutene</i>
2	124	
3	125	129
4	126	37
5	127	130

The dienes *E,E*- and *E,Z*-2,3-bis(ethylidene)bicyclo[2.2.1]heptane, **131**, whose syntheses are described in Scheme 4.2.2, will also be utilized in the *cis,trans*-photoisomerization study.



Scheme 4.2.2. Synthesis of 2,3-bis(ethylidene)bicyclo[2.2.1]heptanes.

The photoisomerization step to the cyclobutene (equation 4.2.1) was useful only for the syntheses of *cis*- and *trans*- isomers of cyclobutenes **129**, **37**, and **130**. *Cis*- and *trans*- **128** ( $n = 2$ ) were synthesized by a route (equation 4.2.2) involving initial zirconocene-mediated cyclization of the dialkyne **133**, hydrogenolysis and photocyclization of the resulting mixture of 3,4-dimethyl-1,2-*bis*(methylene)cyclobutanes **134**. The isomeric dimethylbicyclo[2.2.0]hexenes **128** were thermally labile, but could be separated and purified by semipreparative GC under mild conditions.

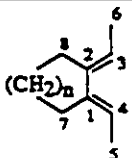
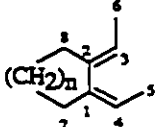


The dienes and cyclobutenes were characterized by  $^1\text{H}$  and  $^{13}\text{C}$  NMR, IR, MS, UV, and High Resolution Mass Spectrometric Measurements. Table 4.2.1 summarizes some diagnostic  $^{13}\text{C}$  nuclear magnetic resonances of dienes **124-127**. The NMR spectra of the *E,E*- diene isomers are much simpler than those of the *E,Z*- isomers due to symmetry factors.

Table 4.2.2 summarizes the UV absorption data of the *E,E*- and *E,Z*- isomers of **124-127**, and **131**. Figure 4.2.1 shows the UV spectra of the *E,E*-isomers of **124-127** and **131**, recorded as dilute ( $\text{ca. } 5 \times 10^{-5} \text{ mol dm}^{-3}$ ) deoxygenated pentane solutions. The UV spectrum of *E,E*-**124** exhibits detailed fine structure centered at 252 nm. The UV

spectrum of *E,E*-131 shows only minor fine structure. The rest of the dienes display a rather broad absorption, devoid of any fine structure.

**Table 4.2.1.** Diagnostic  $^{13}\text{C}$  NMR chemical shifts of 124-127 *E,E*- and *E,Z*- diene isomers determined in deuteriochloroform as solvent.

		$\delta$ [ppm]							
									
$n \rightarrow$		0	1	2	3	0	1	2	3
C	$\downarrow$								
1		141.60	141.12	142.03	146.06	142.47	146.39	142.14	145.31
2						140.22	141.10	137.39	140.27
3		111.47	111.13	115.71	117.40	117.29	120.32	118.85	121.33
4						116.07	116.06	116.48	117.38
5		13.21	14.85	12.92	13.03	14.60	15.41	12.69	14.03
6						13.94	15.10	14.11	14.95
7		29.69	30.35	27.95	31.80	26.42	36.42	37.89	38.00
8						24.98	31.09	28.66	29.68



**Table 4.2.2.** Ultraviolet absorption data for *E,E*- and *E,Z*- dienes 124-127 and 131. The spectra were recorded in *ca.*  $5 \times 10^{-5}$  mol dm<sup>-3</sup> deoxygenated pentane solutions at 23° C.

<i>Diene</i>	$\lambda_{\max}$ [nm]	$\epsilon_{\max}$ [dm <sup>3</sup> mol <sup>-1</sup> cm <sup>1</sup> ]	E [KJ mol <sup>-1</sup> ]
<i>E,E</i> - 124	252	9900	476
<i>E,E</i> - 125	252	9550	476
<i>E,E</i> - 126	221	8500	543
<i>E,E</i> - 127	222	9010	541
<i>E,E</i> - 131	253	11200	474
<i>E,Z</i> - 124	250	10550	480
<i>E,Z</i> - 125	249	9930	482
<i>E,Z</i> - 126	220	9000	545
<i>E,Z</i> - 127	219	8990	548
<i>E,Z</i> - 131	245	11900	490

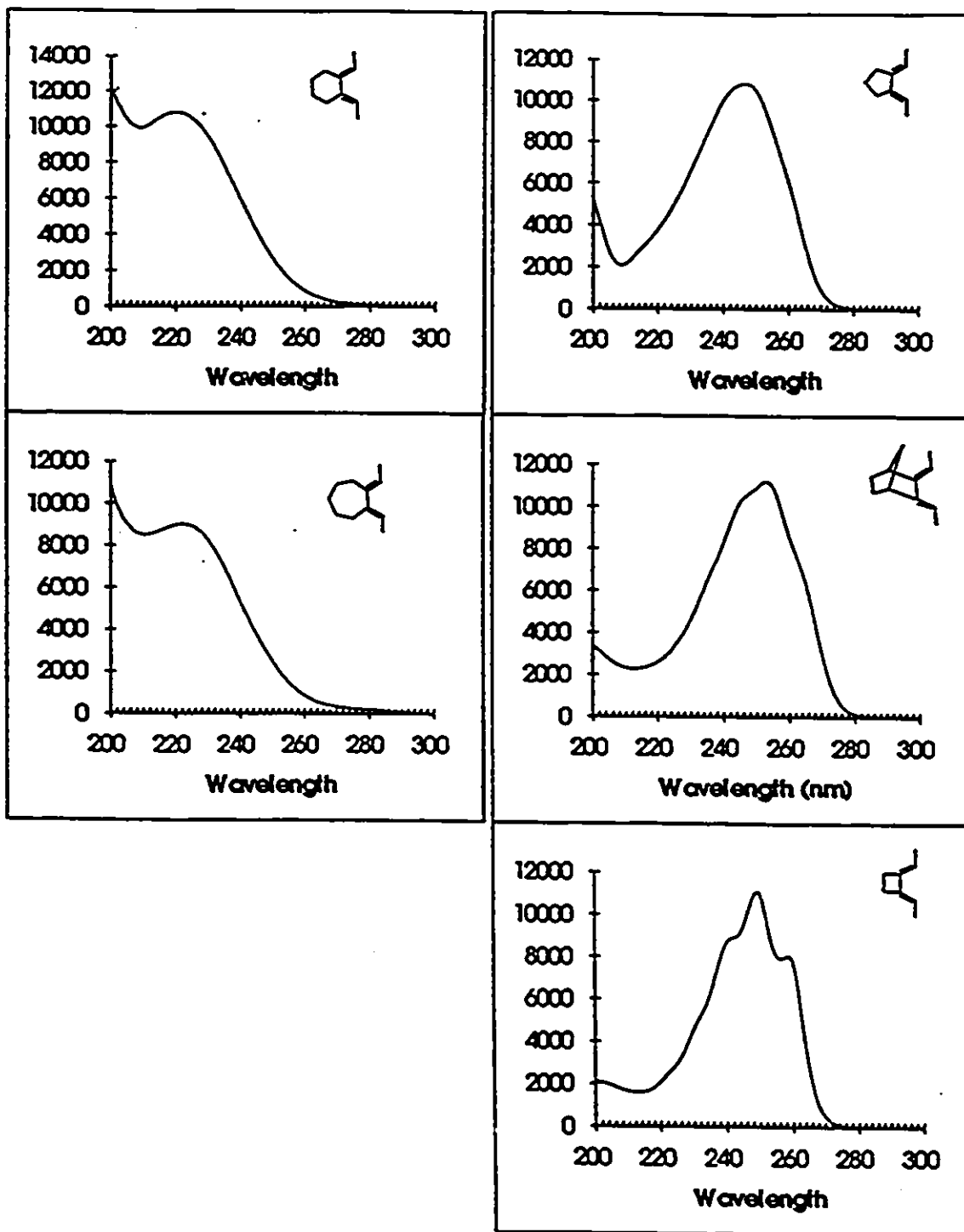
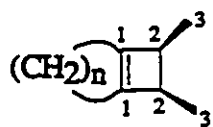
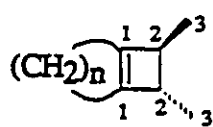


Figure 4.2.1. Solution phase UV absorption spectra of *E,E*- 124-127 and 131 measured at 23 °C, 1.0 cm path length in pentane *ca.*  $1 \times 10^{-4}$  mol dm<sup>-3</sup> solutions

The *cis*- and *trans*-cyclobutene isomers were readily distinguished by their  $^1\text{H}$  and  $^{13}\text{C}$  nuclear magnetic resonance spectra. The proton resonances due to the hydrogens at positions 3 and 4 of the cyclobutene ring are particularly diagnostic<sup>46</sup> of stereochemistry in alkylcyclobutene. In the *trans*-series, these hydrogens are displaced to lower fields with respect to those in the *cis*-isomers; the same trend is observed for the methyl groups. Of particular interest is the  $\gamma$  effect observed in the  $^{13}\text{C}$  nuclear magnetic resonances that confirmed the identification of the *cis*- and *trans*-isomers of the cyclobutene series (Table 4.2.3).

**Table 4.2.3.** Diagnostic  $^{13}\text{C}$  NMR chemical shifts of bicyclic cyclobutenes determined in carbon tetrachloride as solvent.

$\delta$ [ppm]						
						
n	C <sub>1</sub>	C <sub>2</sub>	C <sub>3</sub>	C <sub>1</sub>	C <sub>2</sub>	C <sub>3</sub>
1	154.34	38.67	14.11	152.60	44.62	17.50
2	144.74	40.48	13.19	143.69	46.42	16.94
3	145.12 <sup>§</sup>	38.35 <sup>§</sup>	13.11 <sup>§</sup>	143.99	44.45	17.44

<sup>§</sup> Determined in Deuteriochloroform.

The condensed-phase ultraviolet absorption spectra of the *cis*-, and *trans*-cyclobutenes 128, 129, 37, and 130 follow similar trends to those observed for 95 and

96<sup>42</sup>. The condensed-phase UV absorption spectra of *cis*- and *trans*- cyclobutenes 128, 129, 37, and 130 are shown in Figure 4.2.2.

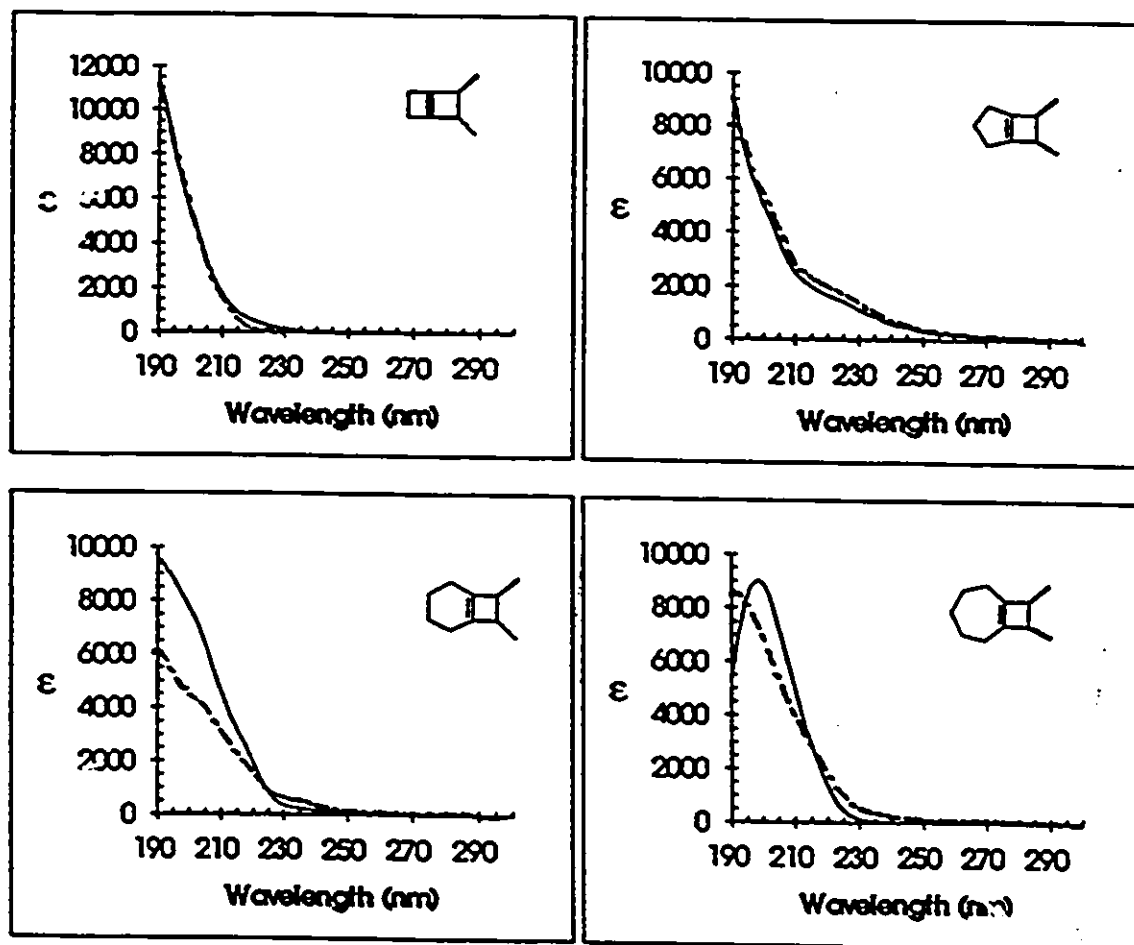
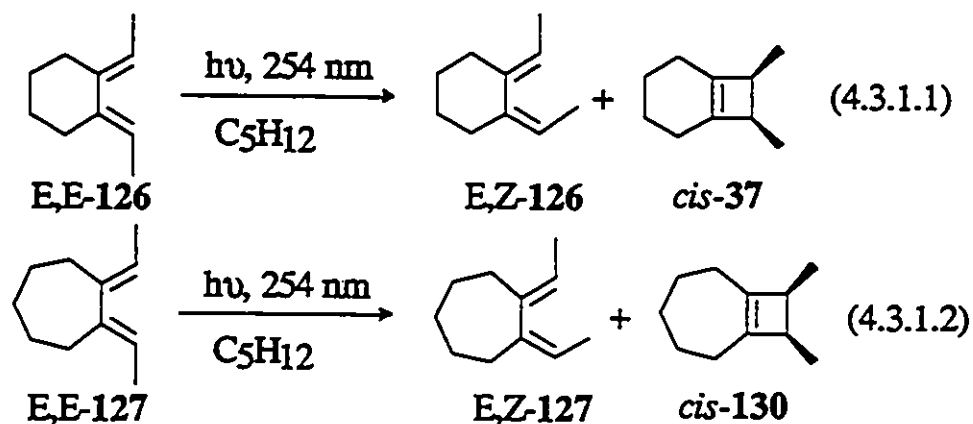


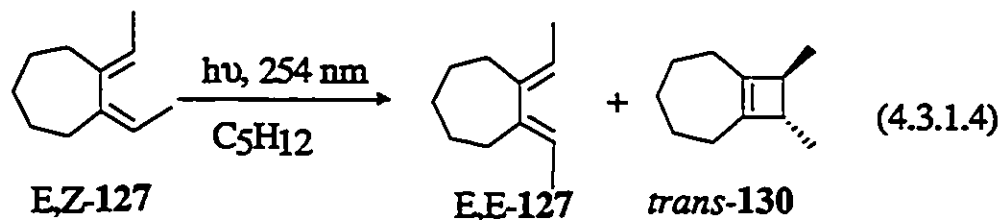
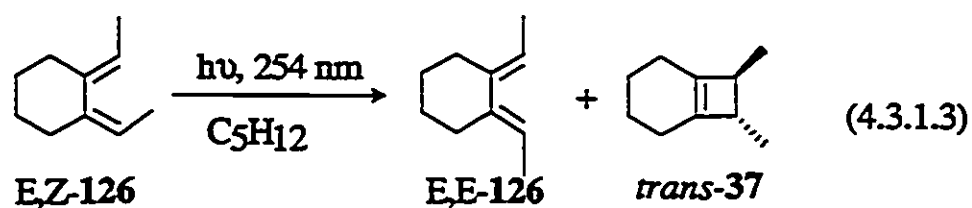
Figure 4.2.2. Solution phase UV absorption spectra for *cis*-(—), and *trans*-(---) 128-130, and 37 measured at 23 °C, in deoxygenated pentane solutions *ca.*  $2 \times 10^{-4}$  mol dm<sup>-3</sup>

### 4.3. Results

#### 4.3.1 Direct Irradiation of Dienes

Direct irradiation (254 nm) of deoxygenated *ca.* 0.02 mol dm<sup>-3</sup> pentane solutions of *E,E*-126 and 127 resulted in the formation of the corresponding *E,Z*-isomers and *cis*-cyclobutenes 37 and 130 according to equations 4.3.1.1-2. Direct irradiation (254 nm) of the *E,Z*-isomers 126 and 127 yielded the corresponding *E,E*-dienes, *trans*-cyclobutenes and small amounts of unidentified products according to equations 4.3.1.3-4. Plots of moles of photoproduct versus irradiation time were constructed for each product and are shown in Figures 4.3.1.1-2. Quantum yields for *cis,trans* isomerization and cyclobutene formation were determined using ferrioxalate actinometry (see Appendix 1), and are collected in Table 4.3.1.1.





**Table 4.3.1.1.** Quantum yields for *cis,trans*- photoisomerization and cyclobutene formation from 254 nm irradiation of *ca.* 0.02 mol dm<sup>-3</sup> deoxygenated pentane solutions of *E,E*- and *E,Z*-126 and 127

<i>Diene</i>	$\phi_{\text{EE-EZ}}$	$\phi_{\text{EZ-EE}}$	$\phi_{\text{EE-CB}}$	$\phi_{\text{EZ-CB}}$	$\Sigma\phi_{\text{other}}^{\text{a}}$ ( <i>cis</i> )	$\phi_{\text{other}}$ ( <i>trans</i> )
126	0.20 ± 0.03	0.29 ± 0.03	0.074 ± 0.001	0.13 ± 0.01	0.041 ± 0.005	0.034 ± 0.009
127	0.21 ± 0.03	0.14 ± 0.06	0.067 ± 0.001	0.032 ± 0.001	0.027 ± 0.008	0.021 ± 0.005

a. No more than of 5 % of total product.

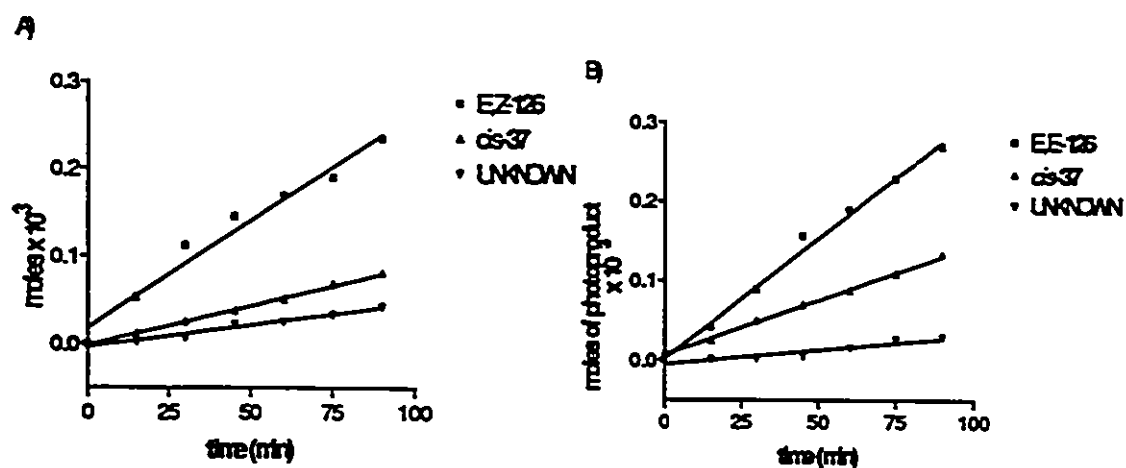


Figure 4.3.1.1 Plots of moles of photoproduct *versus* irradiation time from photolysis of A) *E,E*-1,2-Bis(ethylidene)cyclohexane (*E,E*-126) and B) *E,Z*-1,2-Bis(ethylidene)cyclohexane (*E,Z*-126) in deoxygenated pentane solutions with 254 nm Light

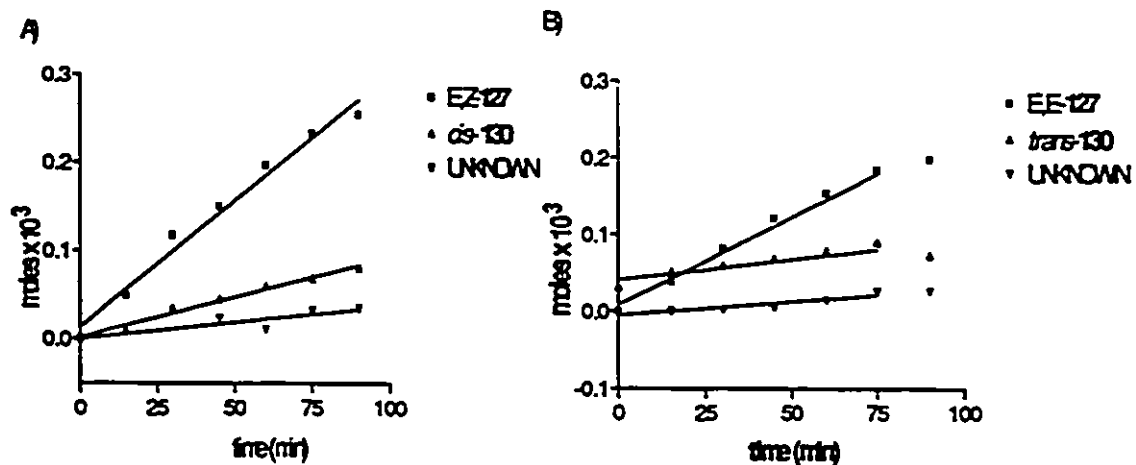
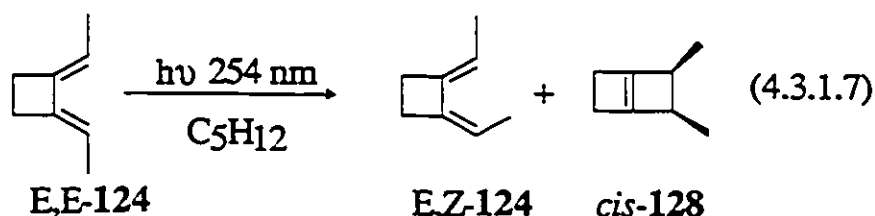
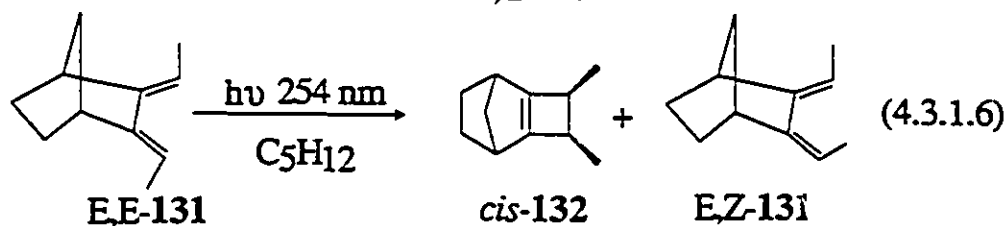
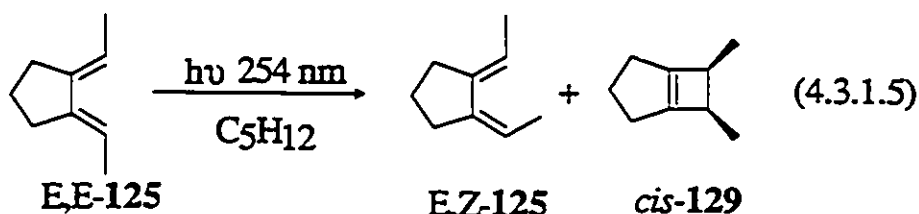
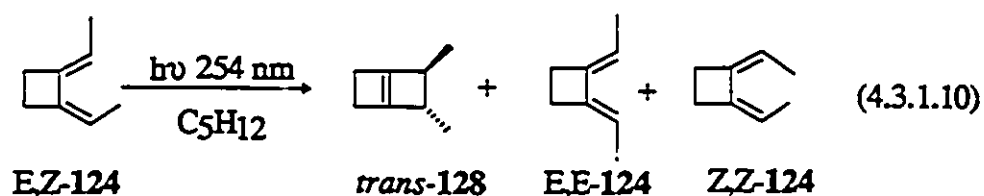
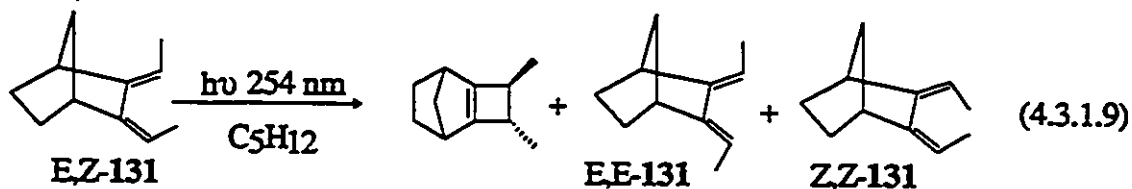
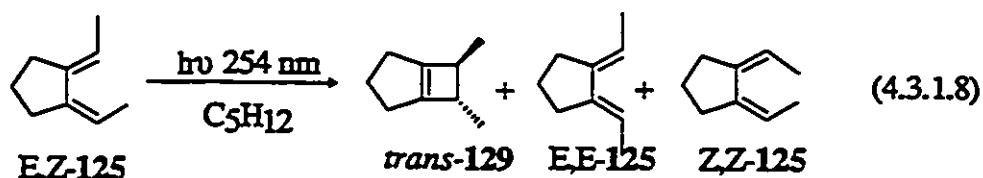


Figure 4.3.1.2. Moles of photoproduct *versus* irradiation time plots for photolysis of A) *E,E*-1,2-Bis(ethylidene)cycloheptane (*E,E*-127) and B) *E,Z*-1,2-bis(ethylidene)cycloheptane (*E,Z*-127) in deoxygenated pentane solutions with 254 nm Light

Direct irradiation (254 nm) of deoxygenated *ca.* 0.02 mol dm<sup>-3</sup> pentane solutions of the *E,E*-isomers of 1,2-bis(ethylidene)-cyclopentane 125 and cyclobutane 124, and 2,3-bis(ethylidene)-norbornane 131 results in the formation of the corresponding *E,Z*-isomers and *cis*-cyclobutenes 129, 132 and 128, as depicted by equations 4.3.1.5-7. Direct irradiation of the *E,Z*-isomers of 125, 131 and 124 yields the corresponding *E,E*- diene and *trans*-cyclobutene derivatives, and small amounts of isomeric compounds which were not identified, according to equations 4.1.3.8-10.







Product yields were determined from plots of moles of photoproduct versus irradiation time as shown in Figures 4.3.1.3-5. Quantum yields for *cis,trans*- photoisomerization and for cyclobutene formation and other minor products were determined for all compounds in the series relative to the *cis,trans*- photoisomerization of *E,E*-125, which was determined to be  $\phi_{E,E \rightarrow E,Z} = 0.24 \pm 0.02$  by ferrioxalate actinometry, and are collected in Table 4.3.1.2.

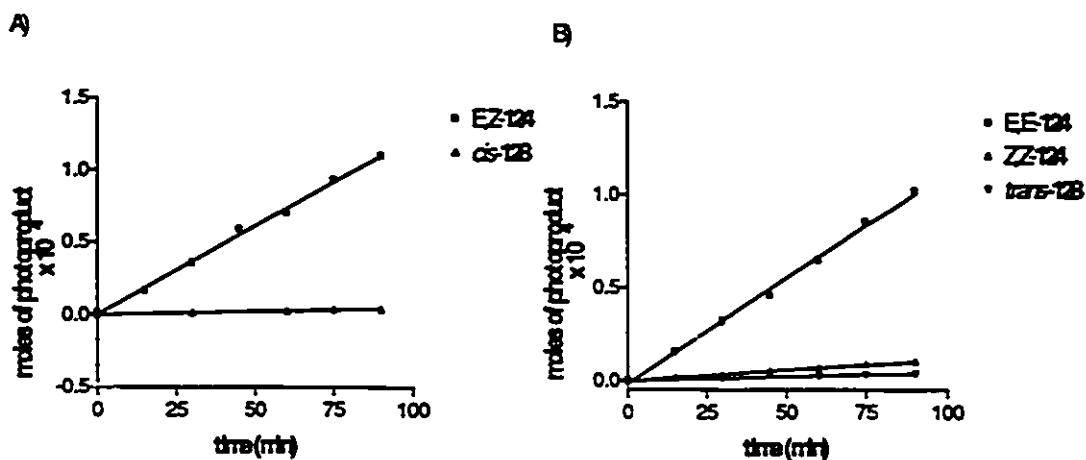


Figure 4.3.1.3. Moles of photoproduct *versus* irradiation time plots for photolysis of A) *E,E*-1,2-*bis*(ethylidene)cyclobutane (*E,E*-124) and B) *E,Z*-1,2-*bis*(ethylidene)cyclobutane (*E,Z*-124) in deoxygenated pentane solutions with 254 nm Light

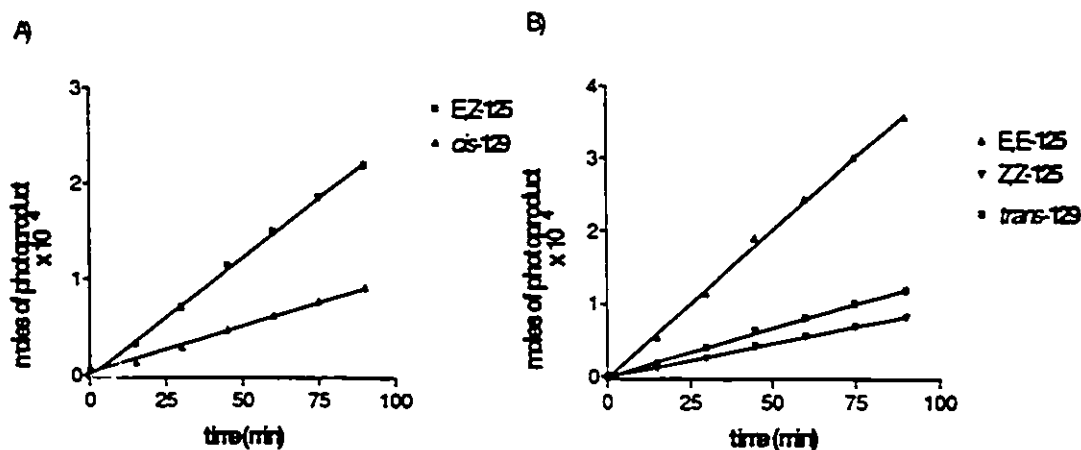


Figure 4.3.1.4. Moles of photoproduct *versus* irradiation time plots for photolysis of A) *E,E*-1,2-*Bis*(ethylidene)cyclopentane (*E,E*-125) and B) *E,Z*-1,2-*Bis*(ethylidene)cyclopentane (*E,Z*-125) in deoxygenated pentane solutions with 254 nm Light

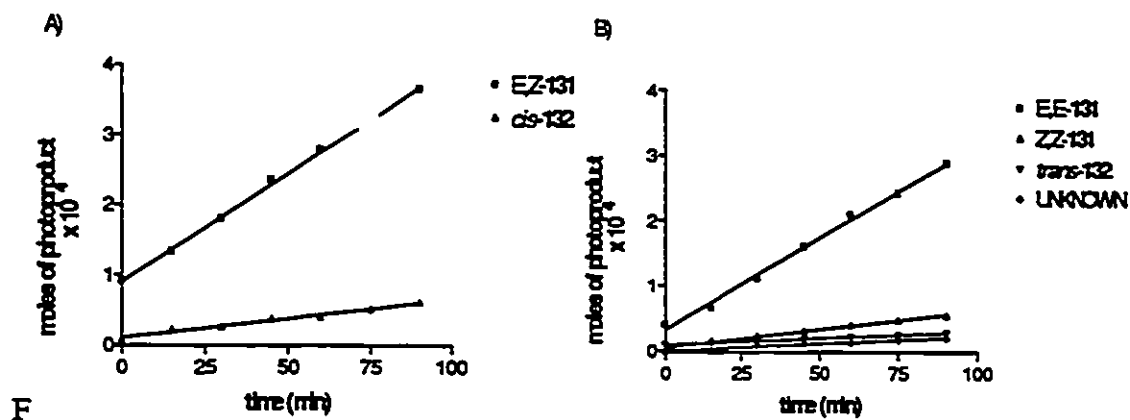


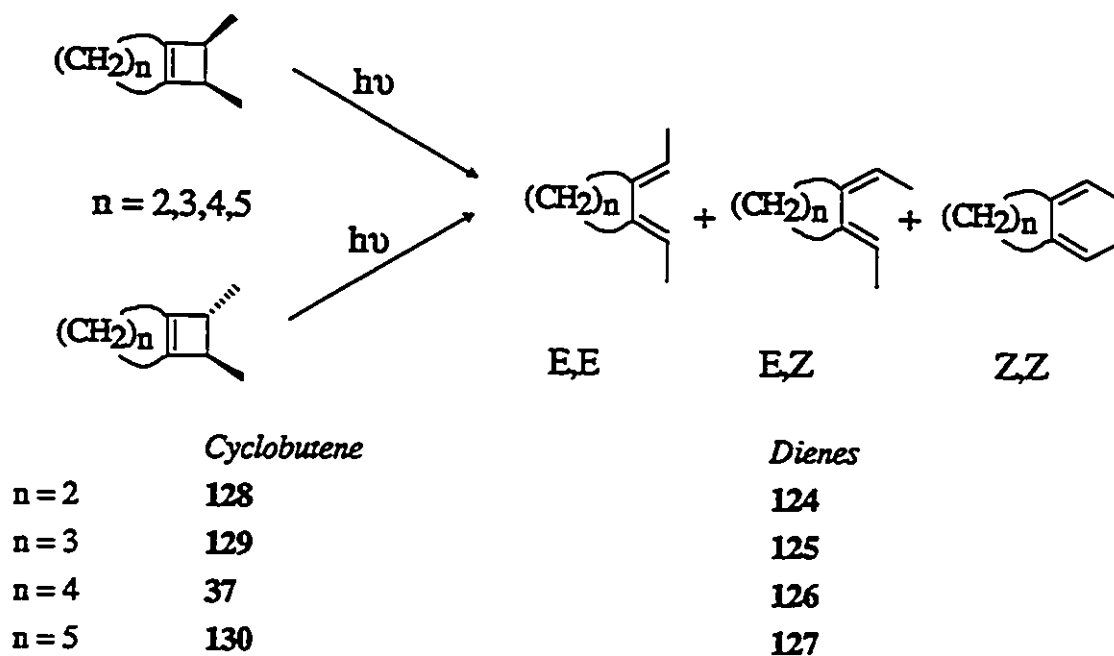
Figure 4.3.1.5. Moles of photoproduct *versus* irradiation time Plots for photolysis of A) *E,E*-2,3-*bis*(ethylidene)bicyclo[2.2.1]Heptane (*E,E*-131) and B) *E,Z*-2,3-*bis*(ethylidene)bicyclo[2.2.1]Heptane (*E,Z*-131) in deoxygenated pentane solutions with 254 nm Light

Table 4.3.1.2. Quantum yields for *cis,trans*- photoisomerization and cyclobutene formation from 254 nm irradiation of 1,2-*bis*(ethylidene)cycloalkanes 125, 131, and 124 in deoxygenated pentane solutions at 23°C

<i>Diene</i>	$\phi_{EE-EZ}$	$\phi_{EZ-EE}$	$\phi_{EZ-ZZ}$	$\phi_{CB}$	$\phi_{other}$
125	$0.24 \pm 0.02$	$0.39 \pm 0.04$	$0.09 \pm 0.01$	$0.10 \pm 0.02$ (EE)	$< 0.002$ (EE)
				$0.13 \pm 0.01$ (EZ)	$= 0.01$ (EZ)
131	$0.30 \pm 0.03$	$0.28 \pm 0.03$	$0.06 \pm 0.01$	$0.03 \pm 0.01$ (EE)	$= 0.003$ (EE)
				$0.03 \pm 0.01$ (EZ)	$< 0.005$ (EZ)
124	$0.12 \pm 0.02$	$0.11 \pm 0.03$	$0.011 \pm 0.005$	$< 0.005$ (EE)	$= 0.01$ (EE)
				$< 0.005$ (EZ)	$= 0.01$ (EZ)

### 4.3.2 Direct Irradiation of *cis*- and *trans*-Dimethylbicyclo[n.2.0]Alk-1<sup>n+2</sup>-enes.

Irradiation of *ca.* 0.02 mol dm<sup>-3</sup> deoxygenated pentane solutions of **128-129**, **37** and **130**, with the pulses from an Ar/F<sub>2</sub> excimer laser (193 nm; 15 ns; 20 mJ; 0.5 Hz repetition rate) or with a 16W Zn resonance lamp (214 nm) resulted in the clean formation of *E,E*- and *E,Z*- **124-127** as the major products, with minor amounts of the *Z,Z*- diene in the irradiations of the *trans*- isomers (Scheme 4.3.2.1). No other products were observed in yields greater than *ca.* 3 % in any case. Product yields were determined from the slopes of moles of photoproduct *versus* photolysis time plots (for the *E,E*- ,*E,Z*- , and *Z,Z*- diene isomers). These plots are shown in Figures 4.3.2.1-5 for the photolyses of *cis*- and *trans*-cyclobutenes **128**, **129**, **37**, and **130** respectively. Quantum yields for product formation from photolysis of cyclobutenes **129**, **37**, and **130** were determined using the ring opening of bicyclo[4.2.0]oct-6(1)-ene as actinometer<sup>181, 182</sup> for 193 nm irradiations. Quantum yields for ring opening of *cis*- and *trans*-**128** were determined with 214 nm excitation, using uranyl oxalate actinometry<sup>113</sup>. Table 4.3.2.1 lists the quantum yield data from photolysis of the eight compounds at the two excitation wavelengths, along with the *E,E*-/*E,Z*- diene ratios calculated from the slopes of moles of photoproduct vs time plots over the 0.5-4% conversion range.



Scheme 4.3.2.1. Photolysis of dimethylbicyclo[n.2.0]alk-1-ene

Table 4.3.2.1. Quantum yields for diene formation from 193 nm and 214 nm irradiation of *ca.* 0.02 mol dm<sup>-3</sup> deoxygenated pentane solutions of *cis*- and *trans*- 128, 129, 37, and 130

<i>Cyclobutene</i>	$\phi_{EE}$	$\phi_{EZ}$	$\phi_{total}$	( <i>E,E</i> -/ <i>E,Z</i> -) <sub>193</sub>	( <i>E,E</i> -/ <i>E,Z</i> -) <sub>214</sub>
<i>cis</i> -128	0.55 ± 0.04	0.32 ± 0.06	0.87		1.7
<i>cis</i> -129	0.42 ± 0.05	0.17 ± 0.03	0.59	2.5	
<i>cis</i> -37	0.48 ± 0.06	0.14 ± 0.02	0.62	3.4	
<i>cis</i> -130	0.68 ± 0.05	0.075 ± 0.008	0.75	9.1	5.38
<i>trans</i> -128	0.066 ± 0.009	0.61 ± 0.04	0.69		0.11
<i>trans</i> -129	0.065 ± 0.008	0.59 ± 0.07	0.66	0.11	
<i>trans</i> -37	0.08 ± 0.02	0.45 ± 0.06	0.53	0.18	
<i>trans</i> -130	0.19 ± 0.03	0.67 ± 0.05	0.86	0.29	0.48

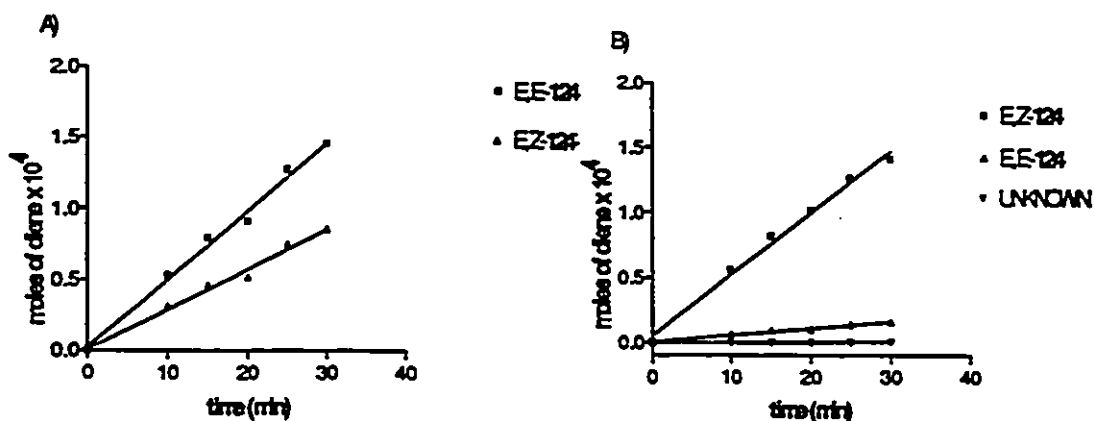


Figure 4.3.2.1. Moles of photoproduct *versus* time plots for the photolysis (214 nm) of *ca*  $1 \times 10^{-2}$  mol  $\text{dm}^{-3}$  deoxygenated pentane solution of A) *cis*-5,6-dimethylbicyclo[2.2.0]hex-1(4)-ene (*cis*-128) and B) *trans*-5,6-dimethylbicyclo[2.2.0]hex-1(4)-ene (*trans*-128) with 214 nm Light

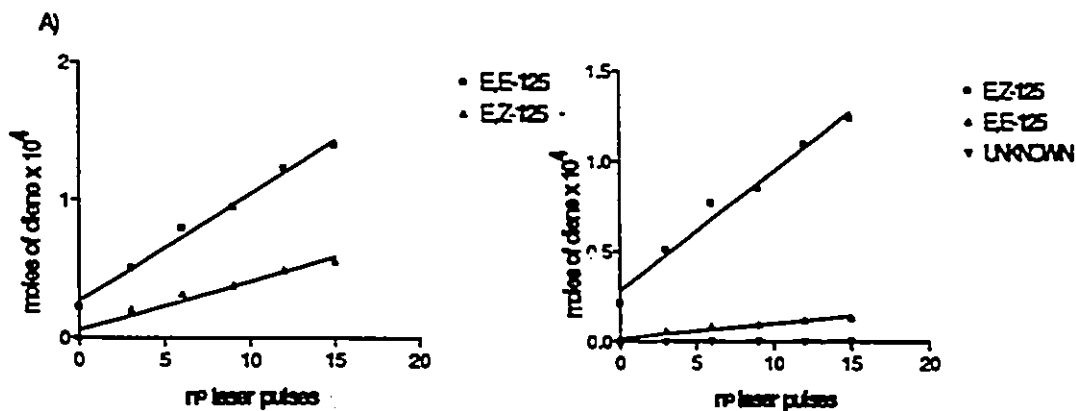


Figure 4.3.2.2. Moles of photoproduct *versus* laser dose for the photolysis (193 nm) of *ca*  $1 \times 10^{-2}$  mol  $\text{dm}^{-3}$  deoxygenated pentane solutions of A) *cis*-6,7-dimethylbicyclo[3.2.0]hept-1(5)-ene (*cis*-129) and B) *trans*-6,7-dimethylbicyclo[3.2.0]hept-1(5)-ene (*trans*-129)

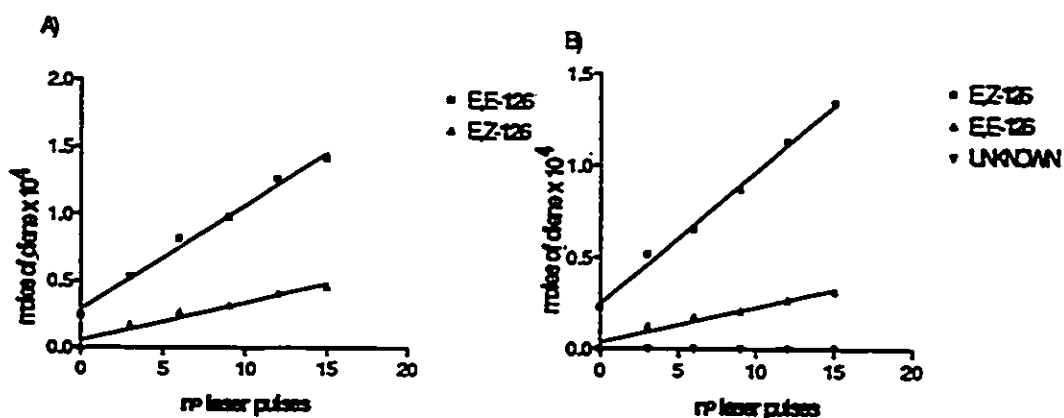


Figure 4.3.2.3. Moles of photoproduct *versus* laser dose for the photolysis (193 nm) of *ca*  $1 \times 10^{-2}$  mol dm<sup>-3</sup> deoxygenated pentane solutions of A) *cis*-7,8-dimethylbicyclo[4.2.0]oct-1(6)-ene (*cis*-37) and B) *trans*-7,8-dimethylbicyclo[4.2.0]oct-1(6)-ene (*trans*-37)

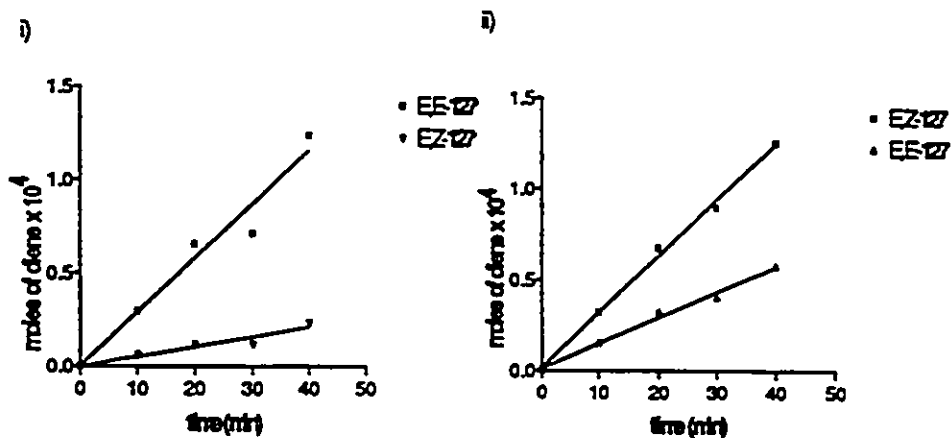


Figure 4.3.2.4. Moles of photoproduct *versus* time plots for the photolysis (214 nm) of *ca*  $1 \times 10^{-2}$  mol dm<sup>-3</sup> deoxygenated pentane solution of i) *cis*-8,9-dimethylbicyclo[5.2.0]non-1(7)-ene (*cis*-130) and ii) *trans*-8,9-dimethylbicyclo[5.2.0]non-1(7)-ene (*trans*-130)

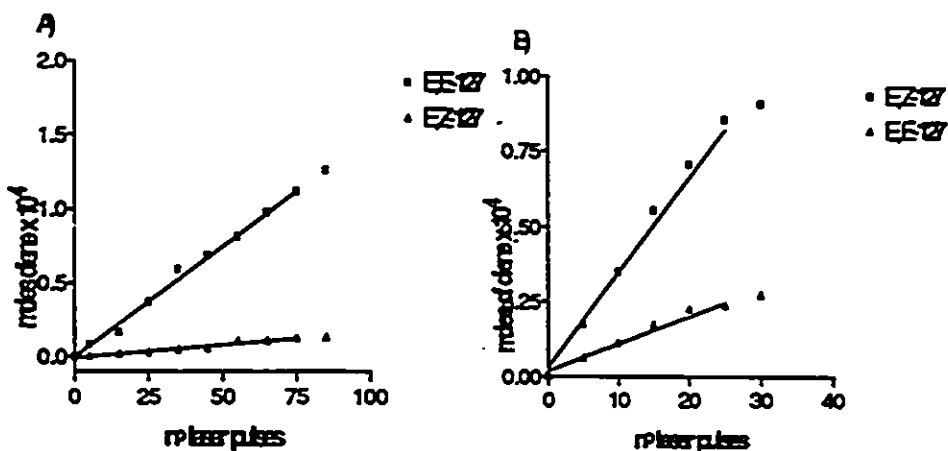


Figure 4.3.2.5. Moles of photoproduct vs laser dose for the photolysis (193 nm) of *ca*  $1 \times 10^{-2}$  mol dm<sup>-3</sup> deoxygenated pentane solution of A) *cis*-8,9-dimethylbicyclo[5.2.0]non-1(7)-ene (*cis*-130) and B) *trans*-8,9-dimethylbicyclo[5.2.0]non-1(7)-ene (*trans*-130).

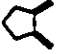
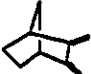

## 4.4 DISCUSSION

### 4.4.1 The *cis,trans* Photoisomerization of Constrained *s-cis* Dienes

The five sets of isomeric dienes studied, 124-127, and 131, have planar *s-cis* structures with central bond dihedral angle close to 0°, but with varying abilities to twist about the dihedral. This is demonstrated by molecular mechanics calculations. The results of MMX dihedral driver calculations for the corresponding *bis*-(methylene)cycloalkanes 110-112 are listed in Table 4.4.1.1. The data listed are the central bond dihedral angle at which the calculated MMX heat of formation of the corresponding *bis*methylene cycloalkanes 110-112 is 12.5 KJ mol<sup>-1</sup> higher than that of its stable ground state geometry<sup>178</sup>.



**Table 4.4.1.1.** Central bond dihedral angles at which the calculated MMX heat of formation of the corresponding *Bis(methyldene)cycloalkanes* is 12.5 KJ mol<sup>-1</sup> higher than that of its stable ground state geometry. C<sub>1</sub>-C<sub>4</sub> distances are included (terminal methylene carbons).

	<i>Diene</i>	Angle for $\Delta H_f = 12.5$ KJ mol <sup>-1</sup>	C <sub>1</sub> -C <sub>4</sub> distance <sup>‡</sup> [Å]
110		37°	1.49961
111		31°	1.51229
112		27°	1.52276

<sup>‡</sup> Ground State Geometry

The quantum yields for *cis,trans*- isomerization of **125** and **131** (Table 4.3.1.2) are of similar magnitude to those reported for the 2,4-hexadienes (Table 1.5.1) and those for **126** and **127** (Table 4.3.1.1), and can thus be considered typical of conjugated dienes in general. In contrast, those for *E,E*- and *E,Z*-**124** are significantly lower. No fluorescence was detected at room temperature for **124** and no evidence was found for the formation of other products, which might account for the reduced quantum yields for *cis,trans*-isomerization.

The results for **124** are incompatible with the classical allylmethylene mechanism for *cis,trans*- photoisomerization (Chapter I, Section 1.6A). This model requires that *cis,trans*- isomerization involves planarization of the diene framework and twisting about one of the terminal C=C bonds. Clearly, constraining the central bond would not be expected to affect the efficiency of the process if it occurred by such a mechanism. It is

possible that distortions of the C<sub>2</sub>-C<sub>3</sub> bond which are caused by the cyclobutyl ring<sup>183</sup> destabilize the allylmethylene structure relative to those of 125 and 131, but to a first approximation, this should also be felt in the fully planar geometry. Thus, it does not seem likely that this factor could account for the observed results .

On the other hand, the results for 124 are qualitatively compatible with the conical intersection mechanism suggested by recent theoretical calculations<sup>79, 104, 179</sup>. As mentioned previously, the geometry of the *s-cisoid* conical intersection (CI) found for the excited singlet state surface of 1,3-butadiene is a tetraradicaloid structure with all three C-C bonds twisted, partly as a result of substantial pyramidalization at one of the two central carbons<sup>104</sup>. In the cases of 124, 125, and 131, structural constraints prevent access to the *s-trans*- conical intersection (50 in Figure 1.6.3, Chapter I), so that only the *s-cis*-structure (48 in Figure 1.6.3) needs to be considered. The theory stipulates that after Franck Condon excitation of *s-cis*- butadiene to the <sup>1</sup>B<sub>u</sub> state, minor distortions allow crossing onto the double excited 2<sup>1</sup>A<sub>g</sub> surface. Once on the 2<sup>1</sup>A<sub>g</sub> surface, the molecule relaxes to the conical intersection region by *disrotatory* twisting around C<sub>1</sub>-C<sub>2</sub> and C<sub>3</sub>-C<sub>4</sub> bonds and pyramidalization at C<sub>2</sub>. Once the conical intersection region is entered, rapid decay to the ground state surface occurs, and the molecule partitions to stable products (the *s-trans*- conformer, cyclobutene, and geometric isomers, Scheme 1.6.4) in relative yields which depend on the trajectories of two vectors that define the conical intersection region<sup>61</sup>.

One might expect that preventing the molecule from undergoing the C<sub>2</sub> pyramidalization process, which is qualitatively similar to C<sub>2</sub>-C<sub>3</sub> bond torsion, would inhibit decay via the conical intersection, resulting in low quantum yields for photoreaction. The results for 124 (anomalously low quantum yields for *cis,trans*-isomerization and no cyclobutene formation) are consistent with this idea.

The calculated geometry for the *s-cis*-conical intersection of 1,3-butadiene (48 in Figure 1.6.2) has a torsional angle of  $52^\circ$  -larger than that obtainable (with a reasonable expenditure of energy) from any of the three compounds studied (124, 125, and 131). If the theoretical model is correct, our results would suggest that is unnecessary for the system to achieve the full  $52^\circ$  angle in order for efficient photochemistry to occur. Theoretical calculations in fact make it clear that efficient passage to the ground state surface can take place anywhere *near* the conical intersection geometry<sup>104, 186, 188</sup>. Our results suggest that this region extends as much as  $20\text{-}25^\circ$  away from the  $52^\circ$  angle.

The quantum yields for cyclobutene formation from 124, 125, and 131 (Table 4.3.1.2) are similar to those reported by Aue and Reynolds for the corresponding *bis*(methylene) analogs 109-112, shown in Scheme 4.1.1. The quantum yields for cyclobutene formation follow a much more consistent trend with torsional freedom than those revealed from the *cis,trans*- isomerization of the dienes 124, 125, and 131 (decreasing central bond torsional flexibility, and shortening of  $C_1\text{-}C_4$  bond distance- $125 > 131 > 124$ ). While this is also consistent with the ramifications of the *conical intersection* mechanism, the reduction in ring closure quantum yields throughout the series is more likely to be the result of increasing  $C_1\text{-}C_4$  bond distances, however (Table 4.4.1.1).

The effects of constraining the  $C_2\text{-}C_3$  torsional angle are also evident in the UV absorption spectra of 124, 125, and 131 (Figure 4.2.1). For *E,E*-124, 125, and 131, the absorption maximum is approximately constant at  $\lambda_{\text{max}} = 250$  nm, indicating (in agreement with MMX) that the most stable ground state conformation is one in which a torsional angle of *ca.*  $0^\circ$  prevails. The increasing fine structure evident in the spectra of

131 and 124 compared to 125 are consistent with increased torsional rigidity since it has been suggested that the diffuseness observed in the absorption spectra of conjugated dienes<sup>21</sup> is due primarily to strong nonadiabatic coupling and internal conversion from the  $^1B_u$  state to the optically forbidden  $2^1A_g$  state. This mixing of states is caused by rapid torsional relaxation of C-C bonds after Franck-Condon excitation, as suggested by the work of Mathies and coworkers<sup>21-24</sup>.

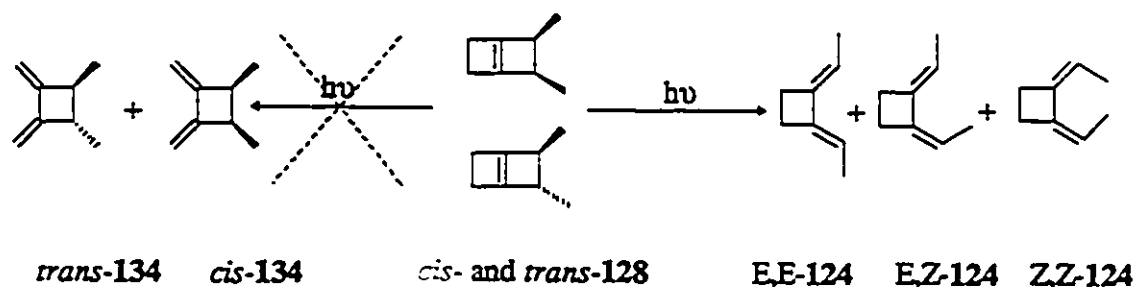
#### 4.4.2 The Photochemical Ring Opening Reaction of Dimethyl-bicyclo[n.2.0]alk-1<sup>n+2</sup>-enes.

In the present study, the dienes produced by photochemical ring opening of cyclobutenes 128 through 130 (Scheme 4.3.2.1) are locked in an *s-cis* conformation which renders them suitable for testing the hypothesis of adiabaticity of the photochemical ring opening reaction. Predicted *E,E*-diene ratios were calculated from the quantum yields for diene photoisomerization according to Tables 4.3.1.1-2., and are collected in Table 4.4.2.1 along with the observed ratios from direct photolysis of 128-130. Comparison of the predicted and observed-diene ratios verifies the preliminary conclusion that the isomeric diene distributions obtained from photochemical ring opening of cyclobutene derivatives cannot be accounted for by the excited state behavior of the single diene isomer formed by *disrotatory* opening; at least for the *trans*- isomers in the series.

In Chapter III the relevance of orbital symmetry selection rules to the photochemical ring opening reaction of monocyclic alkylcyclobutenes was discussed. The results of spectroscopic studies on cyclobutene itself<sup>27</sup> provide a convincing indication that orbital

symmetry plays a role in the ring opening reaction in the first 10 - 20 femtoseconds after Franck Condon excitation. The ring opening of the tricyclic cyclobutenes **10** and **11** (equations 1.4.1.7-8, Introduction 1.4.1) has been mentioned several times throughout this thesis as an example of how orbital symmetry factors can influence the quantum yields for the process, in spite of the fact that, overall, the reaction is nonstereospecific. Supporting evidence for these ideas was provided in Chapter III, from the results of a study of steric effects on the quantum yield for the reaction.

The role of C<sub>3</sub>-C<sub>4</sub> (cyclobutene ring numbering) bond strength in controlling the quantum yield of cyclobutene ring opening was also discussed earlier, and the regiochemistry observed in the ring opening of *cis*- and *trans*- **128** provides further support for these conclusions. *cis*- And *trans*-**128** undergo ring opening *regiospecifically* to yield the various geometric isomers according to Scheme 4.4.1. The fact that **134** is not formed in the photolyses of these compounds suggests that the efficiency of photochemical cyclobutene ring opening depends on the strength of the C<sub>3</sub>-C<sub>4</sub> bond (in cyclobutene numbering)<sup>83, 170</sup>.



Scheme 4.4.1. Regioselectivity observed in the photochemical ring opening of **128**

**Table 4.4.2.1.** Calculated and observed diene ratios at 193 nm and 214 nm from photolyses of cyclobutenes 128, 129, 37, and 130.

cyclobutene	Calculated $E,E-/E,Z-$ <sup>†</sup>	Observed $E,E-/E,Z-$	
		193 nm	214 nm
<i>cis</i> -128	1.2 ± 0.4		1.7
<i>cis</i> -129	2.2 ± 0.4	2.5 ± 0.4	
<i>cis</i> -37	3.7 ± 0.4	3.4 ± 0.6	
<i>cis</i> -130	2.9 ± 0.4	9.1 ± 1.3	5.38
<i>trans</i> -128	0.2 ± 0.1		0.11
<i>trans</i> -129	0.71 ± 0.09	0.11 ± 0.02	
<i>trans</i> -37	0.38 ± 0.05	0.18 ± 0.03	
<i>trans</i> -130	0.19 ± 0.03	0.29 ± 0.04	0.48

<sup>†</sup>Calculated from the quantum yields for photoreaction of the corresponding  $E,E-$  and  $E,Z-$  dienes.  $(E,E-/E,Z-)_{\text{predicted}} = \phi_{EZ \rightarrow EE} / (1 - \phi_{EZ \rightarrow EE} - \sum \phi_i)$

Direct irradiation of *cis*- and *trans*-128, 37, 129, 130 leads to ring opening to the isomeric dienes 124-127, with a high degree of disrotatory stereospecificity in each case (Table 4.4.2.1). The unusual behavior noted previously for *cis* and *trans*-37 (*vide supra*) is a general feature of the photochemistry of bicyclo[n.2.0]alk-1-enes. Furthermore, all the eight cyclobutenes undergo ring opening with quantum yields in the 0.45-0.65 range, a factor 2-3 times higher than those typically observed for monocyclic cyclobutenes. Ring strain clearly cannot account for the unique behavior of these compounds, since there is no





consistent variation in either quantum yield or stereospecificity throughout the series. The opposing trends observed in stereospecificity for the *cis*- and *trans*-cyclobutene isomers (Table 4.4.2.1) is rather intriguing, and may suggest that molecular symmetry plays a role in determining the course of the ring opening reaction. A comparison of the diene distributions reported for the photolysis of *cis* and *trans*-1,3,4-trimethylcyclobutene with those from 95 and 96 also suggests that molecular symmetry may play some role in the reaction<sup>46</sup>. Table 4.4.2.2 summarizes the data for these compounds; the distributions obtained from photolysis of the asymmetric compounds is weighted in favour of the orbital symmetry allowed isomers, in contrast to those obtained from the symmetric compounds 95 and 96. The nature of the role of molecular symmetry in controlling stereospecificity of cyclobutene ring opening is not clear. Dunken et al<sup>189</sup> suggested that high *stereospecificity* (in a concerted electrocyclic rearrangement) is mostly likely to be found when the lowest excited state of the reactant can correlate *directly* with the ground state of the product. Experiments to test the possible role of molecular symmetry are underway in our laboratory.

None of these compounds undergo formal [2+2]-cycloreversion to any discernible extent since this process would lead to the formation of the corresponding highly strained C<sub>4</sub>-C<sub>7</sub> cycloalkyne.

The quantum yields for photochemical ring opening of bicyclic cyclobutenes such as those shown in equations 1.3.2.4-6 (Chapter I, Section 1.3.2)<sup>83</sup> are listed in Table 4.4.2.3<sup>63</sup>. These data contrast with those from the cyclobutenes 128, 37, 129, 130 studied in this chapter (Table 4.3.2.1). Presumably, the increased efficiency in the ring opening process observed for the latter series of compounds is due to some structural feature present in these compounds, but absent in monocyclic cyclobutenes and the

compounds shown in Table 4.4.2.3. Since additional ring strain can be ruled out, the possibilities that remain are the rotational rigidity of the alkyl substituent on the C=C bond, and a lack of torsional mobility about the central (C=C) bond as ring opening commences.



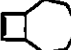
Table 4.4.2.2. Allowed to forbidden diene ratios from photolyses of alkylcyclobutenes in hydrocarbon solutions.

				
193 nm	2.0	2.1	1.2 <sup>†</sup>	1.1 <sup>†</sup>
214 nm	2.1	2.1	0.7 <sup>‡</sup>	1.2 <sup>‡</sup>

<sup>†</sup> Reference<sup>46</sup>

<sup>‡</sup> Chapter III of the present document.

Table 4.4.2.3. Quantum yields for cyclobutene ring opening at 185 nm excitation wavelength

<i>Cyclobutene</i>	Allowed Isomer	Forbidden Isomer
	0.12 (18)	unstable at 25° C
	0.12 (20)	0.40 (21)
	0.16 (24)	0.06 (25)



The latter possibility relates directly to the conical intersection mechanism for cyclobutene/butadiene interconversions. Olivucci and coworkers<sup>62</sup> have proposed that the *nonstereospecific* ring opening of alkylsubstituted cyclobutenes can be rationalized according to a mechanism where the optically-excited cyclobutene evolves on the excited state potential energy surface up to a point where it enters the same low energy conical intersection region as that obtained from *s-cis*-butadiene. Since in cyclobutene, the two terminal CH<sub>2</sub>'s are already twisted by 90° with respect to the carbon framework, it will be possible to enter the conical intersection region without changing the original orientation of the CH<sub>2</sub> groups (or at most, by twisting only one of them). Thus the system can arrive at the conical intersection point along *nonstereospecific* pathways, and product formation will then be determined by the ground state part of the reaction pathway. The ground state part of the ring opening pathway will be dominated by the twisting motion of one or two almost independent CH<sub>2</sub> groups. Thus, there is no reason why only one of the possible torsional motions would be strongly preferred during the distortion toward 1,3-butadiene (Figure 4.4.1). In the present series of compounds, the torsional restrictions imposed on the cyclobutenes could force the systems to follow "restricted" pathways for ring opening on the excited state surface. It is possible that these pathways are directed along the orbital symmetry predicted *disrotatory* reaction coordinates.

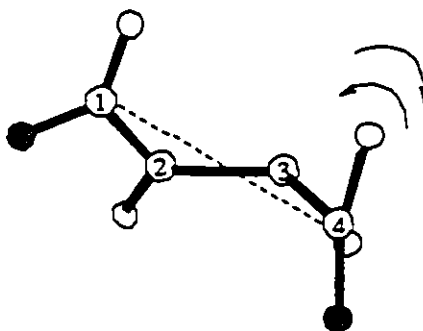


Figure 4.4.1. Structure of cyclobutene at the conical intersection

In the photochemical ring opening of 1,3-cyclohexadiene, Franck Condon excitation to the  $1B_u$  state is thought to be followed by a rapid crossing to the  $2^1A_g$  surface (Chapter I, Figure 1.2.1). Recent *ab-initio* calculations for the 1,3-cyclohexadiene ring opening reaction postulate that depopulation of the  $2^1A_g$  state and subsequent formation of ground state *cZc*-1,3,5-hexatriene (all-*cis*- hexatriene) occurs through a  $2A_g / 1A_g$  conical intersection point<sup>190</sup>. Olivucci and coworkers<sup>192b</sup> explained the experimental quantum yield for 1,3-cyclohexadiene ring opening ( $\phi = 0.44$ <sup>94</sup>) as being consistent with the presence of a conical intersection point located at the top of two different ground state valleys, one leading to formation of *cZc*-1,3,5-hexatriene and the other to regeneration of original reactant. As expected from this model, the quantum yields for ring opening of 1,3-cyclohexadiene and ring closure of *cZc*-1,3,5-hexatriene is close to unity<sup>37, 94</sup>. These authors implied that photoexcitation of both cyclohexadiene and *cZc*-1,3,5-hexatriene must generate the same excited *cZc*-1,3,5-hexatriene intermediate. The involvement of a common intermediate in the direct *cis,trans*- photoisomerization of isomeric dienes has also been suggested<sup>81</sup>. One example of this is given by the direct photoisomerization of *cis,cis*- or *cis,trans*-1,3-cyclooctadiene (Chapter 1.5.1), where the sum of the photoisomerization quantum yields ( $\phi_{cc \rightarrow ct} \approx 0.28$  and  $\phi_{ct \rightarrow cc} \approx 0.80$ ) is close to unity.

In Section 4.4.1, the involvement of torsional motions around the C<sub>2</sub>-C<sub>3</sub> bond (1,3-butadiene numbering) in the *cis,trans*- photoisomerization process of a constrained *s-cis* diene (124) was established. In the present section it was suggested that the locked conformations of the diene products from photochemical ring opening of cyclobutenes 128, 129, 37, and 130 appears to also have an influence on the *stereoselectivity* of the ring opening reaction, presumably because the cyclobutenyl C=C bond (which constitutes the C<sub>2</sub>-C<sub>3</sub> of the diene product) is impeded from torsional motions as ring opening proceeds.

These ideas suggest that ring opening may proceed through an "intermediate" geometry that is common to that involved in the *cis,trans*- photoisomerization of the corresponding isomeric dienes. If this is the case, the sum of the quantum yields for *cis,trans*- isomerization of *E,E*- and *E,Z*- 124 and ring opening of 128 might be expected to be near unity. In fact, the sum exceeds unity by a small amount in most cases.

#### 4.5 Summary and Conclusions.

The results from the photoisomerization of compounds 124 cannot be accommodated by the Oosterhoff model for *cis,trans*- photoisomerization, but are more compatible with a model in which the process involves torsion about all three C-C bonds of the diene- the conical intersection mechanism for diene isomerization. Photochemical ring opening of the bicyclic cyclobutenes 128, 129, 37, and 130 occurs with a high degree of disrotatory stereoselectivity, and strongly suggests that orbital symmetry selection rules are important in this reaction. The present study shows the effect of constraining the C-C central bond in 1,3-dienes on the *cis,trans*- photoisomerization process, and suggests that motions around C=C bond are involved in cyclobutene photochemical ring opening.

Figure 4.5 represents a 3-D surface diagram where the reaction coordinates are motions around the terminal and central C-C bonds in the butadiene  $\leftrightarrow$  cyclobutene system. In this diagram, torsions about the central C=C bond link cyclobutene to [1.1.0]bicyclobutane and *s-cis*- butadiene the *s-trans* conformer. It is implicit in this diagram that *cis,trans*- isomerization of *s-cis*- dienes occurs through a conical intersection

region located inside the cube, whereas cyclobutene ring opening can either proceed through the same conical intersection or through an avoided crossing (front face of the cube), depending upon the C=C bond motions available to the cyclobutene. Thus, cyclobutenes in which the C=C bond is free from torsional constraints, will reach a transition point on the excited state potential energy surface from where immediate funneling to the ground state surface occurs through the so called "conical intersection". After proceeding through the conical intersection, branching to the various photoproducts occurs on the ground state surface. This model can explain the formation of more than one diene isomer from ring opening of simple alkylsubstituted cyclobutenes and therefore the nonstereospecificity of the reaction.

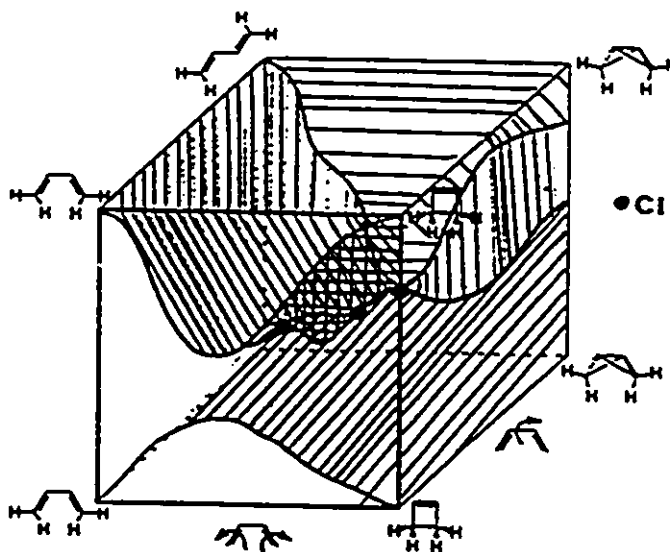


Figure 4.5. Conjectural surface diagram for cyclobutene  $\leftrightarrow$  butadiene interconversion. The spheres inside the cube represent conical intersections

It is then imperative to reconcile the observations that the photochemical ring opening of cyclobutenes appears in general to proceed nonstereospecifically, and the high degree of *stereoselectivity* and high quantum yields encountered for the ring opening reactions of *cis*- and *trans*-dimethylbicyclo[n.2.0]alk-1-enes.

For the cyclobutene  $\leftrightarrow$  butadiene system, this theory explains the stereospecificity of the ring closure reaction of 1,3-butadiene to cyclobutene (*vide infra*) as involving C<sub>1</sub>-C<sub>4</sub> bond formation, and therefore, the terminal CH<sub>2</sub> carbons are prevented from losing their disrotatory relative orientations during the process. In contrast, the ring opening reaction involves double bond formation between C<sub>1</sub>-C<sub>2</sub> and C<sub>3</sub>-C<sub>4</sub> carbons, and can occur by either rotating the CH<sub>2</sub> clockwise or counterclockwise, since according to this model, this CH<sub>2</sub> is almost 90 degrees twisted. The structure of the decay point (at the conical intersection) is given in Figure 4.4.1.

If cyclobutene ring opening indeed follows the mechanism described, then it would be further expected that cyclobutenes with restricted central bond torsional mobility will adopt restricted pathways along their evolution on the 1B<sub>2</sub> and 2A<sub>1</sub> potential energy surfaces that could lead to some degree of orbital symmetry control. The results exposed in Section 4.3.2 show that for cyclobutenes 128-130 and 37, the photochemical ring opening reaction proceeds with high degree of *stereoselectivity*.

According to the general view of this model, both cyclobutene formation and *cis,trans* photoisomerization are processes that are intimately related (*vide supra*); and both could involve a common intermediate. Consequently, these two processes should be connected along the multidimensional potential energy surfaces. It is therefore not surprising that motions that relate cyclobutene ring opening to butadiene ring closure potential energy surfaces also affect the *cis,trans* isomerization process and *vice versa*

(Figure 4.5). The results from the *cis,trans* photoisomerization of the *s-cis* constrained dienes studied in Section 4.3.1, also support the notion of common intermediates in the isomerization processes. Thus, the severely constrained diene 124 shows reduced quantum yields of *cis,trans* isomerization due to its high degree of planarity around the central C-C single bond (1,3-butadiene numbering). This planar structure, as compared to the higher homologs of the series, impedes the molecule from reaching the same low energy conical intersection that is accessible for the higher homologs by rotation around the C-C central bond.

On the other hand, constraining the same central bond (which constitutes the C=C bond in cyclobutene) causes an enhanced reactivity for cyclobutene ring opening, and an increase in the stereoselectivity of the photoreaction perhaps due to forcing the molecule to follow the avoided crossing pathway for ring opening (the front face of the cube in Figure 4.5).

The series of alkylsubstituted monocyclic cyclobutenes studied in Chapter III also supports the idea that the potential energy surfaces traversed during the ring opening reactions are dominated by orbital symmetry factors; that is, *disrotatory* motions are preserved along the excited state coordinates. This is suggested by the diminution in the quantum yields for ring opening upon increasing the methyl substitution in the ring. These results are consistent with those found by Mathies and coworkers on cyclobutene ring opening.

## CHAPTER V

### OVERVIEW

#### 5.1 A New Mechanism for the Photochemical Isomerization of Cyclobutene and 1,3-Butadiene

Three main aspects concerned with the photochemical ring opening of cyclobutenes have been studied in the present document. These are the energetic requirements of the process (1-phenylcyclobutene derivatives; Chapter II); the effects of constraining the C=C bond on the stereoselectivity and efficiency of the reaction (dimethylbicyclo[n.2.0]alk-1<sup>n+2</sup>-enes; Chapter IV); and the influence of steric factors upon *syn*-dimethyl substitution in the ring opening reaction (alkylsubstituted monocyclic cyclobutenes; Chapter III).

It was found that a certain threshold excited state energy is required for the photochemical ring opening reaction to take place. Thus, 1-phenylcyclobutenes do not undergo ring opening due to their low singlet state energy, as compared to alkylsubstituted analogs.

The application of the Woodward and Hoffmann rules to the photochemical ring opening of alkylsubstituted cyclobutenes has proven to be not all successful<sup>43, 74</sup>. There are many examples in the literature that illustrate the general *nonstereospecificity*

associated with the photochemical ring opening of alkylsubstituted cyclobutenes. The theoretical model developed by Van-der-Lugt and Oosterhoff in the early 1970's cannot accommodate these results.

This thesis has been concerned with the development of a new qualitative model to explain the photochemistry of cyclobutene and 1,3-butadiene, in which the internal conversion processes (passage from the excited state to the ground state potential energy surfaces) occur at conical intersections rather than at an avoided surface crossing.

## **5.2 Contributions of the Studies and Future Work**

Many of the important contributions this work has provided to those involved in the studies of the theoretical and photochemical aspects of the cyclobutene  $\leftrightarrow$  1,3-butadiene interconversion have been summarized at the end of each chapter. This chapter integrates in more general terms the conclusions that can be drawn from the present work with regards to the above reaction and the cis,trans photoisomerization processes of substituted 1,3-dienes. It is expected that the knowledge gained in this study will have important ramifications to researchers in the field.

### **5.2.1 Phenylcyclobutenes**

Our studies have offered a detailed understanding of the photochemistry and photophysics of 1-phenylcyclobutene derivatives. The inability of these compounds to undergo ring opening reactions has been found to be related to energetic considerations



rather than polarizability of their excited states. Thus the major distinctive feature of phenylated cyclobutenes with respect to their alkylsubstituted analogues resides in their lower singlet excited state energies that preclude their photochemical ring opening reactions.

Results of the photolyses of 1-phenylcyclobutenes in aprotic solvents have illustrated the extent to which the polarizability of the  $\sigma$  carbon-framework in the cyclobutene ring affects the cycloreversion process. As was pointed out in Chapter II, asymmetrically substituted cyclobutenes are predicted by theory to exhibit polarized excited states. The first series of examples that confirms these predictions has been provided by our 1-phenylsubstituted series (where the diagonals of the cyclobutene ring are not identically substituted). It would be worthwhile to test the extent of the validity of these calculations by studying the photochemistry of a series 1,4-diphenylcyclobutene derivatives with substitution in the phenyl ring, where the diagonals of the cyclobutene ring are "symmetrically" substituted. These compounds are predicted, at a high level of theory, to be deprived of polarized character in the excited state, and hence, substitution in the aryl ring should not have an influence on their photochemistry in aprotic solvents.

The 1-phenylcyclobutenes have proven to be very versatile substrates in reactions such as photoaddition of alcohols. The basicity of their excited states in hydroxylic solvents is enhanced with respect to the corresponding styrene derivatives. It may be possible to construct an excited state substituent constant scale based on the photohydration or alcohol photoaddition to these compounds. This scale can include electron withdrawing substituents such as 3-CF<sub>3</sub>, 4-CF<sub>3</sub>O, and 4-CF<sub>3</sub>. Also, a more thorough comparison between the 1-phenylcyclobutenes and their styrenic analogs is necessary in order to understand the distinctive nature of the former.

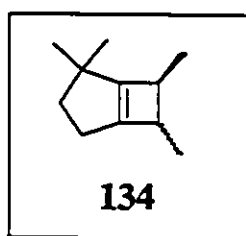
Particular attention will have to be focused on the detection of short-lived ionic intermediates from photolyses of phenylated cyclobutenes in hydroxylic solvents. These cationic intermediates, which are often eclipsed by the presence of high intense triplets, are suspected to have lifetimes of a few hundred nanoseconds. Their detection requires the use of nonnucleophilic solvents and constant flow systems. The present study tentatively assigns the p-tolyl-cyclobutyl cation to a transient spectrum with  $\lambda_{\text{max}} = 337 \text{ nm}$ , but further confirmation of this assignment is necessary. In particular, the determination of rate constants for the quenching of the cation generated in hydroxylic-nonnucleophilic solvents will unambiguously confirm the assignments. Work on this area is in progress in our laboratory.

### 5.2.2 Cyclobutene $\leftrightarrow$ Butadiene Photointerconversion.

The contribution of the work accomplished in Chapter IV (photochemistry of dimethylbicyclo[n.2.0]alk-1<sup>n+2</sup>-enes) has direct relevance on orbital-symmetry conservation arguments for cyclobutene  $\leftrightarrow$  1,3-butadiene interconversions. The high degree of *stereospecificity* observed in the ring opening of these compounds is not related to ring strain factors induced by the presence of the ancillary ring, but rather to the decreased flexibility in the isomeric 1,3-diene products or the rotational flexibility of the substituents on the cyclobutene double bond. This series of cyclobutenes presents the first systematic study which interrelates aspects such as structural modifications and stereospecificity.

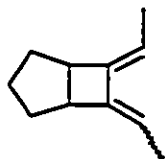
The increased *disrotatory* preference with increased ancillary ring size observed in the ring opening of the *cis*- series of cyclobutenes and decreased *disrotatory* preference

with increased ancillary ring size observed for the *trans*- series of cyclobutenes (Table 4.3.1) is as intriguing an aspect of the photochemistry of these compounds as it is puzzling. This effect may be related to the intervention of states of different symmetry in the photochemistry of the *cis*- or *trans*- series of cyclobutenes. Future work in the area will include the photochemistry of asymmetric cyclobutenes, such as *cis*- and *trans*- 134.

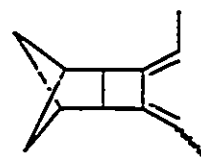


The study of the *cis,trans* photoisomerization of constrained *s-cis* dienes (Chapter IV) has contributed to a more incisive understanding of this fundamental process in organic photochemistry. Laser Raman Spectroscopy and Laser Raman Intensity measurements carried out by Mathies and coworkers<sup>24</sup> demonstrate that the allyl-methylene mechanism (Chapter 1.6) cannot account for the *cis,trans* photoisomerization process. The results presented in Chapter IV are also incompatible with the above mechanism, but are in accord with recent theoretical calculations. Indeed, the lower quantum yield of isomerization of 124 represents the first experimental example of low efficiency in the photoisomerization process of a substituted 1,3-butadiene.

Further work in this area shall include the study of dienes with C-C central bond (in 1,3-butadiene numbering) in a more rigid *s-cis* conformation than 124. These dienes are 135 and 136. Work on the syntheses of these compounds is also under way in our laboratory.

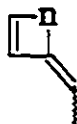


135



136

It is also worthwhile inspecting the photochemistry of a series of *s-trans*-dienes, in order to determine the effect of constraining the central bond on the *cis,trans*-photoisomerization quantum yield.



$n = 1, 2, 3, \text{ and } 4$

## CHAPTER VI

### EXPERIMENTAL

#### 6.1. 1-PHENYLCYLOBUTENES

##### 6.1.1 General

$^1\text{H}$  NMR spectra were recorded on Bruker AM300 (300 MHz) or AM500 (500 MHz) spectrometers in deuteriochloroform (carbon tetrachloride, or dichloromethane- $d_2$  where noted) and  $^{13}\text{C}$  NMR spectra were recorded at 125.6 MHz on the Bruker AM500; all are reported in parts per million downfield from tetramethylsilane.  $^{19}\text{F}$  NMR spectra were recorded at 282.23 MHz on the Bruker AC300; they are reported in parts per million relative to tetramethylsilane and trichlorofluoromethane, respectively.

Mass spectra were recorded on a VGH ZAB-E mass spectrometer, and employed a mass of 12.000 000 for carbon. GC/MS analyses were performed using a Hewlett-Packard 5890 gas chromatograph equipped with a HP-5971A mass selective detector and a DB-1 microbore capillary column (12 m X 0.2 mm; Chromatographic Specialties, Inc.) or a DB-5 microbore capillary column (30 m X 0.2 mm; Chromatographic Specialties, Inc.).

Condensed phase infrared spectra were recorded on a Bio-Rad FT-40 FT infrared spectrometer as neat samples or in carbon tetrachloride solutions where noted. GC/FTIR analyses were carried out using a Hewlett-Packard 5890 gas chromatograph equipped with a DB-17 megabore capillary column (30 m X 0.53 mm;

Chromatographic Specialties) and a Bio-Rad GC/C 32 interface attached to the Bio-Rad FTS-40 FT infrared spectrometer.

Ultraviolet absorption spectra were recorded using a Perkin-Elmer Lambda 9 spectrometer interfaced with an IBM PC PS/2. The spectrometer sample compartment was continuously flushed with nitrogen. Spectra were recorded in 1-cm Suprasil UV cells (Hellma). The sample and reference were deoxygenated with argon prior to recording the spectrum.

Fluorescence emission and excitation spectra were recorded on a Perkin Elmer LS-5 spectrofluorometer, which is also interfaced to the IBM PS/2-286 and controlled by software supplied by the manufacturer or on a PTI-LS 100 spectrofluorometer equipped with both steady state and time resolved capabilities. Phosphorescence spectra were recorded on a PTI-LS 100 spectrofluorometer.

Time Resolved Single Photon Counting measurements were carried out on the PTI-LS 100 spectrofluorometer equipped with a H<sub>2</sub> plasma gas and the software supplied by the manufacturer.

Gas chromatographic analyses were carried out using a Hewlett-Packard 5890 gas chromatograph equipped with a flame ionization detector, a Hewlett-Packard 3396 integrator, and a HP-1 megabore capillary column (12 m x 0.53 mm; Hewlett-Packard, Inc.), a DB-1 megabore capillary column (30 m x 0.53 mm, Chromatography Specialties) or a megabore SPB-1 glass column (Supelco, 30 m x 0.53 mm ID). Semipreparative vpc separations employed a Varian 3300 gas chromatograph equipped with 6' x 0.25 in. stainless steel columns consisting of (a) 5% OV-101 on Supelport or (b) 10% QF-1 on 80/100 Chromosorb (Supelco, Inc.).

### 6.1.2 Commercial Solvents and Reagents Used

n-Pentane (Baker Photorex), cyclohexane (BDH Omnisolv), methanol (Caledon, HPLC grade), and barium oxide (Mallinckrodt) were used as received from the suppliers. Acetonitrile (Omnisolv) was dried over calcium hydride and distilled under dry nitrogen. Benzene (Baker Analyzed) was purified by several extractions with concentrated sulfuric acid, followed by distillation through a Vigreux column. Tetrahydrofuran (Baker Analyzed) was refluxed over sodium/benzophenone and distilled immediately prior to use. Dimethylsulfoxide (Caledon) was dried over potassium hydroxide and distilled under reduced pressure. p-Toluenesulfonic acid monohydrate was used as received from Matheson. Deuterium oxide was from MSD isotopes (Merck division) and used as received. Bromobenzene, 4-bromotoluene, 4-bromo-anisole, 4-bromobenzotrifluoride, 4-trifluoromethoxybromobenzene, bromobenzotrifluoride, tetrakis(triphenylphosphine)palladium(0), cyclobutanone, iodomethane, n-butyl lithium, and n-decane were all used as received from Aldrich Chemical Co.

### 6.1.3 Preparation and Identification of Compounds.

The cyclobutenes 65-70 were prepared by acid-catalyzed dehydration of the corresponding 1-arylcyclobutanol<sup>193</sup>, which was prepared by addition of the appropriate aryllithium to cyclobutanone in anhydrous diethylether at -78°C. The aryllithium reagents were prepared as solutions in ether from the corresponding bromoarene by lithium exchange using n-butyllithium. A typical procedure is described below for the preparation of 1-(4-trifluoromethylphenyl)cyclobutene (68).

*1-(4-trifluoromethylphenyl)cyclobutene* (68). In an oven-dried 50 mL 2-neck round bottom flask equipped with a dropping funnel, magnetic stirrer, rubber septum, and nitrogen inlet were placed 4-bromobenzotrifluoride (3.43 g, 0.015 mol) and anhydrous ether (10 mL). The flask was cooled under an atmosphere of dry nitrogen to  $-78^{\circ}\text{C}$  with a dry ice / acetone bath, and a  $1.6 \text{ mol dm}^{-3}$  hexane solution of *n*-butyllithium (9.5 mL, 0.015 mol) was added dropwise over one hour. The bath and contents of the flask were then allowed to warm to  $0^{\circ}\text{C}$  over *ca.* one hour. The temperature of the resulting yellow solution was again lowered to  $-78^{\circ}\text{C}$ , and a solution of cyclobutanone (0.47 g, 0.0067 mol) in anhydrous ethyl ether (10 mL) was added dropwise over one hour. The resulting yellow solution was then allowed to warm to room temperature over a further one hour. The dark red mixture which resulted was quenched by slow addition of water (20 mL) and then extracted with ether (3 X 10 mL). The combined ether extracts were dried over anhydrous sodium sulfate and filtered. Evaporation of the solvent on a rotary evaporator yielded an orange liquid (1.23 g), which was distilled under vacuum. The major fraction (0.75 g, 0.0035 mol, 70%; b.p. =  $87^{\circ}\text{C}$  (0.3 torr), m.p.:  $52\text{-}54^{\circ}\text{C}$ ) was identified as *1-(4-trifluoromethylphenyl)cyclobutanone*<sup>194</sup> (74), on the basis of the following spectral data:

$^1\text{H}$  NMR:  $\delta$  = 1.55 (br s, 1 H), 1.76 (cplx. m, 1 H), 2.08 (b s, 1 H), 2.36 (cplx. m, 2 H), 2.54 (cplx. m, 2 H), 7.62 (s, 4 H).  $^{13}\text{C}$  NMR:  $\delta$  = 12.96, 37.18, 79.60, 125.51, 125.42, 125.36, 125.27, 126.88, 129.0 (q), 156.39.  $^{19}\text{F}$  NMR:  $\delta$  = -62.67. IR: 3632 (w), 2996 (m), 1328 (s), 1286 (w), 1232 (w), 1172 (m), 1149 (s), 1076 (m), 1017 (w), 846 (w). MS, *m/e* (I) = 216 (2), 215 (3), 197 (17), 188 (98), 173 (100), 151 (35), 147 (42), 145 (96), 125



(33), 91 (75), 69 (33). Exact mass: calc. for  $C_{11}H_{11}F_3O$ , 216.076200; found, 216.0750000.

Significantly higher isolated yields of the cyclobutanols can be obtained using column chromatography (neutral alumina, hexane/ether mixtures) to purify the crude reaction mixtures in the above step.

A solution of 74 (0.50 g, 0.0023 mol) and a few crystals of *p*-toluenesulfonic acid in dry benzene (25 mL) was stirred under mild reflux for six hours, in a 50 mL round bottom flask equipped with a glass tube which contained a small thimble filled with granulated calcium chloride and was topped with a reflux condenser. The resulting light brown solution was cooled to room temperature, water (25 mL) was added, and the mixture was extracted with pentane (3 X 10 mL). The combined extracts were washed with saturated aqueous sodium bicarbonate, dried over anhydrous magnesium sulfate, and the solvent was evaporated to yield a light yellow liquid (0.40 g). The product was isolated as a colorless liquid (0.20 g, 0.001 mol, 43%; b.p. (1 torr) = 77°C, m.p.: 20°C) by vacuum distillation. Better yields can be obtained by purification of the crude product by column chromatography (neutral alumina; 10% ether in hexane). The product was further purified by semi-preparative gas chromatography (vpc) using column (e), and identified as *1-(4-trifluoromethylphenyl)cyclobutene* (68) on the basis of the following data:

$^1H$  NMR:  $\delta$  = 2.40 (m, 2 H), 2.65 (t, 2 H,  $J$  = 4 Hz), 6.25 (br s, 1 H), 7.25 (d, 2 H,  $J$  = 8.2 Hz), 7.39 (d, 2 H,  $J$  = 8.2 Hz).  $^{13}C$  NMR:  $\delta$  = 26.44, 28.65, 124.32, 125.15, 130.27, 137.89, 145.14, 129 (q,  $CF_3$ ).  $^{19}F$  NMR:  $\delta$  = -62.70. IR: 3056 (w),

2962 (m), 2935 (m), 2852 (m), 1330 (s), 1176 (m), 1149 (s), 1073 (s), 1043 (w), 1019 (w), 900 (w), 846 (m), 765 (w). MS: *m/e* (I) = 198 (15), 179 (21), 177 (22), 151 (28), 145 (21), 129 (100), 128 (50), 120 (15), 75 (27), 63 (20), 51 (16). Exact mass: Calcd. for C<sub>11</sub>H<sub>9</sub>F<sub>3</sub>, 198.0656; Found, 198.0688. UV (MeCN):  $\lambda_{\max}$  = 260 nm ( $\epsilon$  14800 M<sup>-1</sup>cm<sup>-1</sup>). M.P.: 22° C.

Cyclobutenes 65-67, 69-70 were prepared in similar fashion to 68, except that the initial lithium exchange in the cyclobutanol synthesis required less or more vigorous conditions depending on substituent. The yields of the intermediate 1-arylcyclobutanols ranged from 50-90% after chromatography, and those of the cyclobutenes from 70-90% after isolation by alumina column chromatography. The latter were all subjected to additional purification (>99% by GC) by semi-preparative gas chromatography. Spectral and analytical data for the remaining 1-arylcyclobutanols- and 1-arylcyclobutenes in the series are listed below.

*1-(4-methoxyphenyl)cyclobutanol* (71). <sup>1</sup>H NMR:  $\delta$  = 1.66 (cplx. m, 1 H), 1.98 (cplx. m, 1 H), 2.36 (m, 2 H), 2.55 (m, 2 H), 3.78 (s 3 H), 7.42 (q, 2 H), 7.77 (q, 2 H). IR: 3576 (m), 2966 (s), 2941 (s), 2883 (m), 1610 (m), 1513 (s), 1472 (m), 1298 (m), 1253 (s), 1224 (m), 1175 (m). MS: *m/e* (I) = 178 (27), 177 (38), 147 (31), 135 (100), 121 (11), 105 (7), 91 (9), 65 (7).

*1-(4-methoxyphenyl)cyclobutene* (65). <sup>1</sup>H NMR:  $\delta$  = 2.50 (m, 2 H), 2.77 (t, 2 H), 3.81 (s, 3 H), 6.13 (t, 1 H), 6.84 (dd, 2 H, J =

2.2 Hz,  $J = 6.8$  Hz), 7.26 (dd, 2 H,  $J = 2.2$  Hz,  $J = 6.9$  Hz).  $^{13}\text{C}$  NMR:  $\delta = 26.02, 55.29, 113.74, 124.57, 125.55$ . IR: 3009 (w), 2956 (m), 2932 (m), 2851 (m), 1605 (m), 1424 (w), 1300 (m), 1258 (s), 1174 (m), 1056 (w), 1038 (w), 835 (m), 760 (w). MS:  $m/e$  (I) = 160 (65), 159 (31), 145 (27), 129 (42), 117 (91), 115 (100), 102 (21), 91 (42), 89 (64), 77 (11), 51 (15). Exact mass: Calcd. for  $\text{C}_{11}\text{H}_{12}\text{O}$ , 160.0888; Found: 160.0904. UV (pentane):  $\lambda_{\text{max}} = 261$  nm ( $\epsilon$  17900  $\text{M}^{-1}\text{cm}^{-1}$ ).

*1-(4-methylphenyl)cyclobutanol* (72)<sup>194</sup>.  $^1\text{H}$  NMR:  $\delta = 1.66$  (cplx. m, 2 H), 1.98 (br s, 2 H), 2.37 (s, 3 H), 2.37 (b s, 2 H), 2.54 (b s, 2 H), 7.17 (d, 0.7 Hz, 2 H), 7.37 (d, 0.7 Hz, 2 H).  $^{13}\text{C}$  NMR:  $\delta = 12.93, 21.02, 36.80, 109.22, 124.92, 129.09, 136.90, 143.29$ . IR: 3634 (m), 3032 (m), 2994 (s), 2958 (s), 2883 (m), 1621 (w), 1517 (m), 1342 (m), 1243 (m), 1136 (m), 1055 (m), 1021 (m), 818 (m), 720 (m). MS:  $m/e$  (I) = 162 (2), 147 (26), 134 (71), 119 (100), 92 (37), 91 (63), 77 (10), 65 (16). Exact mass: calc. for  $\text{C}_{11}\text{H}_{14}\text{O}$ , 162.1044651; found, 162.1037000.

*1-(4-methylphenyl)cyclobutene* (66).  $^1\text{H}$  NMR:  $\delta = 2.27$  (s, 3 H), 2.46 (br t, 2 H), 2.72 (t, 2 H,  $J = 3.3$  Hz), 6.15 (br s, 1 H), 7.05 (d, 2 H), 7.18 (d, 2 H).  $^{13}\text{C}$  NMR:  $\delta = 21.30, 26.15, 28.75, 102.86, 124.12, 125.96, 128.95, 137.14$ . IR: 3057 (m), 3030 (m), 2957 (s), 2932 (s), 2883 (m), 2853 (m), 1510 (m), 1317 (w), 1291 (w), 1241 (w), 1183 (w), 1117 (w), 899 (w).

822 (m), 754 (m). MS:  $m/e$  ( $I$ ) = 144 (24), 129 (100), 128 (59), 115 (90), 90 (9), 89 (11), 63 (18), 51 (12). Exact mass: Calcd. for  $C_{11}H_{12}$ , 144.0939; Found, 144.0930. UV (MeCN):  $\lambda_{\max}$  = 258 nm ( $\epsilon$  15500  $M^{-1} \text{ cm}^{-1}$ ).

*1-phenylcyclobutanol*<sup>193</sup> (73).  $^1\text{H}$  NMR:  $\delta$  = 1.68 (cplx. m, 1 H), 2.01 (cplx. m, 1 H), 2.36 (cplx. m, 2 H), 2.56 (cplx. m, 2 H), 7.27 (m, 1 H), 7.36 (m, 2 H), 7.49 (m, 2 H).  $^{13}\text{C}$  NMR:  $\delta$  = 12.99, 36.83, 124.93, 127.24, 128.44. IR: 3633 (m), 3073 (m), 3041 (m), 2995 (s), 2960 (s), 1448 (m), 1342 (m), 1242 (m), 1177 (w), 1139 (m), 1026 (m), 899 (m), 761 (m). MS:  $m/e$  ( $I$ ) = 148 (8), 147 (7), 130 (12), 120 (58), 115 (18), 105 (100), 102 (15), 91 (63), 78 (89), 77 (99), 74 (21), 63 (16), 51 (48). m.p. = 40-41° C

*1-phenylcyclobutene*<sup>193, 195, 196</sup> (67):  $^1\text{H}$  NMR:  $\delta$  = 2.51 (m, 2 H), 2.79 (t, 2 H), 6.27 (t, 1 H), 7.31 (m, 5 H).  $^{13}\text{C}$  NMR<sup>477</sup>:  $\delta$  = 26.18, 28.72, 124.16, 127.13, 127.36, 128.07, 128.28, 128.64, 135.04, 146.40. IR: 3069 (m), 3041 (m), 2958 (s), 2933 (s), 2888 (w), 2852 (m), 1580 (w), 1491 (w), 1449 (w), 1244 (w), 1070 (w), 901 (w), 850 (w), 729 (s).

*1-(4-trifluoromethoxyphenyl)cyclobutanol* (75).  $^1\text{H}$  NMR:  $\delta$  = 1.18 (cplx m, 1 H), 1.63 (br s, 1 H), 1.97 (cplx m, 2 H), 2.11

(cplx m., 2 H), 6.82 (m, 2 H), 7.13 (m, 2 H).  $^{13}\text{C}$  NMR:  $\delta$  = 12.88, 37.06, 76.56, 120.6 (q), 120.83, 127.08, 134.71, 144.92.  $^{19}\text{F}$  NMR:  $\delta$  = -94.59. IR: 3630 (w), 2996 (m), 2965 (w), 1513 (m), 1273 (s), 1229 (m), 1186 (m), 1142 (w), 1020 (m), 851 (w). MS:  $m/e$  (I) = 232 (1), 231 (1), 204 (74), 189 (100), 175 (7), 162 (23), 147 (15), 95 (22), 69 (15). Exact mass: calc. for  $\text{C}_{11}\text{H}_{11}\text{F}_3\text{O}_2$ , 232.071114437; found, 232.0695000.

*1-(4-trifluoromethoxyphenyl)cyclobutene* (69).  $^1\text{H}$  NMR:  $\delta$  = 2.52 (br d, 2 H), 2.79 (t, 2 H), 6.35 (br s, 1 H), 7.25 (br q, 4 H).  $^{13}\text{C}$  NMR:  $\delta$  = 25.37, 34.94, 118.50, 127.38, 129.56, 130.43, 134.75, 147.80.  $^{19}\text{F}$  NMR:  $\delta$  = -59.08. IR: 3036 (w), 2968 (m), 2911 (w), 1794 (m), 1597 (m), 1502 (m), 1274 (s), 1226 (9s), 1187 (s), 1112 (m), 1023 (w), 901 (m), 836 (m), 790 (m). MS:  $m/e$  (I) = 214 (50), 199 (11), 186 (23), 175 (4), 145 (7), 130 (14), 129 (100), 128 (36), 127 (38), 117 (21), 115 (29), 102 (7), 89 (21), 69 (21), 63 (14), 51 (7). Exact mass: Calcd. for  $\text{C}_{11}\text{H}_9\text{F}_3\text{O}$ , 214.0605; Found, 214.0593. UV (pentane):  $\lambda_{\text{max}}$  = 255 nm ( $\epsilon$  17400  $\text{M}^{-1}\text{cm}^{-1}$ ).

*1-(3-trifluoromethylphenyl)cyclobutanol* (76).  $^1\text{H}$  NMR:  $\delta$  = 1.55 (br s, 1 H), 1.73 (cplx m, 1 H), 2.04 (cplx m, 1 H), 2.34 (cplx m, 2 H), 2.48 (cplx m, 2 H), 7.61 (m, 4 H).  $^{13}\text{C}$  NMR:  $\delta$  = 12.98, 37.15, 76.73, 121.81, 123.98, 124.06, 128.37, 128.92, 130.0 (q), 147.32.  $^{19}\text{F}$  NMR:  $\delta$  = -62.71. IR: 3633 (w), 3080

(w), 2996 (m), 2956 (m), 2889 (w), 1441 (w), 1330 (s), 1272 (m), 1178 (s), 1147 (s), 1077 (m), 1019 (w), 902 (w), 838 (w), 804 (w), 703 (m). MS:  $m/e$  (I) = 216 (2), 215 (1), 197 (13), 188 (94), 173 (100), 159 (6), 145 (56), 127 (7), 91 (19), 75 (6). Exact mass: calc. for  $C_{11}H_{11}F_3O$ , 216.0762000; found, 216.0750000.

*1-(3-trifluoromethylphenyl)cyclobutene* (70).  $^1H$  NMR:  $\delta$  = 2.54 (m, 2 H), 2.81 (t, 2 H,  $J$  = 4.0 Hz), 6.38 (t, 1 H,  $J$  = 1.2 Hz), 7.43 (m, 4 H).  $^{13}C$  NMR:  $\delta$  = 26.38, 28.72, 120.93, 123.89, 127.34, 128.74, 129.36, 146.20.  $^{19}F$  NMR:  $\delta$  = -63.01. IR: 2955 (m), 2816 (m), 1601 (w), 1444 (m), 1348 (m), 1327 (s), 1282 (m), 1256 (m), 1181 (s), 1151 (s), 1076 (m), 981 (w), 891 (w), 799 (m). MS:  $m/e$  (I) = 198 (23), 179 (11), 177 (46), 151 (40), 129 (100), 128 (40), 120 (9), 75 (9), 63 (4), 51 (5). Exact mass: Calcd. for  $C_{11}H_9F_3$ , 198.0656; found 198.0649. UV (MeCN):  $\lambda_{max}$  = 254 nm ( $\epsilon$  15100  $M^{-1}cm^{-1}$ ).

Compounds 65-70 were found to be unstable at room temperature and when kept as highly concentrated solutions. Thus, samples of 65-70 were kept in pentane solutions, at  $-12^\circ C$ , in the presence of radical scavengers such as hydroquinone. The stabilizer was readily removed from the samples by bulb-to-bulb distilling the cyclobutene.

The 1-aryl-1-methoxycyclobutanes 83-88 were prepared by stirring mixtures of the corresponding 1-arylcyclobutanol (0.0009 moles), barium oxide (0.005 mol), iodomethane (0.002 mol), and dry dimethylsulfoxide (10 mL) for 24 hours at room temperature. After addition of 5% aqueous hydrochloric acid, extraction with ether, drying and evaporation of the ether extracts, and finally alumina column chromatography (20% ether in hexane), the compounds were isolated in 70-90% yields as colorless oils. They were identified on the basis of their NMR, IR, and mass spectral data, which are listed below.

*1-methoxy-1-(4-methoxyphenyl)cyclobutane* (83).  $^1\text{H NMR}$ :  $\delta$  = 1.80 (cplx m, 1H), 1.99 (cplx m, 1 H), 2.46 (cplx m, 2 H), 2.55 (cplx m, 2 H), 2.85 (s, 3 H), 3.76 (s, 3 H), 6.89 (d, 2 H), 7.32 (d, 2 H). IR: 2995 (m), 2953 (m), 1652 (m), 1616 (m), 1558 (m), 1517 (m), 1510 (s), 1305 (m), 1252 (s), 1178 (m), 1135 (m), 1047 (w), 972 (w), 833 (m), 777 (w). MS:  $m/e$  (I) = 192 (4), 191 (4), 177 (2), 164 (42), 163 (100), 149 (8), 133 (42), 121 (12), 119 (42), 105 (8), 91 (25), 77 (17), 63 (9). Exact mass: Calcd. for  $\text{C}_{12}\text{H}_{16}\text{O}_2$ , 192.1150; found 192.1127000.

*1-methoxy-1-(4-methylphenyl)cyclobutane* (84).  $^1\text{H NMR}$ :  $\delta$  = 1.68 cplx m, 1 H), 1.97 (cplx m, 1 H), 2.36 (s, 3 H), 2.36 (m, 4 H), 2.92 (s, 3 H), 7.15 (d, 2 H,  $J = 7.9$  Hz), 7.28 (d, 2 H,  $J = 8.0$  Hz).  $^{13}\text{C NMR}$ :  $\delta$  = 12.99, 21.06, 32.88, 50.34, 81.34, 126.29, 128.92, 136.78, 140.10. IR: 3031 (m), 2995 (s), 2950 (s), 2885 (m), 2830 (m), 1621 (w), 1516 (m), 1296 (m), 1249 (m), 1137

(s), 1090 (m), 1056 (m), 815 (m), 786 (w). MS:  $m/e$  (I) = 176 (2), 175 (2), 162 (5), 161 (36), 148 (22), 147 (39), 133 (100), 117 (55), 115 (28), 105 (22), 91 (33), 77 (11), 65 (17), 51 (5). Exact mass: calc. for  $C_{12}H_{16}O$ , 176.120115; found, 176.1190000.

*1-methoxy-1-phenylcyclobutane* (85).  $^1H$  NMR:  $\delta$  = 1.58 (cplx m, 1 H), 1.87 (cplx m, 1 H), 2.32 (cplx m, 4 H), 2.86 (s, 3 H), 7.30 (m, 5 H).  $^{13}C$  NMR:  $\delta$  = 13.01, 32.80, 50.47, 126.28, 127.14, 128.24. IR: 3071 (m), 3037 (m), 2884 (s), 2952 (s), 2914 (m), 2831 (m), 1449 (m), 1289 (m), 1248 (m), 1136 (s), 1090 (m), 1046 (m), 759 (m). MS:  $m/e$  (I) = 161 (3), 134 (37), 133 (100), 115 (6), 104 (31), 91 (34), 77 (35). MS/CI ( $NH_3$ ):  $m/e$  (I) = 131 (100), 148 (50), 162 (4), 180 (5). MS/CI ( $CH_4$ ):  $m/e$  (I) = 61 (9), 79 (28), 85 (34), 131 (100), 163 (11). HRMS ( $M^{+o}-1$ ): calc. for  $C_{11}H_{13}O$ , 161.096640; Found, 161.0944000.

*1-methoxy-1-(4-trifluoromethylphenyl)cyclobutane* (86).  $^1H$  NMR:  $\delta$  = 1.67 (m, 1 H), 1.96 (m, 1 H), 2.36 (d, 2 H), 2.39 (d sextet, 2H), 2.92 (s, 3 H), 7.57 (q, 4 H,  $J$  = 8.4 Hz).  $^{13}C$  NMR:  $\delta$  = 12.90, 32.80, 50.67, 81.26, 125.28, 125.36, 125.42, 126.55,  $CF_3$  not observed.  $^{19}F$  NMR:  $\delta$  = - 62.67. IR: 2997 (m), 2951 (m), 2834 (w), 1620 (w), 1408 (w), 1323 (s), 1300 (w), 1173 (s), 1147 (s), 1087 (m), 1072 (m), 1018 (m), 842 (s). MS:  $m/e$  (I) = 230 (1), 229 (2), 202 (27), 210 (61), 182 (11), 172 (27), 161



(28), 151 (25), 145 (42), 133 (100), 103 (22), 75 (8). Exact mass: calc. for  $C_{12}H_{13}F_3O$ , 230.091850; found, 230.0900000.

*1-methoxy-1-(4-trifluoromethoxyphenyl)cyclobutane* (87).  $^1H$  NMR:  $\delta$  = 1.65 (m, 1 H), 1.98 (m, 1 H), 2.40 (d, 2 H), 2.42 (m, 2 H), 2.93 (s, 3 H), 7.02 (m, 4 H).  $^{13}C$  NMR:  $\delta$  = 12.86, 32.70, 50.63, 78.60, 120.90, 27.14, 134.90, 144.60. MS:  $m/e$  (I) = 245 (3), 230 (6), 218 (48), 217 (100), 188 (45), 175 (15), 161 (15), 133 (36), 119 (18), 91 (9), 77 (6), 69 (15). Exact mass: calc. for  $C_{13}H_{13}F_3O_2$ , 246.08676; found, 246.0901000.

*1-methoxy-1-(3-trifluoromethylphenyl)cyclobutane* (88).  $^1H$  NMR:  $\delta$  = 1.65 (cplx m, 1 H), 1.95 (cplx m, 1 H), 2.36 (d, 2 H), 2.39 (m, 2 H), 2.92 (s, 3 H), 7.60 (m, 4 H).  $^{13}C$  NMR:  $\delta$  = 12.88, 32.71, 50.62, 81.23, 22.92, 124.05, 128.82, 129.62, 144.49.  $^{19}F$  NMR:  $\delta$  = -62.69. IR: 3080 (w), 2997 (m), 2952 (m), 2833 (w), 1489 (w), 1439 (w), 1335 (s), 1270 (s), 1177 (s), 1145 (s), 1100 (m), 1077 (m), 1042 (w), 901 (w), 802 (w). MS:  $m/e$  (I) = 230 (2), 215 (8), 202 (58), 201 (98), 172 (40), 159 (25), 151 (40), 145 (33), 133 (100), 103 (22). Exact mass: calc. for  $C_{12}H_{13}F_3O$ , 230.091850; found, 230.0901000.

*4-Trifluoromethylphenylacetylene*<sup>214</sup>. 4-Bromobenzotrifluoride (0.803 g, 0.5 mL,  $3.57 \times 10^{-3}$  mol) dissolved in freshly distilled toluene (10.0 mL) was added to tetrakis(triphenylphosphine)palladium(0) (0.082 g,  $7.1 \times 10^{-5}$  mol) in deoxygenated

toluene (10.0 mL) under a N<sub>2</sub> atmosphere. The solution was evacuated and refilled with N<sub>2</sub> three times, and the mixture was heated to reflux. To this solution was added dropwise over the period of one hour tributyl-tin-acetylene<sup>‡‡</sup> (0.56 g, 1.78 x 10<sup>-3</sup> mol) in deoxygenated toluene (10 mL). After refluxing for four additional hours, the reaction mixture was cooled down and a brown residue was isolated. Work-up consisted in washing the residue with water and extracting with pentane (5 mL x 4). The dark pentane and toluene layers were dried over anhydrous sodium sulfate and evaporated with a rotary evaporator. A dark brown residue was obtained. Purification consisted in silica gel column chromatography (solvent of elution: pentane) and ulterior bulb-to-bulb distillation. The spectroscopic characterization is in good agreement with the literature information.

*4-trifluoromethylphenylacetylene* (80)<sup>197</sup>. IR: 3314 (s), 3083 (m), 3060 (w), 3035 (w), 2928 (w), 2112 (m), 1601 (m), 1575 (w), 1489 (s), 1444 (m), 1401 (w), 1325 (m), 1223 (m), 1172 (m), 1132 (m), 1102 (w), 1071 (m). MS: *m/e* (*I*) = 170 (100), 169 (25), 151 (40), 120 (40), 99 (10), 75 (20), 74 (20).

‡‡ Sample kindly supplied by Dr. M.A. Brook.

*2,4,4-Trideuterio-1-phenylcyclobutene* (89): Deuteration of cyclobutanone was accomplished by stirring a mixture of cyclobutanone (1 g, 0.014 mol), triglyme (15 mL) deuterium oxide (5.0 mL) and potassium carbonate (5 g) for 24 hrs. at 70°C (not allowing the temperature to rise above 75°C). The resulting solution was extracted 5 times with ethyl ether, and the combined organic layers were distilled off at atmospheric pressure employing a short Vigreux fractionating column. Once the ethyl ether was

removed, two consecutive traps immersed in dry ice / isopropanol were attached in series to the receiving flask that had been cooled at  $-78^{\circ}\text{C}$ , and the temperature of the still was allowed to increase gradually. Deuterated cyclobutanone (0.5 g, 51 % yield), and traces of ethyl ether collected in the receiving flask and the traps.  $^1\text{H}$  NMR analysis of the fractions collected revealed that 80 % tetradeuteration had taken place at the  $\alpha$  positions to the carbonyl group of cyclobutanone. The material was subjected to a second cycle of deuteration following a similar procedure as described (*vide supra*). The  $^1\text{H}$  NMR spectrum of the material isolated, showed H resonances for the methylene groups  $\alpha$  to the carbonyl integrating in a ratio 0.5:20 with respect to the  $\beta$  protons of the cyclobutane ring. The material obtained (0.29 g), was made react with phenyllithium (2.2 mL, 0.0039 mol) in tetrahydrofuran (10 mL) at  $-78^{\circ}\text{C}$ . The solution was stirred at  $-78^{\circ}\text{C}$ , and allowed to reach room temperature. After quenching with deuterium oxide (3.0 mL) and usual work-up (*vide supra*) 0.505 g of a slightly yellow oil was obtained.  $^1\text{H}$  NMR analysis of this oil in  $\text{CDCl}_3$  revealed that the cyclobutane ring had retained four deuteria in its structure. Purification consisted in column chromatography (solvent of elution: hexane : ethyl ether 40:60).

MS: *m/e* (I): 152 (0.5), 151 (0.8), 150 (0.2), 122 (48), 105 (100), 93 (26), 78 (81), 77 (68), 51 (33), 30 (5), 29 (4), 28 (3), 27 (1). IR: 3638 (w), 3073 (m), 3041 (m), 2982 (s), 2943 (m), 2687 (w), 2190 (w), 1606 (w), 1496 (w), 1448 (m), 1378 (m), 1289 (m), 1183 (m), 1103 (m), 1031 (m), 903 (m), 760 (m). m.p.:  $35\text{-}36^{\circ}\text{C}$ .

*2,4,4-Trideuterio-1-phenylcyclobutene* **89** was prepared by refluxing a solution of *2,2,4,4-tetradeuterio-1-phenylcyclobutanol* (0.4 g) in benzene- $d_6$  (5.0 mL) containing traces of deuterium oxide and *p*-toluenesulfonic acid monodeuteriohydrate (recrystallized thrice from  $D_2O$ ) for 5 hours. After cooling to room temperature, the solution was washed with a small amount of 5% aqueous sodium hydroxide and dried over anhydrous magnesium sulfate. The solvent was removed by rotary evaporation to yield a colorless oil (0.35g) from which **89** was isolated by semi-preparative vpc after bulb-to-bulb distillation under vacuum.  $^1H$  NMR analysis indicated the compound to be >95% deuterated at  $C_2$  and  $C_4$  positions of the cyclobutene ring.

$^1H$  NMR ( $CD_3CN$ ):  $\delta$  = 2.48 (s, 2 H), 2.81 (m, 0.12 H), 6.32 (t, 0.05 H), 7.31 (m, 5 H). MS: *m/e* (I): 133 (81), 132 (100), 131 (79), 119 (9), 118 (21), 117 (45), 116 (44), 103 (81), 79 (11), 78 (12), 77 (30), 76 (26), 75 (21), 67 (11), 66 (12), 65 (14), 52 (16), 51 (36), 50 (18), 39 (13). IR: 3074 (m), 3039 (m), 2035 (s), 2291 (w), 2226 (m), 2154 (w), 1954 (w), 1798 (w), 1606 (w), 1493 (m), 1447 (w), 1291 (w), 1019 (w), 753 (s).

Irradiations were carried out on a 0.5 mL scale in 3" x 5 mm quartz tubes, in a Rayonet reactor containing 1 254 lamp. For the purposes of product identification, photolyses were taken to *ca.* 40% conversion, and the products identified by GC/MS, GC/FTIR, and GC coinjection with authentic samples (the synthesized 1-arylmethoxy cyclobutane ethers (83-88)). Identification of the substituted phenylacetylenes was based on their GC retention times, the prominent parent ion and characteristic fragmentation patterns in their mass spectra<sup>198</sup>, their characteristic IR spectra ( $C\equiv C-H$

stretching frequency) obtained by GC/FTIR analyses of the crude photolysis mixtures and coinjection with authentic samples in the case of 4-tolylacetylene<sup>199</sup>, phenylacetylene<sup>200</sup>, and 4-trifluoromethylphenylacetylene (*vide supra*). Mass and gas phase infrared spectral data for the four substituted phenylacetylenes obtained from preparative scale photolysis of phenylcyclobutenes 65, 69, and 70 are given below.

*4-methoxyphenylacetylene* (77)<sup>201</sup>. IR: 3318 (s), 3083 (w), 3031 (w), 2957 (w), 2925 (w), 2838 (w), 2110 (m), 1650 (w), 1598 (m), 1581 (m), 1508 (s), 1489 (s), 1451 (m), 1443 (m), 1290 (m), 1245 (m), 1180 (m), 1103 (w). MS<sup>198</sup>: *m/e* (*I*) = 132 (80), 131 (75), 117 (27), 101 (39), 90 (20), 50 (20).

*4-methylphenylacetylene* (78)<sup>201</sup>. IR: 3317 (s), 3084 (w), 3031 (w), 2962 (m), 2925 (m), 2866 (w), 2111 (m), 1508 (s), 1261 (s), 1215 (m), 1103 (m), 1020 (m), 826 (m), 650 (s), 603 (s), 529 (s). MS: *m/e* (*I*) = 116 (75), 115 (100), 89 (40), 74 (20), 63 (35), 50 (29).

*4-trifluoromethylphenylacetylene* (80)<sup>197</sup>. IR: 3314 (s), 3083 (m), 3060 (w), 3035 (w), 2928 (w), 2112 (m), 1601 (m), 1575 (w), 1489 (s), 1444 (m), 1401 (w), 1325 (m), 1223 (m), 1172 (m), 1132 (m), 1102 (w), 1071 (m). MS: *m/e* (*I*) = 170 (100), 169 (25), 151 (40), 120 (40), 99 (10), 75 (20), 74 (20). <sup>19</sup>F NMR: -62.72.

*4-trifluoromethoxyphenylacetylene* (81). IR: 3314 (s), 2980 (s), 2828 (s), 2869 (m), 2855 (m), 2112 (w), 1671 (w), 1597 (w), 1574 (w), 1489 (m), 1445 (m), 1380 (w), 1261 (s), 1227 (m), 1100 (s), 1070 (m), 1025 (s). MS:  $m/e$  ( $I$ ) = 186 (100), 167 (30), 120 (17), 117 (15), 99 (20), 85 (15), 75 (25), 74 (31).  $^{19}\text{F}$  NMR: -62.76.

*3-trifluoromethylphenylacetylene* (82)<sup>197</sup>. IR: 3314 (s), 3076 (m), 3035 (w), 2923 (w), 2114 (w), 1602 (w), 1579 (s), 1485 (s), 1430 (s), 1348 (s), 1272 (s), 1223 (m), 1174 (s), 1131 (s), 1088 (s), 914 (m). MS:  $m/e$  ( $I$ ) = 170 (100), 169 (30), 151 (40), 120 (42), 99 (10), 75 (20), 74 (30), 69 (10).

The dimers obtained from direct photolysis of 70 in hydrocarbon solutions were tentatively identified on the basis of GC/MS analysis:

*Dimer 1*: 66 % (based on total dimer yield):

MS:  $m/e$  ( $I$ ) = 396 (0.2), 387 (0.1), 290 (100), 271 (21), 251 (4), 240 (6), 219 (23), 201 (94), 170 (10), 152 (50), 126 (3), 99 (1), 69 (19), 50 (0.5).

*Dimer 2*: 33 % (based on total dimer yield):

MS:  $m/e$  ( $I$ ) = 396 (0.5), 387 (0.5), 290 (100), 271 (30), 251 (4), 240 (5), 219 (25), 201 (85), 170 (15), 152 (55), 126 (1), 99 (1), 69 (24), 50 (1).

#### 6.1.4 Quantum Yield Determinations and Fluorescence Lifetimes

Quantum yields were determined by electronic actinometry. The system comprised of an optical bench and a photocounter device. The optical bench consisted of an ultra high pressure Hg lamp housed in a ventilated steel compartment, a monochromator that selected the optical wavelength for excitation and a black box with a mobile shutter. The black box contained a filter (Corning CS7-54) and one splitting lens. Photodiodes collecting the split reference beam and the sample beam were located equidistantly to the splitting lens. A photocounter device provided the number of counts that the photodiodes received. The system was calibrated daily with potassium ferrioxalate. Samples were contained in cylindrical suprasil quartz cells, which were sealed with rubber septa and deoxygenated with a stream of dry nitrogen prior to photolysis. The actinometry was carried out at 260 nm. The conversion of the actinometer (potassium ferrioxalate) was monitored by measuring the absorbance of the complex Fe-(o-phenanthroline-1,10) at 510 nm. A radiant power of ca.  $10^{-8}$  einsteins was achieved after 3 hour photolysis. The conversion of the aryl-cyclobutene **68** to 1-arylacetylene **80** (in aprotic solvents) or to the ether adduct **86** (in protic solvents) was followed by gas chromatographic techniques. Product concentrations were determined relative to an internal standard (n-decane) and were corrected for relative FID response factors using working curves.

Relative quantum yield determinations and Stern-Volmer studies were carried out using a Rayonet reactor equipped with a merry-go-round and one 253.7 nm Hg lamp. Fluorescence lifetimes<sup>202</sup> were measured at ambient temperature (22-25°C) using a PTI-LS 100 single photon counting system and a hydrogen flash lamp. Cuvettes used were Suprasil fluorescence cells sealed with a rubber septa. The cuvettes were

deoxygenated with a stream of dry nitrogen for at least 45 minutes prior to the experiment. Fluorescence decays were recorded using 260 nm excitation and a monitoring wavelength corresponding to the emission maximum of the cyclobutene in the particular solvent being studied (Table 2.2.5.1). For the solutions in the pure solvents, decays were recorded with 10000 counts in the maximum channel, and were deconvoluted and analyzed using the software provided by the manufacturer. In general, the decays were fit to single or double exponential (*e.g.* 65) functions in order to obtain the best possible fit. In cases where the data fit best to a two exponential function, the second component comprised less than *ca.* 10% of the decay. In each case, the lifetimes reported are the average of at least two independent determinations, the results of which invariably differed by less than 5%. For the methanol and HFIP quenching studies, the quencher was added incrementally to the cuvettes by microlitre syringe. In these experiments, decays were recorded with 1000 counts in the maximum channel so as to minimize sample decomposition.

### 6.1.5 Nanosecond Laser Flash Photolysis Experiments

Nanosecond laser flash photolysis experiments employed the pulses (248 nm, *ca.* 12 ns) from a Lumonics 510 excimer laser filled with F<sub>2</sub>/Kr/He or the pulses from a Lumonics TE-861M excimer laser filled with N<sub>2</sub>/He (337 nm, 6 ns, *ca.* 4 mJ) and a microcomputer-controlled detection system that has been described elsewhere<sup>203</sup>. The geometry of the system is such that the excitation beam power is reduced from 80-120 mJ at the source to 2-4.5 mJ at the sample compartment. Solutions of 66-68 were prepared at concentrations such that the absorbance at the excitation wavelength was *ca.*



0.7 (ca.  $5 \times 10^{-5}$  mol dm<sup>-3</sup>.) The 1-arylcyclobutene solutions were flowed continuously through a 3 x 7 Suprasil flow cell, supplied by a calibrated 100 mL capacity reservoir. The solutions were deoxygenated continuously in the reservoir with a stream of nitrogen. Quenchers were added directly to the reservoir by microlitre syringe as aliquots of the neat liquids.

### 6.1.6 Steady State Photolyses

Steady-state photolyses of deoxygenated 0.005 mol dm<sup>-3</sup> pentane, acetonitrile and methanol solutions of 65-70 were carried out in a Rayonet photochemical reactor equipped with a merry-go-round and one or two RPR-254 (254 nm) lamps. Photolysis solutions were contained in 7 x 70 mm quartz tubes sealed with rubber septa which were deoxygenated prior to photolysis with a stream of dry nitrogen.

## 6.2. MONOCYCLIC CYCLOBUTENES

### 6.2.1 General

<sup>1</sup>H / <sup>13</sup>C NMR analyses, IR and mass spectral data were obtained according to Section 6.1.1

Gas chromatographic analyses were carried out using a Hewlett-Packard 5890 gas chromatograph equipped with a flame ionization detector, a Hewlett-Packard 3396 integrator, and a HP-1 megabore capillary column (12 m x 0.53 mm; Hewlett-Packard,

Inc.) or a SP-B1 microbore capillary column (15 m x 0.2 mm; Supelco, Inc.), and a DB-1 megabore capillary column (30 m x 0.53 mm, Chromatography Specialties, Inc.) Semipreparative vpc separations employed a Varian 3300 gas chromatograph and one of the following stainless steel columns: (c) 20 %  $\beta,\beta$ -oxy-bis(dipropionitrile) (ODPN), on 80/100 Chromosorb PNAW (20' x 0.25", stainless steel) or (d) 3.8 % UC W982 on 80/100 Supelport (24' x 0.25", stainless steel).

Ultraviolet absorption spectra were recorded using a Perkin Elmer Lambda 9 spectrophotometer interfaced with an IBM PC PS/2. The spectra were recorded in 0.1 cm Suprasil cells. The sample and the reference were deoxygenated with argon prior to recording the spectra. The cell compartment was constantly flushed with dry nitrogen.

## 6.2.2 Commercial Solvents and Reagents Used

2,3-Dimethyl-1,3-butadiene, 2,3-dimethylmaleic anhydride, acetophenone, propene, *cis* and *trans*-but-2-ene, 2,3-dimethyl-but-2-ene, 2-butyne, lithium aluminum hydride, n-decane, n-nonane, and n-heptane and p-toluenesulphonyl chloride were all purchased from Aldrich Chemical Co., and used as received. Ethyl acetate was Baker Analyzed (HPLC grade). Tetrahydrofuran and ethyl ether were purchased from Fisher Chemical Co., dried over sodium/benzophenone and distilled prior to use. Pentane and cyclohexane were Baker Analyzed (Photorex grade), and used as received from the supplier. Lithium Perchlorite was purchased from Alfa Inorganics, and used as received. n-Hexadecane was purchased from Aldrich, and purified by stirring with concentrated sulfuric acid for 12 hours, separating and discarding the sulfuric layer, and repeating this procedure until the sulfuric layer remained clear. Extraction into an aqueous solution of

sodium bicarbonate followed, and rinsing with distilled water until neutral pH. The *n*-hexadecane was then separated from the aqueous solution, dried over anhydrous sodium sulfate, filtered, and refluxed over calcium hydride overnight. The distillation of the hydrocarbon was carried out under reduced pressure (0.4 torr, 105°C) using a Vigreux fractionating column wrapped in a heating tape. This process yielded the hydrocarbon with very low UV absorption at 200 nm ( $< 0.05$ ), as compared to the commercially available spectroscopic grade hydrocarbons ( $A \geq 1$  at 200 nm).

### 6.2.3 Preparation and Purification of Cyclobutenes

*2,3-dimethylcyclobutene*<sup>93, 143</sup> (93). 2,3-dimethyl-but-1,3-diene (5.0 mL, 3.63 g, 0.044 mol) was dissolved in 45.0 mL of pentane in a 50.0 mL quartz cell. After deoxygenating with a stream of nitrogen for 15 minutes, the solution was irradiated with seven 254 nm light lamps in a Rayonet reactor for six hours until a conversion of 50% of the starting material to the cyclobutene was achieved. The conversion was monitored by gas chromatography using column (c). Further conversion led to increasing amounts of polymeric material. Purification was achieved by bulb-to-bulb distillation of the photolysis mixture. Ulterior purification was carried out by semipreparative gas chromatography on column (c).

$^1\text{H}$  NMR ( $\text{CCl}_4$ )  $\delta$ : 1.56 (s, 6 H), 2.21 (s, 4 H).  $^{13}\text{C}$  NMR  $\delta$ : 3.56, 9.57, 136.04. UV hexadecane),  $\lambda_{\text{max}}$  ( $\epsilon$ ): 191 (8050), 200 (3300), 220 (520).

*1,2,3-trimethylcyclobutene*<sup>145(94)</sup>. 2,3-dimethylmaleic anhydride (15 g, 0.12 mol) and acetophenone (0.57 mL, 0.58 g, 0.0048 mol) were dissolved in 50.0 mL of ethyl acetate in a pyrex reaction kettle equipped with a magnetic stirrer and gas inlet. The solution was deoxygenated at *ca.* -78°C with a stream of dry nitrogen for twenty minutes, and then saturated with propylene. The solution was irradiated with a medium pressure mercury lamp (450W, Hanovia) for 4 hours while the temperature was maintained at -78°C. The irradiation was terminated when more than 95% of the maleic anhydride had been consumed as determined by <sup>1</sup>H NMR, and the solvent was evaporated on the rotary evaporator. The yellow oil that remained was distilled in vacuo (*ca.* 0.3 torr) to remove acetophenone and traces of maleic anhydride. Redistillation of the residue (86-87°C, *ca.* 0.4 torr) afforded a white solid which exhibited a <sup>1</sup>H NMR spectrum consistent with a mixture of *cis* and *trans* 1,2,3-trimethyl-cyclobutane anhydrides.

<sup>1</sup>H NMR  $\delta$  (CD<sub>3</sub>OD): 0.83 (d, 3 H), 0.87 (d, 3 H), 1.12 (s, 6 H), 1.13 (s, 6 H), 2.21 (br. t, 4 H), 3.15 (cplx. m, 2 H).  
GC/FTIR: 919 (m), 970 (s), 1111 (w), 1177 (m), 1219 (m), 1283 (w), 1387 (w), 1459 (w), 1788 (s), 1857 (m), 2883 (w), 2943 (w), 2978 (m). MS, *m/e* (I): 169 (2), 168 (2), 141 (39), 127 (52), 100 (100), 82 (40), 69 (21), 55 (42). MS (NH<sub>3</sub>, DCI): 186.

A portion (10 g) of the white solid was stirred in 20% aqueous hydrochloric acid (30 mL) for 12 h at room temperature, and then extracted with diethyl ether (3 x 15 mL). The extracts were washed with water (30 mL), saturated brine (30 mL), dried over anhydrous sodium sulfate, and the solvent was evaporated to yield a dirty white

solid (9 g). This solid was recrystallized from a mixture of ethyl acetate : water : methanol: 1:1:0.5, to yield needle-like white crystals, (7.2 g, 80 %). The  $^1\text{H}$  NMR spectrum of this material showed resonances that were consistent with 1,2,3-trimethylcyclobutane-1,2-dicarboxylic acid, obtained as a mixture of isomers.

$^1\text{H}$  NMR ( $\text{CD}_3\text{OD}$ ): 0.93 (d, 3 H), 1.11 (s, 6 H), 2.5 (m, 2 H), 3.30 (m, 1 H), 9.05 (br. s, 2 H). MS,  $m/e$  ( $\text{T}$ ): 169 (31), 168 (2), 141 (61), 140 (19), 127 (38), 125 (23), 100 (100), 85 (34), 82 (53), 69 (18), 55 (45). MS ( $\text{NH}_3$ , DCI): 204. IR (KBr pellet): 941 (m), 1061 (w), 1119 (m), 1190 (m), 1310 (s), 1416 (m), 1473 (m), 1701 (s), 2500-3500 (br. s)

A portion of the mixture of diacids (5 g) was then dissolved in acetonitrile (25 mL) in a 150 mL beaker, and 15 mL of an aqueous  $0.1 \text{ mol dm}^{-3}$  solution of lithium perchlorate were added. The mixture was cooled down to  $0^\circ\text{C}$  by means of a cold plate which also stirred the mixture magnetically. Five carbon anodes and one graphite cathode were introduced. The reference electrode consisted of a silver/silver chloride couple ( $E_{\text{OX}} = 2 \text{ v}$  versus  $\text{Ag}^\circ/\text{AgCl}$ ,  $\Delta E_0 = 70 \text{ v}$ ). The solution was then electrolyzed<sup>201</sup> for 36 h, while the temperature was maintained at  $0^\circ\text{C}$  throughout the electrolysis. The progress of the reaction was monitored by taking aliquots at regular intervals of the electrolysis, extracting them with pentane and monitoring the conversion by gas chromatography. After 36 h, more than 85% of the starting material had disappeared to give 1,2,3 trimethylcyclobutene as sole product. Other attempts at shorting the reaction times were made by adding radical scavengers such as p-tert-butyl phenol. These attempts did not lead to any significant improvements to the electrolysis

times. The acetonitrile solution was then extracted with pentane (5 x 15 mL) and the pentane layers distilled off slowly at atmospheric pressure and 35°C. When no less than 10 mL were left, the liquid was bulb-to-bulb distilled at 0.3 torr and room temperature. A transparent liquid was obtained. Gas chromatographic analysis revealed the presence of the very volatile 1,2,3-trimethylcyclobutene. Further purification was achieved by semipreparative gas chromatography, using column (c) (injector temperature 120°C, detector temperature 150°C, oven temperature 50°C).

A second route to the synthesis of 1,2,3-trimethylcyclobutene was attempted. This route involved the oxidative decarboxylation of 1,2,3-trimethylcyclobutanedicarboxylic acid by lead tetraacetate in pyridine. A portion (5 g, 0.027 mol) of the solid was added to pyridine (100 mL, distilled from potassium hydroxide) and the solution was placed in a 250 mL, two necked, round bottom flask fitted with a gas inlet tube and a Vigreux column connected to three sequential dry ice/isopropanol traps. The solution was saturated with oxygen at room temperature, lead tetraacetate (11.9 g, 0.027 mole) was added, a slight positive pressure of dry nitrogen was applied, and the mixture was placed in an oil bath at 70°C where CO<sub>2</sub> evolution occurred within one minute. When gas evolution had subsided, the temperature of the oil bath was increased to 80°C and nitrogen was slowly bubbled through the reaction mixture for 5 hours. The colorless liquid which had collected in the traps (trap 1 contained *ca.* 1.9 mL of pyridine, volume of traps 2 and 3 *ca.* 1.5 mL) was dissolved in pentane (5 mL), washed with 5 % aqueous hydrochloric acid (3 x 2 mL), water (3 x 3 mL), dried over anhydrous sodium sulfate, filtered, and concentrated by distillation at atmospheric pressure. VPC analysis (column (c)) of the product revealed the presence of one major component in *ca.* 96 % (gas chromatographic analysis showed solvent peak integrating for not more than 3 % of the total area). This was separated by semi-preparative vpc (column (c), injector

temperature 100°C, detector temperature 150°C, oven temperature 50°C). The yield of the oxidative decarboxylation of 1,2,3-trimethylcyclobutane dicarboxylic acid with lead tetraacetate was 55 %.

$^1\text{H}$  NMR: 0.91 (d, 3 H), 1.07 (s, 6 H), 2.45 (m, 2 H), 3.21 (m, 1 H). MS,  $m/e$  (I): 96 (45), 95 (12), 81 (100), 80 (75), 79 (51), 68 (61), 55 (65), 54 (66), 42 (39), 41 (29). UV (hexadecane),  $\lambda_{\text{max}}$  ( $\epsilon$ ): 186 (12100).

*Cis and trans-1,2,3,4-tetramethylcyclobutene*<sup>202</sup> (95, 96). A mixture of maleic anhydride (3.55 g, 0.36 mol), and acetophenone (1.5 mL, 1.53 g, 0.0127 mol) were added to 0.190 L of ethyl acetate in a pyrex reaction Kettle equipped with a magnetic stirrer and gas inlet. The solution was cooled down to ca. -78° C, and purged with a stream of dry nitrogen for 30 minutes and then saturated with a mixture of *cis* and *trans* 2-butene, while the temperature was maintained at -78° C. The solution was irradiated with a medium pressure mercury lamp (450W, Hanovia) for 3.5 hours while the temperature was not allowed to rise above -70° C. The irradiation was terminated when more than 95% of the maleic anhydride had been consumed as determined by  $^1\text{H}$  NMR and gas chromatographic analyses, and the solvent was evaporated on the rotary evaporator. The yellow oil that remained was distilled in vacuo (ca 0.3 torr) to remove acetophenone and traces of maleic anhydride, affording a white solid which exhibited a  $^1\text{H}$  NMR spectrum consistent with a mixture of *cis*- and *trans*-1,2,3,4-dimethylcyclobutane-3,4-dicarboxylic acid anhydrides.

$^1\text{H}$  NMR :  $\delta = 0.95$  (b d, 6 H), 1.12 (b s, 6 H), 3.11 (cplx m, 2 H).

The solid from above (1.4 g, 0.01 mol) was stirred in 20 % aqueous hydrochloric acid for ca. 12 hours at 60°C and then extracted with ethyl ether (3 x 10 mL). The extracts were washed with water (5.0 mL), saturated brine (5 mL), dried over sodium sulfate and then distilled to afford a white solid (1.2 g). The  $^1\text{H}$  NMR spectrum of the solid dissolved in DMSO- $d_6$  showed, besides the signals corresponding to methyl and methyne protons, a resonance at ca. 10.1 ppm, indicating the presence of carboxylic protons.

A portion (1 g, 0.005 mol) of the solid was added to pyridine (10 mL, distilled from potassium hydroxide) and the solution was placed in a 50 mL, two necked, round bottom flask fitted with a gas inlet tube and a Vigreux column connected to three sequential dry ice/isopropanol traps. The solution was saturated with oxygen at room temperature, lead tetraacetate (2.5 g, 0.005 mole) was added, a slight positive pressure of dry nitrogen was applied, and the mixture was placed in an oil bath at 70°C where  $\text{CO}_2$  evolution occurred within one minute. When gas evolution had subsided, the temperature of the oil bath was increased to 90°C and nitrogen was slowly bubbled through the reaction mixture for 5 hours. The colorless liquid which had collected in the traps was dissolved in pentane (5 mL), washed with 5 % aqueous hydrochloric acid (3 x 2 mL), water (3 x 3 mL), dried over anhydrous sodium sulfate, filtered, and concentrated by distillation. VPC analysis (column (c)) of the product revealed the presence of two major components in ca. 1:1 ratio. These were separated by semi-preparative vpc (column (c), injector temperature 120°C, detector temperature 150°C, oven temperature 70°C).



*Cis-1,2,3,4-tetramethylcyclobutene*<sup>186</sup> (95). <sup>1</sup>H NMR :  $\delta$  = 0.89 (d, 6 H, J = 6.9 Hz), 1.49 (s, 6 H), 2.56 (q, 2 H, J = 6 Hz). <sup>13</sup>C NMR:  $\delta$  = 10.86, 12.79, 39.45, 139.80. UV (hexadecane),  $\lambda_{\max}$  ( $\epsilon$ ): 190 (11100).

*Trans-1,2,3,4-tetramethylcyclobutene*<sup>186</sup> (96). <sup>1</sup>H NMR :  $\delta$  = 0.99 (d, 6 H), 1.53 (s, 6 H), 1.93 (q, 2 H). UV (hexadecane),  $\lambda_{\max}$  ( $\epsilon$ ): 189 (10500), 205 sh. (7600).

*1,2,3,3,4-Pentamethylcyclobutene*<sup>151</sup>, (97). 2,3-dimethyl-maleic anhydride (15 g, 0.12 mol) and acetophenone (2.80 mL, 2.88 g, 0.024 mol) were dissolved in 100.0 mL of ethyl acetate in a pyrex reaction kettle equipped with a magnetic stirrer and gas inlet. The solution was deoxygenated at ca. -50°C with a stream of dry nitrogen for thirty minutes, and then saturated with 2-methyl-2-butene. The solution was irradiated with a medium pressure mercury lamp (450W, Hanovia) for 5 hours while the temperature was maintained at -50°C. The irradiation was terminated when more than 95% of the maleic anhydride had been consumed as determined by <sup>1</sup>H NMR and gas chromatography analyses, and the solvent was evaporated on the rotary evaporator. The oil that remained was distilled in vacuo (ca. 0.3 torr) to remove acetophenone and traces of maleic anhydride, affording a white solid which upon ulterior recrystallization from a mixture of ethyl acetate : water : methanol (1:1:0.5) yielded white crystals (18.6 g, 80 %), which exhibited a <sup>1</sup>H NMR spectrum consistent with a mixture of *cis* and *trans* 1,2,3,3,4-pentamethyl-cyclobutane anhydrides.

$^1\text{H}$  NMR ( $\text{CD}_3\text{COCD}_3$ ):  $\delta = 0.96$  (d, 3 H,  $J = 7.4$  Hz), 0.97 (s, 3 H), 1.19 (s, 3 H), 1.32 (s, 3 H), 1.38 (s, 3H), 2.24 (q, 1 H,  $J = 7.5$  Hz).  $^{13}\text{C}$  NMR ( $\text{CD}_3\text{COCD}_3$ ):  $\delta = 11.17, 11.32, 17.04, 20.70, 26.59, 39.59, 47.59, 49.63, 175.98, 176.24$ . GC/FTIR: 919 (m), 967 (s), 1005 (w), 1120 (m), 1177 (m), 1242 (m), 1277 (w), 1388 (w), 1459 (m), 1789 (s), 1857 (m), 1931 (w), 2882 (w), 2944 (m), 2978 (m). MS,  $m/e$  (I): 123 (11), 97 (61), 84 (100), 69 (83), 55 (17), 44 (67). MS ( $\text{NH}_3$ , DCI): 228.

The solid from above (10 g, 0.05 mol) was stirred in 20 % aqueous hydrochloric acid for ca. 48 hours at  $80^\circ\text{C}$  and then extracted with ethyl ether (3 x 20 mL). The extracts were washed with water (25.0 mL), saturated brine (25 mL), dried over sodium sulfate and filtered to afford a white solid (9 g, 84 % yield based on anhydride). The  $^1\text{H}$  NMR spectrum of the solid dissolved in  $\text{DMSO}-d_6$  showed, besides the signals corresponding to methyl and methyne protons, a resonance at around 10.0 ppm, indicating the presence of carboxylic protons.

IR (KBr pellet): 519 (w), 601 (w), 801 (s), 1021 (m), 1077 (s), 1261 (m), 1376 (m), 1398 (m), 1458 (m), 1473 (m), 1558 (s), 2871 (w), 2922 (m), 2966 (m), 3394 (br., m).

A portion (5 g, 0.023 mol) of the solid was added to pyridine (50 mL, distilled from potassium hydroxide) and the solution was placed in a 250 mL, two necked, round bottom flask fitted with a gas inlet tube and a Vigreux column connected to three sequential dry ice/isopropanol traps. The solution was saturated with oxygen at room

temperature, lead tetraacetate (10 g, 0.023 mole) was added, a slight positive pressure of dry nitrogen was applied, and the mixture was placed in an oil bath at 70°C where CO<sub>2</sub> evolution occurred within one minute. When gas evolution had subsided, the temperature of the oil bath was increased to 90°C and nitrogen was slowly bubbled through the reaction mixture for 24 hours. The colorless liquid which had collected in the traps was dissolved in pentane (5 mL), washed with 5 % aqueous hydrochloric acid (3 x 5 mL), water (3 x 3 mL), dried over anhydrous sodium sulfate, filtered, and concentrated by distillation. VPC analysis (column f) of the product revealed the presence of one component. This component was separated and purified by semi-preparative vpc (column c), injector temperature 120°C, detector temperature 150°C, oven temperature 70°C).

<sup>1</sup>H NMR (CCl<sub>4</sub>): δ = 1.02 (d, J = 6.8 Hz, 3 H), 1.21 (s, 6 H), 1.37 (s, 6 H), 2.71 (m, 1 H). MS, m/e (I): 124 (32), 123 (5), 109 (54), 108 (23), 96 (31), 82 (52), 70 (100), 69 (67), 68 (32), 55 (47), 54 (43), 53 (32), 37 (21), 27 (12). UV (hexadecane), λ<sub>max</sub> (ε): 187 (7700).

*Hexamethylcyclobutene*<sup>151, 202</sup> (98). 2,3-Dimethyl-maleic anhydride (15 g, 0.12 mol), acetophenone (0.57 mL, 0.58 g, 0.0048 mol), and 2,3-dimethyl-2-butene (10.9 g, 15.5 mL, 0.13 mol) were dissolved in 50.0 mL of ethyl acetate in a pyrex reaction kettle equipped with a magnetic stirrer and gas inlet. The solution was deoxygenated at ca. -30°C with a stream of dry nitrogen for twenty minutes. The solution was irradiated with a medium pressure mercury lamp (450W, Hanovia) for 5 hours while the temperature was maintained at -30°C. The irradiation was terminated

when more than 95% of the maleic anhydride had been consumed as determined by  $^1\text{H}$  NMR and gas chromatography, and the solvent was evaporated on the rotary evaporator. The oil that remained was distilled in vacuo (ca. 0.5 torr) to remove acetophenone and traces of maleic anhydride, affording an oil which was redistilled under high vacuo (ca. 0.05 torr, 146°C) to yield 1,2,3,3,4,4-hexamethylcyclobutane anhydride (18 g, 72 %).

$^1\text{H}$  NMR ( $\text{CDCl}_3$ ):  $\delta = 1.01$  (12 H), 1.15 (6 H). GC/FTIR: 909 (w), 966 (m), 1001 (w), 1211 (w), 1262 (w), 1386 (w), 1462 (w), 1797 (s), 1855 (w), 2884 (w), 2921 (w), 2948 (m).

Attempts at hydrolyzing this compound were unsuccessful. A portion (5 g, 0.023 mol) of the solid was added to pyridine (50 mL, distilled from potassium hydroxide) and the solution was placed in a 250 mL, two-necked, round-bottom flask fitted with a gas inlet tube and a Vigreux column connected to three sequential dry ice/isopropanol traps. The solution was saturated with oxygen at room temperature, lead tetra-acetate (10 g, 0.023 mole) was added, a slight positive pressure of dry nitrogen was applied, and the mixture was placed in an oil bath at 70°C where  $\text{CO}_2$  evolution occurred within one minute. When gas evolution had subsided, the temperature of the oil bath was increased to 90°C and nitrogen was slowly bubbled through the reaction mixture for 24 hours. The colorless liquid which had collected in the traps was dissolved in pentane (5 mL), washed with 5 % aqueous hydrochloric acid (3 x 5 mL), water (3 x 3 mL), dried over anhydrous sodium sulfate, filtered, and concentrated by distillation. VPC analysis (column f) of the product revealed the presence of one component. This component was separated and purified by semi-

preparative vpc (column (c), injector temperature 120°C, detector temperature 150°C, oven temperature 75°C).

An alternative route to the synthesis of 98, is described as follows: 2,3-dimethyl-maleic anhydride (15 g, 0.12 mol), acetophenone (0.57 mL, 0.58 g, 0.0048 mol), and 2-butyne (7.02 g, 0.13 mol) were dissolved in 50.0 mL of ethyl acetate in a pyrex reaction kettle equipped with a magnetic stirrer and gas inlet. The solution was deoxygenated at ca. -55°C with a stream of dry nitrogen for twenty minutes. The resulting solution was irradiated with a medium pressure mercury lamp (450W, Hanovia) for 5 hours while the temperature was maintained at -55°C. The irradiation was terminated when more than 95% of the maleic anhydride had been consumed as determined by  $^1\text{H}$  NMR and gas chromatography, and the solvent was evaporated on the rotary evaporator. The oil that remained was distilled under vacuo (ca. 0.5 torr) to remove acetophenone and traces of 2,3-maleic anhydride, affording an oil which was distilled again under high vacuo (ca. 0.05 torr, 90°C) to yield 1,2,3,4-tetramethylcyclobutene anhydride (18.5 g, 80 %).

$^1\text{H}$  NMR ( $\text{CDCl}_3$ ):  $\delta = 1.45$  (s, 1 H), 1.68 (s, 1 H).

In a 250 mL two-necked round-bottomed flask equipped with a reflux condenser, addition funnel and magnetic stirrer, a suspension of lithium aluminum hydride (6.24 g, 0.166 mol) in tetrahydrofuran (25 mL) was added. The flask was evacuated and blanketed with a nitrogen atmosphere. The mixture was stirred at room temperature when 1,2,3,4-tetramethylcyclobutene anhydride (15 g, 0.083 mol) in tetrahydrofuran (150 mL) was added over a period of 1 hour. The mixture was refluxed for 20 hours with continuous stirring. The solution was then cooled down to -10°C and

quenched carefully by dropwise addition of water (30 mL). The suspension formed was extracted with ethyl ether (20 mL x 5), the organic layers dried over anhydrous sodium sulfate, filtered, and evaporated in a rotary evaporator, to yield a light yellow residue (12.7 g, 91 %). An IR spectrum of the sample dissolved in carbon tetrachloride confirmed the presence of hydroxyl group ( $3507\text{ cm}^{-1}$ ) and the C=C presence ( $1690\text{ cm}^{-1}$ ),  $^1\text{H}$  NMR spectrum confirmed the presence of *1,2,3,4-tetramethyl-1,2-cis-bis-hydroxymethyl-cyclobutene*.

$^1\text{H}$  NMR ( $\text{CDCl}_3$ ):  $\delta = 1.12$  (s, 3 H), 1.45 (s, 3 H), 3.34 (d, 1 H), 3.75 (d, 1 H), 4.64 (br s, 1 H).

A portion of *1,2,3,4-tetramethyl-1,2-cis-bis-hydroxymethylcyclobutene* (8 g, 0.048 mol) dissolved in dry pyridine (25 mL) was added dropwise to p-toluenesulfonyl chloride (14.3 g, 0.1 mol) in pyridine (45 mL) in a 250 mL round-bottom flask at  $0^\circ\text{C}$ , stoppered, and left at  $0^\circ\text{C}$  for 48 hours. The mixture was poured into 250 g of ice, vigorously stirred for 30 min, and then allowed to stand at  $0^\circ\text{C}$  for 1 hour. The solid precipitate was collected by filtration, washed with 2 % hydrochloric acid (25 mL), water (25 mL), filtered, dried under vacuum, and recrystallized from methanol to afford a light brown solid (11.9 g, 52 %).

The ditosylate (10 g, 0.021 mol) was added slowly to a suspension of lithium aluminum hydride (4.74 g, 0.126 mol) in dry tetrahydrofuran (150 mL) in a three-necked, round-bottomed flask equipped with a solid addition funnel, reflux condenser, nitrogen inlet, and magnetic stirrer. The mixture was refluxed for 20 hours, cooled down to  $-10^\circ\text{C}$  and quenched carefully by dropwise addition of water (30 mL). The thick suspension was extracted with ethyl ether (25 mL x 3), pentane (25 mL x 3) and the combined

organic layers were dried over anhydrous magnesium sulfate, filtered, and the solvent removed by slow distillation at atmospheric pressure with the use of a Vigreux column. The product was bulb-to-bulb distilled under vacuum, to afford a clear, transparent liquid with a  $^1\text{H}$  NMR spectrum consistent with *hexamethylcyclobutene* 98.

$^1\text{H}$  NMR ( $\text{CDCl}_3$ ):  $\delta$  = 1.02 (s, 12 H), 1.44 (s, 6 H). MS,  $m/e$  (T): 138 (29), 137 (9), 123 (67), 97 (35), 96 (100), 95 (54), 93 (21), 80 (13), 79 (56), 78 (50), 77 (12), 54 (47), 37 (41), 27 (15). UV (hexadecane),  $\lambda_{\text{max}}$  ( $\epsilon$ ): 185 (6900).

#### 6.2.4 Characterization of Photoproducts

The *cis* and *trans* dienes 101, 103 and 104 were isolated from preparative scale photolyses of cyclobutenes 94, 97, and 98 respectively, using column (c) and (d). Their characterizations follow:

*E*-2,3-Dimethyl-penta-1,3-diene<sup>149, 196</sup> (*trans*-101):  $^1\text{H}$  NMR ( $\text{CCl}_4$ ):  $\delta$  = 1.55 (d,  $J$  = 6.5 Hz, 3 H), 1.73 (s, 6 H), 4.83 (s, 2 H), 5.31 (q,  $J$  = 6.5 Hz, 1 H). MS,  $m/e$  (T): 96 (35), 95 (24), 81 (100), 80 (51), 79 (22), 68 (57), 55 (81), 54 (66), 42 (45), 41 (31), 37 (25), 27 (41). UV (cyclohexane),  $\lambda_{\text{max}}$  ( $\epsilon$ ): 235 (21000).

*Z-2,3-Dimethyl-penta-1,3-diene*<sup>149, 196</sup> (*cis*-101): <sup>1</sup>H NMR (CCl<sub>4</sub>): 1.67 (d, J = 6.8 Hz, 3 H), 1.75 (s, 6 H), 4.83 (s, 1 H), 4.93 (s, 1 H), 5.65 (q, J = 6.5 Hz, 1 H). MS, m/e (I): 96 (31), 95 (25), 81 (100), 80 (61), 79 (25), 68 (60), 55 (80), 54 (65), 42 (54), 41 (30), 37 (25), 27 (45). UV (cyclohexane), λ<sub>max</sub> (ε): 239 (15900).

*E-2,3,4-trimethyl-hexa-2,4-diene*<sup>204</sup> (*trans*- 103): <sup>1</sup>H NMR (CCl<sub>4</sub>): 1.54 (d, J = 6.7 Hz, 3 H), 1.70 (s, 6 H), 1.72 (s, 6 H), 5.37 (q, J = 6.5 Hz, 1 H). MS, m/e (I): 124 (35), 123 (11), 109 (59), 108 (29), 96 (42), 82 (55), 70 (100), 69 (61), 68 (35), 55 (42), 54 (45), 53 (30), 37 (29), 27 (19). UV (cyclohexane), λ<sub>max</sub> (ε): 207 (9500).

*Z-2,3,4-trimethyl-hexa-2,4-diene*<sup>204</sup> (*cis*- 103): <sup>1</sup>H NMR (CCl<sub>4</sub>): 1.61 (d, J = 6.8 Hz, 3 H), 1.72 (s, 6 H), 1.76 (s, 6 H), 5.79 (q, J = 6.5 Hz, 1 H). MS, m/e (I): 124 (365), 123 (11), 109 (55), 108 (25), 96 (42), 82 (54), 70 (100), 69 (62), 68 (36), 55 (45), 54 (45), 53 (39), 37 (29), 27 (21). UV (cyclohexane), λ<sub>max</sub> (ε): 218 (9650).

*2,3,4,5-Tetramethyl-hexa-2,4-diene*<sup>196</sup> (104). <sup>1</sup>H NMR (CCl<sub>4</sub>): 1.47 (s, 6 H), 1.63 (s, 12 H). MS, m/e (I): 138 (31), 137 (10), 123 (57), 97 (41), 96 (100), 95 (55), 93 (24), 80 (18), 79 (50), 78



(55), 77 (15), 54 (49), 37 (45), 27 (18). UV (cyclohexane),  $\lambda_{\max}$  ( $\epsilon$ ): 202 (10200).

The tetramethyl-but-1,3-dienes **102** obtained from photolyses of *cis*- and *trans*-1,2,3,4-tetramethylcyclobutenes **96** and **95** were characterized by co-injection with authentic samples<sup>†</sup>.

*E,E*-3,4-Dimethyl-hexa-2,4-diene<sup>206</sup> (E,E-102). UV  
(cyclohexane),  $\lambda_{\max}$  ( $\epsilon$ ) 206 (5700).

*E,Z*-3,4-Dimethyl-hexa-2,4-diene<sup>206</sup> (E,Z-102). UV  
(cyclohexane),  $\lambda_{\max}$  ( $\epsilon$ ): 210 (4100).

*Z,Z*-3,4-Dimethyl-hexa-2,4-diene<sup>206</sup> (Z,Z-102). UV  
(cyclohexane),  $\lambda_{\max}$  ( $\epsilon$ ): 235 (12000).

<sup>†</sup>The samples of the dienes were kindly provided by Mr. K.C. Zheng.

### 6.2.5 Photolyses and Quantum Yield Determinations

Steady-state photolyses of deoxygenated 0.02 mol dm<sup>-3</sup> n-hexadecane solutions of **93-97** were carried out using 214 nm light provided by a 16W zinc resonance lamp situated in the center of a merry-go-round. Photolysis solutions were contained in 7 x 70 mm quartz tubes sealed with rubber septa which were deoxygenated prior to photolysis with a stream of dry nitrogen. The conversion of the cyclobutenes was

monitored by gas chromatography. The solutions of 93-97 in n-hexadecane contained *ca.*  $10^{-4}$  mol dm<sup>-3</sup> n-heptane as internal standard for quantitation of the dienes and fragmentation products. The FID detector responses toward the dienes (ring opening-type products) and 2-butyne (cycloreversion-type products) were calibrated relative to the internal standard by construction of working curves.

Quantum yields were calculated relative to the ring opening reaction of 1,2-dimethylcyclobutene 93. The absolute quantum yield for ring opening of 93 was determined by uranyl oxalate actinometry and the solutions employed were rigorously deoxygenated for half an hour with a stream of dry nitrogen prior to photolyses. Photolysis solutions of both the actinometer ( $7.002 \times 10^{-3}$  mol dm<sup>-3</sup>) and 93 ( $2.50 \times 10^{-3}$  mol dm<sup>-3</sup>) were contained in cylindrical 3.0 mL quartz cells that were placed very close to the lamp, and were photolyzed at the same time. The absorbance of the unirradiated blank was lower than 0.013 in all cases. A radiant power of *ca.*  $5.5 \times 10^{-8}$  einstein was achieved after 40 minute photolysis as determined by the actinometer. Determinations were carried out in triplicate, and they all resulted in averageable figures. The conversion of the actinometer was calculated by an spectrophotometric technique 113 - 115. The solutions of 93 in hexadecane contained  $10^{-4}$  mol dm<sup>-3</sup> n-heptane as internal standard for quantitation of the product 2,3-dimethyl-buta-1,3-diene by gas chromatographic techniques. The FID detector response toward 2,3-dimethyl-buta-1,3-diene was calibrated relative to an the internal standard by construction of a working curve.

### 6.3 *cis* and *trans*-DIMETHYLBICYCLO[n.2.0]ALK-1<sup>n+2</sup>-ENES and RELATED DIENES

#### 6.3.1 General

<sup>1</sup>H /<sup>13</sup>C NMR analyses, UV, IR and mass spectral data were obtained according to Section 6.1.1

Gas chromatographic analyses were carried out using a Hewlett-Packard 5890 gas chromatograph with a flame ionization detector and a Hewlett-Packard integrator, a SPB-1 microbore capillary column (15 m X 0.2 mm; Chromatographic Specialties, Inc.) with cold on-column injection or a DB-1 megabore capillary column (30 m X 0.53 mm; Chromatographic Specialties, Inc.) with a conventional injector, or a HP-17 megabore capillary column (15 m X 0.53 mm, Hewlett-Packard, Inc.) with conventional injector.

Semipreparative vpc separations employed a Varian 3300 gas chromatograph equipped with a thermal conductivity detector, a Hewlett-Packard 3390A integrator and one of the following stainless steel columns: (e) 20 % TCEP on 80/100 chromosorb PNAW, 20 ft X 1/4 in. (Chromatographic Specialties, Inc.); (f) 20 % TCEP column on 80/100 chromosorb PNAW, 6 ft X 1/4 in., (Chromatographic Specialties); or (g) 3.8 % UC-W982 on 80/100 Supelcoport, 24 ft X 1/4 in. (Supelco).

#### 6.3.2 Commercial Solvents and Reagents Used

Pentane, Photorex reagent, was purchased from Baker Analyzed and used as received from the supplier. Hexamethylphosphoramide, n-Butyllithium, zirconocene

dichloride, methyl iodide, n-decane, *cis,cis*-1,3-cyclooctadiene, and 1,8-nonadiyne were purchased from Aldrich Chemical Co., and used as received. Cerium (IV) sulfate tetra hydrate was purchased from Aldrich and recrystallized from HPLC grade water three times before use. 1,7-Octadiyne and 1,6-heptadiyne were purchased from Wiley Organics, and purified by alumina column chromatography using hexanes as solvent of elution. 1,5-Hexadiyne was purchased from Lancaster and purified in the same way as 1,7-octadiyne and 1,6-heptadiyne. n-Nonane was purchased from Matheson Coleman & Bell and used as received. Uranyl sulfate was purchased from Alfa Inorganics Ventron. Oxalic acid, BDH reagent, was recrystallized three times from water. Tetrahydrofuran was from Caledon and was dried over calcium hydride and distilled from sodium/benzophenone prior to its use. Hexanes was from Fisher and used without further purification.

### 6.3.3 Preparation of Compounds

*Uranyl oxalate* was prepared as described by D.F. Eaton<sup>113</sup>.

The dialkynes precursors of dienes 124-127 were prepared according to a general technique given by Negishi et al.<sup>180</sup>

*2,9-undecadiyne*<sup>180</sup> (119): To 1,8-nonadiyne (10 g, 83.3 mmol) in tetrahydrofuran (160 mL) was added at -78 °C a solution of n-butyllithium in hexane (67 mL, 167 mmol). After stirring for one hour, iodomethane ( 24g, 167 mmol) in hexamethylphosphoramide (50 mL) was added. The reaction mixture was warmed to room temperature, stirred for thirty minutes, poured into water, extracted with pentane,

washed with brine, dried over magnesium sulfate and distilled to provide 12.3 g, (90 %) of a colorless liquid: b.p. 65–66 °C, 0.3 torr.

$^1\text{H}$  NMR,  $\delta$ : 1.45 (br s, 6H), 1.76 (t,  $J = 2.5$  Hz, 6H), 2.10 (cplx. m, 4H);  $^{13}\text{C}$  NMR,  $\delta$ : 3.34, 18.65, 28.64, 75.46, 79.17; MS (m/z (I)): 148 (2), 133(20), 120(20), 105(100), 91(40), 79(30), 67(30), 53(40), 39(40); GC/FTIR: 1335 (w), 1377 (w), 1445 (w), 1461 (w), 2749 (w), 2871 (m), 2939 (s), 3004 (w), 3033 (w).

*2,8-decadiyne*<sup>180</sup> (118): To 1,7-octadiyne (10 g, 94 mmol) in tetrahydrofuran (160 mL) was added at -78 °C a 2.5 mol/dm<sup>3</sup> solution of n-butyllithium in hexane (75 mL, 188 mmol). After stirring for one hour, iodomethane (27 g, 188 mmol) in hexamethylphosphoramide (50 mL) was added. The reaction mixture was warmed to room temperature, stirred for thirty minutes, poured into water, extracted with pentane, washed with brine, dried over magnesium sulfate and distilled to provide 11.3 g, (90 %) of a transparent liquid: b.p. 48°C, 0.3 torr.

MS (m/z (I)): 134 (0.5), 133 (3), 119 (44), 106 (47), 105 (27), 91 (100), 79 (34), 77 (21), 65 (16), 47 (51), 45 (31), 41 (52), 39 (50), 27(48); GC/FTIR: 1334 (m), 1378 (w), 1446 (m), 1461 (m), 2750 (w), 2873 (s), 2936 (s), 2973 (w), 3005 (w), 3062 (w).

*2,7-nonadiyne*<sup>180, 207</sup> (117): To 1,7-octadiyne (8 g, 87 mmol) in tetrahydrofuran (160 mL) was added at -78 °C a 2.5 mol/dm<sup>3</sup> solution of n-butyl lithium

in hexane (70 mL, 174 mmol). After stirring for one hour, iodomethane (24.7 g, 174 mmol) in hexamethylphosphoramide (50 mL) was added. The reaction mixture was warmed to room temperature, stirred for thirty minutes, poured into water, extracted with pentane, washed with brine, dried over magnesium sulfate and distilled to provide 6.3 g, (60 %) of a limpid liquid: b.p. 67°C, 42 torr.

MS (m/z (I)): 120 (1), 119 (4), 105 (100), 92 (39), 91 (73), 79 (50), 77 (41), 65 (44), 47 (36), 45 (50), 41 (50), 39 (97), 27 (71).

GC/FTIR: 1294 (w), 1337 (m), 1380 (w), 1445 (m), 1461 (w), 1541 (w), 2751 (w), 2875 (m), 2937 (s), 3005 (w), 3034 (w).

#### Preparation of (*E,E*)-1,2-bis(ethylidene)cycloalkane

*E,E*-1,2-bis(ethylidene)cycloheptane<sup>180</sup> (127): Zirconocene dichloride (2.45 g, 8.4 mmol) in tetrahydrofuran (28 mL) was treated at -78 °C with *n*-butyllithium in hexane (2.6 mol/dm<sup>3</sup> solution, 6.48 mL, 16.8 mmol). The mixture was stirred for one hour, and 2,9-undecadiyne (1.2 g, 8 mmol) in tetrahydrofuran (12 mL) was added. The reaction mixture was allowed to warm to room temperature and was stirred for four additional hours. The mixture was poured into 6 N hydrochloric acid (15 mL), and extracted with pentane (three times, 10 mL each), washed with brine, dried over magnesium sulfate anhydrous, concentrated, and chromatographed (silica gel, pentane as solvent of elution) to provide 0.52 g (42 %). Further purification was achieved by semipreparative gas-chromatography on column (f).

<sup>1</sup>H NMR  $\delta$ : 1.45-1.55 (m, 6 H), 1.56 (d,  $J = 3.5$  Hz, 6 H), 2.21 (m, 4 H), 5.37 (q,  $J = 7$  Hz, 2 H); <sup>13</sup>C NMR,  $\delta$ : 13.03, 27.78,

29.38, 31.8, 117.40, 146.06. MS ( $m/z$  (I)): 150 (52), 135 (16), 121 (41), 107 (37), 105 (21), 93 (96), 91 (75), 79 (100), 77 (62), 67 (38), 55 (18), 53 (28), 39 (50), 27 (31). UV (pentane):  $\lambda_{\max}$  ( $\epsilon$ ) = 222 nm (9010). GC/FTIR: 806 (w), 840 (w), 977 (w), 1035 (w), 1315 (w), 1346 (w), 1384 (w), 1452 (m), 1647 (w), 1870 (w), 2392 (s), 2868 (m), 3034 (w).

*E,E*-1,2-bis(ethylidene)cyclohexane<sup>67</sup>, 180 (*E,E*-126): This compound was prepared in an analogous fashion as (*E,E*)-1,2-bisethylidenecycloheptane described above.

<sup>1</sup>H NMR  $\delta$ : 1.58 (d,  $J$  = 6.8 Hz, 6 H), 1.59 (superimposed m, 4 H), 2.16 (br s, 4 H), 5.26 (q, 2 H,  $J$  = 6.8 Hz). <sup>13</sup>C NMR (CCl<sub>4</sub>),  $\delta$ : 12.90, 26.29, 27.95, 115.71, 142.03. MS ( $m/z$  (I)): 136 (45), 121 (10), 107 (45), 93 (50), 91 (65), 79 (100), 77 (50), 67 (20), 65 (20), 53 (20), 51 (19), 39 (40). HRMS: calc. for C<sub>10</sub>H<sub>16</sub>, 136.1252006; found, 136.0721000. UV (pentane):  $\lambda_{\max}$  = 221 nm. FTIR: 808 (m), 843 (deg., w), 905 (w), 1001 (w), 1235 (w), 1375 (w), 1443 (m), 2857 (s), 2939 (s), 2959 (m),

*E,E*-1,2-bis(ethylidene)cyclopentane<sup>180</sup>, 208 (*E,E*-125): The synthesis and purification of this compound involved an analogous procedure to that described for *E,E*-126 and 127.

<sup>1</sup>H NMR  $\delta$ : 1.51 (quintet, 2 H), 1.60 (d,  $J$  = 7 Hz, 6 H), 2.23 (t, 4 H), 5.21 (m, 2 H); <sup>13</sup>C NMR (CCl<sub>4</sub>),  $\delta$ : 14.85, 23.79, 30.35, 111.13, 141.12. MS ( $m/z$  (I)): 122 (75), 107 (45), 105 (25), 94

(35), 93 (75), 79 (50), 77 (80), 67 (35), 65 (30), 55 (25), 41 (40).  
 UV (pentane):  $\lambda_{\max} (\epsilon) = 252 \text{ nm} (9550)$ . FTIR: 1011 (s),  
 1068 (s), 1101 (m), 1261 (s), 1561 (s), 1678 (m), 2855 (m), 2928  
 (s), 2961 (m).

*E,E*-1,2-bis(ethylidene)cyclobutane<sup>209, 210</sup> (*E,E*-124):

<sup>1</sup>H NMR  $\delta$ : 1.51 (d, 6 H,  $J = 7 \text{ Hz}$ ), 2.49 (br. s, 4 H), 5.43 (q, 2  
 H,  $J = 6.5 \text{ Hz}$ ). <sup>13</sup>C NMR,  $\delta$ : 13.21, 24.99, 111.47, 141.60.  
 MS (m/z (I)): 108 (45), 93 (86), 91 (96), 79 (100), 77 (83), 66  
 (16), 65 (17), 53 (12), 51 (39), 39 (51), 27 (41). HRMS : found:  
 108.0925000, calculated: UV (pentane):  $\lambda_{\max} (\epsilon) = 252 \text{ nm}$   
 (9900) shoulders at 262 and 240 nm. CG/FTIR: 1011 (s), 1068  
 (s), 1314 (w), 1416 (w), 1561 (s), 1578 (m), 2855 (m), 2929 (m),  
 2928 (m), 2961 (m).

Preparation of (*E,Z*) and (*Z,Z*)-1,2-bis(ethylidene)cycloalkanes and bicyclic  
 cyclobutenes:

Preparative direct irradiation of deoxygenated 1 mol/dm<sup>3</sup> pentane solutions  
 (45.0 mL) of (*E,E*)-1,2-bis(ethylidene)cycloalkane dienes with 253.7 nm light gave the  
 respective (*E,Z*) and (*Z,Z*) diene isomers as well as the *cis*- and *trans*- cyclobutenes. The  
 mixtures were photolyzed until their photostationary state ratios were achieved (35:65,  
 40:60, 45:55 for the (*E,Z*):(*E,E*) isomers of the seven, six, and five member ring dienes  
 respectively). The mixtures of dienes and cyclobutenes (from the five, six and seven  
 member ring diene precursors) were purified by alumina column chromatography



(solvent of elution: hexanes). Further purification was achieved by preparative gas-chromatography (column (f)). The large scale preparative photolysis is depicted in equation 4.2.1. Their spectroscopic characterizations follow:

*E,Z-1,2-bis(ethylidene)cycloheptane (E,Z-127):*

$^1\text{H}$  NMR  $\delta$ : 1.51 (b s, 6 H), 1.59 (d,  $J = 7$  Hz, 3H), 1.63 (d,  $J = 7$  Hz), 2.16-2.22 (m, 4 H), 5.22 (sextet,  $J = 8$  Hz, 2 H);  $^{13}\text{C}$  NMR,  $\delta$ : 14.04, 14.95, 27.42, 29.46, 29.52, 29.68, 38.00, 117.38, 121.33, 140.27, 145.31. MS ( $m/z$  (I)): 150 (56), 135 (18), 121 (43), 107 (39), 105 (21), 93 (97), 91 (69), 81 (28), 79 (100), 77 (60), 69 (3), 67 (41), 55 (17), 53 (29), 39 (54), 27 (30). UV (pentane):  $\lambda_{\text{max}}$  ( $\epsilon$ ) = 219 nm (8990). GC/FTIR: 798 (w), 822 (w), 957 (w), 1350 (w), 1384 (w), 1457 (m), 2864 (m), 2681 (w), 2931 (s), 2968 (m). HRMS: calc. for  $\text{C}_{11}\text{H}_{18}$ , 150.14085066; found, 150.1418000.

*E,Z-1,2-bis(ethylidene)cyclohexane<sup>67</sup> (E,Z-126):*

$^1\text{H}$  NMR  $\delta$ : 1.60 (d, 3 H,  $J = 6.8$  Hz), 1.60 (m, 4 H), 1.67 (d, 3 H,  $J = 6.8$  Hz), 2.10 (m, 2 H), 2.74 (m, 2 H), 5.12 (complex m, 2 H).  $^{13}\text{C}$  NMR ( $\text{CCl}_4$ ),  $\delta$ : 12.69, 14.11, 27.19, 27.94, 28.66, 37.89, 116.48, 118.85, 137.39, 142.16. MS ( $m/z$  (I)): 136 (30), 121 (15), 107 (45), 93 (50), 91 (75), 79 (100), 77 (50), 67 (25), 65 (27), 53 (16), 51 (16), 41 (21), 39 (43). IR (neat): 807 (m),

837 (s), 907 (m), 993 (m), 1238 (w), 1375 (w), 1442 (m), 2860 (s), 2935 (s), 3035 (w).

*E,Z-1,2-bis(ethylidene)cyclopentane*<sup>208</sup> (E,Z-125):

<sup>1</sup>H NMR  $\delta$ : 1.61 (quintet, J = 7 Hz, 2 H), 1.74 (d, J = 7 Hz, 3 H), 1.79 (d, J = 7 Hz, 3 H), 2.35 (complex m, 4 H), 5.48 (m, 1 H), 5.77 (m, 1 H). <sup>13</sup>C NMR,  $\delta$ : 15.10, 15.41, 23.78, 31.09, 36.42, 116.06, 120.32, 141.10. UV (pentane):  $\lambda_{\max}$  ( $\epsilon$ ) = 249 nm (9930).

*E,Z-1,2-bis(ethylidene)cyclobutane*<sup>210</sup> (E,Z-124):

<sup>1</sup>H NMR  $\delta$ : 1.61 (d, J = 7 Hz, 3 H), 1.72 (d, J = 7 Hz, 3 H), 2.48 (br s, 4 H), 5.11 (q with fine structure, J = 7.5 Hz, 1 H), 5.57 (q with fine structure, J = 7.5 Hz, 1 H). <sup>13</sup>C NMR: 13.94, 14.60, 24.98, 26.42, 116.07, 117.29, 140.22, 142.47. MS (m/z (I)): 108 (33), 93 (81), 91 (89), 79 (100), 77 (97), 53 (31), 51 (49), 39 (76), 27 (51). UV (pentane):  $\lambda_{\max}$  ( $\epsilon$ ) = 250 nm (10550), 241 nm sh, 270 nm sh. GC/FTIR: 1015 (s), 1097 (s), 1261 (s), 1382 (s), 1470 (s), 2855 (m), 2929 (m), 2962 (m).

*Z,Z-1,2-bis(ethylidene)cyclobutane*<sup>210</sup> (Z,Z-124):

<sup>1</sup>H NMR  $\delta$ : 1.77 (d, J = 7 Hz, 3 H), 2.41 (br s, 4 H), 5.06 (q, J = 7 Hz, 2 H). MS (m/z (I)): 108 (44), 93 (79), 91 (84), 79 (100),

77 (95), 65 (41), 53 (27), 51 (42), 39 (67), 27 (46). UV (pentane):  $\lambda_{\max}$  ( $\epsilon$ ) = 250 nm (11200). GC/FTIR: 1015 (s), 1097 (s), 1261 (s), 1412 (w), 1448 (w), 1602 (m), 2866 (m), 2928 (m), 2963 (m).

Long term photolysis of the irradiated 1 mol/dm<sup>3</sup> deoxygenated pentane solutions of the *E,E* and *E,Z* diene isomers of *1,2-bis(ethylidene)cycloalkanes* (cycloheptane, cyclohexane and cyclopentane) with 253.7 nm light source afforded the respective ring-closed *cis*- and *trans*- bicyclic cyclobutenes. Purification consisted of alumina column chromatography (hexanes as solvent of elution). Further purification was achieved by semi-preparative gas chromatography (column (f)). Their spectroscopic characterizations follow:

*Cis-8,9-dimethyl-bicyclo[5.2.0]non-1(7)-ene (cis-130):*

<sup>1</sup>H NMR (CD<sub>2</sub>Cl<sub>2</sub>)  $\delta$ : 0.93 (d, J = 7 Hz, 6 H), 1.51 (complex. m, 4 H), 1.67 (complex. m, 2 H), 1.92 (complex. m, 2 H), 2.05 (complex. m, 2 H), 2.58 (b q, 2 H); <sup>13</sup>C NMR,  $\delta$ : 13.11, 28.31, 29.04, 29.67, 38.35, 145.12. MS (m/z (I)): 150 (27), 135 (16), 121 (34), 107 (35), 105 (18), 93 (90), 91 (69), 81 (51), 79 (100), 77 (61), 67 (51), 63 (9), 55 (23), 53 (32), 39 (63), 27 (36). HRMS: calc. for C<sub>11</sub>H<sub>18</sub>, 150.14085066; found, 150.1405000. UV (pentane):  $\lambda_{\max}$  ( $\epsilon$ ) = 199 nm (9050). GC/FTIR: 913 (m), 993 (w), 1452 (m), 1641 (w), 2866 (m), 2932 (s), 2971 (w), 3087 (w).

*Trans-8,9-dimethyl-bicyclo[5.2.0]non-1(7)-ene (trans-130):*

$^1\text{H}$  NMR ( $\text{CCl}_4$ )  $\delta$ : 0.97 (d,  $J = 7$  Hz, 6 H), 1.52 (complex m, 6 H), 1.88 (complex m, 6 H);  $^{13}\text{C}$  NMR, ( $\text{CCl}_4$ )  $\delta$ : 17.44, 28.88, 29.41, 30.02, 44.45, 143.99. GC/MS ( $m/z$  (I)): 150 (33), 135 (17), 121 (39), 107 (42), 105 (22), 93 (99), 91 (77), 81 (25), 79 (100), 77 (61), 67 (39), 65 (25), 55 (16), 53 (25), 39 (52), 27 (29). HRMS: calc. for  $\text{C}_{11}\text{H}_{18}$ , 150.14085066; found, 150.1410000. UV (pentane):  $\lambda_{\text{max}}$  ( $\epsilon$ ) = 191 nm (8650). GC/FTIR: 815 (w), 831 (w), 977 (w), 1378 (w), 1459 (m), 2866 (m), 2920 (s), 2966 (m).

*Cis-7,8-dimethyl-bicyclo[4.2.0]oct-1(6)-ene<sup>67</sup> (cis-37):*

$^1\text{H}$  NMR  $\delta$ : 0.94 (d, 6 H,  $J = 6.7$  Hz), 1.62 (m, 4 H), 1.75 (d, 2 H), 1.86 (d, 2 H), 2.78 (complex q, 2 H).  $^{13}\text{C}$  NMR ( $\text{CCl}_4$ ),  $\delta$ : 13.19, 22.34, 22.92, 40.48, 144.74. MS ( $m/z$  (I)): 136 (22), 121 (17), 107 (40), 105 (13), 93 (51), 91 (59), 79 (100), 77 (46), 67 (21), 65 (18), 53 (20), 51 (19). 41 (25), 39 (43). IR (neat): 805 (w), 815 (w), 885 (w), 928 (w), 968 (w), 1017 (w), 1125 (m), 1233 (m), 1363 (m), 1315 (deg., m), 1375 (m), 1438 (s), 1448 (sh., s), 1465 (m), 2905 (br, s).

*Trans-7,8-dimethyl-bicyclo[4.2.0]oct-1(6)-ene<sup>67</sup> (trans-37):*

$^1\text{H}$  NMR  $\delta$ : 1.08 (d, 6 H,  $J = 6.8$  Hz), 1.60 (m, 2 H), 1.66 (m, 2 H), 1.77 (d, 2 H,  $J = 16$  Hz), 1.85 (d, 2 H,  $J = 16$  Hz), 2.19 (complex q, 2 H,  $J = 6.5$  Hz).  $^{13}\text{C}$  NMR ( $\text{CCl}_4$ ),  $\delta$ : 16.94, 22.44, 23.04, 46.42, 143.69. GC/MS ( $m/z$  (I)): 136 (23), 121 (19), 107 (48), 105 (17), 93 (57), 91 (46), 79 (100), 77 (48), 67 (24), 65 (18), 53 (25), 51 (20), 41 (31), 39 (50). IR (near): 967 (m), 1043 (w), 1123 (w), 1223 (m), 1260 (m), 1291 (m), 1327 (m), 1438 (m), 1443 (s), 2840 (s), 2917 (br. s).

*Cis-6,7-dimethyl-bicyclo[3.2.0]hept-1(5)-ene*<sup>211</sup> (*cis-129*):

$^{13}\text{C}$  NMR,  $\delta$ : 14.11, 26.32, 29.81, 38.67, 153.34. GC/MS ( $m/z$  (I)): 122 (17), 107 (21), 93 (55), 91 (38), 79 (45), 77 (35), 65 (31), 51 (34), 39 (51). UV (pentane):  $\lambda_{\text{max}}$  ( $\epsilon$ ) = 190 (9800).

*Trans-6,7-dimethyl-bicyclo[3.2.0]hept-1(5)-ene*<sup>211</sup> (*trans-129*):

$^{13}\text{C}$  NMR,  $\delta$ : 17.50, 26.20, 29.75, 44.62, 152.60. GC/MS ( $m/z$  (I)): 122 (25), 107 (20), 93 (61), 91 (43), 79 (44), 77 (37), 65 (33), 51 (41), 39 (45). UV (pentane):  $\lambda_{\text{max}}$  ( $\epsilon$ ) = 188 (7260)

Preparation of *cis*- and *trans*- 2,3-dimethyl bicyclo[2.2.0]hex-1(4)-ene (128):

In a 250 mL two-necked flask previously flame-dried, (-)-2,3-butanediol di-*p*-tosylate<sup>199</sup> (19.93 g, 0.05 moles) in tetrahydrofuran (50.0 mL) was placed. The system was cooled to -100 °C, evacuated and refilled with a N<sub>2</sub> atmosphere. This process was repeated three times after which (trimethylsilyl)lithium acetylide<sup>†</sup> (0.1 mol) in tetrahydrofuran was added over a period of one hour by means of a double-end needle (the reservoir was maintained at -78°C) while the solution was stirred continuously. The temperature of the system was maintained at -100 °C throughout the addition of the acetylide. The solution was left stirring for an additional hour at -100 °C, and then the temperature was gradually allowed to reach ambient values. The reaction mixture was quenched with ice water (20 g), and extracted three times with pentane (10.0 mL). The pentane layers were dried with sodium sulfate and evaporated. The residue that was left was chromatographed over alumina (hexanes 100% as solvent of elution, transparent fractions collected). The mass obtained was 4.75 g (0.019 mol, 38 %). The mass spectrum of the compound was consistent with 3,4-dimethyl-1,6-bis(trimethylsilyl)-1,5-hexadiyne. GC/MS (m/z (I)): 235 (13), 207 (3), 162 (75), 161 (43), 156 (2), 147 (22), 138 (13), 110 (14), 96 (14), 83 (12), 81 (11), 73 (100), 59 (12), 43 (11).

<sup>†</sup> Prepared from (trimethylsilyl)acetylene (0.98 g, 0.68 mL, 0.1 mol) and *n*-butyllithium (55 mL, 0.1 mol) at -78°C.

In a 50.0 mL two-necked flask previously flame-dried, zirconocene dichloride (2.92 g, 0.01 mol) in tetrahydrofuran (15.0 mL) was introduced. The system was evacuated and blanketed with a N<sub>2</sub> atmosphere, and stirred by means of a magnetic stirrer. The temperature was lowered to -78 °C when *n*-butyllithium (0.02 mol) in tetrahydrofuran (5.0 mL) was added over a period of one hour by means of a dropping

funnel attached to the flask, while the temperature was maintained at  $-78\text{ }^{\circ}\text{C}$  throughout the addition. The system was left stirring for an additional hour at  $-78\text{ }^{\circ}\text{C}$  and 3,4-dimethyl-1,6-bis(trimethylsilyl)-1,5-hexadiyne (2.50 g, 0.01 mol) in tetrahydrofuran (5 mL) was added to the reaction mixture by means of a canula. After the addition was completed, the solution was kept for an additional three hours at  $-78\text{ }^{\circ}\text{C}$ , and then warmed up to room temperature. The mixture was quenched with ice water (20 g), and extracted three times with pentane (10.0 mL). The pentane layers were evaporated, yielding 1.74 g (69 %) of a yellowish residue. A portion of this material (0.75 g, 0.0030 mol) was dissolved in dichloromethane (10.0 mL) and placed in a 25.0 mL round bottom flask. Trifluoroacetic<sup>204</sup> acid (5 mL) was added, and the mixture was then stirred at room temperature overnight. The resulting brown mixture was quenched with water (10.0 mL) and extracted three times with pentane (5.0 mL each). The organic layers were dried over sodium sulfate, and the solvents distilled off until a volume of 3.0 mL was remained. The residue was bulb-to-bulb distilled employing two liquid nitrogen traps; a mass of 0.29g (90%) of a colorless liquid was obtained. GC/MS analysis indicated two products of the same molecular weight in more than 95% purity. Further purification consisted of semipreparative gas chromatography using  $\alpha$ -alumina (g). These compounds were identified on the basis of their  $^1\text{H}$  NMR spectra and GC/MS analysis and characterized as *cis*-3,4-dimethyl-1,2-(bis)methylenecyclobutane and *trans*-3,4-dimethyl-1,2-(bis)methylenecyclobutane according to their precedent in the literature<sup>210</sup>.

The above mixture of *cis* and *trans* cyclobutanes was taken up in pentane (5.0 mL), deoxygenated with a stream of  $\text{N}_2$  and photolyzed with 253.7 nm light until only 30 % of the starting materials were left, as indicated by gas chromatographic analyses. Two cyclobutene isomers were produced upon this photolysis. The mixture was

maintained at liquid nitrogen temperature until further purification continued. For their final purification, column (e) was used. Their spectroscopic characterizations follow:

*Cis-2,3-dimethylbicyclo[2.2.0]-hex-1(4)ene (cis-128):*

$^1\text{H NMR } \delta$ : 1.60 (d, 6 H,  $J = 7.5$  Hz), 1.76 (t, 4 H,  $J = 2.4$  Hz), 2.21 (q, 2 H,  $J = 6.7$  Hz). UV (pentane):  $\lambda_{\text{max}} (\epsilon) = 188$  (11500). GC/FTIR: 1101 (m), 1261 (m), 1353 (w), 1381 (w), 1450 (w), 2855 (m), 2872 (m), 2929 (s), 2962 (s). GC/MS ( $m/z$  (I)): 108 (39), 93 (78), 91 (83), 79 (100), 77 (94), 66 (24), 65 (29), 53 (29), 51 (41), 39 (63), 27 (41).

*Trans-2,3-dimethylbicyclo[2.2.0]-hex-1(4)ene (trans-128):*

$^1\text{H NMR } \delta$ : 1.60 (dd, 6 H,  $J = 6.7$  Hz,  $J = 1.6$  Hz), 1.76 (t, 4 H,  $J = 2.5$  Hz), 2.15 (m, 2 H), 2.20 (br. q, 2 H). UV (pentane):  $\lambda_{\text{max}} (\epsilon) = 188$  (10800). GC/FTIR: 1261 (m), 1451 (w), 2856 (w), 2872 (w), 2929 (s), 2962 (s). GC/MS ( $m/z$  (I)): 108 (40), 93 (96), 91 (96), 79 (95), 77 (100), 66 (23), 65 (27), 53 (33), 1 (44), 39 (64), 27 (42).

Compounds *cis*- and *trans*- 128 are unstable at room temperature due to rapid polymerization. Thus, it was estimated that the half life (time required for the original concentration of the analyte to be reduced to  $1/e$  of the original concentration) of 128 was approximately 72 hrs at  $20^\circ\text{C}$ . The value of this half life was significantly reduced



in the presence of impurities and dienes. The samples were kept at liquid nitrogen temperature until the experiment took place. The photolyses of 128 were also carried out at  $-78^{\circ}\text{C}$ , in order to check for possible sample-decomposition, or thermal isomerization to dienes during photolysis. The results of the experiments confirmed that no such reactions are detectable if photolysis times are kept under one hour (ratio of dienes from cyclobutene ring opening remain constant at both room temperature and  $-78^{\circ}\text{C}$ ).

Preparation of 2,3-*E,E* and *E,Z*- bisethylidene-bicyclo[2.2.1]heptanes.

*Bicyclo[2.2.1]heptane-2,3-dione*<sup>212</sup> : In a 150.0 mL two-necked flask was placed norcanfor (10.0 g, 0.091 mol), toluene (50.0 mL) and selenium dioxide<sup>199</sup> (7.90 g, 0.1 mol). A condenser was attached to one of the glass joints of the flask and the mixture was heated to reflux for two hours with vigorous stirring, after which the solution turned dark red. Increasing quantities of selenium metal precipitating out of the solution gave the mixture a black color. The selenium metal was filtered off, and the mixture was continued to reflux for an additional hour. The reaction was followed by thin layer chromatography (silica plate, hexane:ethyl acetate 75:25 as developing solvent) and allowed to proceed to 70 % conversion of the starting material. The work-up consisted in boiling the reaction mixture in 95 % ethanol (to destroy the excess of selenium dioxide) and extraction of the toluene-ethanol solution with hydrochloric acid 20% (to remove organic selenium complexes) and then washed three times with ethyl ether. The ether and ethanol solvents were removed by rotary evaporation and toluene was distilled off at atmospheric pressure. The dark orange residue that was left, was

redistilled under very reduced pressure (133°C, 0.05 torr). The distillate that solidified immediately after collection amounted to 9.1 g (0.073 mol, 81%) of a bright yellow solid. An alternate purification procedure consisted in recrystallization of the dark orange residue (obtained after solvent evaporation) from methanol. This compound was identified as *bicyclo[2.2.1]heptane-2,3-dione* on the basis of the following spectroscopic data:

$^1\text{H}$  NMR  $\delta$ : 1.76 (cplx. m, 2 H), 2.01 (t, 9 Hz, 1 H), 2.04 (t, 9 Hz, 1 H), 2.08 (cplx. m, 2 H), 3.04 (cplx. m, 2 H).  $^{13}\text{C}$  NMR,  $\delta$ : 23.78, 31.64, 48.19, 202.05. GC/MS ( $m/z$  (I)): 124 (21), 96 (24), 68 (81), 55 (100), 39 (54), 27 (26). Exact mass: calc for  $\text{C}_7\text{H}_8\text{O}_2$ , 124.052429; found, 124.0522000. IR: 3004 (w), 2970 (m), 2893 (w), 1771 (s), 1459 (w), 1198 (w), 1076 (w), 980 (w), 936 (w), 894 (w), 737 (w).

Into a 500 mL three necked-flask<sup>213</sup> was placed sodium hydride (2.5 g, 0.101 mol), and the solid was washed 3 times with dry pentane. The flask was evacuated and blanketed 3 times with dry nitrogen. Anhydrous dimethyl sulfoxide (50 mL, previously dried over potassium hydroxide and distilled under reduced pressure) was introduced by syringe, and the resulting mixture (white color) was heated at 80°C in an oil bath with stirring for 1.5 hour until hydrogen evolution ceased, which resulted in a green limpid solution. Following cooling to room temperature, a solution of ethyltriphenylphosphonium iodide<sup>§</sup>, (42.2g, 0.101 mol) in warm dimethyl sulfoxide (250 mL) was added. The blood-red solution that resulted was stirred for 15 min before *bicyclo[2.2.1]heptane-2,3-dione* (5 g, 0.0403 mol) dissolved in 50 mL of the same solvent was slowly introduced (warming) by

means of a double-end needle. When addition was complete, the mixture was heated at 60 °C for 20 h and poured into 300 mL of ice water. The product was extracted into petroleum ether (3 x 150 mL), and the combined layers were washed with 50% aqueous dimethylsulfoxide (100 mL) and brine (50 mL). After the solution was dried, the solvent was slowly removed by distillation at atmospheric pressure and the residue was chromatographed by alumina column chromatography (solvent of elution: hexanes 100%), and all the transparent fractions were collected. After solvent evaporation, a colorless liquid was recovered (3.22 g, 0.0218 mol). A GC/MS analysis indicated the presence of a mixture of two isomers of *2,3-bisethylidene-bicyclo[2.2.1]heptane* in over 80% yield. The major component of the mixture of the two isomers was isolated by semipreparative gas chromatography, employing column (f). This compound was identified as *E,E-2,3-bisethylidene-bicyclo[2.2.1]heptane*<sup>213</sup> (**131**) on the basis of the following spectroscopic data:

<sup>1</sup>H NMR δ: 1.24–1.30 (m, 6 H), 1.66 (d, J = 7.5 Hz, 6 H), 3.05 (m, 2 H), 5.48 (q, J = 6.8 Hz, 2 H). <sup>13</sup>C NMR: 14.1, 28.10, 39.10, 40.04, 107.33, 145.08. GC/MS (m/z (I)): 148 (23), 120 (31), 119 (26), 105 (100), 91 (48), 77 (24), 65 (12), 39 (18), 27 (9). IR: 3041 (w), 2986 (s), 2966 (s), 2929 (s), 2877 (s), 1681 (w), 1450 (m), 1262 (w), 1121 (w), 982 (w), 807 (m). UV (pentane): λ<sub>max</sub> (ε) = 253 nm (11200).

To enrich the mixture of isomers (obtained from the synthesis) in the *E,Z* component, compound *E,E-131* (1.5 g) dissolved in pentane (10.0 mL) was photolyzed (254 nm light, 12 lamps, 3 h) in a quartz container after deoxygenation with a stream of

nitrogen. The photolysis was followed up by gas chromatography and interrupted when the mixture reached its photostationary state (50% mixture of the *E,E* and *E,Z* isomers, and minor amounts of other isomers). The second major component in the mixture (with shorter retention time than the *E,E* isomer) was separated by semipreparative gas chromatography employing column (f) and identified as the *E,Z*-2,3-bisethylidene-bicyclo[2.2.1]heptane isomer according to the following spectroscopic data:

$^1\text{H}$  NMR  $\delta$ : 1.30 (cplx. m, 6 H), 1.73 (d,  $J = 7$  Hz, 3 H), 1.75 (d,  $J = 7$  Hz, 3 H), 3.10 (m, 2H), 5.37 (q,  $J = 7.6$  Hz, 1 H), 5.60 (q,  $J = 7.6$  Hz, 1 H).  $^{13}\text{C}$  NMR: 14.89, 14.91, 26.91, 28.13, 38.06, 39.71, 47.38, 112.64, 145.20, 145.96. GC/MS ( $m/z$  (I)): 148 (21), 133 (5), 120 (31), 105 (100), 91 (51), 77 (23) 65 (10), 51 (8), 39 (19), 27 (8). Exact mass: calc. for  $\text{C}_{11}\text{H}_{16}$ , 148.1252006 ;found, 148.1245000. IR: 3069 (w), 2969 (s), 2931 (s), 2878 (s), 1454 (m), 1379 (w), 1261 (w), 1119 (w), 1023 (w), 826 (m). UV (pentane):  $\lambda_{\text{max}}$  ( $\epsilon$ ) = 245 (11900).

§ Prepared from ethyl iodide and triphenylphosphine in scrupulously dried benzene.

#### 6.3.4 Photolyses and Quantum Yield Determinations

Synthetic photolyses employed a Rayonet photochemical chemical reactor fitted with twelve RPR-254 (253.7 nm) lamps and a merry-go-round apparatus.

The cyclobutenes 128, 129, 37, and 130 were photolyzed in deoxygenated  $0.02 \text{ mol dm}^{-3}$  pentane solutions with a 16-W Zn resonance lamp as the light source (214

nm) using an Acton Research Corp. filter (214-B-ID) with a peak wavelength of 2130 Å and a bandwidth of 320 Å to cut off spurious radiation. Ulterior determinations of quantum yields in the absence of such<sup>a</sup> filter did not introduce differences in the results. The unfocused pulses of an ArF excimer laser (193 nm, ca 15 ns, 20 mJ, 0.5 Hz repetition rate) were also employed in the photolyses of cyclobutenes 129, 37, and 130.

For absolute quantum yield determinations utilizing uranyl oxalate photolysis the light source was the Zn resonance lamp. Quartz cells of 3.0 mL were employed. A detailed procedure described by D.F. Eaton<sup>113</sup> was followed. A quantum yield of  $0.500 \pm 0.021$  was used for the actinometer. The conversion of the actinometer was monitored by a spectrophotometric technique as described in Section 6.2.5. The absorbance of the unirradiated blank was lower than 0.10 in all cases. A radiant power of  $ca. 1.0 \times 10^{-8}$  einstein was achieved after 12 hour photolysis (employing the low pass filter) as determined by the actinometer. The conversion of the cyclobutene was determined by gas chromatographic techniques. In determining quantum yields, four single point averageable determinations were employed.

Quantum yields for ring opening of cyclobutenes 129, 37, and 130 were also determined by bicyclo[4.2.0]octene actinometry with 193 nm laser pulse excitation. The actinometric reaction consists in the photochemical ring opening of bicyclooctene to *cis,cis*- and *cis,trans*- cycloocta-1,3-diene. The quantum yield for production of *cis,cis*-cycloocta-1,3-diene is 0.12. Both actinometer ( $2.70 \times 10^{-2}$  mol dm<sup>-3</sup>) and sample ( $ca. 6.5 \times 10^{-3}$  mol dm<sup>-3</sup>) pentane solutions were contained in identical cylindrical suprasil quartz cells that were placed in a cell holder in front of the laser beam and photolyzed separately. The conversions of the actinometer and the sample were followed by gas chromatographic techniques. Quantum yields were determined by following the formation of *cis,cis*-cycloocta-1,3-diene from the actinometer and of dienes 124-127

from the cyclobutenes by vpc analyses between 0 and 5 % conversion. The solutions contained n-octane ( $1.1 \times 10^{-4} \text{ mol dm}^{-3}$ ) and n-decane ( $1.0 \times 10^{-3} \text{ mol dm}^{-3}$ ) as internal standards for quantitation of products. The FID detector responses towards the dienes 124-127 were calibrated relative to the internal standards by construction of working curves.

## REFERENCES

- 1 R.B Woodward, R. Hoffmann *J.Am.Chem.Soc.* **1965**, *87*, 395.
- 2 R.B Woodward, R. Hoffmann *Acc.Chem.Res.* **1968**, *17*, 1.
- 3 R.B Woodward, R. Hoffmann *Angew.Chem.Intl.Ed., Engl.* **1969**, *8*, 781.
- 4 H.C. Longuet-Higgins, E.W. Abrahamson *J.Am.Chem.Soc.*, **1965**, *87*, 2045.
- 5 a) E. Marvel, "Thermal Electrocyclic Reactions", Academic Press, New York, **1980**, Chapter 5. b) P.J. Darcy, R.J. Hart, H.G. Heller *J.Chem.Soc. Perkin Trans. I*, **1978**, 571.
- 6 W.G. Dauben, N. Fonken *J.Am.Chem.Soc.*, **1959**, *81*, 4060.
- 7 L. Chapman *J.Am.Chem.Soc.*, **1962**, *84*, 1220.
- 8 W.G. Dauben *J.Org.Chem.*, **1962**, *27*, 1910.
- 9 W.G. Dauben *J.Am.Chem.Soc.*, **1966**, *88*, 2742.
- 10 R.B. Woodward, R. Hoffmann *J.Am.Chem.Soc.*, **1965**, *87*, 395, 4388.
- 11 W. Adam, K.N. Shumate, P.N. Neuman, G.J. Fonken *Chem.Ber.*, **1964**, *97*, 1811.
- 12 E. Havinga, J.L.M.A. Schlatman *Tetrahedron*, **1961**, *16*, 146.
- 13 E. Havinga, R.J. de Kock, M.P. Rappoldt *Tetrahedron*, **1960**, 276.

- 14 Th. A.M. Van der Lugt, L.J. Oosterhoff *J.Chem.Soc. Chem.Comm.*, **1968**, 1235.
- 15 Th. A.M. Van der Lugt, L.J. Oosterhoff *J.Am.Chem.Soc.*, **1969**, *91*, 6042.  
Y. Osamura, M. Kikuchi *Bull.Soc.Chem.Jpn.*, **1974**, *47(6)*, 1551.
- 16 G. Orlandi, F. Zerbetto *Chem.Phys.*, **1986**, *108*, 127. F. Zerbetto, M.S. Zgierski,  
F. Negri, G. Orlandi *J.Chem.Phys.*, **1987**, *87*, 2505.
- 17 W. Gerhartz, R.D. Poshusta, J. Michl *J.Am.Chem.Soc.*, **1977**, *99*, 4263.
- 18 K.Morihashi, O. Kikuchi *Theo.Chim.Acta*, **1985**, *67*, 293.
- 19 F. Zerbetto, M. Zgierski *J.Chem.Phys.*, **1990**, *93*, 1235.
- 20 M. Olivucci, I.N. Ragazos, F. Bernardi, M.A. Robb *J.Am.Chem.Soc.*, **1983**, *115*,  
3710.
- 21 M.O. Trulson, R.A. Mathies *J.Phys.Chem.*, **1990**, *94*, 5741. G. Strahan, B.  
Hudson *J.Chem.Phys.*, **1993**, *99(8)*, 5780.
- 22 P. Reid, S. Doig, S. Wickham, R.A. Mathies *J.Am.Chem.Soc.*, **1993**, *115*, 4754.
- 23 M.O. Trulson, R.A. Mathies *J.Am.Chem.Soc.*, **1987**, *109*, 586.
- 24 M.O. Trulson, R.A. Mathies *J.Chem.Phys.*, **1989**, *90*, 4274.
- 25 B. Hudson, B. Kohler *Annu. Rev. Phys. Chem.* **1974**, *25*, 437.
- 26 J. Ackermiri, B.E. Kohler *J.Am.Chem.Soc.*, **1984**, *106*, 3681.



- 27 R. A. Mathies, M. K. Lawless *J.Am.Chem.Soc.*, **1994**, *116*, 1593.
- 28 C.D. DeBoer, R.H. Schlessinger *J.Am.Chem.Soc.*, **1968**, *90*, 803.
- 29 G. Kaup, M. Stark *Chem.Ber.*, **1978**, *111*, 3608.
- 30 H. Sakuragi *Chem.Lett.*, **1974**, 29.
- 31 S. Kawamura, G. Schuster *Tetrahedron*, **1986**, *42*, 6195.
- 32 M. Finke, G. Quinkert, K. Opitz, W.W. Wiersdorff *J.Liebigs. Ann.Chem.*, **1966**, *44*, 693
- 33 M. Finke, G. Quinkert, K. Opitz, W.W. Wiersdorff, F. von der Haar *Chem.Ber.*, **1968**, *101*, 2303.
- 34 M. Finke, G. Quinkert, W.W. Wiersdorff, J. Palmowski *Mol.Photochem.*, **1969**, *1*, 433
- 35 J. Michl *J.Am.Chem.Soc.*, **1970**, *92*, 4148.
- 36 J. Michl *Chem.Phys.Lett.*, **1976**, *39*, 57.
- 37 N.C. Yang *J.Am.Chem.Soc.*, **1974**, *96*, 2297.
- 38 R. Srinivasan *J.Am.Chem.Soc.*, **1966**, *88*, 3765.
- 39 R. Srinivasan *J.Am.Chem.Soc.*, **1969**, *91*, 7557.
- 40 J. Saltiel, L.S. Ng Lin *J.Am.Chem.Soc.*, **1969**, *91*, 5404.

- 41 W. Adam, T. Oppenlander, G. Zang *J.Am.Chem.Soc.*, **1985**, *107*, 3921.
- 42 B. Clark, W.J. Leigh *J.Am.Chem.Soc.*, **1987**, *109*, 6086. W.G. Dauben *J.Org.Chem.*, **1988**, *53*, 600. N. Turro, "Modern Molecular Photochemistry", New York, **1985**, Chapter 5.
- 43 K. Zheng, W.J. Leigh *J.Am.Chem.Soc.*, **1991**, *113*, 2163.
- 44 Y. Inoue *Chem.Lett.*, **1983**, 1495
- 45 W.J. Leigh *Can.J.Chem.*, **1988**, *66*, 1571.
- 46 W.J. Leigh *Can.J.Chem.*, **1990**, *68*, 1988.
- 47 A. Merer, R. Mulliken *Chem.Review*, **1969**, *69*, 639.
- 48 R. Mulliken *J.Chem.Phys.*, **1977**, *66*, 2448.
- 49 M.B. Robin "Higher Excited States of Polyatomic Molecules" Academic Press, New York, **1975**, Vol. II.
- 50 N.L. Bauld, D.J. Bellville, R. Pabon, R. Chelsky, G. Green *J.Am.Chem.Soc.*, **1983**, *105*, 2378. C. Dass, M.L. Gross *J.Am.Chem.Soc.*, **1983**, *105*, 5724.
- 51 Kawamura *Tetrahedron*, **1986**, *42*, 6195.
- 52 T. Miyashi *J.Am.Chem.Soc.*, **1987**, *109*, 5270.
- 53 Aebischer, Bally, Roth *J.Am.Chem.Soc.*, **1989**, *111*, 7909.

- 54 P.J. Kropp *J.Org.Photochem.*, **1979**, *4*, 1.
- 55 W. Adam *Angew.Chem.Intl.Ed., Engl.* **1986**, *25*, 661.
- 56 W.J. Leigh *Acc.Chem.Res.*, **1987**, *20*, 107.
- 57 J. Moss "Carbenes", John Wiley and Sons, NEw York, **1973**, *Vol. 1*.
- 58 W.J. Leigh *Can.J.Chem.*, **1990**, *68*, 1961.
- 59 W.J. Leigh, A. Hitchcock, N. Werstiuk, N. Nguyen, A. Wen *Can.J.Chem.*, **1990**, *68I*, 1967, 1973.
- 60 W.J. Leigh *J.Am.Chem.Soc.*, **1991**, *113*, 4993.
- 61 M. Olivucci, M. Robb, F. Bernardi *J.Am.Chem.Soc.*, **1992**, *114*, 2752.
- 62 F. Bernardi, M. Olivucci, M. Robb *Israel J.Chem.*, **1993**, *33*, 265.
- 63 Brady Clark's Ph.D. Thesis, **1987**, McMaster University, Hamilton, Ontario, Canada.
- 64 J. Saltiel, L. Metts *J.Am.Chem.Soc.*, **1970**, *92*, 3227.
- 65 J. Saltiel, J. Charlton "Rearrangements in Ground and Excited States", *Vol. 3* Academic Press. J. Saltiel, S. D'Agostino *Org.Photochem.*, **1973**, *3*, 1.
- 66 J.L. Wooley *Chem.Phys.*, **1946**, *14*, 67.
- 67 W.J. Leigh, K. Zheng *J.Am.Chem.Soc.*, **1991**, *113*, 4019.

- 68 R. Srinivasan *J.Am.Chem.Soc.*, 1962, 84, 4141.
- 69 M. Stephenson, M. Brauman *Acc.Chem.Res.*, 1974, 7, 65.
- 70 R. Srinivasan *Adv.Photochem.*, 1966, 4, 113.
- 71 J. Baldry, J. Baltrop *Chem.Phys.Lett.*, 1977, 46, 430.
- 72 O.A. Mosher, W.M. Flicker, A. Kuppermann *Chem.Phys.Lett.*, 1973, 19, 322.
- 73 K. Knoop, J. Oosterhoff *Chem.Phys.Lett.*, 1973, 22, 247.
- 74 W.J. Leigh *Can.J.Chem.*, 1993, 71, 147.
- 75 G.J. Fonken "Organic Photochemistry", Vol. 1, Orville. L. Chapman and J. Saltiel ,  
Vol. 3.
- 76 Cundall *Progr.React.Kinet.*, 1964, 2, 165.
- 77 S. Peteanu, R.A. Mathies, P. Shank *J.Phys.Chem.*, 1993, 97, 12087.
- 78 S. Peteanu, R.A. Mathies, P. Shank *Proc.Natl.Acad.Sci. USA*, 1993, 90, 11762.
- 79 M. Squillacote, T. Semple *J.Am.Chem.Soc.*, 1990, 112, 5546.
- 80 P. Van der Linden, S. Boue *J.Chem.Soc.Chem.Comm.*, 1975, 932.
- 81 G.J. Fonken, W.J. Nebe *J.Am.Chem.Soc.*, 1969, 91, 1249.
- 82 W.G. Dauben, Kellog *J.Am.Chem.Soc.*, 1980, 102, 4456.

- 83 W.J. Leigh, K. Zheng, B. Clark *J.Org.Chem.*, **1991**, *56*, 1574.
- 84 Y. Inoue, S. Hagiwara, Y. Daino, T. Hakushi *J.Chem.Soc.Chem.Comm.*, **1985**, 1307.
- 85 K.M. Shumate, G.J. Fonken *J.Am.Chem.Soc.*, **1966**, *88*, 1073.
- 86 R.S.H. Liu *J.Am.Chem.Soc.*, **1967**, *89*, 112.
- 87 G.D. Bent, A. Rossi *J.Phys.Chem.*, **1991**, *95*, 7228.
- 88 R. Srinivasan *J.Am.Chem.Soc.*, **1968**, *90*, 4498.
- 89 R. Srinivasan *J.Am.Chem.Soc.*, **1963**, *85*, 4045.
- 90 W.G. Dauben, J.S. Ritscher *J.Am.Chem.Soc.*, **1970**, *92*, 2925.
- 91 D.A. Aue, R.N. Reynolds *J.Am.Chem.Soc.*, **1973**, *95*, 2027.
- 92 W.G. Dauben, J.A. Ross *J.Am.Chem.Soc.*, **1959**, *81*, 6221. W.G. Dauben *Tet.Lett.*, **1962**, 893.
- 93 K.J. Crowley *Tetrahedron*, **1965**, *21*, 1001.
- 94 M. Aoyagi, Y. Osamura *J.Am.Chem.Soc.*, **1989**, *111*, 470.
- 95 A.J.P. Devaquet, R.E. Townshend, W.J. Hehre *J.Am.Chem.Soc.*, **1976**, *98*, 4068.
- 96 I. Baraldi, M.C. Bruni, F. Momicchioli, J. Langlet, J.P. Maleiu *Chem.Phys.Lett.*, **1977**, *51*, 493.

- 97 D. Grimbert, G. Segal, A. Devaquet *J.Am.Chem.Soc.*, **1994**, *98*, 5597.
- 98 P. Reid, M.K. Lawless, S.S. Wickmham, R.A. Mathies *J.Phys.Chem.*, **1994**, *98*, 5597.
- 99 F. Zerbetto, M. Zgierski *J.Chem.Phys.*, **1990**, *93*, 1235.
- 100 M. Olivucci, F. Bernardi, S. Ottani, M. Robb *J.Am.Chem.Soc.*, **1994**, *116*, 2034.
- 101 M. Reguero, M. Olivucci, F. Bernardi, M. Robb *J.Am.Chem.Soc.*, **1994**, *116*, 2103.
- 102 M. Olivucci, F. Bernardi, P. Celani, I. Ragazos, M. Robb *J.Am.Chem.Soc.*, **1994**, *116*, 1077.
- 103 Manthe, Koppel *J.Chem.Phys.*, **1990**, *93*, 1658.
- 104 M. Olivucci, F. Bernardi, M. Robb *J.Am.Chem.Soc.*, **1993**, *115*, 3710
- 105 a) P.J. Kropp *Organic Photochem.*, **1979**, *4*, 1. b) J.F. Ireland, P.A.H. Wyatt *Adv.Phys.Org.Chem.*, **1976**, *12*, 131. c) S.C. Lahiri *J.Sci.Ind.Res.(India)*, **1979**, *38*, 492. d) M. Irie *J.Am.Chem.Soc.*, **1983**, *105*, 2078. e) M Gutman, E. Nachliel, E. Gerson, R Giniger, E. Pines *J.Am.Chem.Soc.*, **1983**, *105*, 2210.
- 106 P.J. Kropp *J.Am.Chem.Soc.*, **1973**, *95*, 7058.
- 107 F.L. Cozins, R.A. McClelland, S. Steenken *J.Am.Chem.Soc.*, **1993**, *115*, 5050.
- 108 K. Yates, R. Anderson *Can.J.Chem.*, **1988**, *66*, 2412.

- 109 K. Yates, S. Culshaw, P. Wan *J.Am.Chem.Soc.*, **1982**, *104*, 2509.
- 110 K. Yates, J. McEwen *J.Am.Chem.Soc.*, **1987**, *109*, 5800.
- 111 K. Ireland, J. Wyatt *Adv.Phys.Org.Chem.*, **1976**, *12*, 163.
- 112 K. Yates, P. Wan *Rev.Chem.Intermed.*, **1984**, *5*, 157.
- 113 D.F. Eaton, *Pure. Applied Chem.*, **1989**, *61*, 187.
- 114 C.G. Hatchard, C.A. Parker *Proc.Roy.Soc.(London)* **1956**, A235, 518.
- 115 C.A. Parker *Proc.Roy.Soc.(London)*, **1953**, A220, 104.
- 116 V. Ramamurthy, J.V. Caspar, D.F. Eaton, E. Kuo, D. Corbin *J.Am.Chem.Soc.*, **1992**, *114*, 3882.
- 117 M. Toth *Chem.Phys.*, **1980**, *46*, 437.
- 118 a) H.E. Zimmerman, K. Kamm, D. Werthermann *J.Am.Chem.Soc.*, **1975**, *97*, 3718. b) F. Wilkinson, J.T. Dubois *J.Chem.Phys.*, **1963**, *39*, 377. K. Sandros *Acta Chem.Scand.*, **1969**, *23*, 2815
- 119 a) T.H. Lowry, K.S. Richardson "Physical Organic Chemistry", 3<sup>rd</sup> edition. b) M.G. Steinmetz *Org.Photochem.*, **1993**. c) S.S. Hixon *J.Am.Chem.Soc.*, **1975**, *97*, 1981. d) P.J. Kropp *J.Am.Che.Soc.* **1973**, *95*, 4611. R.J. Duguid, H. Morrison *J.Am.Chem.Soc.*, **1991**, *113*, 3519.
- 120 J.F. Ireland, P.A.H. Wyatt *Adv.Phys.Org.Chem.*, **1976**, *12*, 131.

- 121 T. Forster, *Z.Elektrochem.*, 1950, 54, 42.
- 122 Weller, *Z.Elektrochem.*, 1956, 56, 662.
- 123 Weller, *Z.Phys.Chem.*, 1955, 3, 238.
- 124 E.L. Wehry, L.B. Rogers *J.Am.Chem.Soc.*, 1965, 87, 4234.
- 125 J. McEwen, K. Yates *J.Phys.Org.Chem.*, 1991, 4, 193.
- 126 P.J. Baldry *J.Chem.Soc.Perkin II*, 1979, 95i.
- 127 H.E. Zimmerman, V.R. Sandel *J.Am.Chem.Soc.*, 1963, 85, 915.
- 128 J.W. Hilborn, E. Macknight, J.A Pincock, P.J. Wedge *J.Am.Chem.Soc.*, 1994, 116, 3337.
- 129 S. Hixon, *J.Am.Che.Soc.*, 1975, 97, 1981.
- 130 P. Wan, K. Yates *J.Photochem.*, 1984, 157.
- 131 P. Wan, K. Yates, *J.Org.Chem.*, 1983, 48, 869.
- 132 S. Anderson, K. Yates *Can.J.Chem.*, 1988, 66, 2412.
- 133 (1) J.P. Malrieu, G. Trinquier *J.Am.Che.Soc.*, 1989, 111, 5916. (2) J.P. Malrieu *Theo.Chim.Acta*, 1981, 64, 251. (3) J.P. Marieu, G. Trinquier *Theo.Chim.Acta*, 1979, 54, 59. (4) J.P. Malrieu, I. Nebot-Gil, J. Sanchez-Marin *Pure&App.Chem.*, 1984, 56, 1241.



- 134 a) K.P. Ghiggino, D. Philips, M.D. Swords, R. Salisbury *J.Photochem.*, **1977**, *7*, 141. b) K. Onodera, G. Furusawa, M. Kojima, M. Tsuchiya, S. Aihara, R. Akaba, H. Sakuragi, K. Tokumaru *Tet.Lett.*, **1985**, *41*, 2215. c) M. Kojima, H. Sakuragi, K. Tokumaru *Tet.Lett.*, **1981**, *22*, 2889.
- 135 K.P. Ghiggino, D. Philips, R. Hara, R. Salisbury *J.Chem.Soc.Faraday Trans. 2*, **1978**, *74*, 607.
- 136 W.G. Dauben, H.C.H.A. van Riel, J.D. Robbins, J.D. Wagner *J.Am.Chem.Soc.*, **1979**, *101*, 6383.
- 137 T. Ni, R.A. Caldwell, L.A. Melton *J.Am.Chem.Soc.*, **1989**, *111*, 457.
- 138 S.R. Meech, D. Phillips *Chem.Phys.Lett.*, **1985**, *116*, 262.
- 139 P. O'Connor, L.A. Chewter, D. Phillips *J.Phys.Chem.*, **1982**, *86*, 3400.
- 140 D. Kivelson, K.G. Spears *J.Phys.Chem.*, **1985**, *89*, 1999.
- 141 D. Ben-Amotz, C.B. Harris *J.Chem.Phys.*, **1987**, *86*, 4856.
- 142 a) R.A. McClelland, C. Chan, F. Cozens, A. Modro, S. Steenken *Angew.Chem.intl.ed.*, **1991**, *30*, 1337. b) R.A. McClelland, F. Cozens, S. Steenken *Tet.Lett.* **1990**, *31(20)*, 2821. c) Electronic aspects of Organic Photochemistry, J. Michl, Vlasta Bonacic-Koutecky, Wiley Interscience Publications, John Wiley & Sons, **1990**, p 244. d) V. Bonacic-Koutecky, K. Schoffel, J. Michl *J.Am.Che.Soc.*, **1989**, *111*, 6140.

- 143 H.M. Frey, D.C. Montague, I.D.R. Stevens *Trans.Faraday Soc.*, **1967**, *63*, 372.
- 144 H.M. Frey *Trans.Faraday Soc.*, **1962**, *58*, 957, 959; **1963**, *59*, 1619; **1964**, *60*, 83.  
H.M. Frey, Marshall, R.F. Skinner *Trans.Faraday Soc.*, **1965**, *65*, 861. H.M. Frey, R.F. Skinner *Trans.Faraday Soc.*, **1965**, *61*, 1918. Ellies, H.M. Frey *J.Chem.Soc.*, **1964**, 5578. Shumate, Neuman, Fonken *J.Am.Chem.Soc.*, **1965**, *87*, 3996. H.M. Frey *J.Chem.Soc.*, **1961**, 957.
- 145 H.M. Frey, J. Metcalfe, B.M. Pope *Trans.Faraday Soc.*, **1971**, *67*, 750.
- 146 H.M. Frey, A.M. Lamont, R. Walsh *J.Chem.Soc.Chem.Comm.*, **1970**, 1583.
- 147 H.M. Frey, G.R. Branton, R.F. Skinner *Trans.Faraday Soc.*, **1966**, 1546.
- 148 H.M. Frey, M. Pope, R.F. Skinner *Trans.Faraday Soc.*, **1967**, *63*, 1166.
- 149 H.M. Frey, A.M. Lamont, Walsh *J.Chem.Soc. A*, **1971**, 2642.
- 150 R. Criegee, U. Zinngibl, H. Furrer, D. Seebach, G. Freund *Chem.Ber.*, **1964**, *97*, 2942.
- 151 R. Criegee, D. Seebach, R.E. Winter, B. Borretzen, H.A. Brune *Chem.Ber.*, **1965**, *98*, 2339.
- 152 D.H. Volman, J.R. Seed *J.Am.Chem.Soc.*, **1964**, *86*, 5095.
- 153 G. Forbes, L. Heidt *J.Am.Chem.Soc.*, **1934**, *56*, 2363.
- 154 J. Pitts, D. Margerum, P. Taylor, W. Brim *J.Am.Chem.Soc.*, **1955**, *77*, 5499.

- 155 H.M. Frey, L. Soller *Trans Faraday Soc.*, **1969**, *65*, 449.
- 156 T. Shida, T. Momose, N. Ono *J Phys.Chem.*, **1985**, *89*, 815.
- 157 B. Thomas IV, J. Evanseck, K. Houk *Israel J.Chem.*, **1993**, *33*, 287.
- 158 W.R. Dolbier, H. Koroniak, D. Burton, P. Heinze *Tet.Lett.*, **1986**, *27*, 4387.
- 159 W.R. Dolbier, T.A. Gray, J. Keaffaber, L. Celewicz, H. Koroniak  
*J.Am.Chem.Soc.*, **1990**, *112*, 363.
- 160 K. Rudolf, D.C. Spellmeyer, K.N. Houk *J.Org.Chem.*, **1987**, *52*, 3708.
- 161 S. Niwayama, K.N. Houk, *Tet.Lett.*, **1992**, *33*, 883; **1993**, *34*, 1251.
- 162 R. Hayes, S. Ingham, S.T. Saenchantara, T.W. Wallace *Tet.Lett.*, **1991**, *32*, 2953.
- 163 S. Niwayama, K.N. Houk, T. Kusumi *Tet.Lett.*, **1994**, *4*, 527.
- 164 B.E. Thomas IV, J.D. Evanseck, K.N. Houk *J.Am.Chem.Soc.*, **1993**, *115*, 4165.
- 165 N. Rondan, K.N. Houk *J.Am.Chem.Soc.*, **1985**, *107*, 2099.
- 166 E.A. Kallel, Y. Wang, D. Spellmeyer, K.N. Houk *J.Am.Chem.Soc.*, **1990**, *112*,  
6759.
- 167 J.E. Baldwin, V.P. Reddy, B.A. Hess, L.J. Schaad *J.Am.Chem.Soc.*, **1988**, *110*,  
8554.

- 168 J.E. Baldwin, V.P. Reddy, B.A. Hess, L.J. Schaad *J.Am.Chem.Soc.*, **1988**, *110*, 8555.
- 169 J. Gajewski "Hydrocarbon Thermal Isomerizations", Academic Press, New York, **1981**, pp 45-48, and references cited therein.
- 170 W.G. Dauben, Haubrich *J.Org.Chem.*, **1988**, *53*, 600.
- 171 Hersberg, Longuet-Higgins *Trans.Faraday Soc.*, **1963**, *35*, 77.
- 172 Mead, Trushler *J.Chem.Phys.*, **1979**, *70*, 2284.
- 173 Mead *Chem.Phys.*, **1980**, *49*, 23.
- 174 S.P. Keating, Mead *J.Chem.Phys.*, **1985**, *82*, 5102.
- 175 S.P. Keating, Mead *J.Chem.Phys.*, **1987**, *86*, 2152.
- 176 M.E. Squillacote, T.C. Semple *J.Am.Chem.Soc.*, **1987**, *109*, 892.
- 177 F. Bernardi, M. Olivucci, M. Robb *J.Am.Chem.Soc.*, **1990**, *112*, 1737.
- 178 A. Postigo, W.J. Leigh *J.Chem.Soc.Chem.Comm.*, **1993**, *24*, 1836.
- 179 R.S.H. Liu, D.T. Browne *Acc.Chem.Res.*, **1986**, *19*, 42.
- 180 Ei-ichi Negishi, S. Holmes, J. Tour, J. Miller, F. Cederbaum, D. Swanson, T. Takashashi *J.Am.Chem.Soc.*, **1989**, *111*, 3336. Ei-ichi Negishi *Chimica Scripta*, **1989**, *29*, 457. Ei-ichi Negishi, S. Miller *J.Org.Chem.*, **1989**, *54*, 6014.

- 181 P. Schuchmann, C. Von Sonntag *J.Photochem.*, **1981**, *15*, 159.
- 182 W.G. Dauben, R. Cargill *J.Am.Chem.Soc.*, **1961**, *83*, 342.
- 183 P.D. Karadokov, J. Gerratt, D. Cooper, M. Raimondi *J.Am.Chem.Soc.*, **1994**, *116*, 7714.
- 184 J. Pitts, D. Margerum, P. Taylor, W. Brim *J.Am.Chem.Soc.*, **1955**, *77*, 5499.
- 185 K. Porter, D.H. Volman *J.Am.Chem.Soc.*, **1962**, *84*, 2011. B. Bagchi, G.R. Fleming *J.Phys.Chem.*, **1990**, *94*, 9. Q. Liu, J.K. Wang, A.H. Zewail *Nature* (London), **1993**, *364*, 427.
- 186 J. Saltiel, L. Metts, M. Wrighton *J.Am.Chem.Soc.*, **1970**, *92*, 3227. S. Boue, R. Srinivasan *Mol. Photochem.* **1972**, *4*, 93.
- 187 R. Srinivasan, S. Boue *J.Am.Chem.Soc.*, **1971**, *93*, 5606.
- 188 J. Saltiel, Metts, Wrighton *J.Am.Chem.Soc.*, **1969**, *91*, 5684.
- 189 I.R. Dunken, L. Andrews *Tetrahedron*, **1985**, *41*, 145.
- 190 L Serrano-Andres, M. Merchan, I. Nebot-Gil, R. Lindh, B.O. Roos, *J.Chem.Phys.*, **1993**, *98*, 3151.
- 191 W.J. Leigh, A. Postigo. "Photochemistry of Bicyclo[n.2.0]alk-1-ene", submitted for publication.

- 192 a) W.J. Leigh, A. Postigo. "Alkyl Substituent Effects on the Photochemistry of Monocyclic Cyclobutenes", submitted for publication. b) P. Celani, S. Ottani, F. Bernardi, M. Robb *J.Am.Chem.Soc.*, 1994, in press.
- 193 A. Burger, R. Bennett *J.Med.&Pharm.Chem.*, 1960, 2, 687.
- 194 H. Tanida, T. Tsushima *J.Am.Chem.Soc.*, 1970, 92, 3397.
- 195 J.L. Derocque, U. Beisswenger, M. Hanack *Tet.Lett.*, 1969, 26, 2149. J. Wilt, D. Roberts *J.Org.Chem.*, 1962, 27, 3430.
- 196 C. Dass, M.L. Gross *Org.Mass Spectr.*, 1983, 18, 544. J. Derocque, M. Jochem *Org.Mass Spectr.*, 1975, 10, 935.
- 197 K. Kodaira, K. Okuhara *Bull.Soc.Chem.Japan*, 1988, 61, 1625.
- 198 S. Safe, *J.Chem.Soc.(B)*, 1971, 962.
- 199 Aldrich Chemical Co.
- 200 Lancaster Chemical Co.
- 201 D. Dawson, W. Reynolds *Can.J.Chem.*, 1975, 53, 373. L. Berthelot, L. Thomas *Spectrochimica Acta*, 1982, 38, 487.
- 202 A. Malliaris *Appl.Spectrosc.Rev.*, 1992, 27, 51.
- 203 W.J. Leigh, M.S. Workentin, D. Andrew *J.Photochem.Photobiol. A*, 1991, 57, 97.
- 204 P. Kraakman, W.de Wolf, F. Bickelhaupt *J.Am.Chem.Soc.*, 1989, 111, 8534.

- 205 Sigma Chemical Co.
- 206 W. Reeve, D.M. Reichel *J.Org.Chem.*, 1972, 37, 68.
- 207 P. Auderset, A. Dreiding, E. Gesing *Synth.Comm.*, 1983, 13, 881.
- 208 R. Sustman, P. Daute, R. Sauer, A Sommer, W. Trahanovsky *Chem.Ber.*, 1989, 122, 1551.
- 209 W. Nugent, D. Thorn, R.L. Harlow *J.Am.Chem.Soc.*, 1987, 109, 2788.
- 210 J. Gajewski, C.N. Shih *J.Org.Chem.*, 1972, 37, 34. J. Gajewski, C.N. Shih , 1972, 94, 1675. P. Humbach, R. Schirpf *Angew.Chem.intl.ed.*, 1969, 8, 206. J. Gajewski, C.N. Shih *J.Am.Chem.Soc.*, 1969, 91, 5900.
- 211 L. Fitjer, S. Moderassi *Tet.Lett.*, 24, 5495. L. Stevens, J. Berson *Tetrahedron*, 1988, 4835.
- 212 R.D. Miller, D.L. Dolce *Tet.Lett.*, 1974, 43, 3813. E. Bolema, J. Stratting, H. Wynberg *Tet.Lett.*, 1972, 1175. N. Rabjohn "Organic Reactions" Chapter 8, pp331-386. H. Scharf, F. Linckens *Synthesis*, 1976, 256.
- 213 L. Paquette, A Schaefer, J. Blount *J.Am.Chem.Soc.*, 1983, 105, 3642.
- 214 a) E. Zimmermann, J.K. Stille *Macromolecules*, 1985, 18, 321. b) M. Kosugi, Y. Kiuchi, T. Migita, *Chem.Lett.*, 1981, 69.

## APPENDIX 1

### Ferrioxalate Actinometer

Calculation of measured radiant power

$$\phi_p = \Delta A \cdot V_1 \cdot 10^{-3} \cdot V_3 / (\phi \cdot \epsilon_{510} \cdot V_2 \cdot t) \text{ [einstein } \cdot \text{s}^{-1}]$$

where  $\Delta A$  = Absorbance of irradiated actinometer minus absorbance of unirradiated actinometer solution measure at 510 nm.

$V_1$  = Volumen of irradiated solution.

$V_2$  = Volumen of aliquote taken from irradiated actinometer.

$V_3$  = Volumen of volumetric flask where the the complex is prepared.

$\phi$  = Quantum yield of actinometer at the given wavelength.

$\epsilon_{510}$  = Molar Extinction Coefficient of complex  $\text{Fe}^{++}$ -o-Phenanthroline  
(11100  $\text{dm}^{-3} \text{mol}^{-1} \text{cm}^{-1}$ )

$t$  = Irradiation Time in seconds.

### Uranyl Oxalate Actinometer

Calculation of measured radiant power:

$$P = V \cdot \Delta A \cdot 10^{-2} / [CF \cdot t \cdot \phi \cdot F \cdot \epsilon]$$



where  $V$  = Volumen of irradiated actinometer solution (mL).

$\Delta A$  = Absorbance of irradiated actinometer minus absorbance of unirradiated actinometer solution (measured at 320 nm).

CF = Conversion factor to convert moles of Cerium analyzed to moles of oxalate photolyzed.

$t$  = Time of irradiation (min).

$\phi$  = Quantum yield of the actinometer ( $\sim 0.50$  at 214 nm).

F = Fraction of incident light absorbed by the actinometer.

$\epsilon$  = Molar Extinction Coefficient of Ce(IV) solution ( $5.41 \times 10^3 \text{ dm}^3 \text{ mol}^{-1} \text{ cm}^{-1}$ ).

The formula reduces to photon flux  $\phi_p$ :

$$\phi_p = \Delta A / (t \cdot \phi) \cdot 2.773 \times 10^{-6} [\text{einstein} \times \text{min}^{-1}]$$

#### Fluorescence Quantum Yield Determinations:

$$\phi_f = \phi_s A_i \eta_i I_i / (A_s \eta_s I_s)$$

Where the subscript "i" refers to the sample and the subscript "s" refers to the standard.

A = Maximum of absorbance (in the range 0.05 - 0.2) at the wavelength of excitation.

$\eta$  = Refractive index of the solvent used.

I = Integration of the gaussian emission band from the fluorescence spectrum.

## APPENDIX 2

Decay Law (Singlet Lifetime) Predicted in the Case of a TransientTerm:

$$G(t) = A \exp(-at - 2bt^{1/2}),$$

Where  $a = 1/\tau_0 + 4\pi R' D_{AQ} N' [Q]$

$b = 4 (R')^2 \times (\pi D_{AQ} N')^{1/2} [Q]$

$R'$  = Encounter distance between fluorophore and quencher.

$D_{AQ}$  = Mutual Diffusion Coefficient of the fluorophore and quencher.

$N$  = Fraction of excited molecules that emit a fluorescence photon.

$[Q]$  = Concentration of quencher.